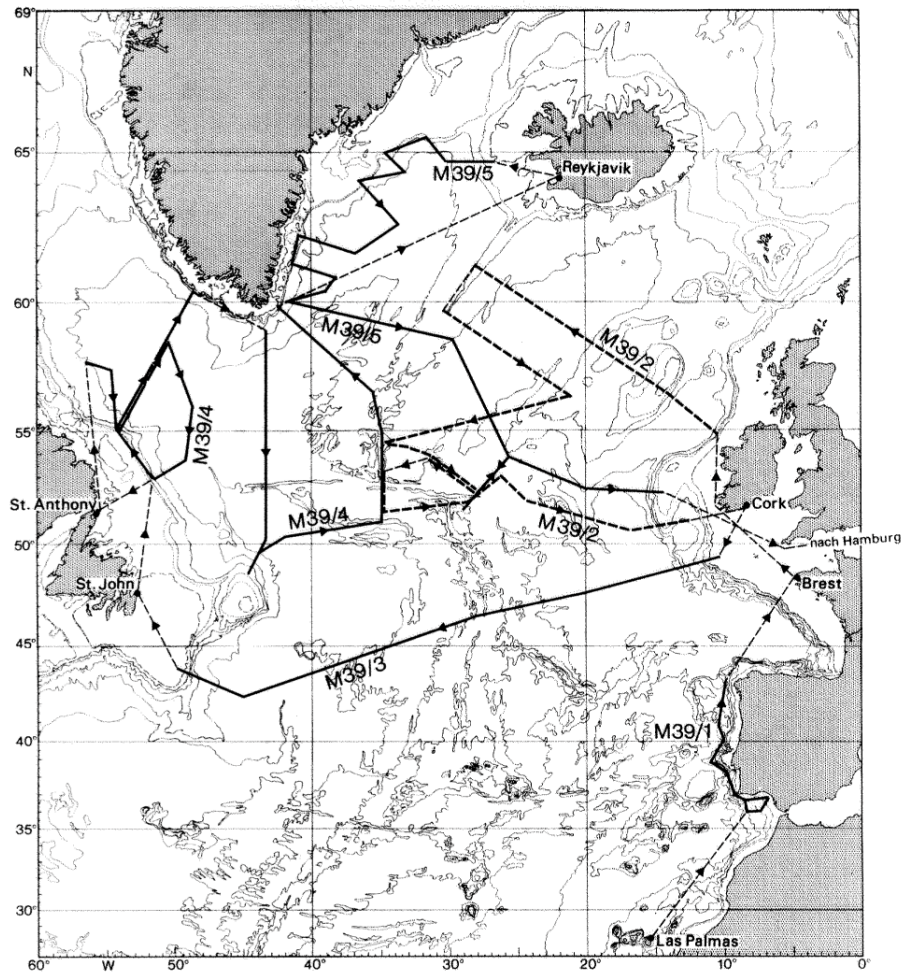


A. Cruise Narrative: 06MT39_1-5 (A02, AR05, AR07E, AR07W, AR12, AR24, AR25



A.1. Highlights

WHP Cruise Summary Information

Ship: **METEOR**

WOCE Line	ExpoCode	Chief Scientist	Dates
AR12, AR24	06MT39_2	Thomas J. Müller, Walter Zenk/IfMK	1997.05.15 – 1997.06.06
A02	06MT39_3	Peter Koltermann/BSH	1997.06.11 – 1997.07.03
AR07W, AR05	06MT39_4	Fritz Schott/IfMK,	1997.07.07 – 1997.08.07
AR07E, AR25	06MT39_5	Alexander Sy/BSH	1997.08.14 – 1997.09.14

06MT39_2 (74 stations)	06MT39_3 (80 stations)	06MT39_4 (102 stations)	06MT39_5 (43 stations)
Brest, France to Cork, Ireland	Cork, Ireland to St. John's Newfoundland, Canada	St. John's, Nfld to St. Anthony to Reykjavik	Reykjavik, Iceland to Hamburg, Germany
Geographic boundaries: 61°10'N 35°9.84'W 9°3.78'W 50°25.32'N	49°13.9'N 50°.4'W 10°38.8'W 42°.9'N	60°18.5'N 56°32'W 34 °50'W 48°51.4'N	65°31'N 42°51'W 14°29.9'W 51°42'
9 RAFOS floats	3 C-PALACE floats	7 Palace floats	0 Floats
Moorings: 2 deployed	1 recovered, 1 deployed	0	6 deployed, 4 recovered

Contributing Authors (as they appear in text)

R. Zahn, W. Zenk, K.P.Koltermann, F. Schott, A. Sy, S. Becker, B. Lenz, T.J. Müller, O. Plähn, A. Körtzinger
L. Stramma, C. Mertens, J. Fischer, U. Send, D. Kindler, M. Rhein, U. Karger, H. Gäng, L. Mintrop, H.-J.
Weichert, G. Stelter, A. Frohse, F. Morsdorf, Ch. Stransky, R. Kramer, H. Tacke, F. Schmiel, A. Gottschalk,
K. Bulsiewicz, U. Fleischmann, G. Fraas, R. Gleiss, V. Sommer, H. Giese, C. Neill, E. Lewis, K. Bakker, D.
Machoczek, H. Mauritz, K. Schulze, M. Stolley, N. Verch, M. Reich, L. Czechel, H. Hildebrandt, C. Mohn, J.
Read, G. Hargreaves, J. Ashley, H. Thomas, B. Schneider, N. Gronau, E. Trost, R. Keir, G. Rehder, M.
Arnold, R. Bayer, M. Huels, S. Jung, A. Müller, C. Willamowski, G. Bozzano, C. Didie, L. Lembke, N.
Loncaric, P. Schäfer, J. Schönfeld, A. Kohly, B. Bader, I. Cacho, K. Heilemann, F.-J. Hollender, T. Karp, K.
Flechtsenhar, B. Brandt, G. Kahl

METEOR – BERICHTE

99-1

North Atlantic 1997

Cruise No. 39

18 April – 14 September 1997

Edited by:

Friedrich Schott, Klaus-Peter Koltermann, Lothar Stramma, Alexander Sy,
Rainer Zahn and Walter Zenk



Editorial Assistance:

Franck Schmieder

Fachbereich Geowissenschaften, Universität Bremen

Leitstelle METEOR

Institut für Meereskunde der Universität Hamburg

1999

WHP Cruise and Data Information

Instructions: Click on items below to locate primary reference(s) or use navigation tools above.

TABLE OF CONTENTS

Abstract

Zusammenfassung

1 Research Objectives

1.1 Introduction

1.2 Projects

2 Participants

3 Research Programs

3.1 WOCE program

3.1.1 Physical Oceanography during WOCE cruises

3.1.1.1 Hydrographic measurements at 48°N in the North Atlantic along the WHP section A

3.1.1.2 WOCE-NORD

3.1.2 Nutrients and tracer measurements during WOCE cruises

3.2 Sonderforschungsbereich (SFB)

3.2.1 Physical Oceanography during SFB cruises

3.2.2 Air-sea fluxes

3.2.3 Carbon dioxide system, oxygen, nutrients during SFB-cruises

3.3 Other programs

3.3.1 VEINS programs

3.3.2 Tracer sampling

3.3.3 Methane

3.3.4 Foraminifera ($\delta^{13}\text{C}$ and $\delta^{18}\text{O}$ data in foraminifera)

3.4 Paleoceanography

3.4.1 Water Column Profiling: Ground-Truth Data Base for Calibration of Paleoceanographic Proxies

3.4.2 Plankton in Surface Waters off Portugal

3.4.3 Benthic Foraminifera: Faunal Composition and Stable Isotopes

3.4.4 Trace Fossils and Bioturbation as Indicators of Paleo-Environmental Conditions

3.4.5 Temperate Water Carbonates

3.4.6 Trace Metals in Calcareous Microorganisms as Paleoceanographic Tracers

3.4.7 Sediment Geochemistry and Mineralogy

4 Narrative of the cruise

- 4.1 Leg M39/1 (R. Zahn)
- 4.2 Leg M39/2 (W. Zenk)
- 4.3 Leg M39/3 (K. P. Koltermann)
- 4.4 Leg M39/4 (F. Schott)
- 4.5 Leg M39/5 (A. Sy)

5 Preliminary Results

- 5.1 SFB
 - 5.1.1 Physical Oceanography of the eastern Basin (M39/2)
 - 5.1.1.1 Hydrography (S. Becker, B. Lenz, T.J. Müller, W. Zenk)
 - 5.1.1.2 Freon Analysis (CFC) (O. Plähn)
 - 5.1.1.3 Carbon Dioxide System, Nutrients and Oxygen (A. Körtzinger)
 - 5.1.2 Physical Oceanography of the Labrador and Irminger Sea (M39/4)
 - 5.1.2.1 Technical aspects
 - 5.1.2.2 Analyses and Evaluations
 - 5.1.2.3 Air-sea fluxes (U.Karger, H.Gäng)
 - 5.1.2.4 Carbon Dioxide System, Nutrients and Oxygen (L. Mintrop)
- 5.2 WOCE and VEINS
 - 5.2.1 Leg M39/3
 - 5.2.1.1 Hydrographic Measurements
 - 5.2.1.2 Nutrients and Oxygen Measurements
 - 5.2.1.4 Mooring work and float deployment (H. Giese, K. P. Koltermann)
 - 5.2.1.5 "TCO₂ and Total Alkalinity Measurements along 48°N on the WHP section A2 1997" (C. Neill, E. Lewis)
 - 5.2.2 Leg M39/5
 - 5.2.2.1 Hydrographic Measurements (A. Sy, K. Bakker, R. Kramer, D. Machoczek, H. Mauritz, F. Schmiel, K. Schulze, G. Stelter, M. Stolley, N. Verch)
 - 5.2.2.2 Tracer Measurements
 - 5.2.2.3 Current Measurements
 - 5.2.2.4 Carbonate chemistry in the Northern Atlantic Ocean (H. Thomas, B. Schneider, N. Gronau and E. Trost)
- 5.3 Other programs
 - 5.3.1 Methane (R.Keir, G.Rehder)
 - 5.3.2 Tritium/helium sampling program results from M39, legs 4 and 5 (H. Hildebrandt, M. Arnold, R.Bayer)
- 5.4 Paleoceanography
 - 5.4.1 Water Column T-S Profiling (M. Huels, S. Jung, R. Zahn)
 - 5.4.2 Seawater Sampling for Trace Element and Nutrient Analysis (A. Müller, C. Willamowski)
 - 5.4.3 Shipboard Sediment Sampling and Core Flow (G. Bozzano, C. Didie, M. Huels, S. Jung, L. Lembke, N. Loncaric, P. Schäfer, J. Schönfeld)
 - 5.4.4 Plankton Hauls (A. Kohly)
 - 5.4.5 Porewater Oxygen Profiling: Reference for Benthic Foraminiferal Assemblage Studies (J. Schönfeld)

- 5.4.6 Trace Fossil Recording and Grab Sampling (P. Schäfer, B. Bader)
- 5.4.7 Geochemistry and Mineralogy (G. Bozzano, I. Cacho)
- 5.4.8 High-Resolution Acoustic Mapping and Core Logging: Paleoceanographic Application (K. Heilemann, F.-J. Hollender, T. Karp)

6 Ship's Meteorological Station

- 6.1 Meteorological conditions during leg M39/1 (K. Flechsenhar)
- 6.2 Meteorological conditions during leg M39/2 (B. Brandt)
- 6.3 Meteorological conditions during leg M39/3 (B. Brandt)
- 6.4 Meteorological conditions during leg M39/4 (G.Kahl)
- 6.5 Meteorological conditions during leg M39/5 (G.Kahl)

7 Lists

- 7.1 Leg M39/1
 - 7.1.1 Locations for sediment and plankton/water samples
 - 7.1.2 Water sampling sites for plankton assemblage studies
 - 7.1.3 Phyto- and zooplankton species found in M39/1 sampling sites
- 7.2 Leg M39/2
 - 7.2.1 CTD Inventory
 - 7.2.2 Mooring Activities
 - 7.2.3 List of RAFOS Float Launches
- 7.3 Leg M39/3
 - 7.3.1 Station list of cruise M39/3
- 7.4 Leg M39/4
 - 7.4.1 CTD-profile station list and water samples taken from the bottles
- 7.5 Leg M39/5
 - 7.5.1 Station listing

8 Concluding remarks and acknowledgements

9 CFC Reports

10 References

Abstract

METEOR cruise M39 took place in the North Atlantic Ocean and consisted of five legs. Work on M39 was carried out mainly in the context of two climate relevant programs: for Sonderforschungsbereich (SFB) 460 (“Dynamics of thermohaline circulation variability”), during legs M39/2 and M39/4, and for the World Ocean Circulation Experiment (WOCE), during M39/3 and M39/5 while paleo-oceanographic studies were carried out on one leg, M39/1.

During the first cruise leg M39/1, departing 18 April 1997 out of Las Palmas, Canary Islands, paleo-oceanographic work was carried out in the eastern Atlantic. The objective was to document the history of the North Atlantic’s thermohaline circulation during the last glacial period. Sediment cores and sediment surfaces along deep transects in the Gulf of Cadiz and off Portugal were sampled. With detailed paleo-oceanographic time series, the hydrographic history of North Atlantic water masses and of Mediterranean water were recorded. Ocean chemistry work documented today’s distribution of paleo-oceanographic trace-elements. Cruise leg M39/1 ended on 10 May in Brest.

METEOR left Brest again on 14 May for leg M39/2. During this leg measurements were conducted in the eastern North Atlantic within the context of the SFB 460 of Kiel University. The aim was to investigate the variability of water masses of the subpolar gyre during their passage through the Iceland Basin as well as its transport rates and pathways. Detailed CTD surveys on seven sections and the deployment of current meter moorings and RAFOS floats were carried out for long-term observations of Overflow- and Labrador Sea Waters. Leg M39/2 was completed on 8 June 1997 in Cork, Ireland.

Cruise leg M39/3 focused once again on a survey of the 48°N WOCE section A2 under one-time survey requirements. Since earlier observations had shown a large interannual variability of all hydrographic properties, this survey was again combined with chemical oceanographic measurements to arrive at a CO₂ budget. Results from this cruise confirm these rapid full-depth changes. The data will be used to calculate indices of the meridional circulation such as transports of heat, freshwater and mass and the meridional overturning. Previous estimates had shown large changes in the heat transports. The observations of cruise M39 are required to advance the understanding of the underlying mechanisms.

Leg M39/4 began in St. John’s on 6 July and investigations were carried out for several projects of the SFB 460. Since leg M39/4 had as an essential objective the retrieval and redeployment of a variety of moorings, it had to be subdivided into two segments with an interim stop on 16 July in St. Anthony (New Foundland). During the first part of leg M39/4 several moorings were successfully recovered, a boundary current meter array was deployed, CTD-profiles were taken and profiling ALACE floats deployed in the western part of the Labrador Sea. After the interim stop in St. Anthony the mooring work was continued in the Labrador Sea. Here, as well as in the Irminger Basin, a large amount of CTD stations were carried out to investigate the water mass distribution, spreading paths and transports in the western North Atlantic. Leg M39/4 had accomplished its objectives and ended on 11 August in Reykjavik, Iceland.

Cruise M39/5 by R.V. METEOR was another contribution to the "World Ocean Circulation Experiment" (WOCE). In addition, work was carried out for the EC program "Variability of Exchanges in the Northern Seas" (VEINS). This leg started in Reykjavik (Iceland) on 14 August and finished in Hamburg (Germany) on 14 September, 1997. The purpose of the first part of the cruise (VEINS) was to carry out CTD sections and to recover and redeploy current meter moorings in the overflow waters off East Greenland, between the Denmark Straits and Cape Farvel. Work was part of a cooperation effort between British, Finnish, Icelandic and German institutions. The objective of the second part of this cruise leg was a repeat of the WOCE Hydrographic Programme section A1E/AR7E, running from Cape Farvel to the southern tip of the Porcupine Bank off the west coast of Ireland.

Overall METEOR cruise 39 was successful, and the intended work could be carried out according to plan.

Zusammenfassung

Die METEOR-Reise M39 fand im Nordatlantischen Ozean statt. Im Verlauf von fünf Fahrtabschnitten wurden Arbeiten hauptsächlich im Zusammenhang mit zwei klimarelevanten Programmen durchgeführt, dem Sonderforschungsbereich (SFB) 460 "Dynamik thermohaliner Zirkulationsschwankungen" (Abschnitte M39/2 und M39/4) und dem "World Ocean Circulation Experimentis (WOCE) (Abschnitte M39/3 und M39/5). Ein Fahrtabschnitt (M39/1) diente Paleo-Ozeanographischen Untersuchungen.

FS METEOR lief am 18. April 1997 von Las Palmas auf den Kanarischen Inseln für den ersten Abschnitt M39/1 aus. Paleo-Ozeanographische Arbeiten wurden im östlichen Nordatlantik durchgeführt. Das Ziel der Arbeiten war die Erforschung der Geschichte der Nordatlantischen Thermohalinen Zirkulation während der letzten Glazialperiode. Dafür wurden Sedimentkerne und Sedimentverteilungen entlang tiefer Schnitte im Golf von Cadiz und vor Portugal gesammelt. Meereschemische Arbeiten dokumentierten dabei die heutigen Verteilungen der Paleo-Ozeanographischen Spurenelemente. Das wissenschaftliche Programm von M39/1 wurde mit der Ankunft in Brest am 10. Mai beendet.

METEOR verließ Brest am 14. Mai für den Abschnitt M39/2. Auf diesem Abschnitt wurden Messungen im östlichen Nordatlantik für den SFB 460 der Universität Kiel durchgeführt. Ziel war die Untersuchung der Variabilität von Wassermassen des subpolaren Wirbels während ihres Durchquerens des Islandbeckens sowie ihre Ausbreitungswege und Transporte. Detaillierte CTD-Untersuchungen auf sieben Schnitten und Verankerung von Strommessern und RAFOS Floats wurden zur Beobachtung des Langzeitverhaltens des Overflow und des Labradorsee-Wassers durchgeführt. Der Abschnitt M39/2 wurde am 8. Juni 1997 mit der Ankunft in Cork, Irland beendet.

Der Abschnitt M39/3 diente der erneuten hydrographischen Aufnahme des WOCE-Schnitts A2. Damit verbunden war die Wiederholung der Aufnahme der CO₂-Verteilung auf diesem Schnitt im Rahmen von JGOFS. Die vorangegangene Aufnahme mit FS METEOR im Herbst 1994 hatte bereits die deutlichen und schnellen Veränderungen der hydrographischen Kenngrößen in diesem Übergangsbereich zwischen dem Subpolar- und dem Subtropenwirbel

im Vergleich mit den Vorgängeruntersuchungen aufgezeigt. Diese signifikante Variabilität wurde auf der jetzigen Reise bestätigt. Die Daten dieser Reise werden ebenfalls für die Berechnung der meridionalen Zirkulationsgrößen wie Wärme-, Süßwassertransport und Meridionalzirkulation verwendet. Frühere Aufnahmen in den 90er Jahren hatten Schwankungen besonders im Wärmetransport gezeigt, die zu verstehen Ziel der jetzigen Untersuchungen ist.

Der Abschnitt M39/4 begann in St. John's am 6. Juli, und die durchgeführten Untersuchungen standen im Zusammenhang mit mehreren Teilprojekten des SFB 460. Da M39/4 als eines der Hauptarbeitsziele die Aufnahme und erneute Auslegung einer Vielzahl von Verankerungen hatte, mußte M39/4 aus logistischen Gründen in zwei Teile mit einem kurzen Zwischenstop in St. Anthony am 16. Juli aufgespalten werden. Während des ersten Teils von M39/4 wurden mehrere Verankerungen erfolgreich geborgen, ein Strommesser- und Randstromarray ausgelegt, CTD- Profile gewonnen und profilierende ALACE Floats im westlichen Teil der Labrador See ausgesetzt. Nach dem Zwischenstop in St. Anthony wurden zunächst die Verankerungsarbeiten in der Labrador See fortgesetzt. Hier als auch im folgenden im Irminger Becken wurde eine Vielzahl von CTD-Profilen gewonnen, um die Wassermassenverteilung, und Ausbreitungspfade und Transporte im westlichen Nordatlantik zu untersuchen. Der Abschnitt endete am 11. August in Reykjavik, Island.

Reise M39/5 war ein weiterer Beitrag zum deutschen WOCE-Programm. Weiterhin wurden Arbeiten für das EG-Programm "Variability of Exchanges in the Northern Seas" (VEINS) durchgeführt. Der Fahrtabschnitt begann am 14. August in Reykjavik (Island) und endete am 14. September 1997 in Hamburg. Der Beitrag zu VEINS während des ersten Teils von M39/5 waren CTD-Messungen sowie Aufnahme und Wiederauslegung von Strommesserverankerungen zwischen dem ostgrönländischen Kontinentalabhang, der Dänemarkstraße und Kap Farvel. Diese Arbeiten wurde in Kooperation zwischen britischen, finnischen, isländischen und deutschen Instituten durchgeführt. Das Hauptziel des zweiten Teils des Abschnitts war eine Wiederholung des WOCE Schnittes A1E/AR7E, einem hydrographischen Schnitt zwischen Kap Farvel und dem Südende der Porcupine Bank vor der Westküste Irlands. Insgesamt war METEOR-Reise M39 erfolgreich und die vorgegebenen Aufgaben konnten in vollem Umfang abgewickelt werden.

1 Research Objectives

1.1 Introduction

METEOR-cruise 39 took place in the North Atlantic Ocean with measurements mainly north of 40°N (Figure 1) except for some work off Portugal and near the entrance to the Mediterranean Sea during the first leg. The cruise began on 18 April 1997 in Las Palmas and ended on 14 September 1997 in Hamburg. METEOR-cruise 39 combined during five legs (Table 1) activities of paleo-oceanographic, physical oceanography, marine chemistry, meteorological, geological and tracer physics working groups.

After cruise M39 started in Las Palmas, METEOR headed towards the entrance of the Mediterranean. The work during the first leg off the southwest European shelf combined different working groups and measurement techniques to investigate paleo-oceanographic problems with regard to the thermohaline circulation during the last glacial period.

The aims during the second and forth leg were regional investigations of the thermohaline circulation in the western and eastern basins within the context of the new "Sonderforschungsbereich" at the University of Kiel SFB-460 "Dynamics of thermohaline circulation variability". The main objectives during the SFB-460 related cruise legs were hydrographic measurements as well as intense mooring work.

Besides the hydrographic and mooring work during the two SFB-460 related cruise legs distributions of total dissolved inorganic carbon and total alkalinity were measured at the hydrocast locations. Nutrients and dissolved oxygen were determined in parallel. This combined analysis will allow the calculation of the penetration of anthropogenic CO₂ into the water column. Additionally, a system to continuously monitor the CO₂ partial pressure in surface waters and air operated during the two legs. This will allow calculating the CO₂ flux between atmosphere and ocean.

During the third and fifth leg measurements of the thermohaline overturning circulation of the North Atlantic along two trans-Atlantic sections were carried out as final contributions of the Hamburg groups to the World Ocean Circulation Experiment (WOCE). Both sections were repeated several times since 1991 to investigate the transport rates of the meridional overturning circulation and its variability. Besides hydrography, marine chemistry and tracer measurements were carried out. During the fifth leg, measurements were made also for the "Variability of Exchanges in the Northern Seas (VEINS)" Project as part of the EC-MAST II program.

As part of the joint operation between WOCE and JGOFS (Joint Global Ocean Flux Study), on the leg M39/3, the components of the CO₂-system, such as dissolved and particular carbon CO₂, were measured along the WHP-section A2 throughout the water column to describe the ocean's role as a buffer of atmospheric CO₂. Its input into these highly to moderately convective regions covered by section A2 is strongly variable and therefore calls for more frequent sampling than elsewhere in the ocean.

Several other groups not imbedded in the large projects summarized about participated in some of the cruise legs and their work is detailed under sections 3 and 5.

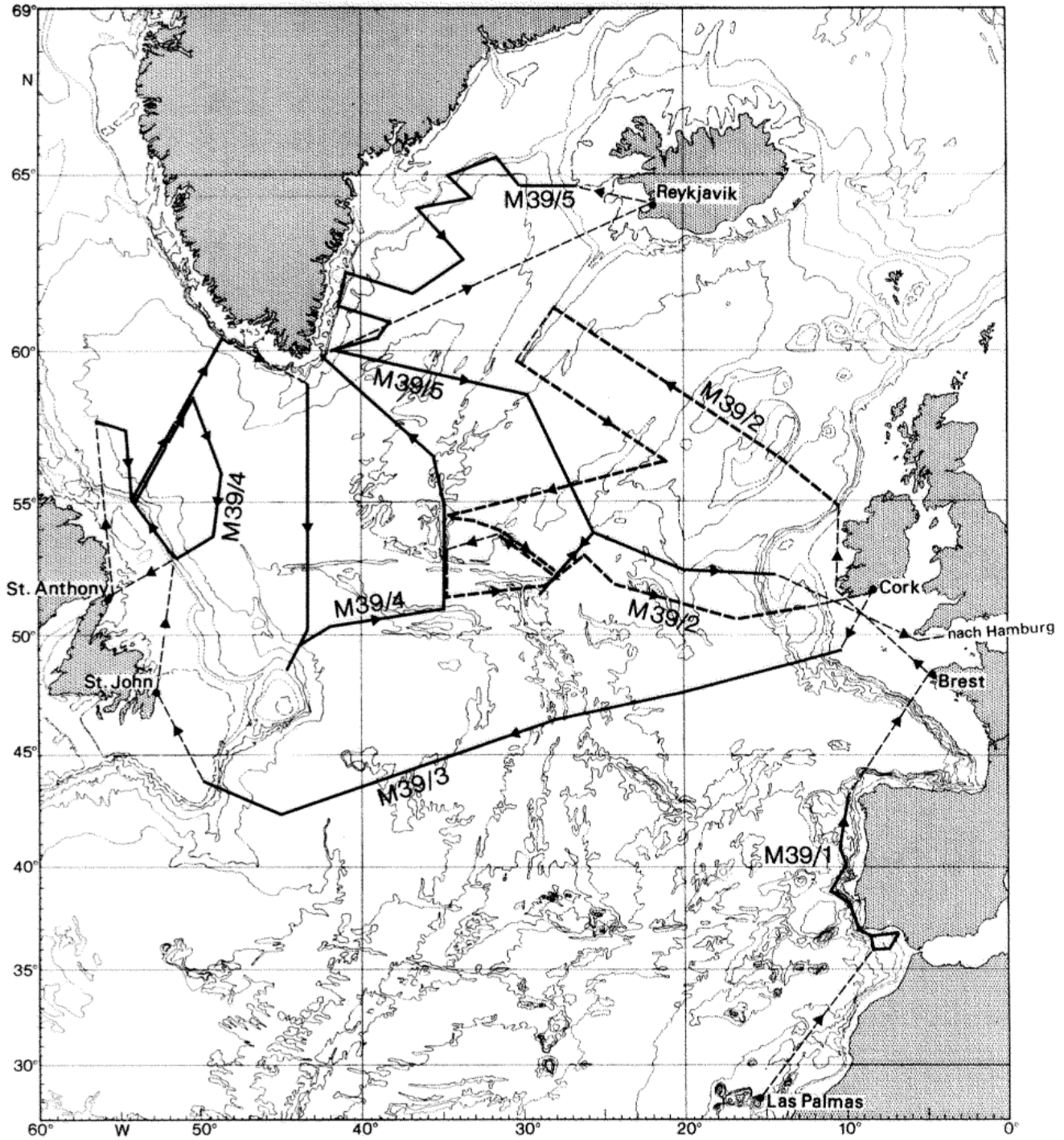


Fig. 1: Cruise track of the 5 legs of METEOR cruise no. 39. To separate the different cruise legs M39/2 is shown as dashed line. Transit sections are shown as thin dashed lines.

Tab.1: Legs and chief scientists of METEOR cruise No. 39

Leg	Chief scientist
M39/1	Dr. R. Zahn
18.04.-12.05.1997, Las Palmas, Canary Islands, Spain - Brest, France	
M39/2	Dr. W. Zenk
15.05.-08.06.1997, Brest, France - Cork, Ireland	
M39/3	Dr. K. P. Koltermann
11.06.-03.07.1997, Cork, Ireland - St. John's, Canada	
M39/4	Prof. Dr. F. Schott
06.07.-11.08.1997, St. John's, Canada - Reykjavik, Iceland	
M39/5	Dr. A. Sy
14.08.-14.09.1997, Reykjavik, Iceland - Hamburg, Germany	
Coordination:	Prof. Dr. F. Schott
Masters:	Captain D. Kalthoff
	Captain M. Kull

1.2 Projects

A large fraction of the work carried out on cruise M39 is imbedded in the international WOCE program and the SFB-460, which both are shortly introduced here:

The goal of the World Ocean Circulation Experiment (WOCE) is to develop models for improved descriptions of the ocean circulation and prediction of climate changes and to collect the appropriate data in the World Ocean. The North Atlantic Ocean is characterized through an intensive meridional circulation cell, carrying near surface waters of tropical and subtropical origin northwards and deep waters of arctic and subarctic origin southwards. The transformation and sinking of water masses at high latitudes are the important processes for the "overturning" of the ocean. The overturning rates and the intensity of the meridional transports of mass, heat, and salt are control parameters for the modeling of the ocean's role in climate.

The two legs M39/3 and M39/5 provided two complete full-depth transoceanic hydrographic sections in the North Atlantic as a prominent contribution to the WOCE Hydrographic Programme (WHP), completing the German WOCE field work that started with METEOR cruise M18 in 1991. Both legs: M39/3 and M39/5 were also part of the seven-year observational programme WOCE-NORD (World Ocean Circulation Experiment – North Atlantic Overturning Rate Determination), a German contribution to WOCE and funded by the Ministry of Education and Research. Using repeated hydrographic sections between the southern tip of Greenland and Ireland in combination with current measurements the overturning rates of the North Atlantic will be estimated. Quantifying both input and output in the meridional overturning cell (MOC) will help to improve modeling the role of the ocean in the climate system.

The Sonderforschungsbereich SFB 460 “Dynamics of Thermohaline Circulation Variability” began in 1996 at Kiel University. Main objective of the SFB 460 is to investigate the variability of the water mass formation and transport processes in the subpolar North Atlantic and to gain an understanding of its role in the dynamics of the thermohaline circulation and the ocean uptake of anthropogenic CO₂. The variability of circulation and water mass distribution appears to be related through the North Atlantic Oscillation (NAO) with climate changes in northern Europe. These connections shall be investigated.

Legs M39/2 and M39/4 were carried out within the context of the SFB 460 with a wide range of hydrographic, tracer and current measurement techniques to investigate the variability of the circulation in the North Atlantic. The cruises were part of the opening phase of the SFB although the leg to the Labrador Sea was already the second cruise to this area of annually planned cruises within the SFB. During these two legs the focus was on the pathways of the deep circulation and the associated signals in the water mass distributions. Besides the shipboard measurements, a large part of the work was mooring work and the deployment of floats.

2 Participants

Tab.2: Participants of METEOR cruise no. 39

Leg M39/1

Name	Specialty	Institute
Zahn, Rainer, Dr.	Chief Scientist	GEO
Bader, Beate	Sedimentology	GIK
Bassek, Dieter	Meteorol. radio operator	DWD
Bozzano, Graziella	Sedimentology	ICM
Didie, Claudia	Sedimentology	GEO
Flechtenhar, Kurt	Meteorologist	DWD
Harder, Angela	Inorganic chemistry	GEO
Heidemann, Kristina	Geophysics	GEO
Hollender, Franz-Josef	Geophysics	GEO
Hüls, Matthias	Paleocenaography	GEO
Jung, Simon	Paleocenaography	GEO
Karp, Tobias	Geophysics	GEO
Kohly, Alexander	Sedimentology	GIK
Lembke, Lester	Paleocenaography	GEO
Loncaric, Neven	Sedimentology IGM	
Müller, Anja	Sedimentology	GEO
Neufeld, Sergeij	Technician	GTG
Schäfer, Prisca, Prof. Dr.	Sedimentology, Paleontol.	GIK
Schönfeld, Joachim	Micropaleontology	GEO
Stüber, Arndt	Inorganic chemistry	GEO
Willamowski, Claudia	Inorganic chemistry	GEO

Leg M39/2

Name	Specialty	Institute
Zenk, Walter, Dr.	Chief scientist	IfMK
Amman, Lars	Marine Chemistry	IfMK
Bahrenfuß, Kristin	Tracer Oceanography	IfMK
Becker, Sylvia	Marine Physics	IfMK
Brandt, Benno	Meteorology	DWD
Carlsen, Dieter	Marine Physics	IfMK
Csernok, Tiberiu	Marine Physics	IfMK
Friedrich, Olaf	Marine Physics	IfMK
Johannsen, Hergen	Marine Chemistry	IfMK
Keir, Robin, Dr.	Geochemistry	GEO
Körtzinger, Arne, Dr.	Marine Chemistry	IfMK
Lenz, Bernd	Marine Physics	IfMK
Link, Rudolf	Marine Physics	IfMK
Meyer, Peter	Marine Physics	IfMK
Müller, Thomas J., Dr.	Marine Physics	IfMK
Nielsen, Martina	Marine Physics	IfMK
Heygen, Ronald	Logistic	RF
Ochsenhirt, Wolf-Thilo	Meteorology	DWD
Pinck, Andreas	Marine Physics	IfMK
Plähn, Olaf	Tracer Oceanography	IfMK
Rehder, Gregor, Dr.	Geochemistry	GEO
Schweinsberg, Susanne	Marine Chemistry	IfMK
Trieschmann, Babette	Tracer Oceanography	IfMK
Wehrend, Dirk	Marine Physics	IfMK

Leg M39/3

Name	Specialty	Institute
Koltermann, Klaus Peter, Dr.	Chief Scientist	BSH
Wöckel, Peter	CTD engineer	BSH
Stelter, Gerd	data scout and manager	BSH
Weichert, Hans-Jürgen	CTD data processing	BSH
Frohse, Alexander	Salinometer	BSH
Lohrbacher, Katja	Hydrowatch captain	BSH
Esselborn, Saskia	Hydrowatch	IfMH
Gouretski, Victor, Dr.	Hydrowatch captain	BSH/MPI
Stransky, Christoph	Hydrowatch captain, XBT	BSH
Morsdorf, Felix	Hydrowatch, L-ADCP	IfMK
Gottschalk, Ilse	Hydrowatch	BSH
Fick, Michael	Hydrowatch	IfMH
Giese, Holger	Moorings	BSH
Tacke, Helga	Nutrient Analyst	BSH
Gottschalk, Anke	Oxygen Analyst	BSH
Schmiel, Franziska	Oxygen Analyst	BSH
Kramer, Rita	Nutrient Analyst	BSH
Bulsiewicz, Klaus	Tracer/CFC	UB
Plep, Wilfried	Tracer/CFC	UB
Fleischmann, Ulrich	Tracer/CFC	UB
Sommer, Volker	Tracer/CFC	UB
Gleiss, Ralf	Tracer/CFC	UB
Neill, Craig	CO ₂ Analysis, DIC	BNL
Lewis, Ernie	CO ₂ Analysis, Alkalinity	BNL
Brandt, Benno	Meteorology	DWD
Ochsenhirt, Wolf-Thilo	Meteorology	DWD

Leg M39/4

a) 06.07. - 16.07.1997 St. John's, Canada - St. Anthony, Canada

b) 16.07. - 11.08.1997 St. Anthony, Canada - Reykjavik, Iceland

Name	Specialty	Institute
Schott, Friedrich, Prof., Dr.	Chief Scientist (a,b)	IFMK
Adam, Dorothee	Tracer (b)	IFMK
Arnold Matthias	Helium/Tritium (a)	IUP
Bahrenfuß, Kristin	Tracer (a, b)	IfMK
Begler, Christian	Oceanography (a, b)	IfMK
Dombrowsky, Uwe	Oceanography (a, b)	IfMK
Eisele, Alfred	Oceanography (a, b)	IfMK
Fischer, Jürgen, Dr.	Oceanography, (a, b)	IfMK
Friis, Karsten	CO ₂ (b)	IfMK
Fürhaupter, Karin	Foraminifera	GEO
Gäng, Holger, Dr.	Meteorology (a, b)	IfMK
Kahl, Gerhard	Meteorology, (a, b)	DWD
Karger, Uwe	Meteorology (a, b)	IfMK
Keir, Robin, Dr.	Methan (b)	GEO
Kindler, Detlef	Oceanography (a, b)	IfMK
König, Holger	Oceanography (a, b)	IfMK
Malien, Frank	Oxygen, Nutrients (a, b)	IfMK
Mauuary, Didier, Dr.	Tomography (a)	CEP
Meinke, Claus	Oceanography (a, b)	IfMK
Mertens, Christian	Oceanography (a, b)	IfMK
Mintrop, Ludger, Dr.	CO ₂ (a, b)	GeoB
Ochsenhirt, Wolf-Thilo	Meteorology (a, b)	DWD
Papenburg, Uwe	Oceanography (a, b)	IfMK
Plähn, Olaf	Tracer (a)	IfMK
Rehder, Gregor, Dr.	Methan (b)	GEO
Rhein, Monika, Dr.	Tracer (b)	IfMK
Schweinsberg, Susanne	CO ₂ (a, b)	IfMK
Send, Uwe, Dr.	Tomography (b)	IfMK
Stramma, Lothar, Dr.	Oceanography (a, b)	IfMK
Walter, Maren	Oceanography (a, b)	IfMK
Winckler, Gisela	Helium/Tritium (b)	IUP

Leg M39/5

Name	Specialty	Institute
Sy, Alexander, Dr.	Chief Scientist	BSH
Stolley, Martin	Hydro Watch, XBT	BSH
Mohn, Christian	Hydro Watch, VM-ADCP	IfMH
Berger, Ralf	Hydro Watch, CTD, L-ADCP	IfMK
Gottschalk, Ilse	Hydro Watch	BSH
Weigle, Rainer	Hydro Watch	IfMH
Struck, Petra	Hydro Watch	BSH
Verch, Norbert	Salinity	IfMH
Stelter, Gerd	Bottle Data management	BSH
Mauritz, Heiko	CTD DATA Processing	BSH
Schulze, Klaus	TSG, Ship's Data management	IfMH
Bakker, Karel	Nutrients	NIOZ
Kramer, Rita	Nutrients, Oxygen	BSH
Schmiel, Franziska	Oxygen	BSH
Machoczek, Detlev	Oxygen	BSH
Read, John	Moorings	CEFAS
Hargreaves, Geoff	IES, Moorings	POL
Ashley, John IES,	Moorings	POL
Hildebrandt, Hauke	Tritium/He, 0-18, SF-6	IUP
Rhein, Monika, Dr.	CFC, L-ADCP	IfMK
Elbrächter, Martina	CFC	IfMK
Czeschel, Lars	CFC	IfMK
Reich, Michael	CFC	IfMK
Thomas, Helmuth, Dr.	CO ₂	IOW
Trost, Erika	CO ₂	IOW
Gronau, Nicole	CO ₂	IOW
Kahl, Gerhard	Meteorology	DWD
Bassek, Dieter	Meteorology	DWD
Henning, Arndt	Film Team	AmPuls
Schäfer, Werner	Film Team	AmPuls

Tab.3: Participating Institutions

AmPuls	AmPuls Film Film und TV Produktion Curschmannstr. 13 20251 Hamburg – Germany
BNL	Oceanographic and Atmospheric Sciences Division Department of Applied Sciences Brookhaven National Laboratory Upton, NY 11973 – USA
BSH	Bundesamt für Seeschifffahrt und Hydrographie Bernhard-Nocht-Str. 78 20597 Hamburg – Germany
CEFAS	Centre for Environment Fisheries & Aquaculture Science Lowestoft Laboratory Lowestoft, Suffolk NR33 0HT – England
CEP	Centre d'Etude des Phénomènes Aléatoires et Géophysiques EINSIEG-CAMPUS Universitaire BP 46, 38402 Saint Martin d'hères Cedex-France
DWD	Deutscher Wetterdienst Geschäftsfeld Seeschifffahrt Bernhard-Nocht-Str. 76 20359 Hamburg – Germany
GEO	Geomar Forschungszentrum für Marine Geowissenschaften Universität Kiel Wischhofstr. 1-3 24148 Kiel – Germany
GeoB	Universität Bremen Fachbereich 5, Geowissenschaften Klagenfurter Str. 28359 Bremen – Germany
GIK	Geologisch-Paläontologisches Institut Universität Kiel Olshausenstr. 40 24118 Kiel – Germany
GTG	Geomar Technologie GmbH Wischhofstr. 1-3 24148 Kiel – Germany
ICM	Institut de Ciencies del Mar Consejo Superior de Investigaciones Científicas Passeig Joan de Borbó, s/n 08039 Barcelona-Spain

IfMH	Institut für Meereskunde der Universität Hamburg Tropowitzstr. 7 22529 Hamburg – Germany
IfMK	Institut für Meereskunde an der Universität Kiel Düsternbrooker Weg 20 24105 Kiel – Germany
IGM	Instituto Geológico e Mineiro Rua Academia das Ciências, 19-2° 1200 Lisboa-Portugal
IOW	Institut für Ostseeforschung Warnemünde Seestraße 15 18119 Rostock-Warnemünde – Germany
IUP	Institut für Umweltphysik der Universität Heidelberg Im Neuenheimer Feld 366 69120 Heidelberg – Germany
MPI	Max-Planck-Institut für Meteorologie Bundesstr. 55 20146 Hamburg – Germany
NIOZ	Nederlands Instituut voor Onderzoek der Zee Postbus 59 1790 AB Den Burg, Texel –Netherlands
POL	Proudman Oceanographic Laboratory Bidston Observatory Birkenhead, Merseyside L43 7RA – England
RF	R/F Reedereigemeinschaft Forschungsschiffahrt GmbH Haferwende 3 28357 Bremen – Germany
UB	Universität Bremen Institut für Umweltphysik, Abt. Tracer-Oceanographie Bibliotheksstraße 28359 Bremen – Germany

3 Research Programs

3.1 WOCE program

Two hydrographic sections were carried out within the WOCE program. The northern section from Greenland to Ireland (WHP A1-East) cuts across the convective regime of the Subpolar Gyre, whereas the southern of the two sections, running from the English Channel to the Grand Banks off Newfoundland (WHP A2), spans the non or weakly-convective regime of the transition zone between the subpolar and subtropical gyres. The data are used to estimate the transports of heat and matter of the meridional circulation and contribute towards estimating the so-called “overturning” of the oceanic meridional circulation regarded as the main driving mechanism for the global thermohaline circulation and its temporal changes. Special emphasis is put on the intensive propagation of newly formed Labrador Sea Water (LSW) into the North Atlantic, first seen in the 1993 coverage of A2. These coverages of sections A1 and A2 repeat

some earlier measurements that have shown a high temporal and spatial variability of both the water mass characteristics and the meridional transports of heat, salt and freshwater.

3.1.1 Physical Oceanography during WOCE cruises

3.1.1.1 Hydrographic measurements at 48°N in the North Atlantic along the WHP section A2

The meridional transports of heat, freshwater and salt in the Atlantic Ocean and their seasonal and inter-annual changes have been determined for the 90s across the latitude of the global maximum freshwater transport at ca. 50°N in the Atlantic Ocean. Results are compared with previous measurements in the 50s and 80s. They show surprisingly variable transports, suggesting time scales of 10 years for changes originating in the subpolar and some 30 years for those originating in the subtropical gyre.

Working the section A2/AR19 at about 48°N in the summer of 1993 with FS Gauss (G226) has shown the Labrador Sea Water temperatures some 0.4°C below its historical characteristic temperature, and deeper in the water column by some 700 m. This fits with the observations for the early 90s along 60°N and 24°30'N and indicates a rapid reaction of the intermediate circulation of the northern North Atlantic to changes in the buoyancy forcing in the Labrador Sea. This situation seems to have ended in 1995/96 when the NAO-Index, characterizing the prevailing atmospheric forcing over the region, changed from an all-time high to moderate values. First reactions of the ocean to these changes can be seen in the coverage of the sections A2 with FS Gauss (G276/1) and A1 with FS Meteor in the fall of 1994. The cruise M39/3 served also to document this tendency.

Following the WOCE Hydrographic Programme requirements, the section WHP-A2 along nominally 48°N was worked again as under "One - Time Survey" conditions. In addition to the classical hydrographic parameters, nutrients and small volume tracer concentrations were determined. Continuous ADCP (Acoustic Doppler Current Profiler) data provided the absolute vertical current shear of the top 500 m to calculate, from geostrophic transports, the absolute transport through this section. Additionally, velocity profiles have been acquired using a LADCP to support calculations of the absolute velocities. With a horizontal station spacing between 5 and 35 nm, a 24x10 l - rosette system was deployed to collect at up to 36 discrete depth levels water samples together with the quasi-continuous profiles of T, P, S and O₂ with a CTDO₂ -probe. The track and station spacing essentially follows the Gauss section from 1993, covering 66 stations with 86 casts. Some additional casts for performance tests of the CTD/rosette system, calibrations and for the instruments for the chemical analyses have been worked.

Since the summer 1996 a mooring array again covers over the full water depth the deep eastern boundary current on the west side of the Mid-Atlantic Ridge on A2. The velocity, temperature and salinity data will describe the long-term changes of this current system that seems to play an important role in the exchange of newly formed water masses such as the LSW within the ocean basin or across the ridge. The moorings were turned around for another

deployment of one year to be recovered in the summer of 1998. There were no problems in locating, retrieving or setting the moorings.

3.1.1.2 WOCE-NORD

The second part of leg M39/5 was part of the WOCE-NORD project funded by BMBF and was the sixth repeat of the WHP section A1E/AR7E. Meridional transports of heat and matter in the North Atlantic will be quantified through a section connecting Ireland and South Greenland. This section runs south of the region where the atmospheric forcing transforms the water advected to high latitudes such that it will sink to greater depths and spreads further south, forming the source water masses of the North Atlantic Deep Water. For several years we have been observing a cooling trend in the LSW caused by the spreading of newly formed LSW in the Labrador Sea. Estimates of circulation times derived by linking single LSW vintages, using hydrographic and tracer data independently, lead to trans-Atlantic propagation times of 4 to 5.5 years from the source region to the West European Basin. During the second part of leg M39/5 the A1E/AR7E section was sampled successfully.

3.1.2 Nutrients and tracer measurements during WOCE cruises

a) Nutrients along the WHP section A2

Along the WHP section A2 the nutrients PO_4 , NO_3 , NO_2 , NH_4 , $\text{Si}(\text{OH})_4$ and the content of dissolved oxygen O_2 from all water samples were determined to differentiate water masses and their origin.

From 1591 water samples nutrients and dissolved oxygen were determined on board according to the WHP Standards. For quality assurance purposes additional samples were taken as duplicates or replicates. All data will be processed on board, subjected to detailed consistency and quality checks and compared to existing data sets from this region. An annotated data file was produced at the end of the cruise, containing all relevant information and documentation on methodology and the quality of the data.

b) CFCs and helium/tritium on WHP section A2 and A1E

In addition to the classical hydrographic data the measurements of anthropogenic tracers provide additional parameters for water mass analysis. They are particularly important for the determination of water mass transports and mixing processes making use of their well-known time-dependent input history at the ocean surface.

As on the A2-survey in 1994 (M30/2) measurements were carried out for the determination of the CFCs F-11, F-12, F-113, and CCl_4 and samples for the laboratory measurements of helium isotopes and tritium have been taken.

Since most of these tracers provide transient signals, the main objective will be to measure their time dependence. The hydrographic parameters for the mainly stationary flowing water masses like NADW or the deep waters of the eastern basin will not show much changes. But

the tracer concentrations (except possibly for tritium) of these waters are expected to increase. The differences in tracer concentrations from these two cruises and the knowledge of the different input histories will allow us to determine the age structure of these water masses. The age structure is caused by mixing of waters of different age within a water mass, a process hardly detectable by hydrographic parameters. The “width” of the age structure gives an indication of the turbulent exchange coefficient, a parameter of general interest.

We expect further information on the intrusion of younger water from the north close to the bottom in the eastern basin which has been seen on the previous cruises M30/2 and further north during M18. This water is in contrast to older waters coming from the south as an eastern boundary current.

The highest tracer concentrations for NADW are expected in the western boundary current. The extension in zonal direction to and across the Mid Atlantic Ridge (recirculation) is easily detectable by the tracers. The LSW has changed its characteristic properties during the last years. To determine the development of these changes will be an objective of the cruise. The tracer concentrations will help to identify and to date the changes in the LSW.

The CFCs on section A2 were measured on the majority of the water samples. Helium and tritium sampling was restricted to about every second station, but with a high vertical resolution. The CFC data were available in preliminary form within about 24 h after sampling, so that they served to assist selecting sampling depths further on.

The CFC distributions in 1991 and 1994 along WHP section A1 led to estimates of the spreading times of LSW into the Irminger Sea and into the Northeast Atlantic, which were significantly shorter than previously thought. They correspond, however, with estimates derived independently from the cooling signal of LSW.

The CFC analysis at M39/5 did continue the CFC time series of the deep water masses. In combination with the analysis at M39/2 and M39/4 the spreading and mixing of the deep water masses in the subpolar North Atlantic will be studied.

c) TCO₂ and total alkalinity measurements on WHP section A2

Measurements were made of total dissolved inorganic carbon (TCO₂) and total alkalinity from full water column profiles collected along 48°N. At least one full profile (36 samples) was analyzed each day. TCO₂ was analyzed using a SOMMA-coulometer system that belongs to IfM Kiel; total alkalinity was measured by potentiometric titration (open cell titration) again using equipment which belongs to IfM Kiel. Certified Reference Materials for these parameters was analyzed daily.

With accurate preliminary hydrographic data provided to the analysts at the completion of the cruise, a final TCO₂ and alkalinity data set was made available for incorporation into the cruise data file.

The CO₂ measurements will be used for the following purposes:

- (1) The zonal section of TCO₂ measurements will be combined with estimates of baroclinic, barotropic and Ekman water transport across the section to estimate the meridional transport of inorganic carbon at this latitude. These estimates should assist with the delineation of large scale patterns of divergence or convergence of the inorganic carbon transport in the North Atlantic ocean. These patterns in turn can be used as important constraints for large scale ocean carbon cycle models. Previous work during METEOR cruise M30/2 in 1994 has shown strong contrasts between waters from the source regions further to the North and particularly the deep Eastern Basin which was CO₂ free. We expect, because of the observed large changes in the intermediate waters in the 1990s, considerable changes of the CO₂ budget during this 1997 cruise.
- (2) The observed TCO₂ can be separated into anthropogenic and preindustrial components. Such a separation has been attempted for an earlier CO₂ data set collected along this section and showed a large anthropogenic component penetrating to the ocean floor in the western basin and to approx. 4000 m in the eastern basin. However the influence of upper ocean seasonal changes can potentially obscure this anthropogenic signal: comparison of anthropogenic CO₂ components estimated from data collected during November 1994 and summer, 1997 should allow the magnitude of this possible seasonal contamination of the anthropogenic CO₂ signal to be addressed.
- (3) TCO₂ is remineralized at depth in the ocean together with nutrients and in association with the removal of dissolved oxygen: as a result there are very robust inter-relationships between dissolved oxygen, TCO₂ and dissolved nutrient concentrations in the deep ocean. Whereas

Certified Reference Materials are available for quality control of measurements of the TCO₂ content of seawater, there are unfortunately no such standards for nutrients or oxygen. The observed empirical relationships between TCO₂ and the other parameters should, however, remain constant in the deep ocean for periods of at least several years to decades. Hence comparison of the quality controlled TCO₂ data with measured nutrients and oxygen concentrations provides one means by which the internal consistency of nutrient and oxygen measurements made on different cruises can be assessed. Simply put, any inaccuracies in the measurement of nutrients (for example) would show up as offsets or slope changes in the TCO₂ -nutrient plots derived from various cruises. Hence measurement of TCO₂, because it is a parameter that can be traced to a Certified Standard, provides a means by which the quality of other closely related chemical parameter measurements can be assessed.

3.2 Sonderforschungsbereich (SFB) 460

The research program of the SFB is based on a combination of physical-oceanographic, marine chemistry and meteorological observation programs, which are carried out in close interaction with a series of numerical models with moderate (50 km), high (15 km) and very high resolution (5 km), which will allow a simulation of current structures and variability over a wide range of space and time scales. The main interests during the first SFB phase are, first of

all, the water mass formation processes and the circulation of deep waters in the subpolar North Atlantic, their interaction and integral effects, especially with regard to the uptake of anthropogenic CO₂. Second, the variability of the ocean - atmosphere interaction is investigated, and modeling investigations of large-scale aspects and causes of this variability are supplemented by the analysis of fluxes from different meteorological standard models in comparison with observations, with emphasis on the fresh water exchange.

3.2.1 Physical Oceanography during SFB cruises

The western subpolar North Atlantic is a critical region for the climate of the North Atlantic region. Here, strong water mass transformations take place, with far-reaching consequences. This region is formation as well as transformation region of cold water masses, which are exported and as a consequence require northward compensating flow of warm water masses. The deep western boundary current, fed by the Denmark-Strait-Overflow at the lowest level and by the Deep Water from the Gibbs-Fracture-Zone above, flows along the topography in the Labrador Sea and continues past the Grand Banks. Indications exist for a deep cyclonic recirculation cell located between the Grand Banks and the Mid-Atlantic Ridge, its physical explanation is still unclear.

The work on leg M39/2 was related to subproject A3 of the SFB 460. The project focus deals with the variability of water masses of the subpolar gyre during their passage through the Iceland Basin. Some critical data gaps in observations east of the Reykjanes Ridge and at the depth level of the eastward spreading Labrador Sea Water could be closed. Data collection was concentrated on seven hydrographic sections cutting through the Iceland Basin and the western European Basin. With one exception all were oriented near-zonally between 60° and 52°N, i.e. between WOCE sections A1 and A2. The latter was occupied again during legs 3 and 5 of METEOR cruise 39. Detailed CTD surveys and the deployment of current meters and RAFOS floats were conducted for long-term observations of Overflow and Labrador Sea Water. The distribution of temperature, salinity, nutrients and CFC tracers were mapped by four sections across the subpolar gyre in the central eastern basin. Properties of Labrador Sea Deep and Overflow Water from the Iceland Faroer Ridge were of importance for the survey. In addition to the section work, two low-energy signal generators and the first RAFOS floats were deployed.

Further work was concentrated at the Middle Atlantic Ridge, where detailed investigation of the spreading paths and transports of overflow water approaching the Gibbs Fracture Zone was conducted. In addition to a number of short hydrographic sections, a group of three current meter moorings, which also include a third signal generator, were deployed. Traditional RAFOS floats and, for the first time, a float park was deployed. The latter array contains a number of independent floats temporarily moored at the sea floor. They will leave their fixed position in a delayed mode after the METEOR has left the site. After release from their moorings these floats ascend to their mission level (appr. 1500 m) of the Labrador Sea Water. The purpose of the float park is to provide a Lagrangian time series of the inflow of Labrador Sea Water into the Iceland Basin. Float missions amount between one and two years.

The SFB program in the northwestern Atlantic began with a “Valdivia”-cruise in summer 1996 and was continued with cruise M39/4. A main water mass of the investigation during M39/4 was the Labrador Sea Water. After its formation in late winter in the central Labrador Sea it seems to circulate along complicated paths in the western basin and crosses the Mid-Atlantic Ridge far into the eastern basin. Only much later the LSW export to the south within the deep western boundary current takes place. The LSW seems to participate also in the recirculation east of the Grand Banks.

Large differences might exist between different years. Further, the flow paths of the LSW are not continuous, but its spreading paths are actually made up by a complicated interaction of eddy transport and mean advection. Until recently it was believed that the exchange of LSW with the water masses of the Irminger Sea takes place on time scales of several years, but recent measurements within WOCE indicated that the LSW can progress within less than a year far into the Irminger Sea.

Recent investigations indicate that convection takes place not only in the central Labrador Sea, but also at its southern margin. The water mass formed there seems to make up the upper part of the deep water export south of New Foundland, and as tracer data show, it moves there faster and more directly than the LSW. In addition, the possibility of convection in the Irminger Sea cannot be excluded. In late winter surface-mixed layers of more than 600 m appear regularly in the Irminger Sea, which forms the Subpolar Mode Water of the North Atlantic. So far, deep convection in this region could not be proved.

The main objective of leg M39/4 was the investigation of the different paths of the deep water circulation in the western subpolar basin of the North Atlantic and its water mass distribution.

Especially the focus was on the outflow of Labrador Sea Water into the western basin and its recirculation. To investigate the water mass transports, profiling current measurements from the ship by the ADCP lowered with the CTD (LADCP) were made. To characterize the water masses, CTD-hydrography and tracer measurements (Freon) and tritium/helium and ^{18}O as well as nutrients and CO_2 measurements were carried out.

To investigate small scale convection processes (“plumes”), ADCP moorings were deployed in the convection regions of the central and southern Labrador Sea. To measure the integral effects of convection, acoustic tomography was used.

The deployment of the Deep Labrador Current (DLC) array was one of the major objectives of project A4 of the SFB 460. The array is designed to determine the transports of the DLC south of Hamilton Bank. The array is oriented perpendicular to the continental slope near $52^{\circ}51'\text{N}$, $51^{\circ}36'\text{W}$ and then northeastward. There the topography is very steep and the measurements from summer 1996 (Valdivia 161) showed a well defined DLC. In addition to the current meters and ADCPs the array also contains several conductivity/temperature probes (SEACATs) to monitor the water mass characteristics in key layers.

3.2.2 Air-sea fluxes

The meteorological aim in the SFB 460 is the investigation of air-sea interaction parameters in the Labrador Sea. Especially the focus is on the variability of surface fluxes and their feedback with ocean deep convection events in this region. The comparison of model results, field experiments and satellite remote sensing data should lead to a better understanding of variability of air-sea fluxes on different time scales.

The METEOR cruise M39/4 was the second field experiment in the context of the SFB 460 in the Labrador Sea region. Data under meteorological winter conditions were sampled on a cruise on the RV Knorr during February and March 1997. The meteorological program on cruise M39 was divided up in two parts. The first part was the collection of data for the eddy correlation calculation of air-sea fluxes. For this purpose high resolution time series of three dimensional wind components, air temperature and humidity are necessary. The second part of the program was to get atmospheric data for the improvement and development of air-sea flux algorithms for satellite remote sensing applications.

3.2.3 Carbon dioxide system, oxygen, nutrients during SFB-cruises

The determination of the carbon dioxide system parameters total dissolved inorganic carbon and alkalinity and their depth distribution is a prerequisite to understand the carbon cycle. While the nutrient concentrations determined in parallel are mainly used as indicators for water mass properties, the carbon parameters and dissolved oxygen values allow also for the calculation of uptake of anthropogenic carbon into the water column. A significant anthropogenic signal even at greater depth is expected for the study area where the transport of anthropogenic carbon into the Deep Water is achieved mainly through the thermohaline circulation. Another aspect of air-sea carbon exchange is the CO₂ partial pressure difference between surface seawater and the atmosphere. This difference indicates the degree of saturation of the surface waters and allows for the calculation of momentary air-sea exchange fluxes.

On the second and fourth leg of the METEOR cruise 39, the depth distribution of the parameters total dissolved inorganic carbon, alkalinity, nutrient- and dissolved oxygen concentrations were measured at the hydrocast locations. One aspect also was the determination of a baseline to detect variations in later studies within the SFB. In parallel, an automated system to measure CO₂ partial pressure in atmosphere and surface seawater was run during the whole length of both legs.

3.3 Other programs

3.3.1 VEINS programs

VEINS (Variability of Exchanges in the Northern Seas) is an EU-MAST III programme to measure and model the variability of fluxes of water, heat and dissolved matters between the Arctic Ocean and the North Atlantic over a period of three years. It is aimed at developing an efficient observation design to measure time series resolving up to decadal time scales which are considered crucial for advancing our predictive capabilities for shorter term climate

changes. For this purpose VEINS covers four key regions with recording current meters and repeat hydrography. One of these regions is the Denmark Strait (including the Greenland continental slope to the southwest) which was the working area for cruise METEOR 39/5. Here Atlantic input (Irminger Current) and output of polar surface waters (East-Greenland Current) as well as Arctic deep water (overflow) are the components of the exchange between the North Atlantic and the Seas of high latitudes. The measurements east of Greenland during the first part of leg M39/5 were carried out in the context of VEINS. Forty-three hydrographic stations were taken, six current meter moorings and two Inverted Echo Sounders (IES) were deployed and four moorings and one IES were recovered.

3.3.2 Tracer sampling

- a) Helium/Tritium An extended sample set for on-shore analysis of helium isotopes, tritium concentrations and oxygen isotopes was collected along the cruise tracks of M39/4 and M39/5. In addition to the classical hydrographic parameters these tracer data will provide additional information for water mass analysis: making use of their well known time-dependent input history at the ocean surface the helium/tritium distribution will be used to estimate apparent $^3\text{H}/^3\text{He}$ ages of the prominent water masses and to determine spreading times and mixing rates. In particular, the interpretation of different tracer distributions characterized by different input histories (such as $^3\text{H}/^3\text{He}$ and CFCs) allows to describe mixing processes and to determine the age structure of the water masses. Interpretation of the tritium/helium data obtained will be done in context to the tracer information accomplished during former occupations of the area and will especially refer to the investigations performed during the WOCE cruises M18 (1991) and M30/3 (1994).

Use of $^{18}\text{O}/^{16}\text{O}$ ratios as oceanographic tracer is based on the fact that isotopic fractionation processes during evaporation and condensation lead to a typical $\delta^{18}\text{O}$ signature of different oceanic reservoirs. The $\delta^{18}\text{O}$ analysis allows to separate fresh water components e.g. arctic run-off transported by polar water or contributions of melted ice derived from the Greenland ice-shield. A total of 400 samples for helium isotope and tritium analyses was taken along the cruise track M39/4. The vertical and horizontal resolution of the sampling grid was determined by the topography and the dynamic structures of the water column. Special focus was on the distribution of the Labrador Sea Water as well as on the deep boundary currents resulting in a dense station coverage at the shelf sections of the track (off Labrador, off SW Greenland, off Cape Farewell and off Flemish Cap). Another focus was on the Gibbs Fracture Zone outflow. The helium isotope and tritium analyses will be performed using a sectorfield mass spectrometer at the IUP in Heidelberg. In addition, a total of 145 samples for $^{18}\text{O}/^{16}\text{O}$ analyses was collected along the cruise track of M39/4. Samples were taken in the upper 600 m of the water column focusing on sections marked by surface boundary currents. The analytical work will be done on shore at the IUP (Heidelberg) after the cruise.

b) *delta* ^{18}O As supplement to the tritium, helium and $^{18}\text{O}/^{16}\text{O}$ samples taken by the Institut für Umweltphysik Heidelberg oxygen-18 (^{18}O) samples were taken during leg M39/4 for two other groups. ^{18}O samples were taken for Robert Houghton at the Lamont Earth Observatory U.S.A. at the legs M39/4 and also M39/5 and for Tim Winters at the University of East Anglia, U.K. during M39/ 4. ^{18}O samples for Robert Houghton were taken during M39/4 at 6 short near coastal stations of the upper 200 m at the Labrador and Greenland coasts and of the Flemish Cap. In collaboration with Rick Fairbanks, Houghton studies the freshwater balance along the northeast continental margin from Labrador to Georges Bank using oxygen isotope analysis to trace freshwater sources. In the Labrador Sea they are attempting to resolve conflicting estimates of the relative importance of freshwater input via the Baffin Basin and the West Greenland Current.

The ^{18}O samples for Tim Winters were taken at the AR7 section from Labrador to West Greenland and for a short section at the southeastern shelf of Greenland over the full depth range. The samples are for measuring the ^{18}O content of the water in the Labrador Sea. Winters will use an unmixing model to quantify the amounts of the various components of NADW as it flows south in the Deep Western Boundary Current through 50°N . It is intended to utilize ^{18}O content of the water as an extra conservative parameter to identify the relative amounts of source waters in the NADW.

3.3.3 Methane

The overall goal of the methane program is to understand the nature of various processes that influence the distribution of this dissolved gas in the ocean. Methane appears to be slowly consumed in deep waters by oxidation and its concentration in old deep waters is very low. Sources include exchange with the atmosphere, production in the upper few hundred meters of the ocean by a biological process that is not fully understood, and bottom sources where hydrothermal and cold vents occur. In connection with the first of these, the concentration of methane in the atmosphere has varied over time. Proxy measurements made in ice cores indicate that over the last 200 years, the atmospheric methane has risen from about 700 to 1800 ppb volume, and, on a percentage basis, the rise has accelerated during the last decades at a rate faster than the rise of atmospheric CO_2 . As has already been observed in other transient tracers such as tritium and chlorofluorocarbons, the changing atmospheric concentration should result in a time dependent net input of methane to the ocean, the signature of which should be observable in recently formed deep waters.

Since the majority of the ocean's deep water is produced in the northern Atlantic, it is an area where the changing atmospheric exchange should influence the distribution of methane most strongly. Research objectives include determination of the concentrations of the dissolved CH_4 in the various water masses of the northwestern Atlantic, particularly in the various sources of North Atlantic Deep Water, and determination of the $^{13}\text{C}/^{12}\text{C}$ isotope ratio of the dissolved methane. The isotope measurements should provide an indication of the extent of the methane decrease in the water column that is due to oxidation, because this process consumes the lighter isotope preferentially. In contrast, the carbon isotope ratio of methane in the atmosphere has remained nearly constant over time, and changes in the distribution due to varying atmospheric concentration should not strongly affect the isotope ratio in the ocean.

Discrete CH₄ Measurements

Measurements of the dissolved methane concentration in the water column were made from the hydrocast collections during M39/2 and M39/4. In order to conduct these measurements, a new procedure for separating the gas phase from the water was employed. Water from the Niskin bottles is drawn into a 200 ml glass syringe without contact to the air. The syringe is then connected to an evacuated 500 ml bottle. As the water is drawn into this bottle from the syringe, most of the dissolved gas separates from the liquid phase. Altogether, 400 ml of water from 2 syringes is added to each bottle. The gas is now led into an evacuated burette by injecting a degassed brine into the bottom of the sample through a sidearm at atmospheric pressure. At this point, 1 ml of gas is extracted and injected into a gas chromatograph equipped with a flame ionization detector.

The gas remaining in the burette is collected in an evacuated vial for carbon isotopic analysis by mass spectrometry ashore. In addition to the gas samples, on a few stations separate water samples were collected in air free bottles, and these will be returned to the shore-based laboratory for carbon isotope analysis. The dissolved gas in these samples will be stripped using helium, and the trapped methane injected directly into the mass spectrometer. These isotope measurements will be compared to those on the already separated gas samples.

Surface Water pCH₄

Since deep waters are formed from surface waters, one needs to observe whether the atmosphere does indeed tightly control the methane concentration in the open ocean where this formation occurs. The partial pressure of methane in the surface layer of the ocean as well as in the atmosphere was surveyed continuously underway with a gas equilibrator connected to a pump 5 meters below the water line. A sample of the air recirculated in the equilibrator is periodically shunted into a gas chromatograph equipped with a flame-ionization detector. Both the methane and the CO₂ partial pressure were measured, the latter by catalytic conversion to methane. These measurements were also carried out continuously on air pumped from overtop the bridge into the wet lab. The apparatus provides a semi-continuous measurement of the partial pressures in the water every twenty minutes and atmospheric measurements every 40 minutes.

3.3.4 Foraminifera ($\delta^{13}\text{C}$ and $\delta^{18}\text{O}$ data in foraminifera)

The isotopic signal of carbonate shells of planktonic foraminifera is used to deduce water mass temperatures or climatic changes in the past. However, without knowledge of the influence of biological factors on the isotopic composition of these shells, there is considerable latitude for false interpretation of the data.

Therefore plankton samples at different sites of leg M39/4 should give more information about horizontal and vertical distribution patterns, calcification depth and population dynamics of the foraminifera, *Neogloboquadrina pachyderma* (sin.) (Ehrenberg), an important species in palaeo-oceanography. The values of $\delta^{13}\text{C}$ and $\delta^{18}\text{O}$ of the foraminifera shells can then be compared with values of the water.

Some specimens of *N. pachyderma* (*sin.*) will be used for culture experiments under controlled temperature and food conditions in order to gain a paleo-temperature-equation for low temperature ranges.

On 18 different stations in polar and subpolar water masses plankton samples were taken with a multinet at specific depth intervals (500-300 m, 300-200 m, 200-100 m, 100-50 m, 50-0m). These samples were preserved in ethanol for later inspection.

4 samples were taken for culture experiments. The foraminifera of the species *N. pachyderma* (*sin.*) were sorted out and held in cell wells containing filtered sea water at a temperature of 4°C (similar to natural environment) Culture medium was changed every week and food (fresh algae cells about 20-64 µm in diameter) was added once a week. The culture experiments themselves will start immediately following this expedition.

3.4 Paleooceanography

The scientific program of R/V METEOR cruise M39/1 concentrated on the history of the North Atlantic's thermohaline circulation during the last glacial period. A primary cruise objective was to monitor the evolution of Mediterranean Outflow Water that today constitutes an important hydrographic component for North Atlantic mid-depth waters. Of special interest were short-term climatic anomalies that occurred sporadically during the last ice age and their effects on the regional circulation. Temperatures in the North Atlantic region rose between 2° and 7°C during these abrupt climatic shifts, and remained high for several 100 to 1000 years. Then they dropped back abruptly - within few 10-100 years - to 'normal' ice age values. These anomalies caused distinctive changes in the North Atlantic's thermohaline circulation: melt water surges flooded the North Atlantic and resulted in an almost complete shut-down of surface water convection and deep water formation. The oceanographic signals that were caused by these anomalies reached the Portuguese margin. Further interest concentrated on benthic growth habitats and carbonate production at the Iberian shelf and Gulf of Cadiz which may serve as an example of extra-tropical carbonate production.

R/V METEOR cruise M39/1 consisted of acoustic surveys of sediment drifts in the Gulf of Cadiz, and a sampling program including sediment sampling along depth transects immediately west of the Gibraltar Strait and at the western Iberian margin as well as plankton hauls and hydrocasts. Shorebased sedimentological and geochemical analyses that will be carried out post-cruise will provide data that are needed to decipher the history of climate change and ocean variability in the northeastern Atlantic in association with changes of climate and ocean circulation in the northern North Atlantic and the Mediterranean Sea.

The intended paleoceanographic and paleoclimatic research depends critically on the quality of the sediment samples. Acoustic surveys that map the sea floor topography and the internal structure of the upper sediment layers are essential to locate coring positions that are suitable for this research and provide continuous and undisturbed sediment records. The combination of R/V METEOR's Hydrosweep and Parasound systems allows integrative mapping of topography and sediment structure which is an important prerequisite to reconstruct current-induced sediment redeposition and erosion, and to detect current patterns - e.g., of

Mediterranean Outflow Water in the Gulf of Cadiz. Paleoceanographic proxy-records to be established by using M39/1 sediment samples will include a wide range of biological-micropaleontological and organic and inorganic geochemical parameters. The most viable paleoceanographic proxies are benthic and planktonic foraminiferal community structures, stable oxygen and carbon isotope composition of benthic and planktonic foraminiferal shells and foraminiferal trace element composition that all trace various physical and chemical oceanographic parameters.

Interpretation of paleo-oceanographic time series requires knowledge about how tightly individual proxies are linked to environmental parameters such as water temperature and salinity, and nutrient concentration. To gain better control on the sediment data, continuous water column temperature and salinity profiles as well as profiles of trace element and nutrient concentration provide ground-truth data bases that are essential for calibrating the paleoceanographic proxy- records. Hydrographic surveys using CTD-probes in conjunction with water sampling bottles²⁵ and separate sets of clean GoFlo bottles for trace-metal water sampling were thus a central research program of R/V METEOR cruise M39/1.

3.4.1 Water Column Profiling: Ground-Truth Data Base for Calibration of Paleoceanographic Proxies

The hydrography of deeper water masses at the Portuguese margin is defined by the advection of North Atlantic Central Water (NACW), Mediterranean Outflow Water (MOW), upper and lower North Atlantic Deep Water (NADW), and Antarctic Bottom Water (AABW) (HARVEY and THEODOROU, 1986; McCARTNEY, 1992; SCHMITZ and McCARTNEY, 1993). MOW is the most outstanding hydrographic component in that it comprises a prominent salinity maximum. MOW today enters the North Atlantic with temperature-salinity (T-S) values of 13°C/38.4 (HOWE, 1982; 1975; AMBAR et al., 1976). Potential density of this water is around 37.4 (σ_t = density on 2000 dbar surface), i.e. considerably higher than that of 36.7 for North Atlantic Deep Water (NADW). Rapid mixing with less saline North Atlantic Central Water (T-S=13°/35.6; ZENK (1975)) and Labrador Sea Water (LSW, a component of upper NADW; T-S=3°/34.85; TALLEY and McCARTNEY (1982)) that both flow at the depth level of MOW reduces the density of MOW so that it flows northward along the upper Portuguese Margin in an upper (750 m) and lower (1250 m) core layer (ZENK and ARMI, 1990). Immediately west of the Gulf of Cadiz, T-S values for upper and lower MOW are around 12.5°/36.2 and 11.5°/36.4, respectively; northward advection (compared to the 2000 dbar surface) in the upper layer is highest, around 2.73 Sv (1 Sverdrup = $10^6 \text{ m}^3 \text{ s}^{-1}$), compared to 1.24 Sv in the lower layer (ZENK and ARMI, 1990).

The paleoceanographic evolution of deeper water masses in the Northeast Atlantic has been reconstructed by mapping benthic foraminiferal stable carbon isotope ratios from sediment cores at the Northeast Atlantic continental margin, the open North Atlantic, and the Norwegian-Greenland Seas (BOYLE and KEIGWIN, 1987; ZAHN et al., 1987; DUPLESSY et al., 1988; VEUM et al., 1992; OPPO and LEHMANN, 1993; SARNTHEIN et al., 1994; JUNG, 1996). These studies infer enhanced ventilation of the mid-depth North Atlantic, in response to the formation of a Glacial North Atlantic Intermediate Water (GNAIW, sensu DUPLESSY et al. (1988)) or enhanced formation of Upper North Atlantic Deep Water at the expense of Lower

North Atlantic Deep Water (BOYLE and KEIGWIN, 1987; SARNTHEIN et al., 1994). Northward advance of AABW far into the northern North Atlantic caused significantly decreased ventilation there at depths below 3500. The net result of the reorganization of vertical water mass architecture in the North Atlantic was a steeper vertical gradient of biologically cycled nutrients between nutrient depleted mid-depth and nutrient-enriched deep and bottom waters.

From this pattern it is concluded that during the last glacial the upper Portuguese margin, at water depth above 1500 m, was influenced by the presence of a well ventilated water mass. Enhanced glacial benthic carbon isotope levels at the upper Moroccan continental margin have been inferred to document a stronger influence of MOW on the North Atlantic mid-depth hydrography (ZAHN et al., 1987). This hypothesis has also been used to explain enhanced benthic carbon isotope values further north, at the Portuguese margin and the Rockall Plateau area in the open northern North Atlantic (SARNTHEIN et al., 1994; JUNG, 1996). Evaluating benthic oxygen isotope in view of equilibrium $\delta^{18}O$ fractionation as a function of ambient water temperature and salinity, however, implies that MOW contribution must have been reduced during the last glacial, and that enhanced mid-depth ventilation at the Portuguese margin must have come from a North Atlantic source, similar to today's North Atlantic Central Water (ZAHN et al., 1997).

An important aspect of the M39/1 paleoceanographic work was to collect water column data that will serve as an oceanographic ground-truth data base to better define the paleoceanographic proxy-signals of MOW close to the Strait of Gibraltar i.e., prior to large-scale mixing of MOW with Atlantic waters. T-S profiles in conjunction with water column oxygen, phosphorus and stable oxygen and carbon isotope analyses (as well as water column trace element analysis; see below) will serve as a modern control for the interpretation of paleoceanographic proxy records and their interpretation in terms of glacial-interglacial changes in physical circulation and regional nutrient inventories. To obtain high-quality water samples from paleoceanographically important depth intervals, CTD-derived T-S profiles in conjunction with Rosette and GoFlo water sampling were a central scientific objective of M39/1.

3.4.2 Plankton in Surface Waters off Portugal

Plankton organisms represent the base of the marine trophic chain. Seasonally varying abundances indicate varying bio productivity at the sea surface. During settling to the sea floor, the plankton assemblage changes mainly due to grazing and shell dissolution. Moreover, lateral advection of plankton organisms by ocean currents might as well affect the sedimentary assemblage. A comparative study of plankton at the sea surface and in surface sediments was carried out to shed light on the loss of primary produced material and the loss of species during settling. Analysis of living and the dead (fossil) assemblages and documentation of the autochthonous plankton signal in surface waters and underlying sediments, as well as an evaluation of MOW- related advection/transport of allochthonous plankton was thus an important objective of the cruise.

3.4.3 Benthic Foraminifera: Faunal Composition and Stable Isotopes

Benthic foraminiferal studies are part of an ongoing research project on late Quaternary water mass patterns at the western Iberian margin. Main objectives are to document (i) the impact of sporadic North Atlantic melt water events on water mass stratification and advection in the northeastern Atlantic during the late Quaternary and (ii) the dynamics of the Mediterranean Outflow Water (MOW) during the last glacial, deglacial, and Holocene. Benthic carbon isotope data from the western Iberian margin document distinct anomalies that are coeval with glacial melt water events in the open North Atlantic (ZAHN et al., 1997). The data imply that the hydrographic response to sporadic collapses of thermohaline overturn in the northern North Atlantic was felt outside the immediate region of maximum melt water fluxes i.e., at the Portuguese margin, and may have been of ocean-wide importance. Detailed evaluation of water mass patterns during these events is hindered by a lack of information on the advection history of MOW during the melt water pulses. M39/1 was designed to retrieve sediment cores close enough to the Strait of Gibraltar to allow for the documentation of MOW flow in that the proxy-records would trace the source signal of Mediterranean waters at their entrance into the North Atlantic. The benthic foraminiferal community structure also shows distinct changes of faunistic constituents that are coeval with periods of sporadic thermohaline spin-down (Baas et al., submitted). The faunistic proxies closely complement the isotope data. They need to be refined and calibrated with oceanographic data to corroborate reconstructions of glacial and deglacial deep-water circulation from benthic isotopes (KAIHO, 1994; BAAS et al., submitted). An epibenthic foraminiferal association indicative of recent current MOW advection off southern Portugal is to be traced further towards the MOW source in the Gulf of Cadiz to monitor the response of the biota to higher current strength. The study also needs to be extended further to the north to document the correlation between epibenthic foraminiferal assemblages and the spreading of MOW (SCHÖNFELD, 1997). New surface samples and sediment cores from suitable locations are needed to fill in gaps in the present data sets which inhibit a conclusive interpretation and application of foraminiferal faunal and isotope proxies. Sediment sampling is complemented by water column measurements of oxygen concentration, nutrients, stable isotopes, temperature and salinity of near-bottom waters to provide environmental data for calibration.

An important aspect of this work is the potential influence of pore water chemistry on benthic foraminiferal assemblages. The faunal composition of benthic foraminiferal assemblages in surface sediments is closely linked to organic carbon fluxes to the seafloor (ALTENBACH, 1985; LUTZE and COULBORN, 1984; ALTENBACH et al., 1989). A relation to oxygen concentrations of ambient bottom waters is also indicated (KOUTSOUKOS et al., 1990; HERMELIN, 1992; ALVE, 1995). Species adapted to dysoxic conditions such as *Globobulimina affinis* and *Chilostomella ovoidea* commonly prefer a deep endobenthic microhabitat (CORLISS, 1985), but they appear close to the sediment surface in regions of low-oxic bottom waters and/or of high flux rates of organic matter (HARMAN, 1964; MULLINEAUX and LOHMANN, 1981). A detailed examination of the relation between dysoxic species and pore-water oxygen levels will help to discern the impacts of both environmental factors (LOUBERE, 1997). Only few studies report on depth habitats of *Globobulimina* and oxygen concentrations in ambient pore waters (REIMERS et al., 1992). This is mainly reflects the fact that micropaleontological studies and geochemical measurements are rarely carried

on the same sets of sediment samples. Our strategy is to provide *in situ* oxygen data for the same samples that will be used later for analysis of the benthic foraminiferal fauna. For the porewater oxygen measurements we use an oxygen needle-probe and determine pore-water oxygen concentrations in subsurface sediments of that multicorer tube, which was later sampled for benthic foraminiferal depth-habitat studies.

3.4.4 Trace Fossils and Bioturbation as Indicators of Paleo-Environmental Conditions

Trace fossil assemblages are related to environmental conditions at the sediment/water interface e.g., temperature, salinity, oxygen and nutrient concentrations, sediment stability and grain size. Thus, a comparative study of trace fossil assemblages at different water depths is carried out to improve their paleoceanographic application. In particular, the relation of trace fossil changes to MOW-advection changes e.g., in the course of glacial-interglacial climatic cycles, will be studied. The primary intention is to revise and improve the concept of trace fossils as monitors of environmental change.

3.4.5 Temperate Water Carbonates

Modern and late Quaternary changes of biogenic carbonate production and carbonate accumulation are investigated at the western Iberian continental shelf and margin, and in the Gulf of Cadiz. The response of benthic carbonate organisms to environmental factors such as productivity of surface waters, terrigenous sediment input and redeposition and their relation to the global state of climate are studied. Warm temperate carbonate shelf sediments that are formed under variable upwelling regimes are compared to carbonate sediments in temperate, high boreal, and subarctic shelf settings.

3.4.6 Trace Metals in Calcareous Microorganisms as Paleoceanographic Tracers

a) Cadmium

The distribution of dissolved cadmium is globally correlated with the distribution of biologically cycled nutrients (BOYLE, 1988; FREW and HUNTER, 1992) and is used in paleoceanographic studies in conjunction with benthic $\delta^{13}\text{C}$ data as an independent tool to reconstruct past ocean circulation patterns and nutrient inventories (BOYLE, 1994). The great potential of cadmium as a paleoceanographic proxy comes from the fact that - in contrast to $\delta^{13}\text{C}$ - Cd is cycled within the ocean only and no iexternallr pathways are know (except for leaching at some continental slope deposits; FREW, 1995). The ocean carbon cycle, on the other hand, also involves air-sea gas exchange which is associated with carbon isotope fractionation (BROECKER and MAIER- REIMER, 1992). In high latitudes, the isotope fractionation during outgassing or carbon uptake may exceed the biologically-driven iiRedfieldly $\delta^{13}\text{C}$ fractionation and severely hamper extraction of nutrient information from paleoceanographic $\delta^{13}\text{C}$ data sets. Cd is not involved in air-sea fluxes and thus, it is considered a faithful recorder of ocean nutrient cycling (ZAHN and KEIR, 1994). Apparent disparities between benthic foraminiferal Cd and $\delta^{13}\text{C}$ signals thus bear information on water mass source regions and can be used in paleo-ocean circulation studies as conservative tracers for water mass tracking (LYNCH-STIEGLITZ et al., 1996).

Basin-wide compilation of benthic foraminiferal $\delta^{13}\text{C}$ from glacial sections of North Atlantic sediment cores documents large-scale changes in the regional water mass pattern that went along with changes in northern North Atlantic surface ocean conditions (DUPLESSY et al., 1988; SARNTHEIN et al., 1994). The principal change was a shift in depth of the core layer from 3000 m to around 2000 m during the last glacial in response to enhanced buoyancy of convecting water masses. Only in the immediate vicinity of convection, i.e. north of 45°N , did the influence of newly-convected deep waters reach water depths similar to today (SARNTHEIN et al., 1994). At depths below 3000 m, depleted benthic $\delta^{13}\text{C}$ values signify an enhanced influx of a chemically aged water mass of presumably Southern Ocean origin (DUPLESSY et al., 1988; SARNTHEIN et al., 1994). Benthic $\delta^{13}\text{C}$ records from the upper Portuguese margin, at water depths of 1000- 1200 m, display distinct negative anomalies that were associated with sporadic melt water events (ZAHN, 1997; ZAHN et al., 1997). The data imply a rapid slow-down of thermohaline circulation in the North Atlantic during these events. Benthic foraminiferal Cd records imply increased nutrient concentrations in ambient mid-depth waters during these periods and thus confirm convective slow-down. The data, however, are inconclusive as to whether these "old" waters originated from the southern hemisphere (e.g., a glacial Antarctic Intermediate Water) or whether limited convection still occurred in the northern North Atlantic.

Water column cadmium analysis in conjunction with the determination of oxygen and phosphorus concentrations was a primary scientific objective of M39/1. The data are intended to provide information on regional Cd distribution in the Gulf of Cadiz and at the western Iberian margin that would allow to calibrate the Cd-to-P relation in the northeastern Atlantic. Special emphasis is on MOW in terms of Cd and nutrients concentrations to better constrain the paleoceanographic patterns observed in sediment cores from the upper Portuguese and Moroccan margins.

b) Strontium, Magnesium

The general objective of this project is to test and improve the application of Sr/Ca and Mg/Ca records of calcareous planktonic and benthic microorganisms as proxies for paleoceanographic reconstructions. Aspects to be addressed are i) processes which determine the uptake of trace metals during biomineralisation in the water column; ii) the influence of diagenetic alteration on trace metal composition of fossil carbonate shells; iii) chemical variability during climatic changes. The western Iberian margin is well suited for these investigations, because: (i) distinct variations of surface water temperature during glacial-interglacial times are documented from the N-Atlantic (BOND et al., 1993), changes that should also be documented in the Mg/Ca signals of planktonic foraminifera off Iberia; (ii) sporadic glacial melt water events documented by ice-rafted detritus and temperature anomalies (BOND et al., 1992, 1993; MASLIN et al., 1995) induced severe changes in the surface hydrography. Due to a insensitivity of the Mg/Ca-ratio to minor salinity changes (NÜRNBERG et al., 1996a), Mg/Ca-time series should primarily reflect temperatures changes, and thus, should help to detect melt water events when compared to $\delta^{18}\text{O}$ -data. (iii) Fluctuation of the late Pleistocene Mediterranean outflow, that are documented in marked temperature and salinity anomalies (ZAHN et al., 1987), should have caused distinct chemical signals in the shells of benthic ostracods. The Western Iberian continental slope will therefore

serve for a case study to test whether the temperature reconstruction from Mg/Ca-ratios can compete against conventional temperature reconstructions based on stable oxygen isotopes and/ or faunal analysis. Furthermore, the characteristic MOW water properties should be clearly depicted in the shell chemistry of benthic ostracods. A primary goal is to study the relationship between foraminiferal Sr/Ca ratios and Sr-depletion in surface waters to improve the potential of foraminiferal Sr record as paleoceanographic tools. Comparison of trace metal concentration in seawater and benthic ostracods will elucidate if MOW carries a characteristic Mg/Ca signal, and if the signal is picked up by benthic organisms.

3.4.7 Sediment Geochemistry and Mineralogy

The Gulf of Cadiz has been one of the most interesting research areas for the ICM Marine Geology group of Barcelona. In this area, geophysical, geochemical, sedimentological and stratigraphic studies have been carried out, which resulted in a dense grid of seismic profiles and a large number of sediment cores of the eastern part. Here, gas-charged sediments and seafloor pockmarks-like features were recognized on the slope area and described in BARAZA and ERCILLA (1996). Furthermore, this work will focus on the impact of the Mediterranean Outflow on the sea floor, e.g. formation of contourites and sea floor bed forms. These processes are either linked to changes of sea level or the strength of the undercurrent itself (NELSON et al., 1993). Moreover, geochemical studies will be carried out to improve our understanding of contamination of suspended particles and surface sediments by heavy metals from mining factories, and its relationship to modern sedimentary processes of the area (PALANQUES et al., 1995; VAN GEEN et al., 1997).

The overall intention is, to study the paleoclimatic record in Pleistocene-Holocene sediments, based on different mineralogical and geochemical parameters. Mineralogically, smectite apparently offers a great paleoceanographic potential. Today, smectite is discharged through the Guedalquivir River into the Gulf of Cadiz, partially even into the Alboran Sea (AUFFRET et al., 1974; GROUSSET et al., 1988; BOZZANO, 1996). Variations of this clay mineral, as recorded in the Alboran Sea cores possibly depend on changes of the Atlantic inflow during the past, a hypothesis, which we intend to verify with sediment cores from the Gulf of Cadiz. An important objective of this study is to follow the path of the smectite track from the Atlantic into the Mediterranean, and improve our understanding of the oceanographic constraints implied in this transfer process.

The main objectives of the geochemical study are to characterize the conditions of past sea surface waters in the Gulf of Cadiz. Based on a high-resolution biomarker studies, the paleoceanographic response in the Gulf of Cadiz to rapid climatic changes in the North Atlantic should be depicted. A second objective is to compare records from the Gulf of Cadiz and the Alboran Sea to elucidate the impact of the inflowing Atlantic water on water mass dynamics in the Alboran Sea. Finally, the Gulf of Cadiz, the Alboran Sea and the Agadir zone are ideally suited for a prospective study of slope-sediment instability. P-wave velocity, density and magnetic susceptibility of regional sediments will also be studied.

4 Narrative of the cruise

4.1 Leg M39/1

(R. Zahn)

The M39/1 scientific party arrived in Las Palmas on 16 April 1997. After the ISO 9002 certification of R/V METEOR was successfully completed, all scientists embarked R/V METEOR the next day. On April 18, 09:00, R/V METEOR left Las Palmas and headed north-north-east to the Gulf of Cadiz. After a transit of 53 hours in good weather and calm seas we reached our first working area in the outer Gulf of Cadiz (Figure 2). Functionality and handling trials were successfully run with the full suite of sediment sampling devices and the CTD/Rosette. During the following 10 days, extensive PARASOUND and HYDROSWEEP surveys were carried out that were followed by sediment and water sampling at 29 sites. The sampling sites were targeted to cover the depth ranges of North Atlantic Central Water, MOW, upper North Atlantic Deep Water (NADW) and uppermost lower NADW. Spectacular temperature and salinity profiles were collected across the MOW flow path at four hydrographic stations and water samples were collected to measure stable isotope, nutrient and trace element compositions of the key water masses.

The second half of the cruise was devoted to sediment and water sampling along the western Iberian margin. 48 sampling stations between Cabo Sao Vicente in the south to Cabo Finisterre up north at water depths from 20 m to >3000 m were occupied. The shallow stations on the shelf were designed to recover surface carbonate sediments which are to be used to estimate the carbonate production potential on the Portuguese shelf and its influence on the sedimentary regime of the upper continental slope. Core log profiles, namely magnetic susceptibility and color reflectance, along sediment cores from the upper and central slope revealed quasi-cyclic changes of sediment properties that could tentatively be correlated with high-frequency climatic oscillations known from Greenland ice cores. Distinctive positive anomalies in the susceptibility logs further indicated the sporadic incursion of ice rafted debris horizons which have already been documented in sediment cores that were collected during earlier cruises to the area. The scientific program of M39/1 was completed on 10 May, 13:00. After a 41 hour transit, R/V METEOR arrived in Brest in the early morning hours of 12 May. In total, 78 stations were occupied during the cruise and a rich collection of water and sediment samples, and of hydroacoustic profiles were retrieved. As such, the cruise was successful in that all major scientific objectives were achieved. This success to no small extent was made possible by the ship's master, Kapitän Dirk Kalthoff, his officers and the crew who cooperatively collaborated with the scientists and made our work possible even under difficult conditions. To all of them we owe our sincere thanks.

We are also indebted to the Portuguese and Spanish governments for granting us clearance to carry out our scientific work in their national waters. In particular, we appreciate the good collaboration with the Portuguese naval command and the Spanish ship traffic control that made it possible for us to work in intricate terrain such as major ship traffic areas and at near-shore, shallow water sampling sites.

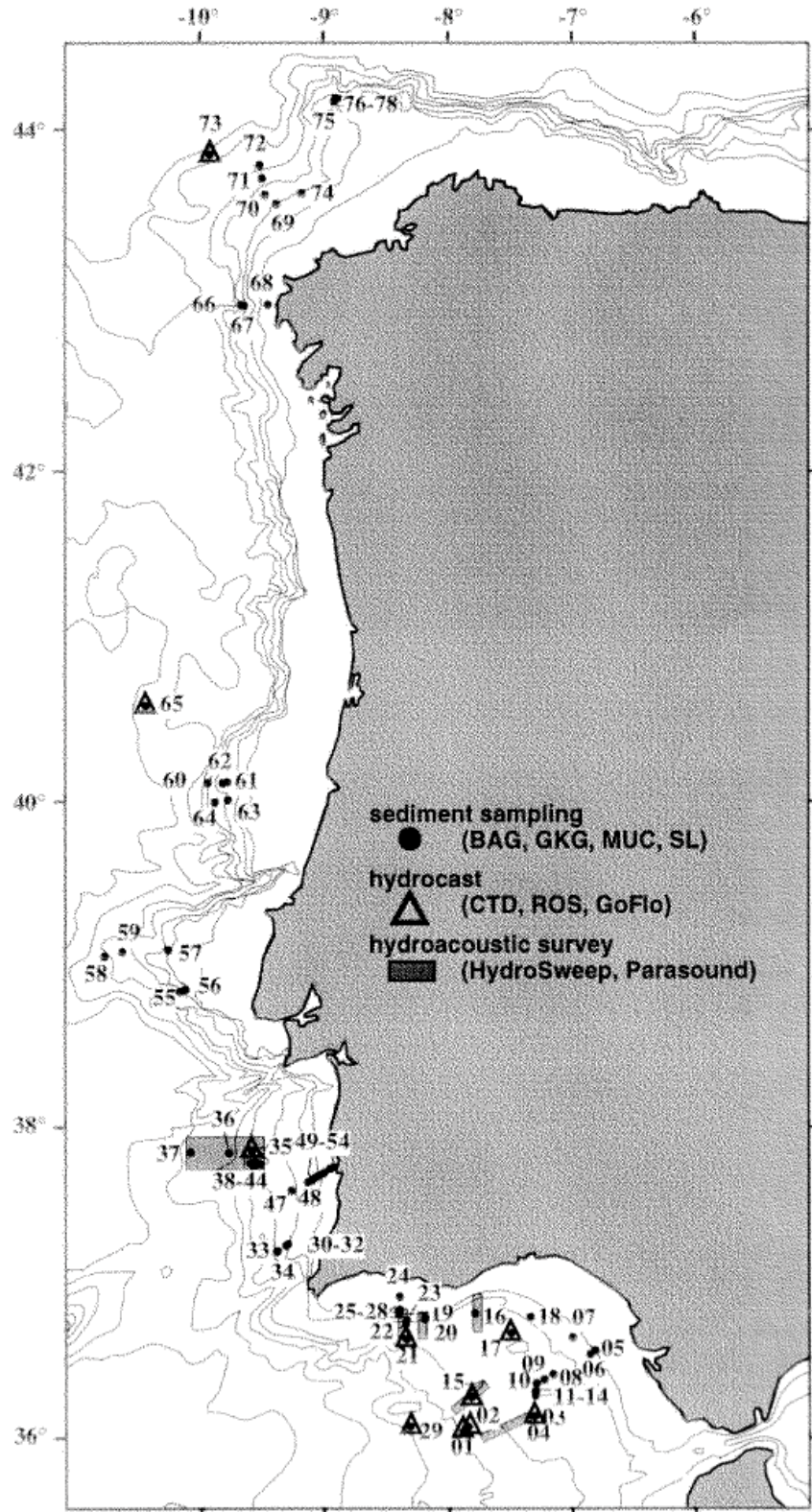


Fig. 2: Location map of M39/1 sediment and water sampling sites in the Gulf of Cadiz and at the western Iberian margin.

4.2 Leg M39/2 Brest - Cork (W. Zenk)

On the evening of the 13 May an informal reception was held for the participants of an Eurofloat meeting at IFREMER together with a number of local representatives from IFREMER and from the *Service Hydrographique et Oceanographique de la Marine* (SHOM).

On the afternoon of the 14th, the majority of cruise participants arrived in Brest and installation of equipment on board started immediately. After initial testing of the chemical instrumentation and of various computer systems was successfully concluded, the METEOR left Brest at 14:00. The next two days we sailed for the starting point of our scientific mission on the northwestern shelf edge of Ireland north of Porcupine Bank. This location was reached on the morning of May 17 on Sta. 200 (see chapter 7, list 7.2.1). An essential test station had been occupied the day before. Starting from the continental slope, METEOR cruised straight (306°) towards the Middle Atlantic Ridge, crossing Rockall Trough, Rockall Bank, and Maury Channel in the Central Iceland Basin (Fig. 3). This first hydrographic Sect. A (Sta. 200-224) was paralleled by a second (B) positioned 230 km southwestward between the Ridge and the southern flank of the Hutton Bank (Sta. 225-232). A third section (C) followed subsequently. It brought us back to the Middle Atlantic Ridge north of Charles Gibbs Fracture Zone (Sta. 240) where METEOR arrived on May 28.

On the initial Sections A-C, 40 full depth CTD stations were occupied, those at Maury Channel (215, 230, 234) being the deepest. With the exception of four stations during strong gale conditions on Sect. A the CTD system included a rosette sampler (RO) and an acoustic Doppler current profiler (LADCP). Two interruptions in the CTD work were necessary to launch moorings IM1 and IM2 (see list 7.2.2). They contain low-energy signal generators, an essential infrastructure for the application of the RAFOS technology (see Fig. 5). Nine RAFOS floats were launched up to May 26 (see list 7.2.3). Over the following 12-24 months they will monitor the spreading of Labrador Sea Water in the Iceland Basin at approximately 1500 m depth.

After reaching Sta.240 we set course on a fourth section (D) with CTD stations 243, 242, 244, 249, 245-248 (see Fig. 3). The non-monotonic station sequence over this section was the result of the difficult weather conditions in the northern West European Basin. It is positioned just north of Charlie Gibbs Fracture Zone where we expected the Overflow Water to still be confined to the eastern flanks of the Reykjanes Ridge before escaping westward through the fracture zone into the Irminger Sea. For this reason, we deployed three current meter moorings (V386, V 387, and V388 [IM3] see list 7.2.2) at this gateway. The array hosts 13 recording instruments and a further RAFOS generator at the depth of the Labrador Sea Water and at several levels below within the Overflow Water. From these long-term current observations we expect continuous records of transport fluctuations at intermediate and near-bottom depths at Gibbs Fracture Zone, the major conduit for water mass exchange in the central North Atlantic.

These efforts were be complemented by the installation of 'Float Park North' at Sta. 245, where four RAFOS floats were launched from the METEOR. While one of them descended to its mission depth, the rest have been temporarily moored at the bottom (3170 m) for 2, 4, and 6 months, respectively. The stepped delays of the three new dual-release floats will enable us

to establish a modest Lagrangian time-series at the entrance of mid-depth water masses into the eastern basin (Fig. 4). The latter is a major research topic of the initiative SFB 460 of the University of Kiel. It features the dynamics of the thermohaline circulation variability, thought to be relevant for climate variability.

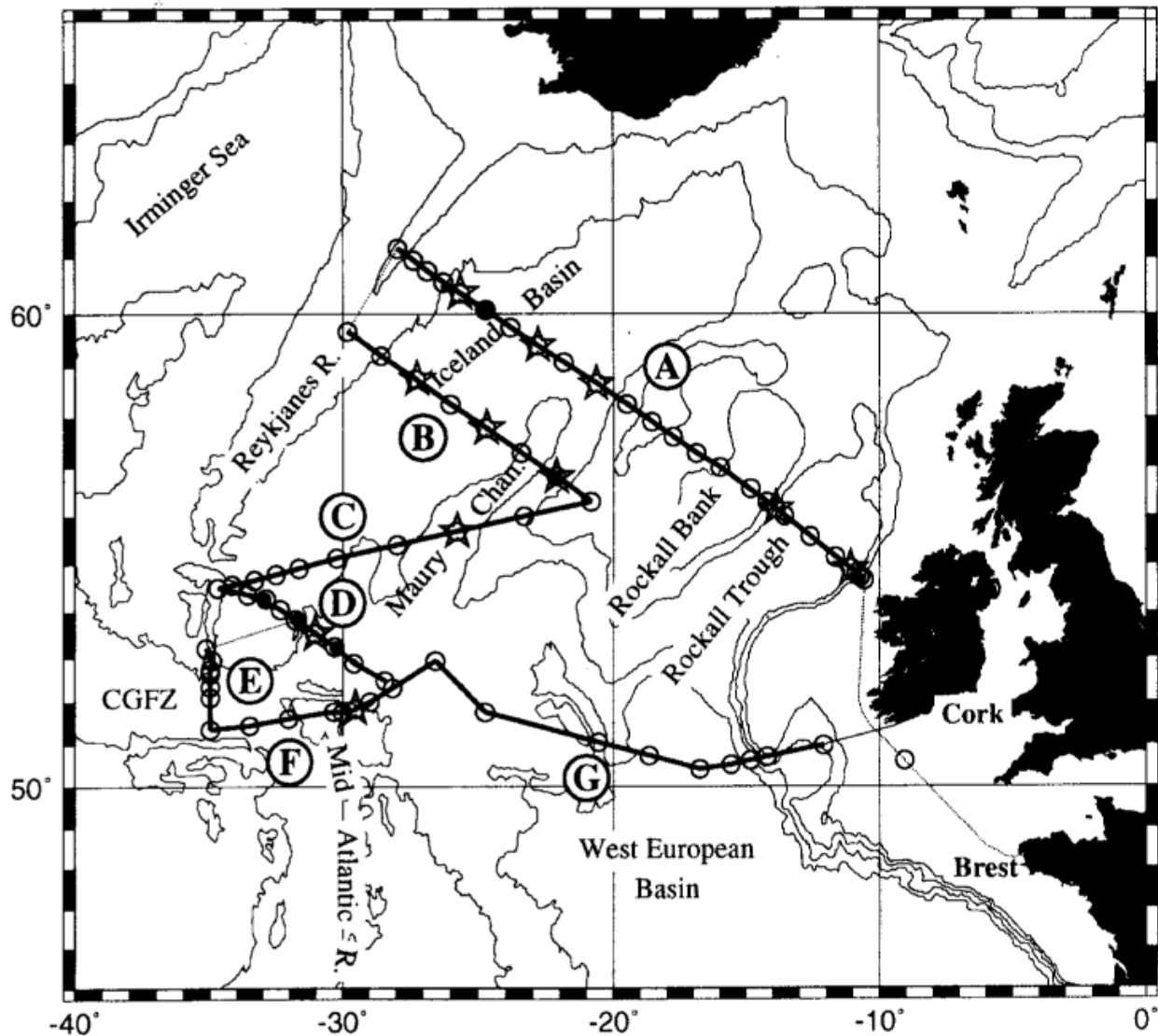


Fig. 3: Geographical setting of METEOR cruise 39/2. Capital letters denominate sections. Hydrographic stations (cf. list 7.2.1) are shown as circles. Stars represent RAFOS float launch positions (cf. list 7.2.3). Dots stand for mooring locations (cf. list 7.2.2).

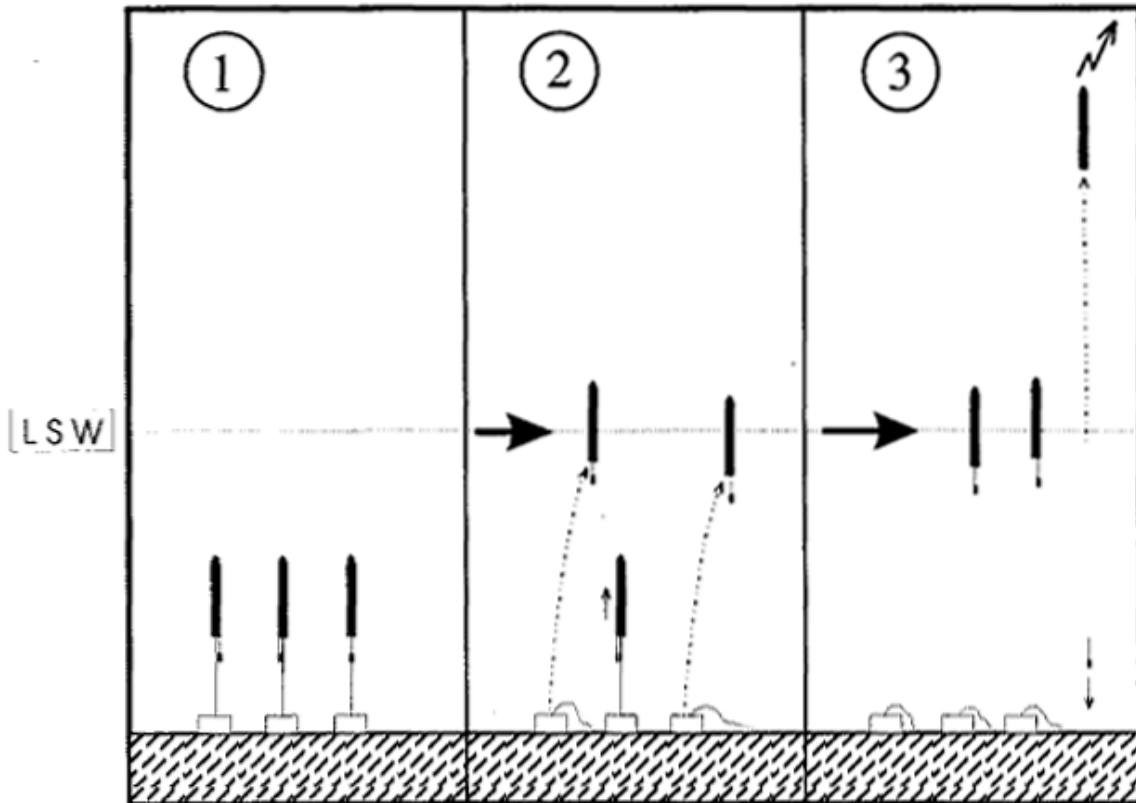


Fig. 4: Principle of the “Float Park” deployed during METEOR cruise 39/2. During phase 1 RAFOS floats with dual-releases are moored temporarily at the bottom. Phase 2 begins with the anchor release. It enables floats to reach their mission level at the Labrador Sea Water (LSW) plume. Finally they drop their ballast weight (phase 3), return to the surface and transmit their recorded data. For mission lengths see Table 7.2.3.

After we had lost more than a day due to unfavorable weather conditions with three attempts to occupy Sta. 245 at mooring V387, METEOR cruised towards the Gibbs Fracture Zone on 31 May, where a meridional hydrographic section (E) on 35°W was occupied. It consisted of seven closely spaced deep CTD stations (250-256) and was finished early in the morning on 2 June. Then, METEOR proceeded eastward, initially cutting through the Middle Atlantic Ridge at a nominal latitude of 51°N. During the next two days until 4 June, Sect. F consisting of Sta. 256 to 264, was completed. On Sta. 261, ‘Float Park South’ was installed (see Fig. 5 and 6). Again, it contains four RAFOS floats of which only one drifts immediately at its mission depth while the rest of the group remains anchored for the next 3, 6, and 9 months. We expect the combination of Sections D, E and F to allow a synoptic budget of the transports of Overflow Waters at the 3- way junction ‘Gibbs Fracture Zone’. Furthermore, it is worth noting that the chemists on board detected elevated methane concentrations in the rift valley at Sta. 260, which is situated at the extension of the Middle Atlantic Ridge south of Gibbs Fracture Zone.



Fig. 5: Deployment of RAFOS sound source (IfM Nr. V385) on Station 231.

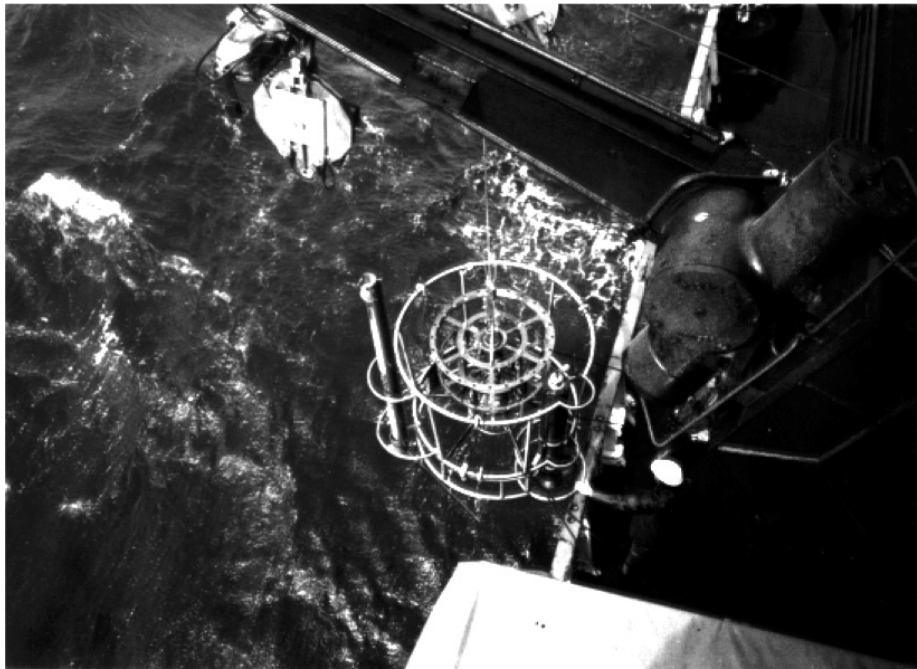


Fig. 6: Deployment of the CTD probe on Station 261 carrying a RAFOS float to be moored temporarily in a float park on the ground.

The final Sect. G, with much widely spaced station intervals, was completed on 7 June. It consists of Sta. 263, 265-271, connecting the Middle Atlantic Ridge with the western approaches of the British Isles. In the afternoon of 7 June, the hydrographic observations were terminated and the METEOR sailed towards Cork. All CTD stations, mooring and float deployments are compiled in lists 7.2.1, 7.2.2 and 7.2.3.

While on passage to the western approaches of Ireland we contacted Prof. L. TALLEY from the Scripps Institution of Oceanography. She and her team had just started their hydrographic work aboard the research vessel KNORR. After the exchange of the latest information about our observations on the METEOR the American group on the KNORR considered an adjustment of their cruise track in order to optimize the hydrographic coverage of the Iceland Basin on a quasi-synoptic scale in early summer 1997. On an unexpected stop-over of the KNORR we missed our colleagues in the port of Cork by only a few hours.

METEOR cruise 39, leg 2, was completed in Cork, Ireland, on 8 June 1997. Because of tunnel construction work under the River Lee, METEOR had to stay the same day at the new ferry terminal outside of Cork. In the afternoon of the next day she moved to Tivoli pier, right in the centre of the city. Disembarkation of the scientific party had taken place at the container pier before reaching Tivoli pier.

4.3 Leg M39/3 (K. P. Koltermann)

METEOR sailed from Cork, Ireland on 11 June 1997 the single day of Irish weather we encountered in Ireland, rain. A test station (273) was worked on 12 June 1997 in more than 4300 m depth at 49°30'W, 14°W. Tests of the 36 x 10 l Rosette were not successful. After finally testing the established 24 x 10 l rosette package successfully, a further test station was worked on stat. 274 on 3722 m of water to get blank values for the CFC measurements (274 KAL). The ship worked then the A2 section (Figure 7) onto the European shelf towards East. At all station positions and halfway between stations XBT drop were added to the spatial resolution of the temperature field. In the mean time work on both the 36 x 10 l rosette and the DHI1 CTD was continued. On 14 June 1997 after working the easternmost station of the section (stat. 282) the ship sailed for the position of the second test station (274) to finally take up the section work westward. We used mainly the 24x10 l rosette equipped for the L-ADCP on loan from IfM Kiel. No difficulties were encountered with either rosette, L-ADCP or the CTD NB3. In the mean time the repair work of the other CTDs, planned to be the main stay of this work, left us with the NB3, a MkIIIB and the BSH2 without an oxygen sensor, MKIIIC.

On 20 June 1997 with stat 302 we crossed the Mid-Atlantic Ridge MAR and worked this station at the deepest part of the Rift Valley. There we also deployed the first of three C-PALACE floats, #719. On 21 June the mooring K1 was successfully recovered and another mooring deployed. No damage or losses were incurred. After another hydro station at the site, section work was continued. C-PALACE #720 was deployed on 20 June at stat 304 on the west side of the MAR. The last C-PALACE #718 was successfully launched on 22 June at station 307. The next day the mooring K3 was recovered at dawn and a new mooring deployed. After reaching depths in excess of 4100 m, on stations we deployed first the 24x10 l rosette B24

together with the CTD NB3 for a shallow cast to nominally 1200 m, followed by the deep cast with the 24 x 10 I rosette K24 and the BSH2 CTD, that included the LADCP. Two bottle positions had been sacrificed to incorporate the LADCP. The deep North American Basin was crossed until 29 June. Single cast stations were resumed up the slope towards the tail of the Grand Banks. On 30 June 1997 the last station was worked at 59 m depth.

Rosette work, after settling in on the work packages, was only effected by leakages, slipped O-rings and occasionally leaking spittoons. These leakage problems were the only but quite numerous handicaps in the water sampling. At some time a re-definition of the starting position of the rosette trigger had to be checked and confirmed with deliberate firings on deck. Throughout the cruise, as on all other previous ones, we used the BIO sample numbering scheme. Again, all who did not have previous experiences adopted it right away.

After passage on 1 July towards St John's, Nfld, METEOR docked on 2 July, 1700 at pier 10. During the passage all wire work was concluded, the ship's measurement systems such as thermosalinograph, ADCP and underway measurements were stopped when passing the 50 nm limit of Canada.

Meteor M39/3 , 6/13/97 - 06/13/1997

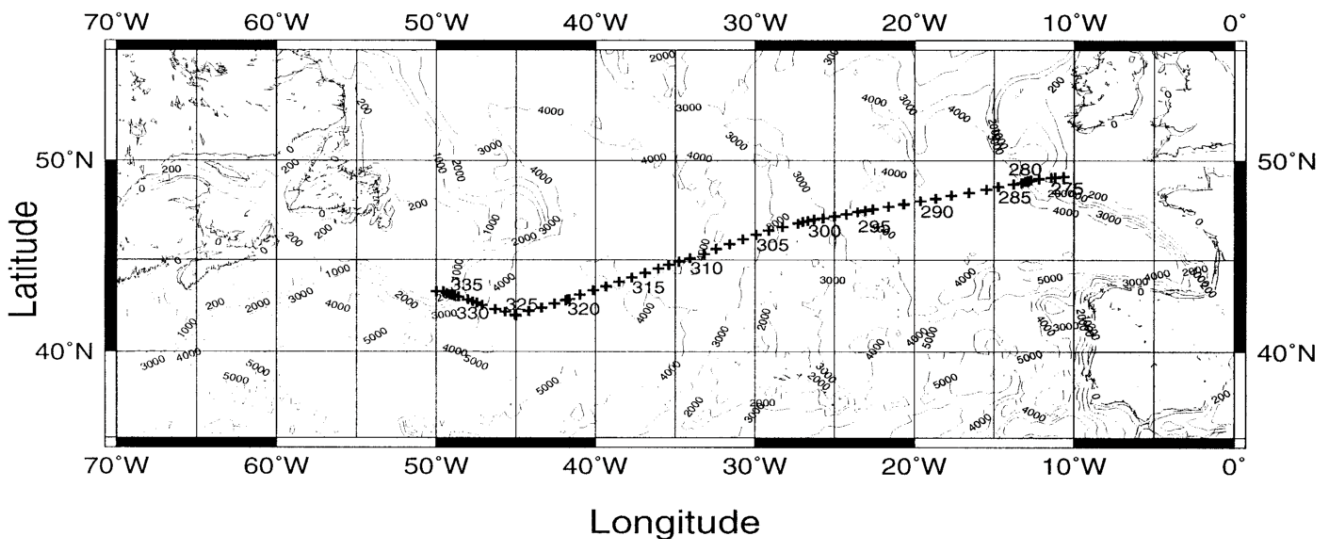


Fig. 7: Cruise track of METEOR cruise M39/3, WOCE Hydrographic section A2 between Goban Spur on the Irish shelf and the Canadian Tail of the Grand Banks.

4.4 Leg M39/4
(F. Schott)

Since cruise leg M39/4 had as an essential objective the retrieval and redeployment of a variety of moorings, it had to be subdivided into two segments with an interim stop on 16 July in St. Anthony, in case last-minute repairs needed to be made on tomography transceivers or convection observing instrumentation. The cruise began in St. John's amidst festivities to celebrate the 500th anniversary of Cabot's crossing with the 'Matthews'. A Japanese TV

camera team escorted the ship out of the port, filming for an educational channel; they passed along a camera to the METEOR for underway filming.

The first part of the cruise repeated the 'Valdivia' track of 1996, beginning north of Hamilton Bank along the WOCE line AR7 with retrieving moorings K2, K6 (Fig. 8) that had been deployed in August 1996 by 'Valdivia'. The moorings were both recovered on 8 July in good condition, thus alleviating fears that deep-reaching icebergs or shelf edge fishery might have jeopardized them. Across the boundary current 3 profiling ALACE floats (PALACE) were deployed to continue our Lagrangian observations across the boundary circulation that were started with deployment of 6 PALACEs in February 1997 by the 'Knorr'. On 10 July, an Inverted Echosounder (IES) of URI was recovered under unfavourable conditions (insufficient acoustic tracking signals and fog). Working our way northwestward along AR 7 to tomography station K4, this mooring was recovered intact in the evening of 10 July, but two of its transponders only sent weak signals and did not release. Then a southwesterly course was taken, back to the Labrador shelf. On 12 July, tomography mooring K3 and its three navigation transponders were recovered and during 14-20 July the boundary current meter array K7-K16 (Fig. 8) was deployed, while at nighttime CTD/LADCP stations across the Labrador Current were taken. This time period was particularly intense for those of the scientific party dealing with the equipment, since many of the instruments to be used for these deployments (tomotransceivers, acoustic releases, transponders, current meters, seacats) had to be turned around, after just having been retrieved. A special worry some problem was that the data evaluation of the tomographic stations just recovered indicated that there had been phases of large mooring inclinations. These were larger than experienced anywhere else, although the mean currents in the interior Labrador Sea were small. The effect appeared to be dominantly due to small-scale but deep-reaching energetic eddies, that slowly drifted by a mooring position. One remedy was to increase net buoyancy of the moorings to the absolute limit of wire breaking strength.

On 16 July this first part of M39/4 was terminated according to plan. The quality of the shipboard and lowered ADCP profiles was much improved by the significantly increased navigation accuracy that was made possible by the newly introduced GPS/GLONASS receiver. It reduced the scatter on the GPS positions noticeably, and thus even more on their derivatives which should constitute the ship's motion vector. The new 75 kHz shipboard ADCP had been successfully put to work and routinely yielded depth ranges of more than 500 m except under very rough sea state conditions. A system that did not satisfactorily work when we got on board was the Ashtech direction determination unit. Two reasons were discovered: First, the antenna locations are less than adequate for the purpose and second, a new firmware had been developed by the manufacturer that was not yet installed on the vessel. When we received that by e-mail, the data return improved drastically.

The interim stop in St. Anthony allowed the exchange of a number of personnel (3 departing, 7 coming) and gave a welcome break for those aboard, which was used for an outing to a Viking settlement ('L'Anse aux Meadows'). From St. Anthony METEOR headed northward for deployment of tomography mooring K17 and of the moored cycling CTD (K15, Fig. 8). After deployment of tomography mooring K17 with the heavy HLF-5 sound source it turned out that the station did not operate properly. In the night the mooring was picked up again, a highly

commendable effort by the crew who had by now been up and working for long hours. After installation of K15 and K17 this time with a Webb transceiver on 20 July the ship headed to the southeastern end of the WOCE line. Tomography/convection moorings K12 and K11 (Fig. 8) were deployed on 21/22 July and the last of the deployments was K14 on 23 July.

The northern boundary circulation was then investigated with 4 CTD/LADCP stations across the northern end of the WOCE-AR7 line whereupon the ship transited to Cape Farewell, past a beautiful scenery of icebergs and ice floes occupied by seals, to begin profiling the meridional section along 43.5°W. That meridional section away from the boundary was filled with energetic mesoscale eddies, but in order to have enough time for sampling the Gibbs Fracture Zone (GFZ) through flow and the other deep boundary currents, fairly wide station spacing had to be used until reaching Flemish Cap. There the Labrador Sea Water was found to circulate southeastward offshore, separated by a front from the “Northeast Corner” of the North Atlantic Current. After another connection section to 35°W, the investigation of the GFZ was begun on 1 August with increasingly closely spaced stations until reaching the main cross-connecting valley. On this approach, the Hydrosweep bottom observations taken on M39/2 could well be used for station planning, even more so since rough weather degraded the quality of our own soundings. The interesting result of that small-scale survey was that much through flow also seems to originate in a valley a few km north of the main cross roads.

Following the axis of the Mid-Atlantic Ridge (MAR) northward it was found that it carries a deep valley along its crest that might play a role in the interbasin exchange through openings of other cross-ridge valleys in the north. On 6 August, the final transect was begun, running from the MAR to the Greenland coast just north of Cape Farewell (Fig. 8). Dense station spacing across the topographic slopes on both sides covered the deep boundary circulation. This last phase of the work was hampered by strong head wind. The station work was terminated in the night of 8/9 August and the transit to Iceland was commenced. After weeks and weeks of westward winds along this track the winds were now from the northeast, delaying our advance to port somewhat unexpectedly. Leg M39/4 had accomplished its objectives and ended around noon of 11 August in Reykjavik.

4.5 Leg M39/5 (A. Sy)

After three days in Reykjavik to exchange the scientific staff and set up the laboratory installations, R.V. METEOR sailed from Reykjavik (Iceland) on 14 August, 09:00 UTC heading for the startup position at 64°45'N, 26°40'W (stat. # 451; Fig. 9). Station work began the same day. The dense station spacing in conjunction with quiet weather facilitated the establishment of the necessary station work routine. We worked 5 short sections down the Greenland slope which covers the range from the cold and fresh East Greenland Current of polar origin to the warm and saline Atlantic water of the Irminger Sea (Fig. 10). During the VEINS part of our programme, which was finished on 24 August, 23:30 UTC (stat # 505), we worked 43 CTD/LADCP/Rosette stations, deployed 6 current meter moorings, 2 inverted echo sounders (IES) and recovered 4 moorings and one IES (see station listing 7.5.1, Fig. 9). Unfortunately, the recovery (dredging) of 5 moorings deployed in 1995 and 1996 failed. Stat. # 505 was also used as a test station for a performance check of all 3 CTD systems available.

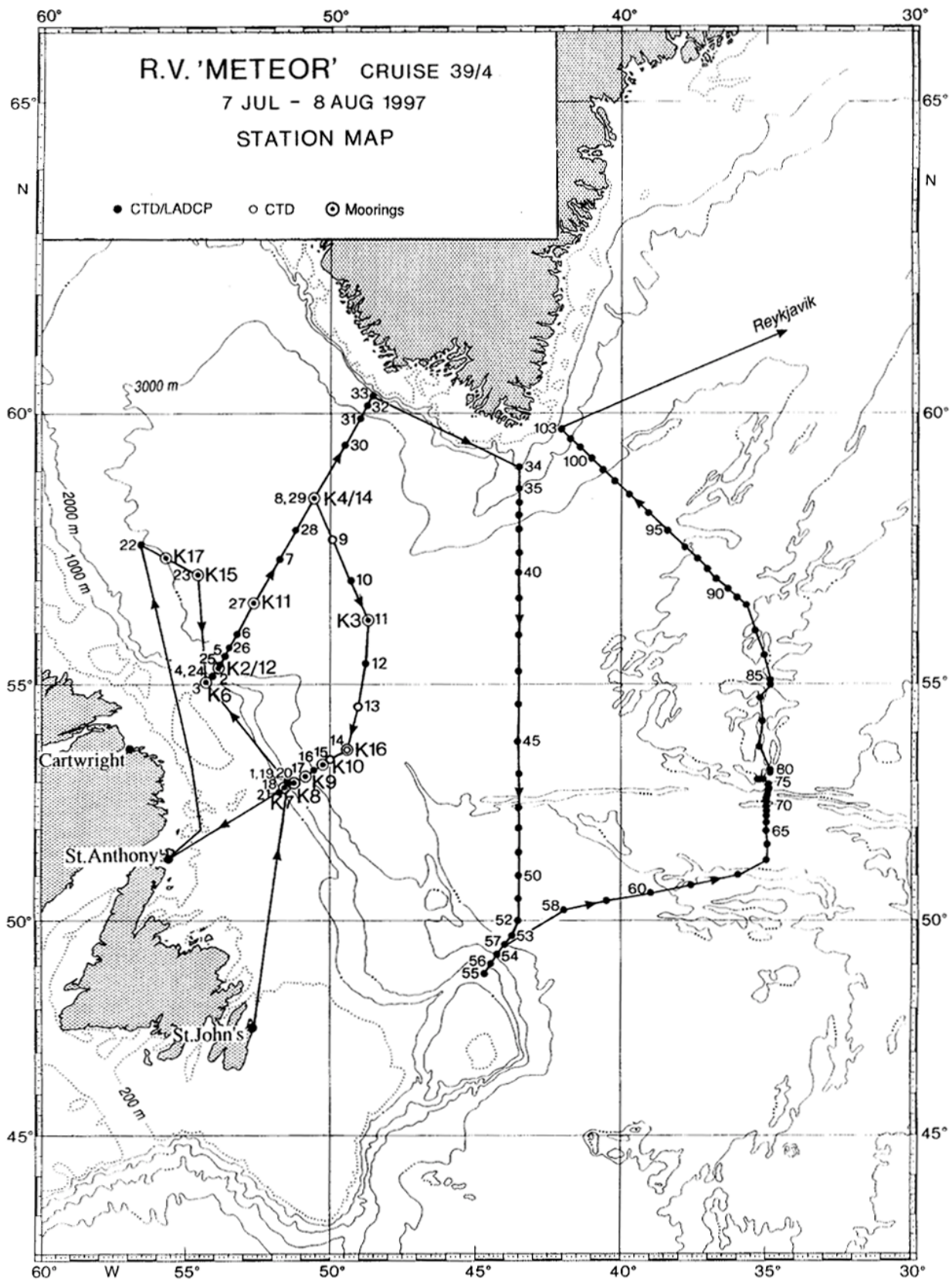
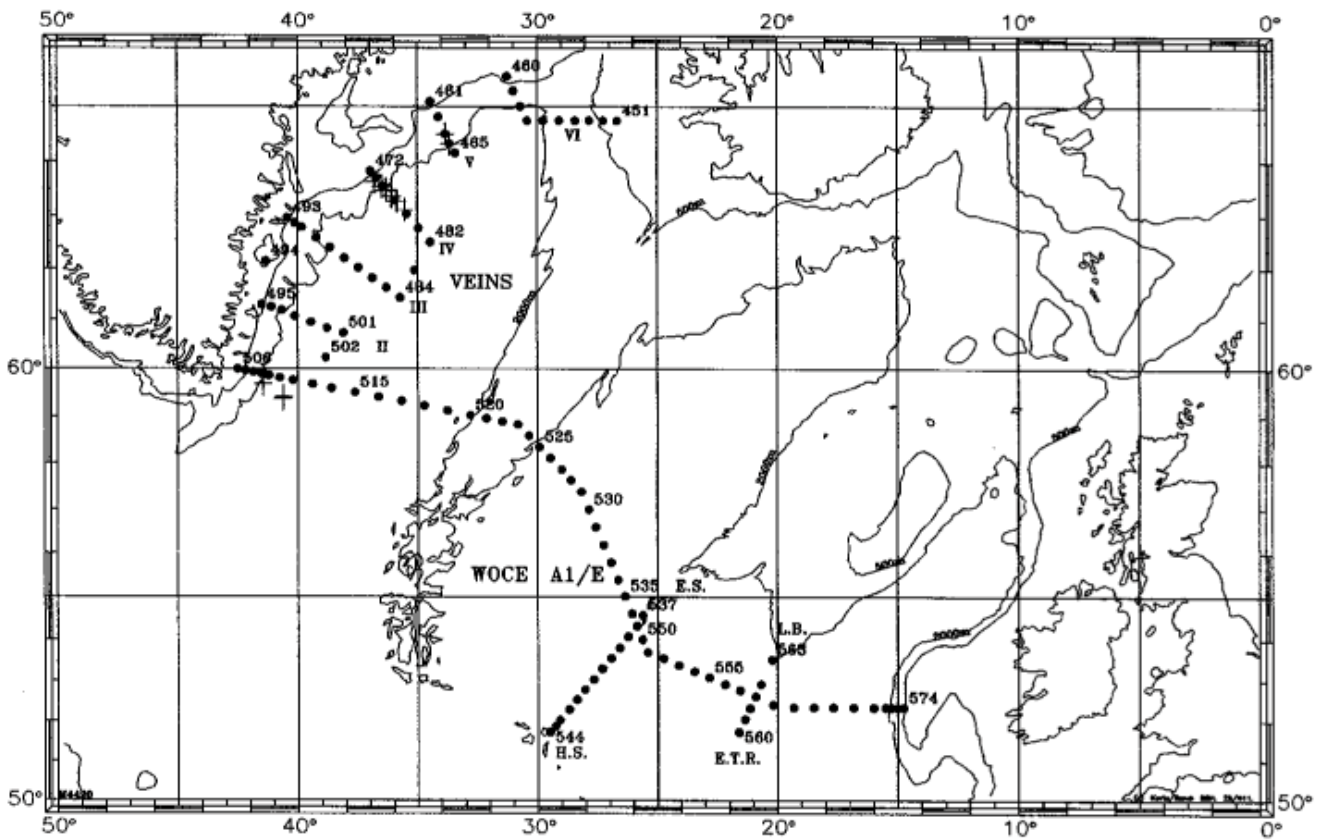


Fig. 8: Cruise track and station map of METEOR leg M39/4.

CTD station work was resumed on 25 August at 07:00 UTC at the western end of the WOCE section A1/E on the eastern Greenland shelf at 60°N, 42.5°W. Because wind and sea conditions (see section 6.5) were moderate throughout, and we encountered no serious technical problems, station work proceeded fast and without any interruptions until 6 September. We were thus in the favourable position of having time to spare, which we used for two additional sections. These were orientated normal to the WOCE section from Eriador Seamount to Hecate Seamount (stat # 537 - 549) and from Lorien Bank to East Thulean Rise (stat # 558 - 563).

From 6 September, 17:00 UTC to 8 September, 04:30 UTC, station work had to be interrupted for the recovery of an ill crew member by an Irish rescue helicopter (MRCC Dublin). After that action and a detour of 360 nm, station work was resumed and the WOCE section was completed successfully on 9 September, 22:30 UTC. METEOR set course for the English Channel and reached Hamburg on 14 September 1997, at 10:00 LT.



R.V. "METEOR" cruise # 39/5 VEINS and WOCE, 14.08.97-09.09.1997, station work: ● CTD, + Mooring

Fig. 9: positions of CTD_{O₂}/rosette stations for R.V. METEOR cruise M39/5.

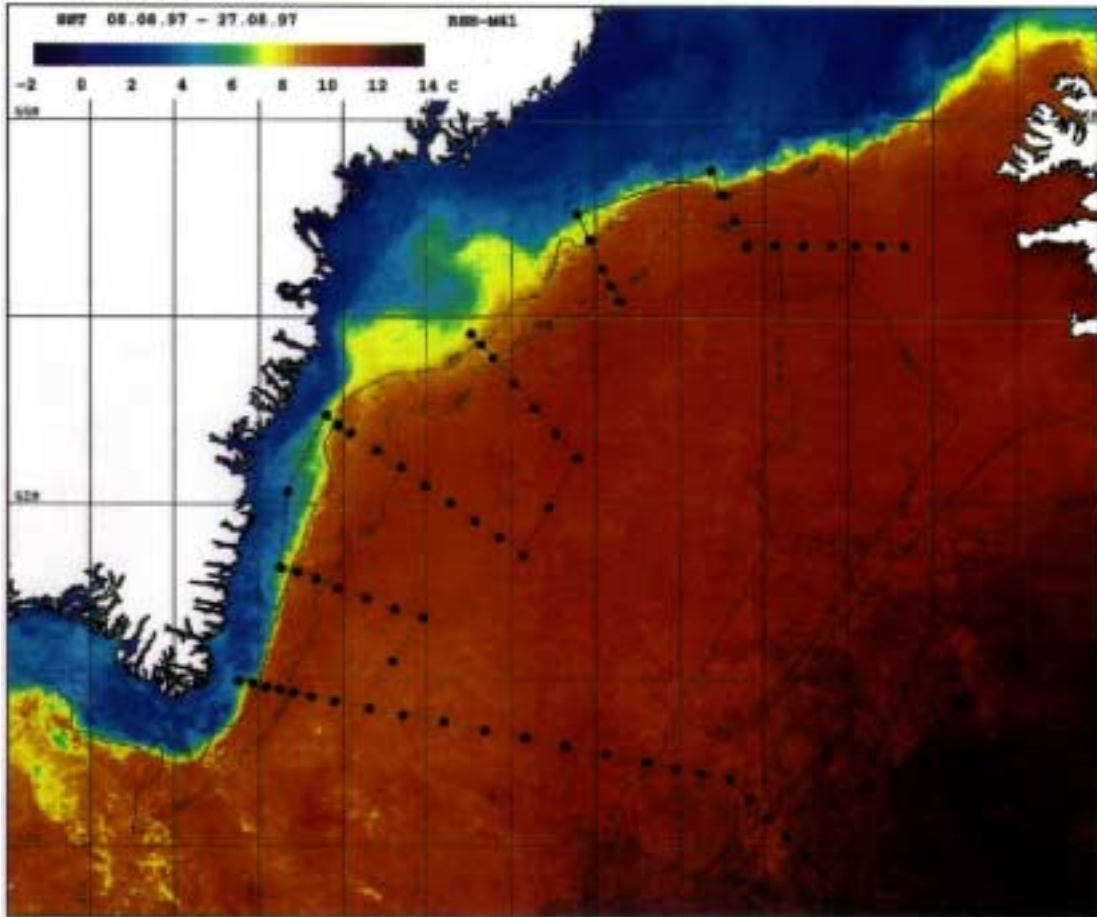


Fig. 10: Irminger Sea SST with M39/5 CTD stations (sea surface temperature composed from NOAA-12 and NOAA-14, 8.8.-27.8.97).

5 Preliminary Results

5.1 SFB 460

5.1.1 Physical Oceanography of the eastern Basin (M39/2)

5.1.1.1 Hydrography

(S. Becker, B. Lenz, T.J. Müller, W. Zenk)

A CTD in combination with a rosette sampler (21x10 l bottles) for the analysis of dissolved oxygen and nutrients was used to investigate the structure of water masses on sections (see Fig. 3) in The Iceland Basin north of 50°N. The water masses are:

- Subpolar Mode Water (SPMW)
- North Atlantic Central Water (NACW)
- Intermediate Water (IW)
- Mediterranean Water (MW)
- Labrador Sea Water (LSW)
- Lower Deep Water (LDW)
- Iceland Scotland Overflow Water (ISOW)
- North East Atlantic Deep Water (NEADW)
- Antarctic Bottom Water (AABW) Fig. 11 shows the potential temperature salinity (θ/S) relation in four selected regions:
- Western European Basin (WE)
- Rockall Trough (RT)
- Northwestern Iceland Basin (NI)
- Charlie Gibbs Fracture Zone (GF)

Three representative stations per region are plotted for each of the above regions. Surface and mode water vary between 9 and 15°C in potential temperature θ and 35.0-35.7 in salinity S (Fig. 11a). Remnants of NACW occupy the main thermocline. Traces of Mediterranean Water are most prominent in the Western European Basin, with core salinities $S > 35.4$. Isolated lenses of this water mass were found in Rockall Trough and even in the northwestern corner of the Iceland Basin. The base of NACW range overlaps with IW which primarily is identified by low oxygen (O_2) and high nitrate (NO_3) concentrations (VAN AKEN and DE BOER, 1995), and which is found at approximately 7-8°C in the relations of θ/O_2 (Fig. 12) and θ/NO_3 (not shown here).

The deeper water masses can be identified more clearly in for $\theta < 4^\circ\text{C}$ in Fig. 11b. The minimum salinity in the core of the LSW is found in the Gibbs Fracture Zone ($S_{\min} = 34.87$). Also, LSW is coldest in this region, and with $\theta < 2.95^\circ\text{C}$, its temperature is well below that observed by SY et al. (1997) who found minimum temperatures on WOCE section A2 (48°N) of 3.20°C one year before. The cold ($\theta < 2.5^\circ\text{C}$), salty ($S > 34.96$) and oxygen-rich ISOW like LSW shows pronounced horizontal gradients. Being almost at the same density as ISOW, LDW is marked by higher salinity and nutrients. In silica, e.g., the concentrations in water with high amount of LDW are about three times larger ($> 45 \mu\text{mol/l}$) than those for with high amounts of ISOW ($< 18 \mu\text{mol/l}$, Fig. 13). Note that in the deep Rockall Trough phosphate contents are relatively high when compared to the other regions in terms of the Redfield ratio (Fig. 14).

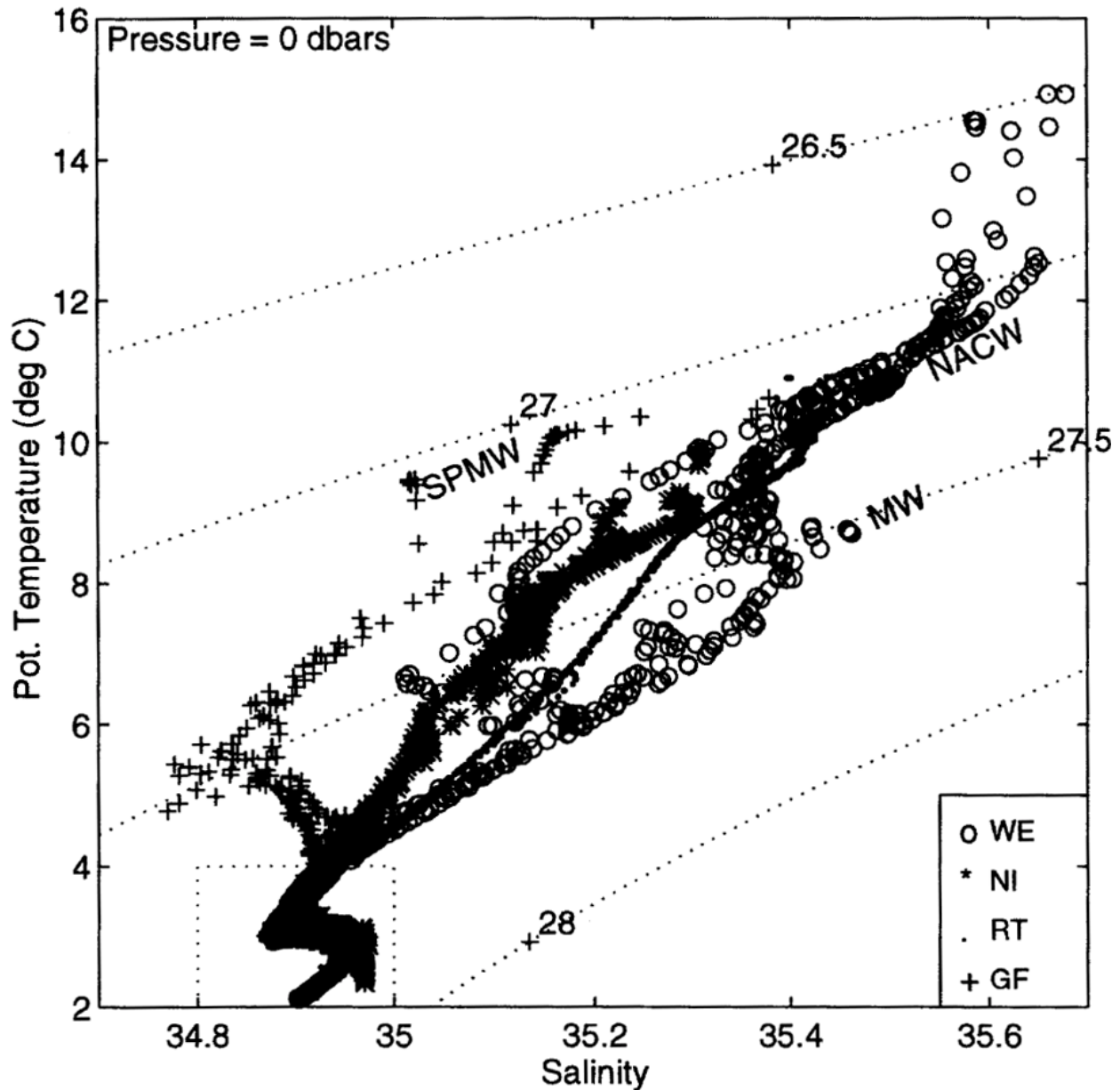


Fig. 11a: Potential temperature (θ) salinity diagram from 4 representative regions in the Iceland Basin. Their locations are shown in Fig. 3: WE-Western European Basin (Sta. 267-269), NI-northern Iceland Basin (Sta. 216-218), RT-Rockall Trough (Sta. 203-205), and GF-Charlie Gibbs Fracture Zone (Sta. 254-256). Lines of equal density are shown as σ_θ (kg m^{-3})-isolines. Subpolar Mode Water (SPMW) primarily is found in the southwestern region of the basin (GF), North Atlantic Central Water (NACW) is restricted to the more easterly located regions off the European shelf and likewise the remainders of the Mediterranean Water (MW) with their clear intermediate salinity maximum. A subset of these stations with $\theta \pm 4^\circ\text{C}$ are shown in Fig. 11b. Data are based on CTD stations from M39/2, equally spaced at 10 dbar.

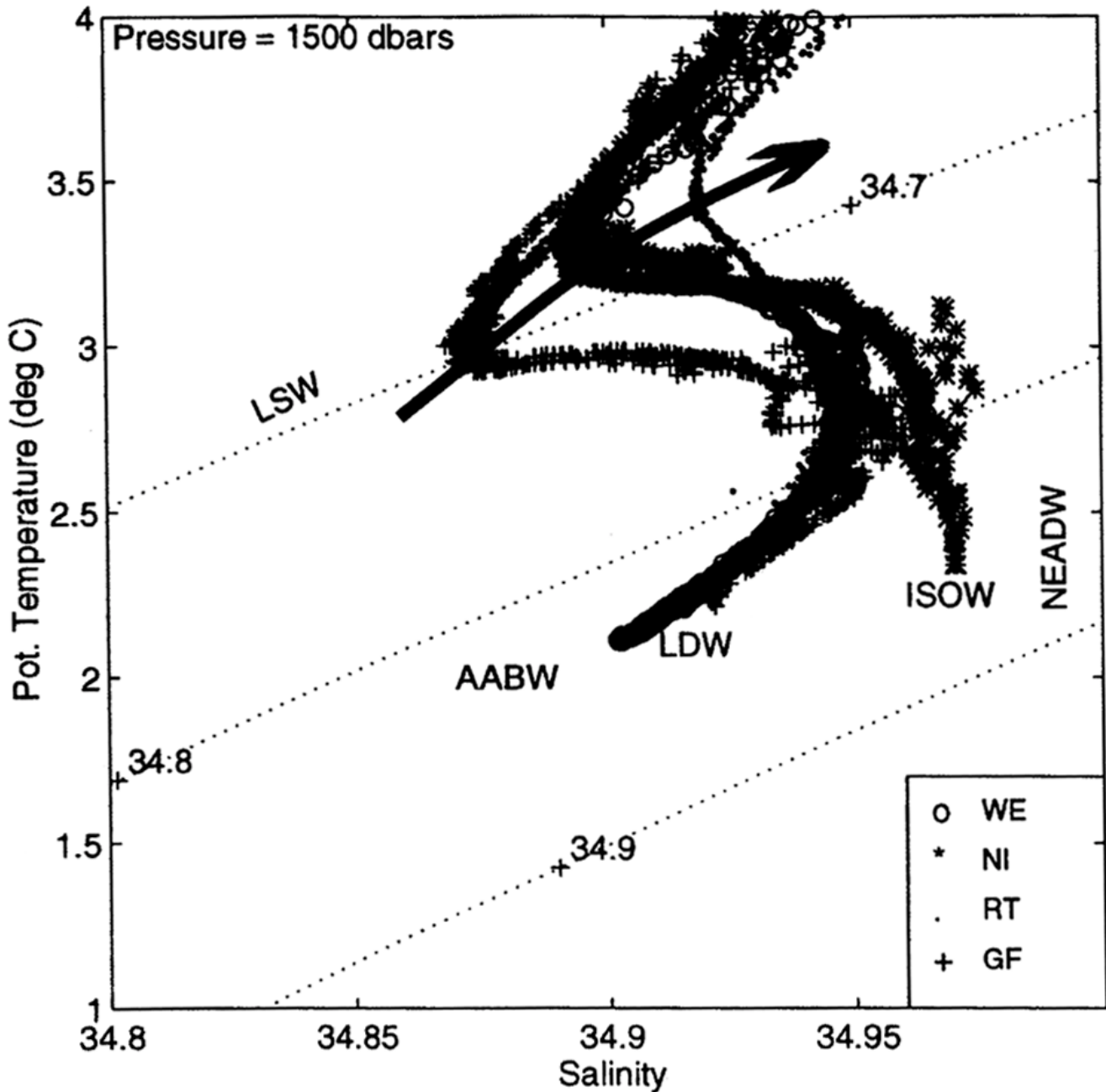


Fig. 11b: Enlarged θ/S diagram for $\theta \leq 4^\circ\text{C}$ inferred from Fig. 11a (box). Water masses of the Cold Water Sphere can be identified: LSW at $\sigma_{1.5}=34.7 \text{ kg m}^{-3}$ is characterized by its clear minimum in salinity. While progressing eastward through Gibb Fracture (SY et al., 1997) it mixes with SPMW, resulting in a systematic increase of temperature and salinity (arrow). Below LSW we encounter LDW penetrating into the Western European Basins as an eastern boundary current derived from AABW ($\theta \leq 2^\circ\text{C}$). At comparable density levels we find ISOW on the flanks of the Reykjanes Ridge in the NW corner of the basin. As this water mass follows the Ridge, it mixes horizontally contributing to the NEADW formation.

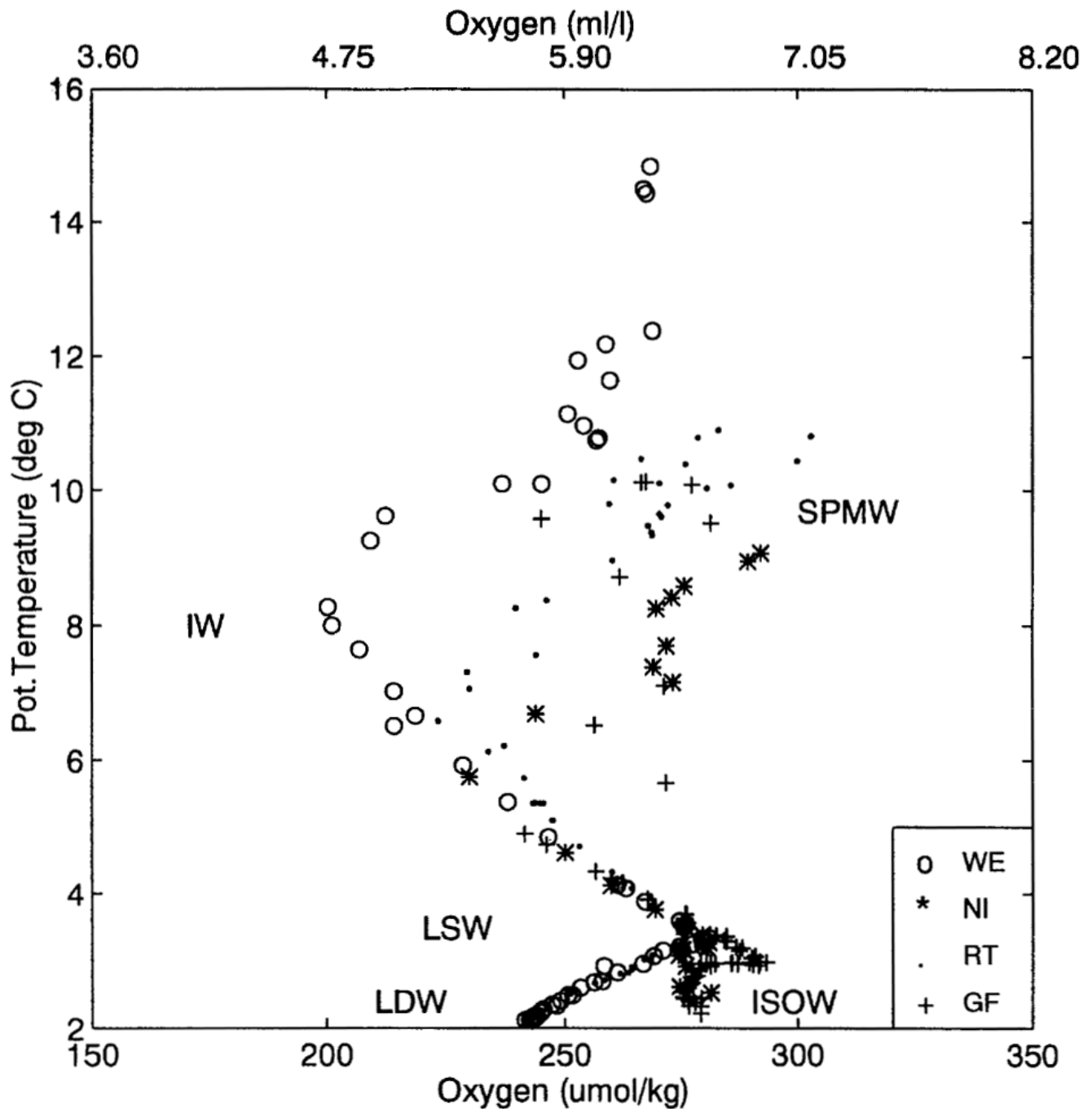


Fig. 12: θ/O_2 diagram from rosette samples from CTD stations indicated in Fig. 11a. Remnants of local deep winter convection result in highly ventilated water masses of the thermocline, SPMW. Additional highs in O_2 are found in the LSW and the ISOW. The deepest water masses in the east have their origin in remnants of AABW, called LDW. Lowest O_2 values were encountered in the Western European Basin where VAN AKEN and DE BOER (1995) define their Intermediate Water (IW) at $\theta \sim 8^\circ\text{C}$.

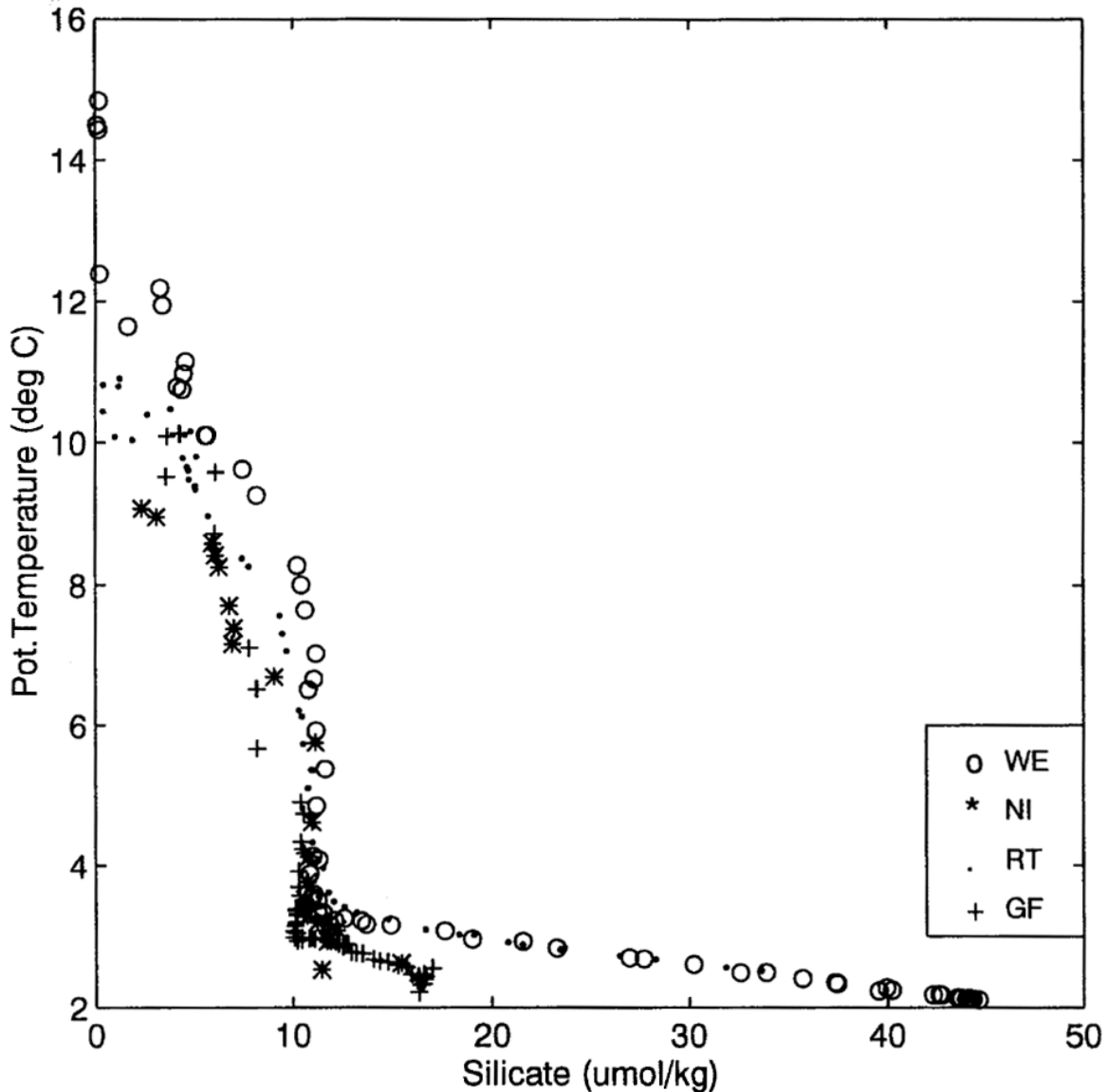


Fig. 13: At the surface SiO_4 is a deficit nutrient salt. The most distinct signal was encountered in the LDW. Values $> 40 \mu\text{mol/kg}$ identify clearly their origin in AABW source waters. Some minor amount is advected through Gibbs Fracture ($>17 \mu\text{mol/kg}$).

We briefly discuss two of the four sections (locations see Fig. 3) as examples: Section A from the northern edge of Porcupine Bank to the northern end of Reykjanes Ridge and section D which runs parallel to the array of current meter moorings.

At the thermocline level of the northern (ca. 58°N) section A (Fig. 15) we find the 8°C -isotherm crossing the 250 m level as an indicator of the Subpolar Front which is closely related to the North Atlantic Current (KRAUSS, 1986). The thermal stratification decreases at the level of the Labrador Sea Water (1200-2000 dbar) where we also find the pronounced minimum in the θ/S -relation. In the Iceland basin the associated core layer sinks from approximately 1200 dbar on the eastern flanks of the Reykjanes Ridge down to 1800 dbar above Maury Channel. Beneath

the Labrador Sea Water we recognize the cold ($\theta < 2.9^{\circ}\text{C}$) and saline ($S > 34.96$) contours of the Iceland Scotland Overflow Water. As expected, intermediate and bottom water parameters are absent in the Iceland Basin and less pronounced in the Rockall Trough.

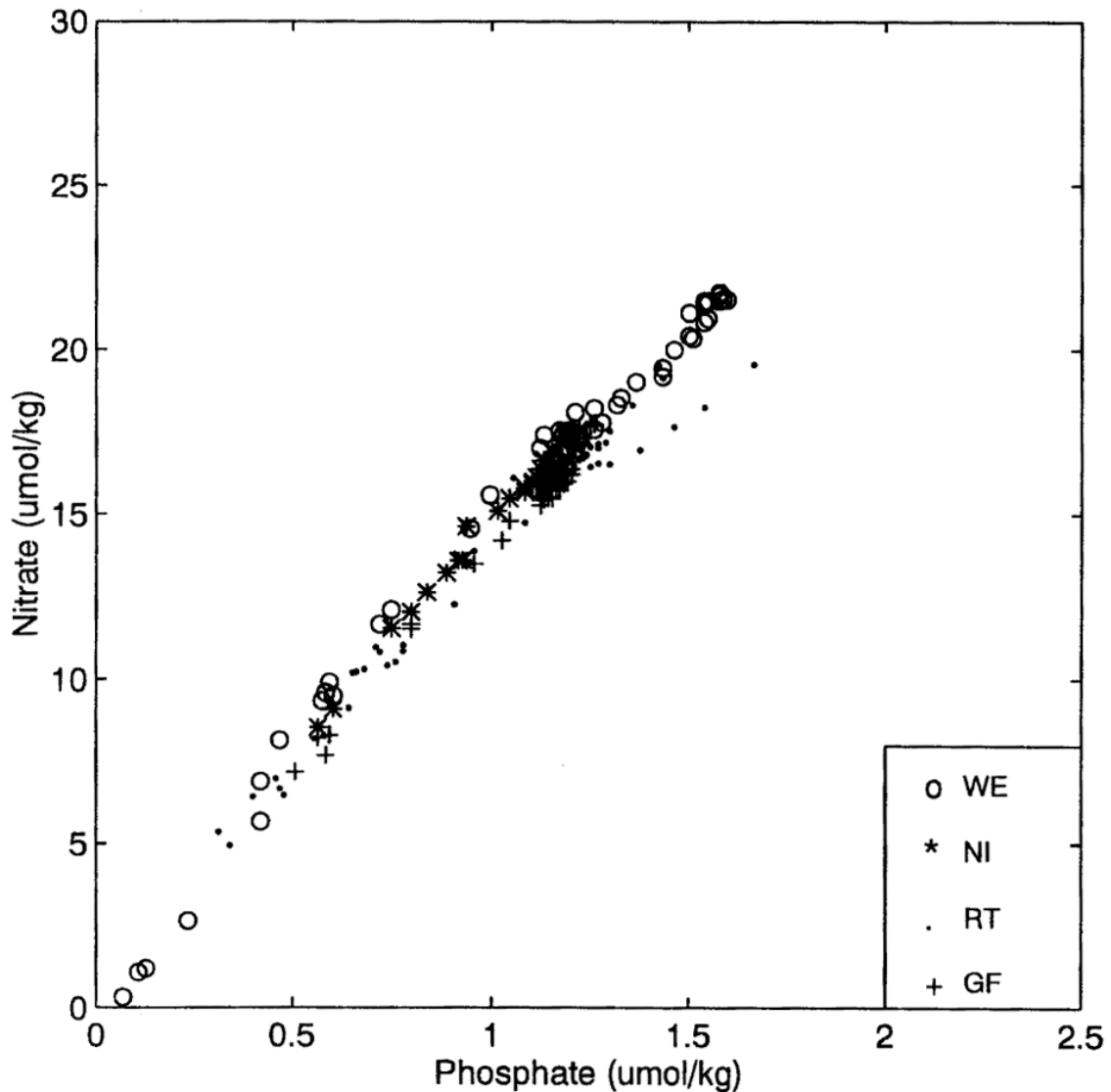


Fig. 14: The Redfield ratio in the four test regions of the Iceland Basin. The slope derived from all data excluding stations from the Rockall Trough (RT) is 12:1. Apparently the Rockall Trough is enriched by PO_4 .

We show the distribution of salinity, oxygen and silicate on Section D (Fig. 16) just north of Gibbs Fracture as background information for our current meter array (see Table 7.2.2 upper half). Current recording instruments are concentrated on the low saline and oxygen rich Labrador Sea Water and on the more saline Iceland Scotland Overflow Water which on its way southward has been already entrained by silicate-rich Northeastern Atlantic Deep Waters.

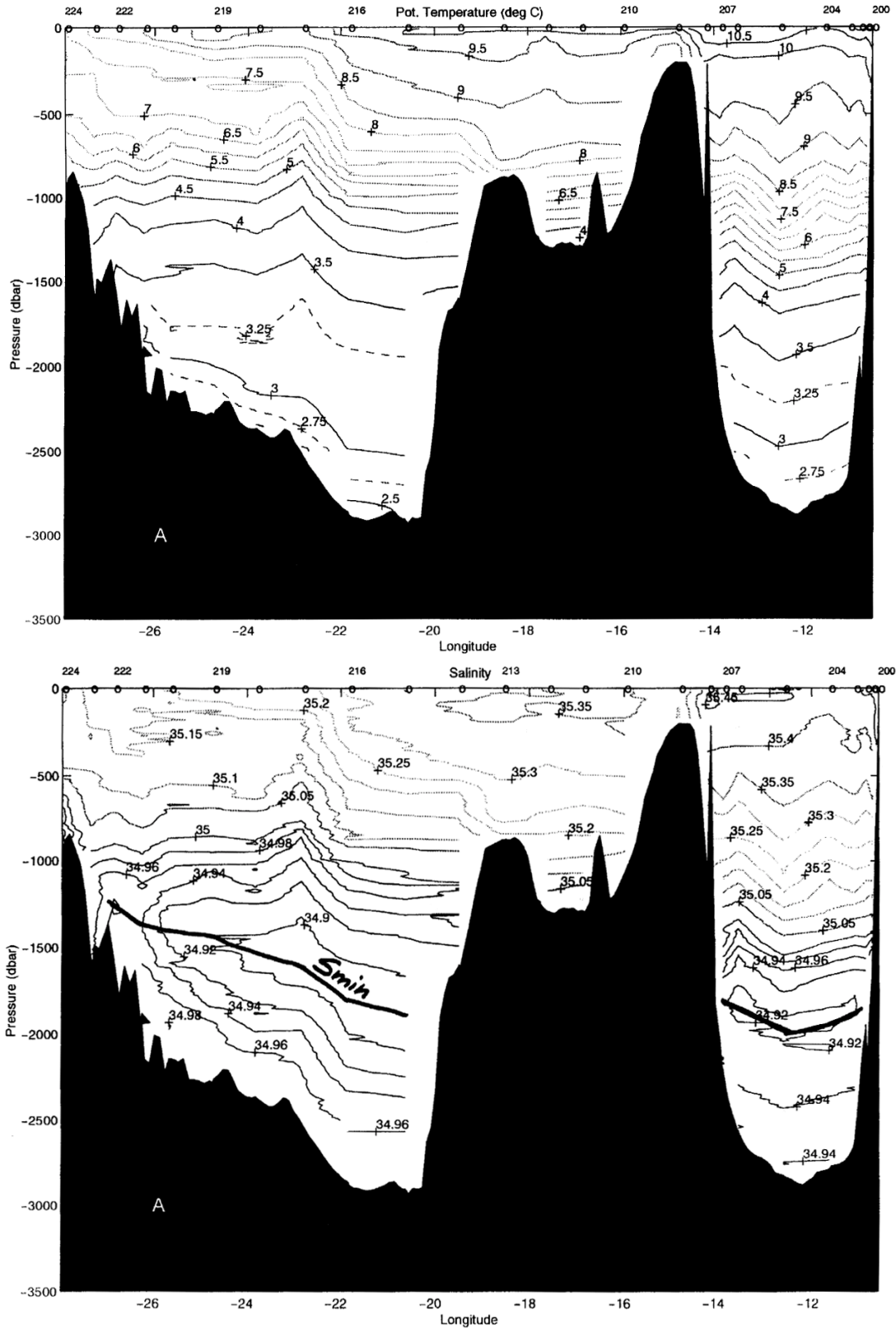


Fig. 15: Section A (see Fig. 3) at nominally 58°N showing the distribution of potential temperature (a) and salinity (b).

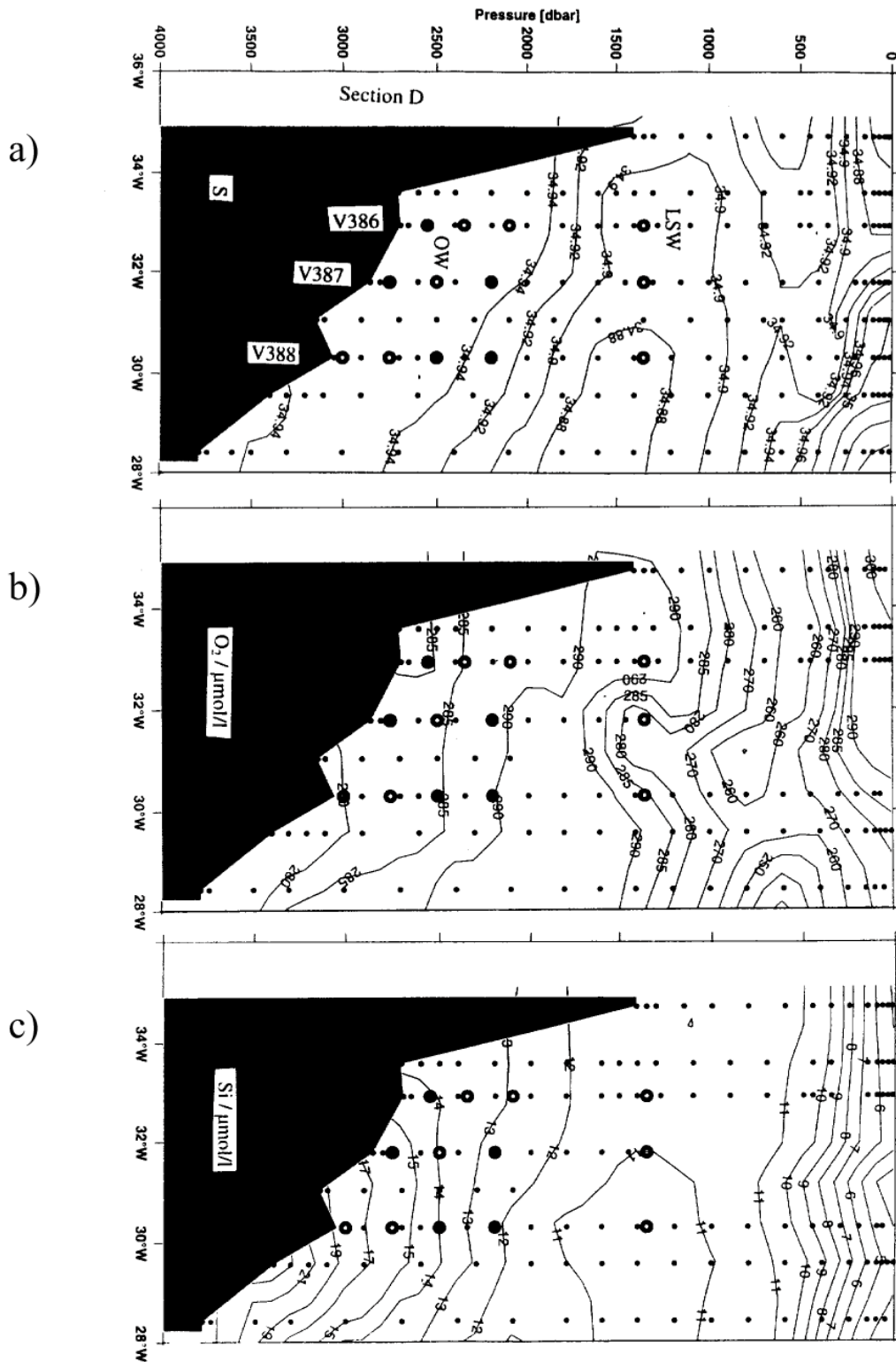


Fig. 16: Distribution of salinity (a), oxygen (b) and silicate (c) on Section D (see Fig. 3). Data (black dots) were collected by the rosette sampler operated jointly with the CTD probe. Overlaid circles represent locations of moored current meters for the observation of deep boundary currents along Reykjanes Ridge.

5.1.1.2 Freon Analysis (CFC) (O. Plähn)

Methods

During M39/2 about 1200 water samples have been measured on 66 CTD station to analyse the CFC components F11 and F12. About 10 to 25 ml of seawater are transferred from precleaned 10 L Niskin bottles to a purge and trap unit. The gases are separated on a gas chromatographic column and detected with an electron capture detector (ECD). Before and after each station, a calibration curve with 6 different gas volumes was taken. Assuming a linear drift between both calibrations, the ECD signals are converted into CFC concentrations.

The observed temporal variations of the ECD were very stable for the F12 component, whereas for F11 the observed variability was in the order of 30%. The mean blank of the sample transfer and the measurements procedure was determined by degassing CFC free water, produced by purging ECD clean Nitrogen permanently through 5 L seawater. The blanks were in the order of 0.004 pmol/kg for both components.

The accuracy was checked by analysing about 350 water samples twice or more. It was found to be 0.6% for CFC-11 and 0.7% for CFC-12. At some stations, the F12 peak was disturbed by a high N₂O level of the samples. Air samples were taken regularly, to find possible contamination inside the vessel and to analyse the clean air outside the vessel. The saturation at the surface of both components was about 100%±5%.

Preliminary results

Along the first section (Ireland-Reykjanes Ridge) the lowest CFC concentrations -less than 1 mol/kg for CFC-11- were measured at the bottom of the Rockall Trough. The high silicate concentration (>20 µmol/kg) at that region, leads to the assumption that this water comes partly from the southern hemisphere. Overflow water masses from the Arctic are not found at this trough, in contrast to the Maury Channel. In this deep basin a significant signal of Iceland Scotland Overflow Water (ISOW) was found at the bottom. The high CFC concentrations (CFC- 11>2.3 pmol/kg) correlate with salinity (>34.95). The small tongue of overflow water had an vertical extension of only 200 m, with a density of sig >27.87. Above the ISOW water with lower salinities (<34.95) and lower CFC-11 (<2 pmol/kg) are found. Whereas the concentrations of the CFC minimum increase to the north, with values of less than 1.6 pmol/kg (CFC-11) at the southwestern edge of the Rockall Bank.

Along the eastern flank of the Reykjanes Ridge, ISOW spreads southward, with a mean CFC-11 signal of 2.5 pmol/kg at 60°N. Along its pathway the concentration decreases, and perpendicular to the flow direction, the concentration gradient increase. In the flow through the Charlie-Gibbs-Fracture-Zone, the CFC-11 concentration was 2.3 pmol/kg in the core of the ISOW, at the northern edge of the fracture zone.

The largest freon signal of the LSW was measured southwest of the Charlie-Gibbs-Fracture-Zone with concentrations of more than 3.2 pmol/kg. Spreading eastwards this strong signal decreases steadily. In the density range between 27.75 and 27.78, the average CFC-11

concentration was less than 2 pmol/kg in the Rockall Trough and about 2.7 pmol/kg in the Iceland Basin. Due to vertical mixing along the Reykjanes Ridge, in some profiles no concentration maximum could be observed. Along the 51°N section the LSW signal was observed east of 15°W, marked by oxygen and CFC-11 maxima.

5.1.1.3 Carbon Dioxide System, Nutrients and Oxygen (A. Körtzinger)

a) Background

The ever increasing demands of our expanding human population have led to considerable anthropogenic emissions of greenhouse gases with carbon dioxide being the most prominent one. The well-known impact of these greenhouse gases on the radiative balance of our planet has brought the whole question of climate change into discussion. This problem has been fully recognized during the last decades and ambitious international research programs focusing on the different reservoirs of the global carbon cycle have been launched. The ocean has long since been identified as a significant sink of this anthropogenic or “excess” CO₂. However, the marine carbon cycle with its complex coupling to physical, chemical and biological processes is still not fully understood. Reliable predictions of future climate change can only be achieved on the basis of a profound understanding of the natural carbon cycle, the largest rapidly exchanging reservoir of which is the ocean.

The North Atlantic plays a major role in the climate system with its large air-sea exchange fluxes. This is not only true for heat and freshwater but also for carbon dioxide. With the downward moving limb of the global ocean conveyor being located in the North Atlantic Ocean this part of the world ocean seems to play a key role. While the mean ventilation of the ocean constitutes the main kinetic barrier for equilibration with the perturbed atmosphere, the North Atlantic provides a “window” of the deep ocean to the atmosphere which allows the excess CO₂ to penetrate more rapidly. We have shown previously that the anthropogenic CO₂ has penetrated through the entire water column down to depths of 5000 m in the western basin of the North Atlantic. The eastern basin still shows much deeper penetration (3000-4000 m) than anywhere else in the oceans. The new Sonderforschungsbereich 460 at the University of Kiel on the decadal variability of the thermohaline circulation is focusing on the formation and modification of deep and intermediate waters in the North Atlantic Ocean. As part of this ambitious program a marine chemistry project has been implemented to study the importance of the thermohaline circulation and its variability for the natural carbon cycle and the uptake of anthropogenic CO₂. After completion of the WOCE-WHP section A2 in Nov 1994 (METEOR 30/2) this project has now started field work in the ocean domain of the new SFB 460.

b) Methods

Nutrient and Oxygen Measurements

Dissolved oxygen was measured based on a titration method first proposed by Winkler as described in GRASSHOFF et al. (1983). This method yields an accuracy of the order of 0.5 µmol/l.

Nutrient concentrations were measured photometrically after conversion of the analytes into colored substances as described in GRASSHOFF et al. (1983). All measurements were carried out with an Auto-Analyzer continuous flow technique. Estimated accuracy is 0.02 $\mu\text{mol/l}$ for nitrite, 0.1 $\mu\text{mol/l}$ for nitrate, 0.05 $\mu\text{mol/l}$ for phosphate and 0.5 $\mu\text{mol/l}$ for silicate.

Measurements of Carbon Dioxide System Parameters

The collection of extensive, reliable, oceanic carbon data is a key component of the Joint Global Ocean Flux Study (JGOFS) and has also been an important aspect of the World Ocean Circulation Experiment (WOCE). Based on these international efforts to understand the marine carbon cycle on a global scale, standard methods and operating procedures have been defined to allow for a global synthesis of the vast amount of data obtained. All carbon dioxide system measurements carried out during cruise M39/2 of R/V METEOR are based on such well-tested analytical methods and procedures as described in DOE (1994).

Unfortunately, the concentrations of the individual species of the carbon dioxide system in solution cannot be measured directly. There are, however, four parameters (i.e. CO_2 partial pressure, pH value, total dissolved inorganic carbon, alkalinity) that can be measured. Together with knowledge of the thermodynamics involved any combination of two of these parameters can be used to obtain a complete description of the carbon dioxide system in seawater. Two different sampling strategies were followed during cruise M39/2. The first comprised continuous measurements of the partial pressure of CO_2 in surface seawater and air along the cruise track. The second sampling strategy followed "classical" collection of water samples from hydrocasts along 7 transects for measurements of total dissolved inorganic carbon and alkalinity. This also included sampling at selected sites for measurements of the $\delta^{13}\text{C}$ value of the dissolved inorganic carbon.

Underway Measurements

Profiles of the partial pressure of CO_2 ($p\text{CO}_2$) in surface seawater and overlying air were obtained with a newly designed, automated underway $p\text{CO}_2$ system (KÖRTZINGER et al., 1996). This system has shown excellent agreement with another system developed at the Institute for Baltic Research in Warnemünde/Germany (ibid). Seawater was pumped from the moon pool of R/V METEOR by means of a submersible pump (ITT Flygt Pumpen GmbH, Langenhagen/ Germany) at a pump rate of about 30 L/min. The flow of about 2 L/min required for the analysis was teed-off close the equilibrator. *In-situ* temperature and salinity were measured at the seawater intake with a CTD probe (ECO, ME Meerestechnik Elektronik GmbH, Trappenkamp/Germany). Clean air was pumped from an intake on "monkey's island". The measurement routine comprised recalibration of the system every six hours using two standard gases with known CO_2 concentrations in natural air prepared by the NOAA Climate Monitoring and Diagnostics Laboratory in Boulder, Colorado/U.S.A. as well as nitrogen as a zero gas. The resulting accuracy of the measurements is better than 1 ppm. Air was measured every hour for two minutes. All data were logged as 1-minute averages together with T/S data from the CTD as well as navigational data (position, speed and course over ground) from a separate GPS receiver.

The $p\text{CO}_2$ data are corrected for the non-ideal behavior of CO_2 (i.e. they are given as fugacity of CO_2 or $f\text{CO}_2$). They are also corrected back to *in-situ* temperature accounting for the slight warming during passage of the seawater to the system. All $f\text{CO}_2$ values are calculated for 100% humidity at the air-sea interface to allow for direct flux calculations.

Discrete Measurements

The total dissolved inorganic carbon content (C_T) was measured using the so-called SOMMA system, which has become the standard method for a major part of the JGOFS and WOCE activities especially in the U.S. community. The system consists of an automated extraction unit with a coulometric detector (JOHNSON et al., 1993). It was calibrated with known amounts of pure CO_2 . The calibration was checked regularly (i.e. roughly every 15 samples) with certified reference material provided by Andrew Dickson from the Scripps Institution of Oceanography, Marine Physical Laboratory, La Jolla, California/U.S.A. The obtained precision is of the order of 0.5-1 $\mu\text{mol/kg}$. The achieved accuracy is better than 2 $\mu\text{mol/kg}$ as judged from repeated measurements of the certified reference material.

The alkalinity (A_T) was measured by potentiometric titration of a known volume of seawater with hydrochloric acid basically according to MILLERO et al. (1993), but carried out in an open vessel (VINDTA system, MINTROP (1996), unpubl.). The progress of titration was monitored using a glass electrode/reference electrode pH cell. Total alkalinity was computed from the titrant volume and the electromotoric force data using a least-squares procedure based on a non-linear curve fitting. The titration factor of the hydrochloric acid was measured at high accuracy by Andrew Dickson. The system was also checked regularly (i.e. roughly every 15 samples) with the same certified reference material provided by Andrew Dickson. The precision as estimated from repeated measurements of the certified reference material was about 3 $\mu\text{mol/kg}$. Due to the lack of a superior reference method the accuracy of the method is difficult to estimate. It is probably of the order of 5 $\mu\text{mol/kg}$.

c) First Glance at the Data

Sample Statistics

A total of 1209 samples from 64 stations were analyzed for nutrients (nitrate, nitrite, phosphate, silicate) and dissolved oxygen. A total of 529 samples from 30 stations were analyzed for C_T and A_T . All systems operated throughout the cruise without any major problems or unusual quality restrictions.

The $p\text{CO}_2$ system was also operated throughout the cruise with two minor exceptions, an initial delay (until May 26, 08:30 UTC) caused by computer problems and a short break (May 24, 21:00 UTC to May 25, 10:00 UTC) due to failure of the submersible pump. The total distance covered by these underway measurements of $p\text{CO}_2$ (in seawater and air), temperature and salinity is about 3600 nm.

Underway Measurements

The measured CO₂ mole fraction in dry air ranged between 367 and 370 ppm for most of the cruise. An atmospheric temperature inversion encountered during May 16 close to the coast of Ireland was accompanied by increased atmospheric CO₂ concentrations of up to 380 ppmv. This increase reflects the influence of CO₂ from sources on the European continent accumulating under the inversion, which serves as a barrier for vertical mixing in the atmosphere. Due to the relative large observed range in barometric pressure (approx. 997-1026 hPa) the resulting atmospheric *f*CO₂ is roughly 366±6 µatm.

The observed range of *f*CO₂ in surface seawater is 260 to 360 µatm. Lowest values were found close to the Irish coast, probably due to the influence of riverine freshwater input. The *f*CO₂ in seawater generally increased towards the west and highest values were found at the western ends of most transects. The covered area of the eastern North Atlantic Ocean has been found to serve as a significant sink for atmospheric CO₂. In the eastern part this sink was as large as 60-80 µatm difference between air and seawater *f*CO₂ ($\Delta f\text{CO}_2$), which translates into large air-to-sea fluxes of CO₂ under the prevailing high wind stress (i.e. high transfer coefficients). Close to the Mid-Atlantic Ridge the sink was considerably smaller with a $\Delta f\text{CO}_2$ of 5-50 µatm and some areas close to equilibrium. The mean undersaturation of surface waters along the cruise tracks was of the order of 30-40 µatm. The temperature range between up to 15°C in the east and around 7°C in the west was not found to be the major driving force behind the general *f*CO₂ patterns in surface waters. These more likely reflect the different “history” of the surface waters, i.e. their source region and contact time with the atmosphere.

These findings are in good agreement with the current understanding of the role of the North Atlantic in the global carbon cycle. Large volumes of surface waters are transported northwards through the Gulf Stream and the North Atlantic Current. These waters are strongly cooled during their passage hereby decreasing significantly their *f*CO₂ due to the temperature dependant solubility of CO₂. This process generates a strong undersaturation of surface waters which drives large air-sea exchange fluxes of CO₂. Furthermore this effect can be strongly enhanced during spring bloom situations as marine phytoplankton take up CO₂ during photosynthesis. An indication of such bloom situations was found at some locations in the eastern part of some transects. While chlorophyll measurements were not carried out during this cruise the strong changes in water colour give valuable hints for biological productivity.

Water Column Data

From the broad set of water column data only the vertical distribution of total dissolved inorganic carbon (C_T) shall be discussed here briefly. A typical C_T profile shows lowest values at the surface, where waters are generally not too far from equilibrium with the atmosphere. Below the surface mixed layer C_T values increase with depth as a result of the remineralization of particulate organic carbon in the water column and the dissolution of particulate biogenic carbonates. The first process takes place in much shallower depths generating a C_T maximum at depths of about 800-1200 m. The second process generally takes place much deeper depending on the depth of the lysocline of calcite (and aragonite). These are deepest in the

North Atlantic Ocean (>4000 m for calcite) so that carbonate dissolution is a minor process and no significant C_T increase from this source is found at greater depths.

The C_T profiles of three stations (205, 251, 268) are shown in Fig. 17. Station 205 is located on transect "A" in the Rockall Basin, station 251 on transect "E" in the Charly Gibbs Fracture Zone and station 268 on transect "G" in the eastern basin of the North Atlantic Ocean. The three profiles show quite different patterns. At station 205 the extreme depth of the winter mixed layer is still reflected in the profile. While a much more shallow mixed layer of around 100 m was present at the time sampling; C_T values around 2132 $\mu\text{mol/kg}$ at depths of 100-700 m represent the remains of the very deep winter mixing in this area. This can also be seen at station 268 at 100-400 m depth. The remineralization maximum is found at depths between 400 m (station 251) and 1200 m (station 205). Station 205 and 268 show a strong increase in C_T values of up to 50 $\mu\text{mol/kg}$ at depths greater than 2000 m. This is indicative of much older waters which carry a higher signal of respiratory CO_2 and represent the northernmost extensions of the Antarctic Bottom Water. There is no comparable increase in the deep waters at station 251.

As the distribution of C_T in the water is influenced by different processes (physical, chemical and biological) the presence of "excess" CO_2 cannot be identified directly. There are, however, techniques to identify the anthropogenic fraction which makes up between 0 and 60 $\mu\text{mol/kg}$ depending on the time of ventilation. It is assumed that overflow water found at the western ends of the transects and in the Charly Gibbs Fracture Zone as well as the recently formed Labrador Sea Water carry a higher anthropogenic CO_2 signal. With the present data set we have a very good basis to understand the distribution of anthropogenic CO_2 in the eastern North Atlantic and to improve previous estimates of total inventory of anthropogenic CO_2 .

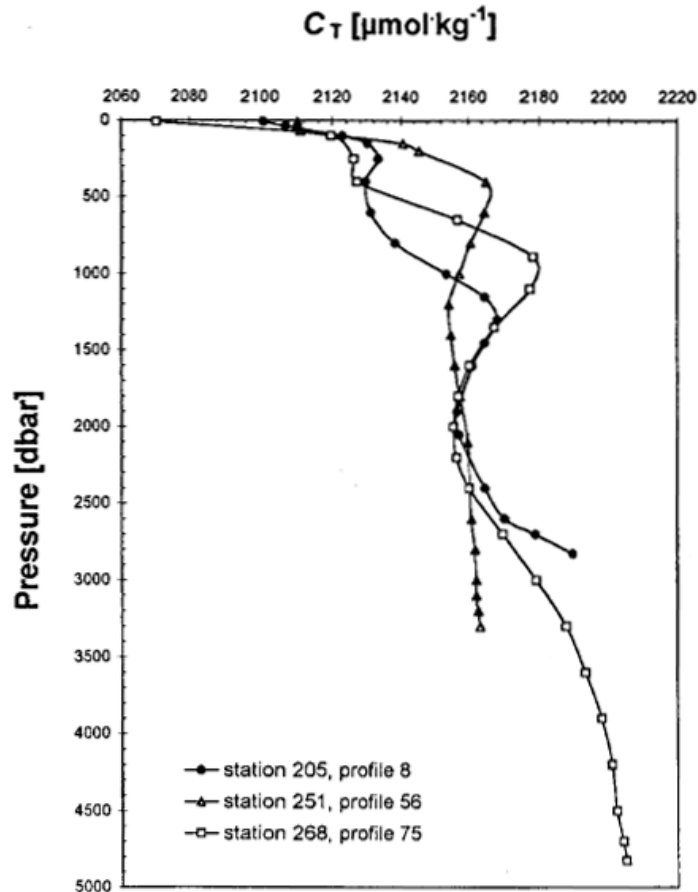


Fig. 17: Profiles of total dissolved inorganic carbon (C_T) at three selected stations of METEOR cruise M39/2. Stations are located on transect "A" in the Rockall Basin (205), on transect "E" in the Charly Gibbs Fracture Zone (251) and on transect "G" in eastern basin of the North Atlantic (268).

5.1.2 Physical Oceanography of the Labrador and Irminger Sea (M39/4)

5.1.2.1 Technical aspects

a) CTD analysis (L. Stramma, C. Mertens)

The CTD probe used was a Neil Brown Mark IIIB additional equipped with a Beckman oxygen sensor. It was attached to a 24 bottle 10 l General Oceanic rosette water sampler. As a LADCP was built into the rosette frame, a maximum of 22 bottles was used throughout the cruise. Five of the bottles were equipped with deep-sea reversing thermometers for temperature and pressure calibration.

Calibration of the pressure and temperature sensors was done at IfM Kiel in July 1996 and April 1997. The thermometer readings were used to check the laboratory calibration of the pressure and temperature sensors. Within the accuracy of the reversing thermometers no deviations were found and no further correction to the laboratory calibration was applied.

The salinity samples, typically six per profile, were analysed with two Guildline Autosal Salinometers. The IfM Kiel AS4 showed some jumps within the salinometer readings and stable calibrations could be done only after the jump in the readings happened. Therefore, part of the time the BSH-3 salinometer was used, which showed a very stable calibration and no reading jumps. In the CTD salinity calibration the readings of both salinometers showed similar variations, hence the IfM Kiel AS4 salinometer despite the reading jumps did not result in a reduced accuracy. The calibration of the CTD salinities was carried out with an rms-error of 0.0025 for leg M39/4. The oxygen samples were analyzed in the marine chemistry group with traditional Winkler titration. Typically samples were taken from all bottles on each station plus additional double samples at some stations. The CTD oxygen sensor had hardware problems in recording continuous oxygen current and oxygen temperature values and filled gaps by zero or low values. This problem could be solved within the software of the CTD processing and calibration routines.

Due to time dependant drift of the CTD oxygen sensor, the calibration was done for three individual periods. The rms-error for the oxygen sensor was 0.044ml/l for leg M39/4.

b) Mooring retrievals and deployments (J. Fischer, F. Schott)

Mooring retrievals

The mooring work began 8 July with the recovery of moorings K6 and K2 near the shelf break at Hamilton Bank. Inspection of the recovered mooring hardware showed almost no corrosion, confirming that it should be possible to extend deployment periods to two years. The recovered instruments were in good shape, and with the exception of one acoustic current meter all instruments (SEACATS, ADCPs and Thermistor Strings) returned a full data set. With the following recovery of the tomography moorings K4 and K3, and the recovery of moorings K1, K5 and L by RV Hudson a month before the METEOR cruise, all moorings were successfully recovered. All 5 ADCPs (including one in the Canadian ,'BRAVO" mooring) returned 100% data. The FSI inductive temperature probes, used for the first time worked fairly well, and data gaps occurred only for those sensors mounted at great distance from the data logger.

Inspection of the depth records either by the ADCPs or the pressure sensors in the tomographic instruments showed periods of large vertical excursions. To reduce mooring motion we increased the net buoyancy in moorings K11, K12, K14 and K17 to more than 700 kp and increased the anchor weight to 2000 kp.

The Deep Labrador Current Array 1997/99

Mooring positions and deployment dates of the Deep Labrador Current (DLC) array are summarized in table 4. The instruments (current meters, ADCPs and SEACATs) were programmed for two years duration, with the exception of the instruments in mooring K9 which will be recovered summer 1998.

Tab. 4: Mooring deployments during M39/4

mooring	date	UTC	Latitude	Longitude	comment
K7	14. July 1997	22:31	52°51.1'N	51°35.8'W	DLC-array
K8	15. July 1997	13:30	52°57.5'N	51°18.0'W	DLC-array
K9	14. July 1997	14:20	53°08.5'N	50°52.0'W	DLC-array
K10	13. July 1997	23:30	53°22.8'N	50°15.6'W	DLC-array
K16	13. July 1997	13:04	53°41.5'N	49°26.2'W	DLC-array
K11	22. July 1997	23:39	56°33.6'N	52°39.5'W	Tomography/Convection
K12	21. July 1997	19:48	55°19.5'N	53°53.6'W	Tomography/Convection
K14	23. July 1997	22:35	58°30.0'N	50°34.2'W	Tomography
K17	20. July 1997	19:09	57°24.8'N	55°40.0'W	Tomography
K15	20. July 1997	09:44	57°06.1'N	54°40.0'W	moored CTD

Convection Moorings 1997/1998

As in the previous deployment (1996/97) two moorings, K12 and K11, are equipped with ADCPs to measure vertical currents associated with convection, and with temperature and conductivity sensors to measure the development of the stratification. Two new instruments are deployed for the first time, a new generation of Seabird sondes ("Micro-Cat") and small temperature/depth sondes (developed and assembled by C. Meinke). The latter are thought to replace thermistor strings in order to reduce the drag in the mooring (leading to large vertical excursions), and to increase the flexibility of the vertical distribution of temperature measurements in convection moorings. Both moorings had tomography sources.

The moored CTD The moored CTD was repaired and prepared for its second deployment period at Woods Hole Oceanographic Institution, and it arrived in St. Johns just prior to the cruise. The position of this mooring was planned to be near the center of the deep winter mixing regime west of the WOCE-AR7 line, and it should be located on the acoustic ray path between the tomography sources in K1 and K17. The deployment on July 20 went very smooth, and we were able to avoid any slippage of the CTD along the mooring wire; this was thought to be the reason for the instrument failure in the previous deployment. In addition to the CTD a down-looking ADCP for three-dimensional current measurements was incorporated near 70 m.

c) Acoustic Tomography

(U. Send, D. Kindler)

During the winter 1996/97 four moorings with tomography instruments had been deployed in the Labrador Sea (K1, K3, K4, L). Two of these were recovered already in May/June during a cruise of the Canadian research vessel 'Hudson', while the remaining two, K3 and K4, were retrieved on this METEOR cruise. The mooring operation proceeded without obvious problems; however, a small quantity of water was found inside instrument K4, below the electronics and the battery pack. At present, it is unclear how and when this leakage occurred.

The recovery of the acoustic transponders turned out to be problematic in some cases. These transponders are important for the mooring-motion navigation of the tomography instruments,

and three transponders are located around each mooring. This time, we were using recoverable transponders, which can be released through an acoustic command. In total, 9 of these were to be recovered on the METEOR cruise, however one was not responding anymore, while the other was so weak (battery problem ?) that it could not be released. Thus a total of 7 transponders was retrieved.

During the cruise, 5 tomography instruments were originally planned to be deployed again. This number had to be reduced to 4 due to the leakage in the instrument from K4. The fifth unit was the larger HLF-5 sound source, which had been prepared in Kiel complete with two powerful lithium battery packs. The two instruments recovered on the 'Hudson' had in the meantime been at the manufacturer for service and repair, whereas the remaining instrument retrieved on the first leg of M39/4 had to be serviced and prepared for re-deployment on board. These activities went according to plan, until a short-circuit occurred in both lithium battery packs during/after deployment of the HLF-5 source. This was due to a leaking underwater electrical connector. Fortunately, multiple fuses prevented a fire of these potentially dangerous batteries, but the packs were unusable afterwards. With help from the ship's electronics department an improvised battery pack with reduced capacity was then built from the alkaline batteries originally meant for the instrument from K4. This new pack would allow transmissions with the HLF-5 sound source once a day, starting November 1. Two short test transmissions shortly after deployment could not be verified, possibly due to high ship noise.

In total then four moorings with tomography instruments were deployed, which were K11, K12, K14, K17. Again three transponders were placed around each of these moorings, whose exact position was determined with a special acoustic survey.

d) Navigation requirements , shipboard ADCP and LADCP

(J. Fischer, C. Mertens, F. Schott)

Lowered ADCP

On all of the CTD profiles an ADCP was attached to the rosette to obtain profile-deep currents. The profiles were all referenced by GPS/GLONASS positioning, and the much improved positioning accuracy will reduce errors in the barotropic current component (see also "shipboard ADCP"). During the first leg of cruise M39/4 the Broad-Band ADCP S/N 1002 was used until a failure appeared and some profiles were considerably distorted. These profiles need individual processing and adjustment to shipboard ADCP currents.

From profile 17 onwards the Narrow-Band ADCP S/N 301 was used. This instrument was in already in use during the previous cruises M39/2 and M39/3. It worked fine with the usual unavoidable data loss by bottom interference; this needs careful postprocessing and checking with bottom tracking.

Shipboard ADCP

In St. Johns a new 75kHz shipboard ADCP was mounted in the ships well. This was the first use of a low frequency ADCP, as the standard METEOR ADCP was a 150 kHz system. Other

components of the system were a 3D-ASHTECH GPS receiver for positioning and attitude (mainly heading) parameters, and the above mentioned GPS/GLONASS receiver as a standalone system for parallel storage of more precise positioning data.

During calm conditions the profiling range of the ADCP was near 700 m, but when the ship was heading into the swell the range was significantly reduced; there were even periods of total data loss during the more windy days.

At the end of the cruise all shipboard ADCP data were edited and calibrated. The calibration improved due to external navigation from the GPS/GLONASS system, and by using the Ashtech heading for gyro correction. During the cruise the ADCP had to be lifted up, as there was a seawater pump attached to the same mounting platform which had to be replaced. We suspected that this would reset the ADCP calibration, but fortunately the transducer orientation did not change. The accuracy of the transducer misalignment angle determination was estimated to 0.1° degs on the basis of 160 reliable calibration points.

In general the vertical shear of the currents was rather weak, and the reference layer velocity (depth range 60 - 140 m) is representative for the currents over the total depth range of the ADCP. An overview over the existing data base along the three major sections of the cruise is shown in figure 18.

As another example for the final shipboard ADCP data the section along the moored boundary current array is shown in figure 19.

GPS/GLONASS precision of navigation

This system was received in St. Johns, and it was planned to be used for improving the accuracy of lowered and shipboard ADCP data as well as for better transponder navigation.

During most of the time the number of satellites locked exceeded 10 with an equivalent number of GPS and GLONASS satellites; sometimes even 15 satellites were locked, resulting in a very smooth ship track. Only in rare occasions at a number of satellites less than 8, some noise could be detected on the plotted cruise track.

As the ship was underway wenn the GPS/GLONASS system was started we were not able to perform a statistical test with the ship at rest. Instead we compared the influence of pure GPS data stored with the shipboard ADCP data string (5 minute data) with that of GPS/GLONASS in terms of statistical noise in the absolute reference layer velocity. This is the vertically averaged ADCP current (bins 5 to 10) minus the ships drift (the latter determined by either positioning system). While referenced with GPS only the scatter of the absolute reference layer velocity was large (12cm/s) it was significantly reduced (to 5cm/s) by using GPS/ GLONASS (Figure 20). As an additional benefit the higher accuracy of the reference layer velocity helped to improve the determination of the transducer misalignment angle.

Summarizing, the GPS/GLONASS receiver led to significantly higher accuracy of positioning data, thereby improving both shipboard and lowered ADCP data. In cases where the GPS P-

code or differential GPS quality is not available this system should be routinely used. GPS/GLONASS positioning for example should be linked directly to the shipboard ADCP as the primary navigation source.

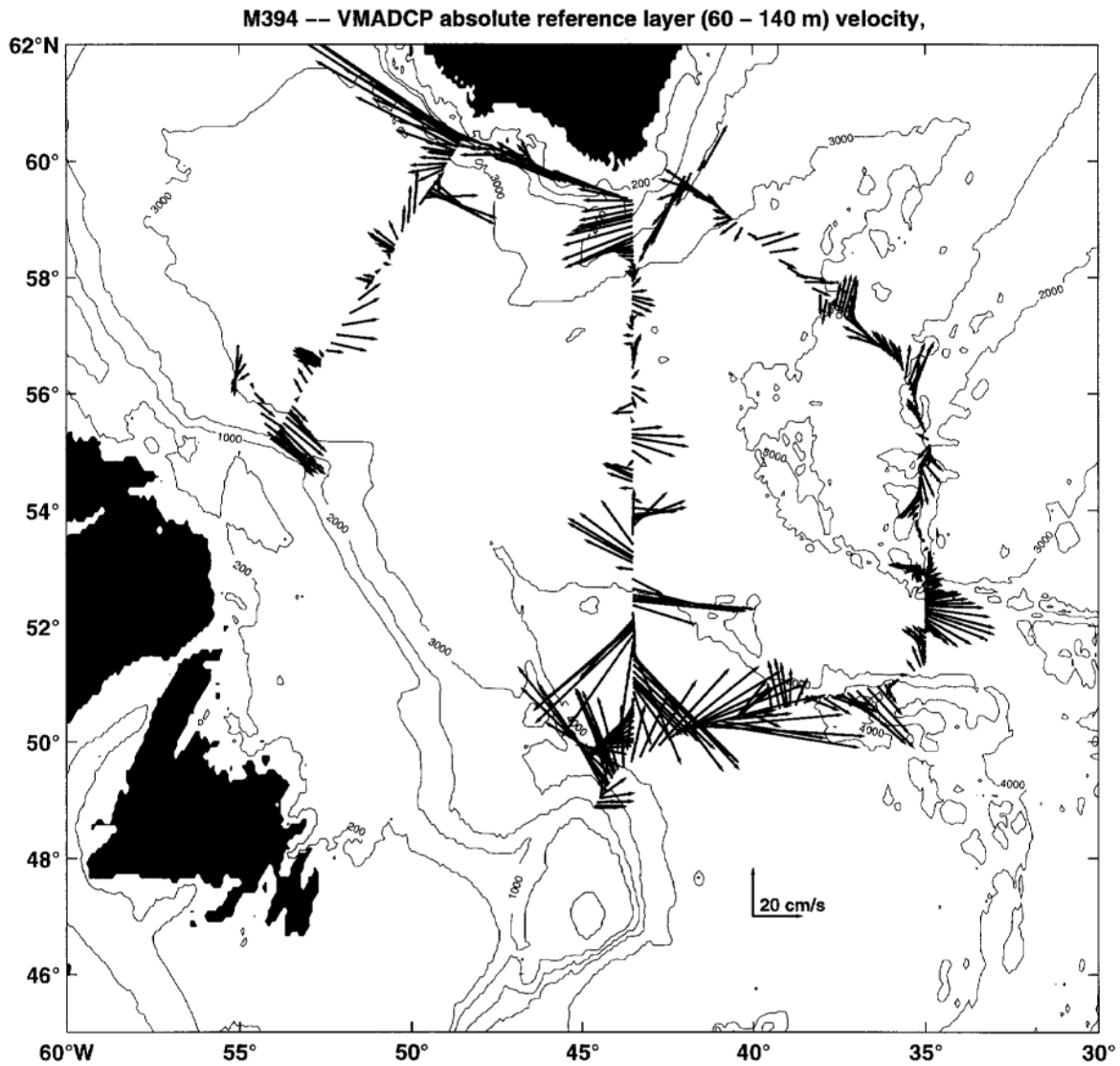


Fig. 18: Shipboard ADCP currents during the second part of leg M394/4; St. Anthony to Greenland.

METEOR 39-4

VM-ADCP

Database: ../adcpdb/m394

Filename: m394

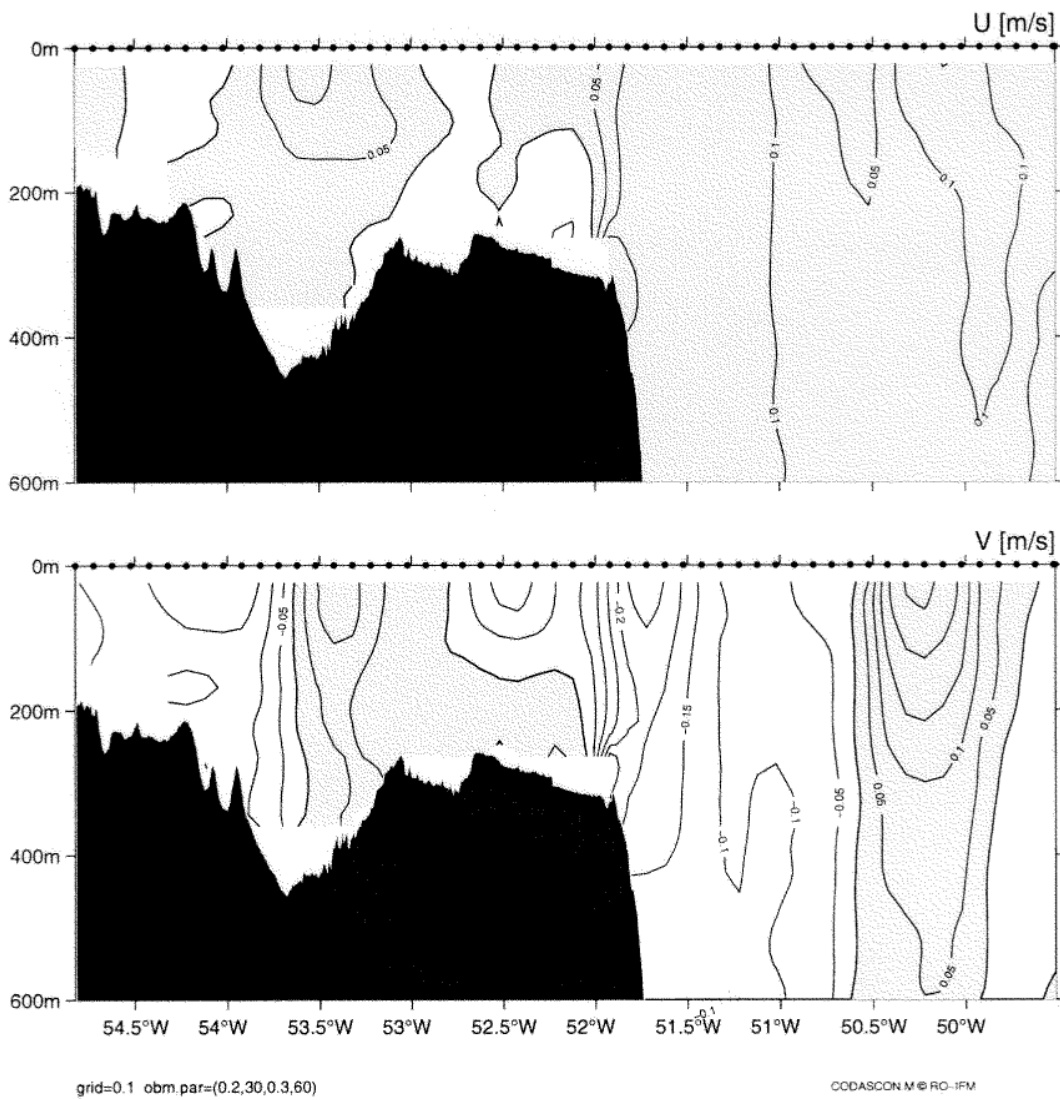
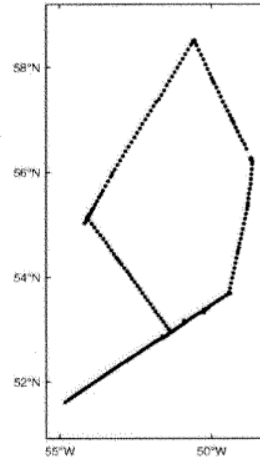


Fig. 19: Shipboard ADCP currents (east and north component) along the boundary current array and across the Newfoundland shelf to St. Anthony. The topography is from the METEOR depth sounding system (Parasound).

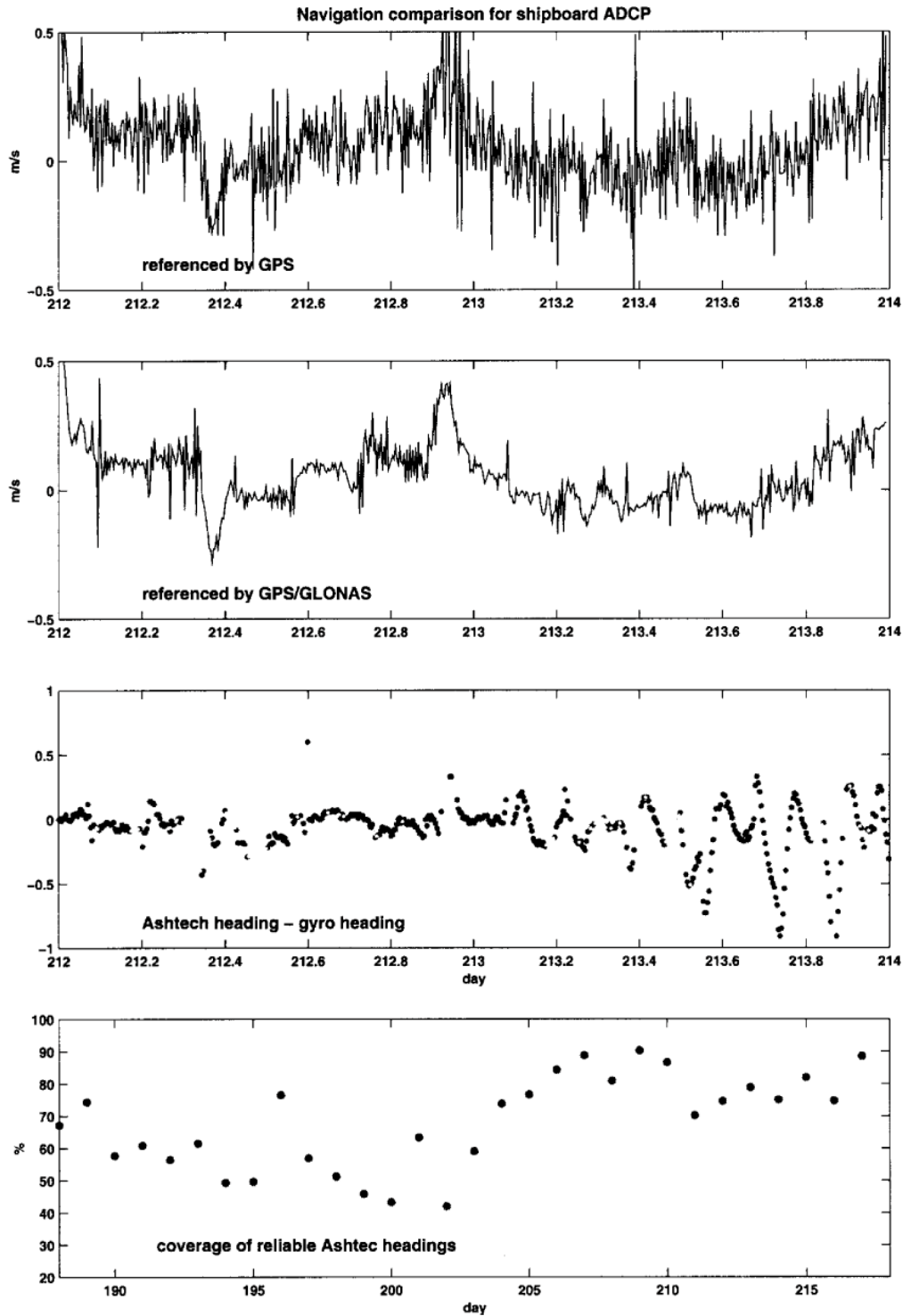


Fig. 20: Navigation data comparison: top graph shows ADCP currents minus ships speed over ground (SOG) determined from GPS positions, second graph shows the same but SOG determined by GPS/GLONASS positions. The third timeseries shows the difference between Ashtech 3D- GPS heading and gyro heading; note some gaps between the dots. The lowest graph shows the coverage of reliable Ashtech headings in %/day.

Ashtec 3DF attitude parameters

Gyro errors are one of the major error sources in shipboard ADCP data. High frequency (Schuler) oscillations show heading fluctuations of more than a degree during acceleration phases. Since these periods are important for calibration of the misalignment angle between ADCP-transducers and gyro heading, any improvement of heading accuracy should be considered. With METEOR's Ashtec 3DF-GPS receiver it is possible to obtain an independent estimate for ship's heading, which is not contaminated by these oscillations. However, due to data gaps this correction could not be done on a ping to ping basis, but for ensembles (5 min) with good data coverage. During the first part of the cruise the data coverage was in the 50% range, but with the new firmware (obtained underway) the data covered improved to near 80%.

A heading correction file was prepared by using the GPS-Gyro heading difference whenever the GPS data quality was sufficient. Short gaps were filled by interpolation, for longer gaps the difference was set to zero. Then all ensembles were rotated accordingly.

e) PALACE launches (J. Fischer)

Seven Palace floats were deployed during the cruise, two with CTD-sensors and 5 with temperature and pressure. All floats were ballasted to drift at 1500 dbar, and they were programmed for surfacing every 5-days until April 1998 and for 14-day cycles afterwards. All floats were deployed in the boundary current regime; for dates and positions see table 5.

Tab. 5 Palace floats deployed during M39/4

Float	code	sensors	date	UTC	Latitude	Longitude
9L	8632	TD	09. July 1997	09:49	55°15.55'N	53°57.12'N
14L	8637	CTD	09. July 1997	10:58	55°24.83'N	53°48.45'W
8L	8631	TD	09. July 1997	12:04	55°33.64'N	53°39.96'W
15L	8638	CTD	14. July 1997	14:39	53°08.84'N	50°52.53'W
7L	8630	TD	15. July 1997	15:04	52°56.99'N	51°18.130'W
46	9211	TD	20. July 1997	22:14	57°25.00'N	55°40.94'W
23	9210	TD	21. July 1997	03:10	56°48.11'N	55°00.06'W

f) CFC analysis

(M. Rhein)

During the cruise, the CFC system worked continuously and about 1850 water samples have been analysed. The survey was dedicated to the circulation of the deep water masses. During periods of dense station spacing, sampling was focused on the water column below 800 m depth. Calibration was done with a gas standard kindly provided by D. Wallace, PMEL, USA. The CFC concentrations are reported on the SIO93 scale. CFC-11 analysis was successfully carried out during the cruise, the analysis of the CFC-12 concentrations however was partly interrupted by an unknown substance with a similar retention time as CFC-12. The blanks for CFC-11 and CFC-12 were negligible. Accuracy was checked by analyzing 10 percent of the water samples twice, and was for both substances $\pm 0.8\%$.

5.1.2.2 Analyses and Evaluations

a) Water mass distribution, Labrador Sea Water properties

(M. Rhein, L. Stramma)

Labrador Sea Water (LSW)

Along the WOCE section AR7-W (Fig.21), the CTD stations were mainly centered in the boundary current regions leaving 5 stations for the central Labrador Sea. Two of these stations show peculiar features. Profile 7 (57°23'N, 51°47'W) exhibits the lowest salinities in the range of the LSW, which are associated with a temperature minimum (Figure 21) and with elevated CFC-11 concentrations at 1000-1600 m depth, higher by 0.6 pmol/kg than anywhere else in this water mass. All three parameters point to formation by deep convective renewal in late spring 1997, reaching to depth around 1500 m. The core density was $\sigma_t = 27.76$ ($\sigma_{\theta} = 34.67$), lower than the density of the convective product in spring 1994, which still lingers in the Labrador Sea with core densities of $\sigma_t = 27.78$ ($\sigma_{\theta} = 34.69$). The CTD profile at the nearby profile 28 (57°56'N, 51°10'W) was characterized by a low vertical temperature gradient at 500 - 900 m, lifting the isopycnal $\sigma_t = 27.76$ from 1000 m to 700 m depth. The lower bound of the LSW ($\sigma_t = 27.8$) was 2200 m (Prof. 7), and 1800-2000 m for the other central stations. CFC-11 concentrations in the LSW along the AR7 section varied between 4.0-4.6 pmol/kg, except at the before mentioned profile 7 where values as high as 5.03 pmol/kg were observed.

South of the Gibbs Fracture Zone (52°30' - 53°N) along the 35°W section (Figure 22), the LSW layer is about 1300 m thick. Due to the rising of the lower bound of the LSW ($\sigma_t = 27.8$) over the Reykjanes Ridge from about 2100 m to 1500 m LSW grows thinner above the ridge. Salinities of the LSW were higher than 34.87 and CFC-11 concentrations did not exceed 3.5 pmol/kg (profile 68, south of Gibbs Fracture Zone), the lowest values were measured on the northernmost station on the Reykjanes Ridge. The salinity minimum at $\sigma_t = 27.78$, the product of deep convection in 1994, was only found on the stations south of profile 71 (52°39'N, 35°01'W), the salinity minimum further north was broader, less distinct and centered at higher densities (around 27.785).

Gibbs Fracture Zone Water (GFZW)

The Salinity-F11 relation of GFZW in the Eastern Atlantic differs from the one in the Western Atlantic: in the east, CFC-11 is elevated with increasing salinity, because the water surrounding the GFZW are less saline and CFC-11 poor. In the west, however, the GFZW encounters the low saline but CFC rich LSW and DSOW, leading to increasing CFC-11 values in the GFZW with decreasing salinity. When entering the western part, the CFC-11 concentrations in the high saline core of the GFZW can only decrease further when mixing with older deep water flowing into the subpolar North Atlantic from the south.

The 35°W section includes the detailed survey of the Gibbs Fracture Zone (Figure 22), and of channels which might allow the GFZW to spill over the Reykjanes Ridge into the western Atlantic. In the Western Atlantic, the isopycnals $\sigma_t = 27.8$ - 27.88 enclose the GFZW. In the GFZ itself, the salinity maximum ($S > 34.96$) located on the northern flank reaches down to

about 3200 m ($\sigma_t = 27.882$). Below, the salinity AND the CFCs decrease, indicating that this deeper part is also water from the Eastern Atlantic. The lowest GFZW concentration in the GFZ was 1.8 pmol/kg. The concentrations in the GFZW increased towards the north up to 2.5 pmol/kg, north of 53°N, CFC-11 values were everywhere greater than 2.2 pmol/kg. The highest density found on the Reykjanes Ridge was 27.876 ($\sigma_t = 37.03$, $S = 34.968$, CFC-11 = 2.4 pmol/kg, profile 85).

The salinity maximum, denoting the core of the GFZW is located in the Irminger Sea at densities $\sigma_t = 36.99 - 37.01$ with increasing densities towards the west and more saline at the Reykjanes Ridge (34.93) than at 41°W (34.92). The salinity maximum could not be identified west of 41°W. The most saline and thus purest GFZW in the Irminger Sea has CFC-11 concentrations smaller than 1.9 pmol/kg, much lower than the concentrations above the Reykjanes Ridge, but close to the lowest values below the salinity maximum flowing through the GFZ.

A close investigation of the CFC-distribution showed that spilling of GFZW across the Reykjanes Ridge through gaps other than the GFZ can only influence the GFZW in the Irminger Sea at densities $\sigma_t < 37.03$, the CFC-11 - density relation seems to limit the density range $\sigma_t < 37.0$.

Along the 43°30'W section and in the Labrador Sea, the most saline and CFC-11 poorest GFZW was found away from the boundary regions. CFC-11 concentrations below 2 pmol/kg are found along 43°30'W between 51°30'N and 57°0'N and in the Labrador Sea on the easternmost profiles 11-15.

Denmark Strait Overflow Water (DSOW)

In 1996, the temperature minimum of the DSOW was found not in the Irminger Sea but in the Labrador Sea (1.12°C coldest temperature in the Labrador Sea in August 1996, found in the center (profile 61). Compared to 1996, the temperature in the Labrador Sea increased to 1.4-1.6°C, with the coldest temperatures at profiles 14 and 15 in the southern section. Only two locations on our survey were colder: at the northern boundary at the 43°30'W section (profiles 35, 36, 37) and in the western part of the Irminger Sea section west of 40°W with a minimum temperature of 1.19°C. The warmest temperatures (higher than 1.8°C) were found at the 43°30'W section (profiles 40-46) and east of 37°W.

The CFC-11 concentration of the DSOW in the Labrador Sea has decreased, caused by the change in temperature. The CFC-11 values at the same temperature level showed no difference between the 1996 and 1997 data. The characteristic of the DSOW, i.e. decreasing salinities and increasing CFCs towards the bottom were found on all deep profiles except the region east of 37°W.

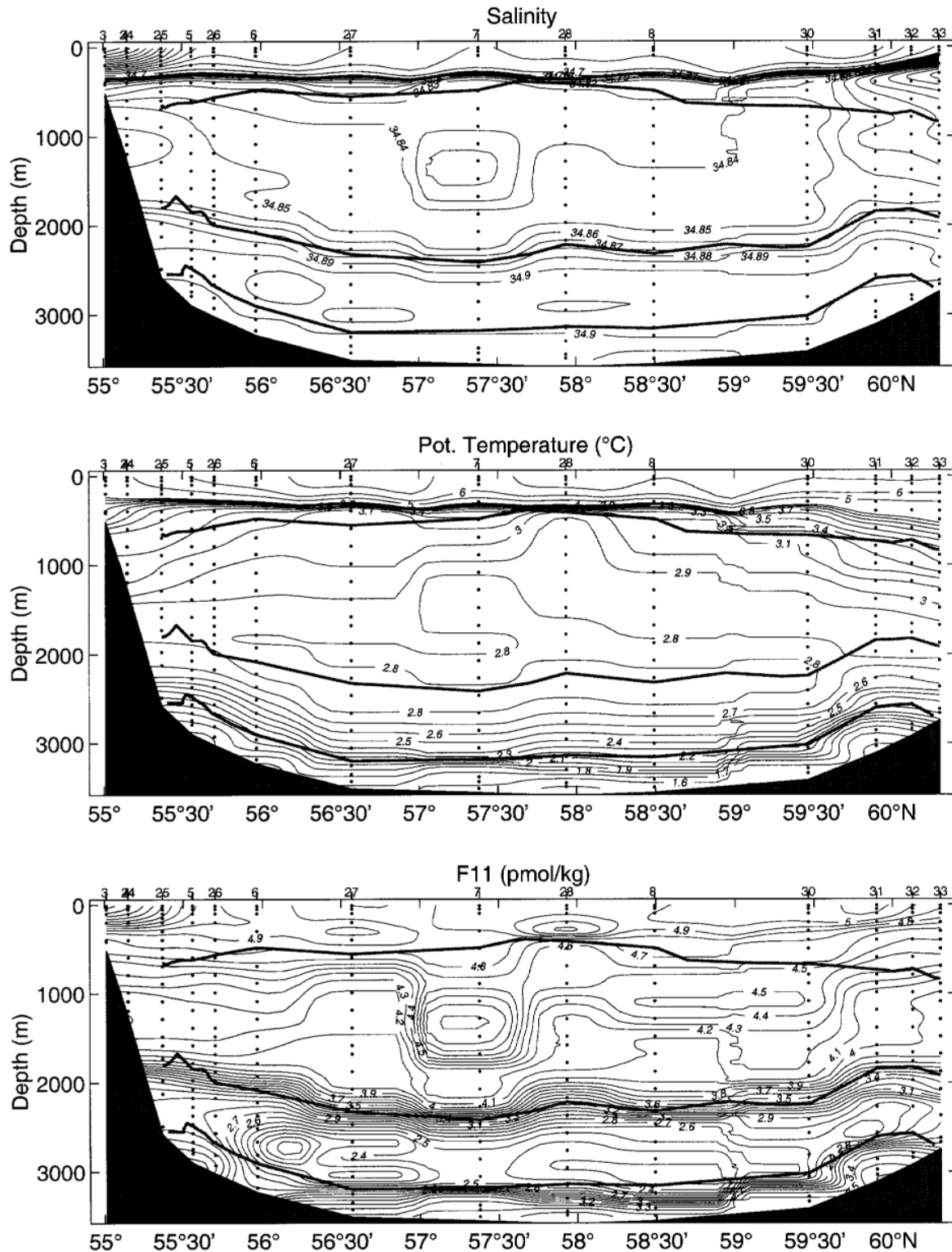


Fig. 21: Distribution of salinity (top), potential temperature (center) and CFC-11 in pmol/kg (bottom) along section AR7-W. The isopycnals $\sigma_t = 27.74$, 27.8 and 27.88 as boundaries for the LSW ($27.74 - 27.8$) and Gibbs Fracture Zone Water ($27.8 - 27.88$) are included as solid lines.

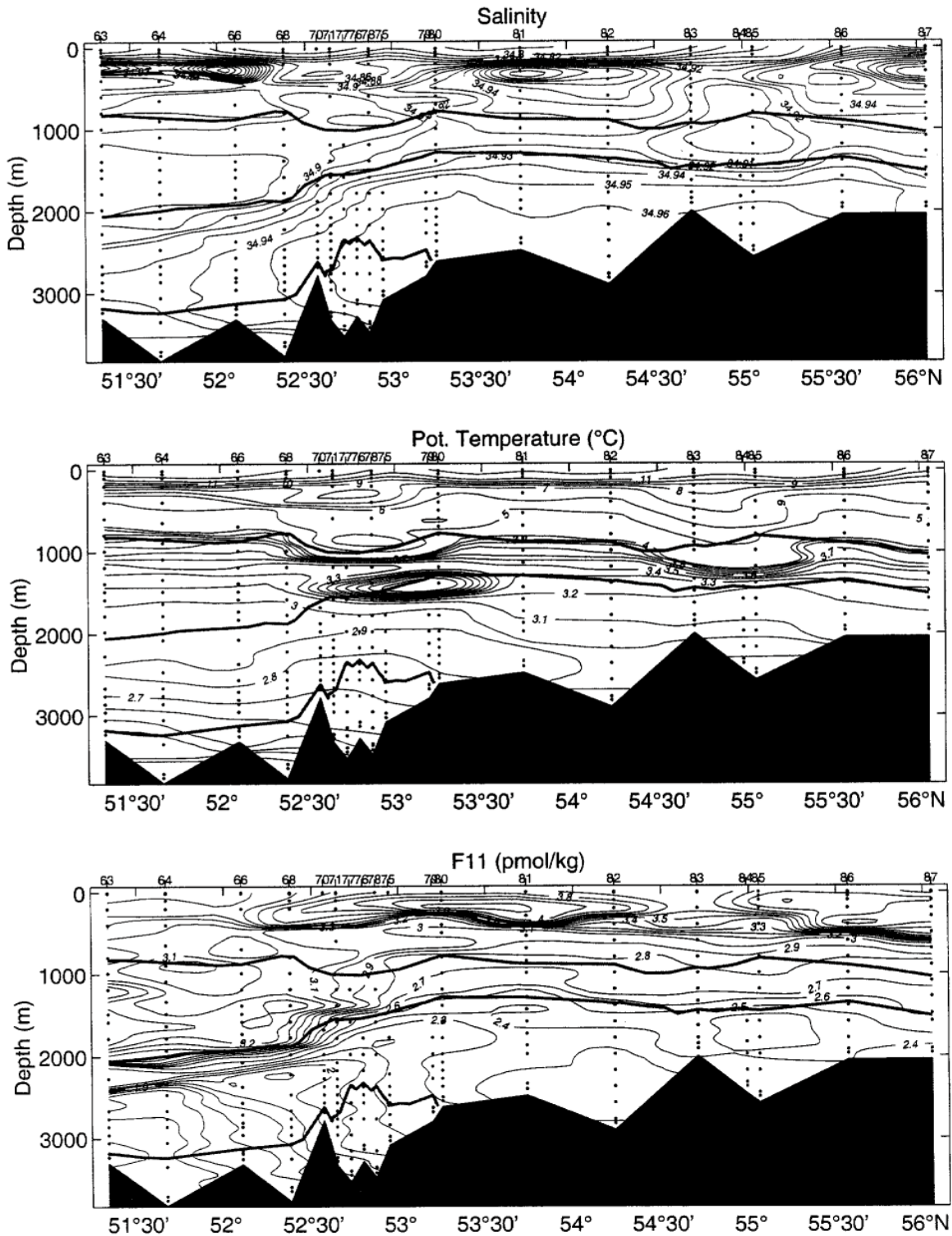


Fig. 22: Distribution of salinity (top), potential temperature (center) and CFC-11 in pmol/kg (bottom) along 35°W. The isopycnals $\sigma_t = 27.74$, 27.8 and 27.88 as boundaries for the LSW ($27.74 - 27.8$) and Gibbs Fracture Zone Water ($27.8 - 27.88$) are included as solid lines.

b) Boundary circulation and transports

(F. Schott, J. Fischer)

The cruise track of M 39/4 was especially designed to investigate the deep boundary currents of the Labrador- and Irminger seas. Deep boundary current velocities are determined by geostrophy and by LADCP current profiling. The evaluation of both kinds of observations showed that on most boundary sections a satisfactory level of no motion cannot be determined. A significant barotropic component is mostly present.

The western Labrador Sea boundary currents were sampled by two sections, north of Hamilton Bank and near 53°N, where the array K7-K16 was then deployed (Fig.8), the northern Labrador Sea by the AR-7 line. The directly-measured (by LADCP) top to bottom currents across the western end of the AR-7 section yield quite substantial transports, of 33 Sv total between the shelf edge and 56°N. This number is in close agreement with the value of 31 Sv that was determined along the same section segment in August 1996 from LADCP profiling during “Valdivia” cruise VA161. A bit more will have to be added when the shipboard ADCP observations on the shelf are brought into the analysis. The total boundary current transport is made up by the addition of the near-barotropic flow due to Sverdrup forcing, superimposed by the deep boundary current. The Sverdrup flow and the thermohaline DWBC are both cyclonic, hence a zero-reference level cannot be expected.

The absolute current field along the boundary sections is determined by geostrophy referenced by vertically integrated LADCP currents. This procedure is recommended as the vertically integrated LADCP currents are accurate estimates of the barotropic flow component, while the baroclinic flow estimated from geostrophy is preferable to that obtained by the direct measurements. The resulting transports for the deep water masses (DSOW, GFZW and LSW) at the boundary sections are summarized in Table 6. However, the result is to be considered preliminary, since it is somewhat dependent on the treatment of bottom triangles and might also be subject to larger changes, when the direct measurements are corrected for tidal currents.

Tab. 6: Total transport at Boundary Current sections (Sv)

Section	DSOW	GFZW	LSW	DWBC
AR7-S	5.0	4.4	11.8	21.6
53°N	4.0	4.6	11.0	19.6
Cape Farw.	6.0	6.5	13.0	25.5
Flem. Cap	1.5	3.0	8.0	12.5

c) Convection moorings 1996-97

(C. Mertens, J. Fischer, F. Schott)

Four of the moorings, deployed over the winter of 1996/97, were designed for the purpose of observing deep convection activity using acoustic current meters and temperature/salinity recorders. Two of the moorings (K1 and K5) were located in the central Labrador Sea and the other two (K2 and K6) in the boundary current region.

The meteorological conditions during the winter of 1996/97 showed a dramatic transition of the flow regime over the North Atlantic which resulted in a significant change in the magnitude of surface cooling in the Labrador Sea region. Until mid January the presence of a blocking high over Europe and anomalously high pressure over Greenland caused a significant westward shift of cyclonic activity with the effect of rather low heat loss over the Labrador Sea. In contrast, February 1997 was a month in which the circulation pattern over the North Atlantic was significantly stronger than average, resulting in strong heat loss over the Labrador Sea. NCEP/ NCAR reanalysis data show peak values greater than 1000 W/m^2 (Fig. 23a).

The temperature development at mooring K1 during the winter of 1996/97 is shown in Fig. 23b. In late autumn a warming is found in the near-surface sensors, resulting from the deepening of the summer mixed-layer. Owing to the first rather mild winter, only a slow cooling of the surface layer set in by mid December. After the transition of the meteorological conditions in mid January, strong cooling took place and a rapid deepening of the mixed-layer to about 1000 m. Temporary fluctuations in the records of deeper temperature sensors indicate convection activity to about 1300 m. Acoustic Doppler current profiler (ADCP) measurements show strong downward vertical currents for several hours duration during this period. The maximum vertical velocity of about 10 cm/s was found at the beginning of March.

The time series of horizontal currents obtained at K1 show, except for a number of eddy events, a rather small amplitude (Fig. 23c). Prior to the convection two of those barotropic eddies advected past the mooring, one at the beginning of December and one in January. Their low core temperature suggest, that their water-mass properties have been formed by convection during the previous winter. After convection a number of strong eddy events have been observed.

Mooring K2 was also equipped with a large number of temperature sensors in order to observe possible convection activity. In contrast to the central Labrador Sea, an instantaneous cooling of the upper 800 m has been observed here in mid February, which could not result from local convection activity and hence must have been advected by the Labrador Current. Further, no pronounced events of downward vertical velocity could be found in the ADCP records, most likely due to the reduced density of the lower-salinity Labrador Current on top.

d) Gibbs Fracture Zone study

(F. Schott, J. Fischer, L. Stramma).

The Charly Gibbs Fracture Zone near 52°N is the key location for the exchange of deep water masses between the eastern and western basin of the subpolar North Atlantic. As detailed bathymetric surveys showed a bottom depth exceeding 3500 m this allows North East Atlantic Deep Water (NEADW) to pass the Mid-Atlantic Ridge (MAR) through the GFZ. Owing to its density this water mass, also called Gibbs Fracture Zone Water (GFZW), is located beneath the Labrador Sea Water (LSW). Framed by potential densities 27.8 and 27.88 the GFZW is clearly detectable by its high salinity.

Earlier moored observations of the throughflow by SAUNDERS (1994) had shown a mean westward flow organized in inter-mittent events with the currents even reversed to eastward during some periods. Such a situation was met during M39/4 when we conducted a detailed study of the water masses (CTDO 2 and CFC's) and flow (LADCP) in the passage (Figure 24), farther up north along the MAR, and across the Irminger Sea. Geostrophic shears revealed the expected structure with deep westward shears between the LSW and the GFZW, and currents relative to 1000 m showed deep westward flow in the range of the GFZW yielding a westward transport of approximately 7 Sv for the layers below 1500 m. However, the directly measured currents gave a different result. Although showing approximately the same baroclinic structure, even with the relative transports being in good agreement with the geostrophic estimates, the barotropic current component was directed towards the east leading to net eastward transport. Regarding the deep flow alone, i.e. below 1500 m, this led to net eastward transports of about 6.5 Sv. The surface flow at this time showed a well defined eastward jet accompanied by salinities above 35 and was presumably associated with the North Atlantic Current (NAC), which was located right on top of the GFZ at this time.

A study of historical hydrography and XBT data from the region showed that at some times in the past the NAC took a more northerly route than usual. The consequence seems to be a deep-reaching effect on the GFZ and deep-water through flow into the western basin. A paper on this subject was prepared for publications.

e) Acoustic tomography

(U. Send)

In some of the tomography moorings, isolated components had failed, which reduces the information available quantitatively or qualitatively. Among these is a gap in the data disk in instrument K1, mis-formatted information from the mooring navigator in instrument L, and two essentially non-functioning transponders in mooring K3. All these units had passed pre-deployment tests, and the source of the problem must be intermittent in nature.

The quality of the acoustic receptions was found to be highly variable. There are periods with good, clearly resolved receptions, while at times no signal is visible at all. Detailed analyses revealed increased noise levels (and sometimes also reduced signal levels) during the periods with worse signal-to-noise (S/N) ratio. These intervals are highly correlated with times at which the moorings are displaced horizontally and vertically due to currents, which might indicate a

problem with mooring strumming, flow noise, or related effects. However, we cannot exclude the possibility of an instrumental problem in the receiver part of the electronics. There seems to be enough information still in the data to analyze the large-scale temperature stratification at various times from the tomography array, but these results depend on more careful evaluation of error sources and sizes, and choice of a suitable set of basis functions (vertical modes) for inversions.

For the redeployment of the instruments, every effort was taken to verify the functioning of the modules in each unit, and to reduce noise in the moorings (e.g. by covering shackles and rings). Also, the distances between the moorings were somewhat reduced in this deployment period, and the more powerful HLF-5 sound source should further improve the S/N ratio.

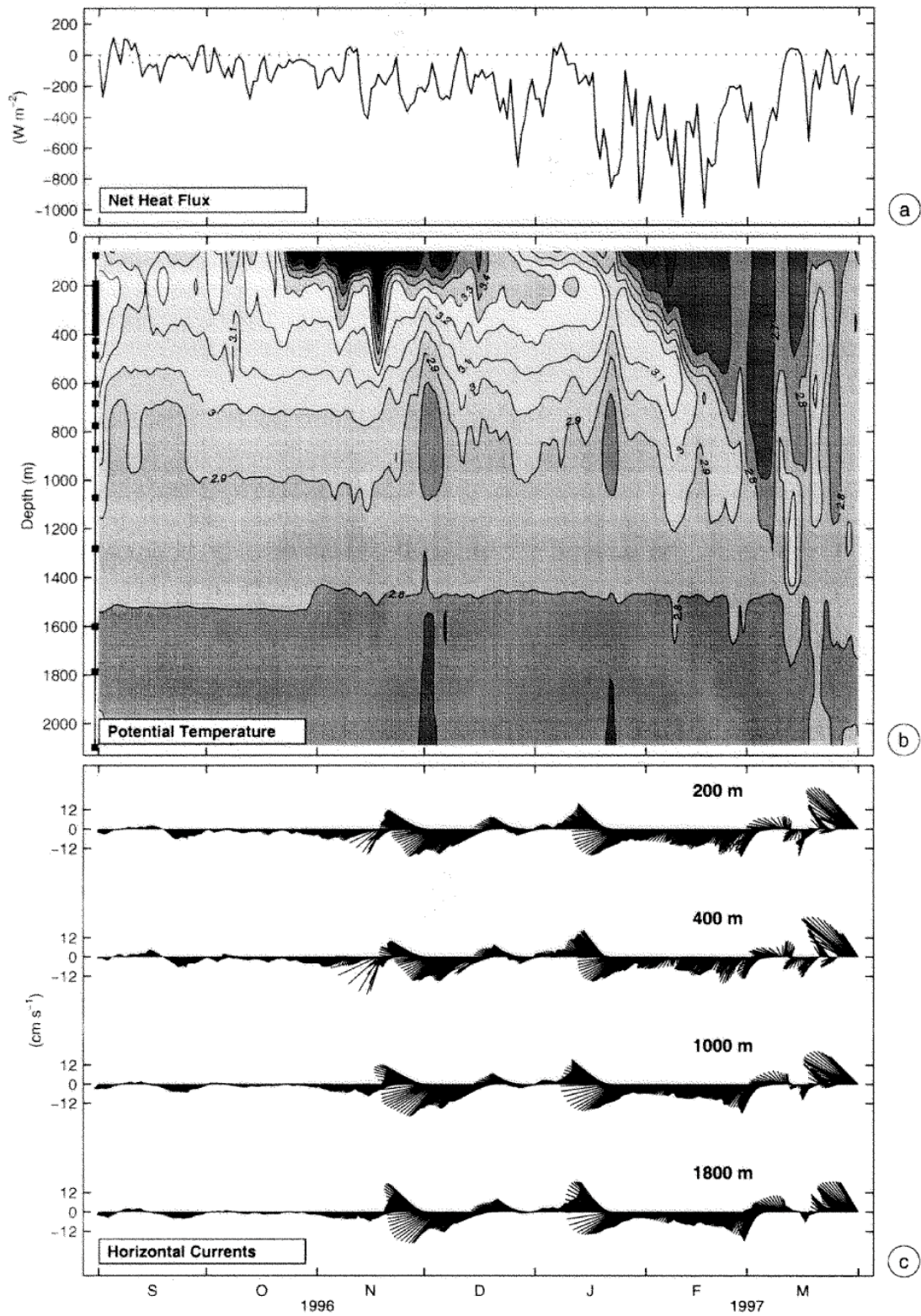


Fig. 23: a) Net heat flux from NCEP/NCAR reanalysis at a grid point near mooring K1; b) potential temperature from all K1 instruments, instrument depths are marked as squares; c) horizontal current vectors for selected depths.

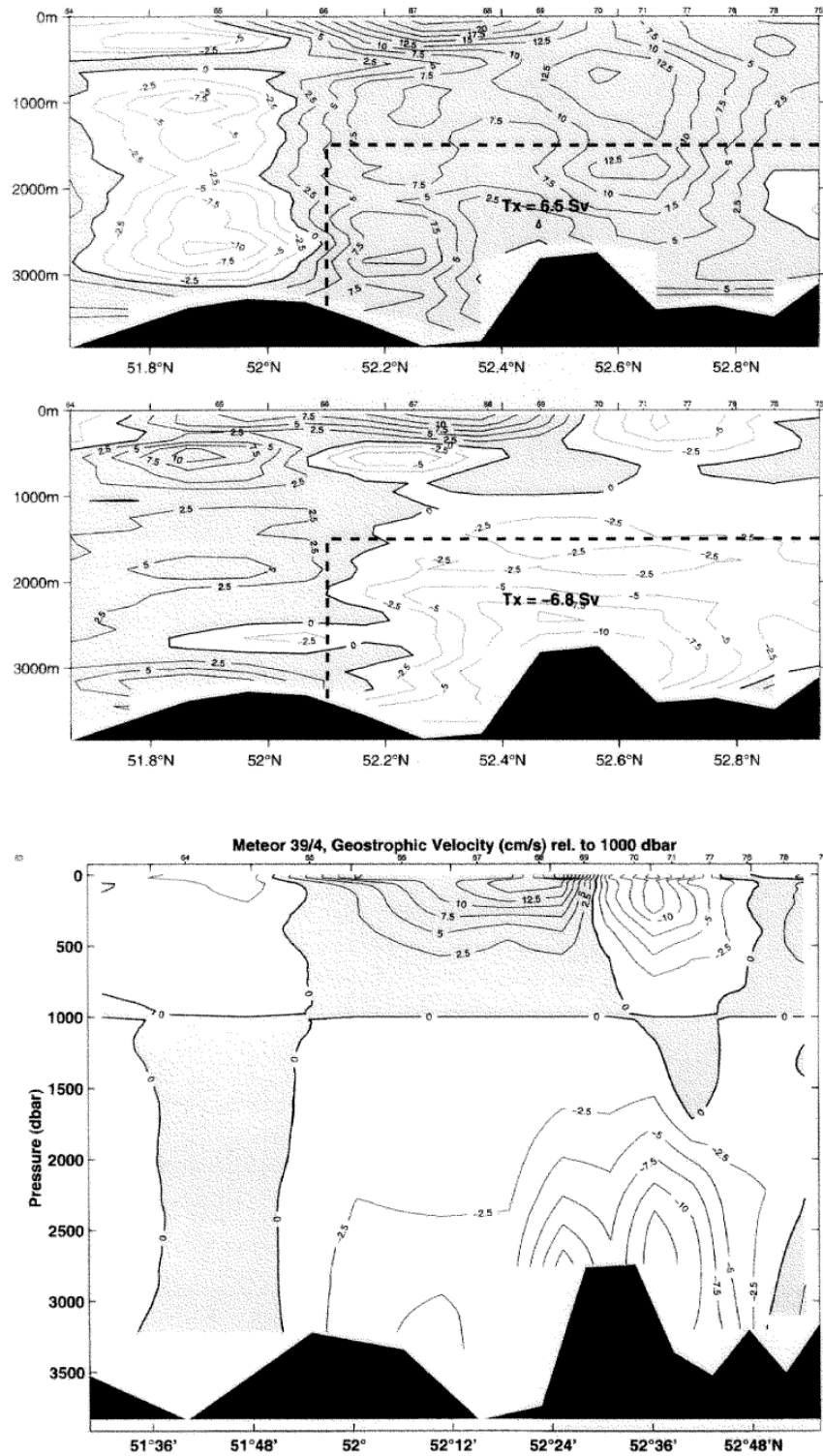


Fig. 24: Zonal flow through the Charly Gibbs Fracture Zone obtained by LADCP (top) currents relative to the flow in 1000 m depth (middle) and by geostrophy relative to 1000 m depth (lower graph). Transports below 1500 m and between stations 65 and 75 are included; units are in Sv.

5.1.2.3 Air-sea fluxes

(U .Karger, H. Gäng)

Measurements of the turbulent structure of the wind were gathered using a 3-dimensional sonic anemometer with a sampling rate of 30Hz. The spectra of turbulent wind speed fluctuations will give an estimate of the momentum exchange. Coincident temperature and humidity samples, measured with a fast-response psychrometer lead, together with the vertical fluctuations of wind speed, to the fluxes of sensible and latent heat. Since ship movements will have an impact on the measurement of the wind components, the pitch and roll angle of vessel was taken with a frequency of 5Hz. Both instruments were located port beside the foremast at a height of 20 m. Most of the time these measurements were under good conditions, because the relative wind direction was often North to Northwest, so that the data should not be disturbed directly by the ship's superstructure and the foremast.

Different kinds of data of the vertical atmospheric structure for the evaluation of remote-sensing based air-sea flux algorithms were sampled. More than 160 radiosonde launches were made, together with the German Weather service, during overpasses of DMSP-satellites with the SSM/ I (Special Sensor Microwave/Imager) radiometer on board. The soundings provide the real state of the atmosphere, measuring temperature and humidity profiles, which will influence the atmospheric microwave emission. With a ship borne 20-30 Ghz passive microwave radiometer down-welling radiances of the atmosphere were obtained, from which also water vapour and especially cloud liquid water will be deduced. Additional information about the ocean surface skin temperature and the cloud-base temperature were detected by two infrared thermometers. Meteorological standard synoptical observations were performed hourly to give further information about the atmospheric conditions, e.g. distribution, height, and kind of clouds.

5.1.2.4 Carbon Dioxide System, Nutrients and Oxygen

(L. Mintrop)

Technical aspects

On this leg the same methodology and sampling strategy for CO₂, oxygen and nutrients was followed as on the second leg of the cruise (see 5.1.1.3.). This involved discrete water sampling from 46 hydrocasts on this leg. A total of 862 samples were drawn and immediately analyzed for total dissolved inorganic carbon (C_T) and total alkalinity (A_T). The analytical methods involved have been described previously (5.1.1.3.). Due to some improvements of the alkalinity method, precision for A_T could be raised further to 0.5 μmol·kg⁻¹ (between-bottle reproducibility) as judged from regular measurements of duplicate samples. Accuracy of the data has been estimated to be about 2.0 μmol·kg⁻¹ for A_T.

The continuous determination of the partial pressure of CO₂ (pCO₂, closely equivalent to fugacity of CO₂ which more correctly takes into account the non-ideal nature of this gas) in surface seawater and overlying air was carried out during the entire cruise using the automated underway pCO₂ system described previously (see 5.1.1.3.). During the cruise a

data set of more than 2600 one-minute-averages for atmospheric $p\text{CO}_2$ and approx. 45000 averages for surface seawater $p\text{CO}_2$ was generated.

In contrast to the situation in the Pacific, data on isotope ratios for ^{13}C and ^{14}C are scarce for the North Atlantic; one objective during legs 2 through 5 therefore was taking samples to improve this situation. Carbon isotope ratios will give additional information on anthropogenic CO_2 invasion and assist in distinguishing the physical and biological carbon pumps. A total of 239 samples were taken on 12 hydrographic stations on leg 4. A subset of samples will be selected for ^{14}C AMS-measurement.

The calculation of anthropogenic CO_2 from measured concentrations of total dissolved inorganic carbon involves the reconstruction of the "history" of the water sample under consideration. So the measured value is to be corrected for the changes incurred due to remineralization of organic matter and the dissolution of carbonates since the water lost contact with the surface and the preformed pre-industrial value. Difficulties associated with this approach is the role of mixing of different water types with poorly known initial concentrations, possibly leading to non linear effects, the difficulty of choosing appropriate pre-industrial end-member water types and some uncertainties in the assumptions relating to the constant stoichiometric ratios and the resulting from the use of the apparent oxygen utilization (AOU) for determining the contribution of the remineralization of organic matter.

AOU was calculated from the measured dissolved oxygen concentrations; 1907 samples were drawn from a total of 99 hydrographic stations. The samples were measured using standard WINKLER titration, the method was refined to meet WOCE quality criteria (see 5.1.1.3.). Standard deviation as determined from sets of 10 replicates were 0.12%.

The nutrient data, necessary to evaluate atom ratios in the remineralization of organic matter and therefore provide the stoichiometric factors necessary for anthropogenic CO_2 calculation, were obtained from 1905 samples from 97 hydrocasts. Standard photometric procedures (see 5.1.1.3.) were applied using an autoanalyzer system. Standard deviation from measurements of 10 replicates were 0.09%, 1.1%, 1.1% for nitrate, phosphate, and silicate, respectively.

First results

As mentioned earlier, the calculation of anthropogenic CO_2 requires a number of assumptions, which have to be verified for the area under consideration. The data obtained on the various legs of the METEOR 39 cruise therefore should serve as a data baseline to elaborate from property-property plots relations of nutrients and oxygen with the carbon system parameters for different water masses. Also, preformed values from several water types found in the area were also taken from data collected on previous cruises covering their source regions. These relations are currently used to refine the method of back-calculation for the North Atlantic published recently (KÖRTZINGER et al. 1998).

Some more general features of the measured parameters shall be mentioned in the following:

C_T: In contrast to profiles measured in the Eastern Basin of the North Atlantic earlier, those of the Labrador and Irminger Seas are characterized by very little variation below the top 500 meters approximately. Concentrations are about 2152-2156 $\mu\text{mol/kg}$, only in the deeper waters at the Gibbs-Fracture Zone (St. 415-430) elevated values up to 2162 $\mu\text{mol/kg}$ were found. However, despite the low variability, a close positive correlation with AOU and also with nutrient maxima is obvious, as should be expected due to remineralization processes. The little variation found is favorable to detect any alteration of the C_T level in future cruises, as are planned in the SFB 460.

A_T: Alkalinity as well shows remarkable little variation in the Labrador and Irminger Seas, ranging from 2302 to 2312 $\mu\text{mol/kg}$ below 500 meters. The range is even reduced, when the specific alkalinity, normalized to S=35, is considered. This shows the partly conservative behavior of alkalinity. However, positive correlation with silicate is also observed. This is a feature of Southern Component Water, characterized by higher silicate and specific alkalinity. This water is found below 3000 m, most pronounced between St. 393 and 399. Alkalinity rises to 2320 $\mu\text{mol/kg}$ there.

Nutrients: The silicate profiles mainly reflect waters with southern origin, as has been mentioned above. Peak levels reach 16 $\mu\text{mol/L}$ at depth below 3000 m. However, this is only a weak signal, considering a silicate concentration around 120-130 $\mu\text{mol/L}$ for the AABW endmember. Nitrate and phosphate are correlated, but a more detailed investigation will be required to deduce Redfield ratios from the data. Nitrite is close to the detection limit throughout, with occasional peak values up to 0.5 $\mu\text{mol/kg}$ in the 50 m samples. Nutrient maxima in the 1000 m level accompanied with low oxygen indicate the zone of mayor remineralization in the water column.

Oxygen: AOU calculated from oxygen concentrations reach fairly low maxima around 50 to 70 $\mu\text{mol/L}$, both associated with silicate maxima in deep waters and nitrate/phosphate maxima at intermediate levels.

To give an example, Fig. 25 shows isoplots of several parameters along the transect between stations 381 and 404 (roughly a meridional transect along 43°30'W). From the nitrate values the mayor remineralization zone between 500 and 1500 m is clearly visible. High silicate values centered at about 3500 m indicate the prevalence of Southern Component waters. High AOU accompanies both features. Maxima in C_T parallel those in AOU, while the deep silicate maxima between 51 and 53°N is associated with a pronounced A_T maximum. Low values of all parameters around the northern slope indicate the NADW boundary current.

Surface water pCO₂: A first look at the pCO₂ of surface water showed a constant undersaturation of 30-40 μatm throughout the cruise. It was closely related to surface temperature, but also correlated with salinity. The data will have to be compiled after the cruise.

The profiles of $p\text{CO}_2$ co-vary with temperature, indicating that water mass characteristics and their short time variability and local patchiness govern the $p\text{CO}_2$. Positive correlation between $p\text{CO}_2$ and temperature would indicate rising $p\text{CO}_2$ when a water mass gets warmer (theoretically about 4% per °C). Since co-variation is observed also without positive correlation, it is more likely that temperature indicates different water parcels and their patchy distribution in this cases, which due to their inherent preformed $p\text{CO}_2$ cause the observed $p\text{CO}_2$ variability. Negative correlation would also be the result of CO_2 uptake after a water parcel had been cooled due to higher solubility of CO_2 in cold water. However, in most cases CO_2 exchange is slow compared to temperature change of surface waters.

During the first part of the cruise, very low $p\text{CO}_2$ values of as low as 180 μatm were measured. These are not accompanied by a temperature decrease and strongly indicate massive fixation of CO_2 by a plankton bloom.

Fig. 26 gives an example of a $p\text{CO}_2$ registration over 24 hours; given is the $X \text{CO}_2$ (molar fraction of CO_2), the temperature and the salinity. The different water masses, characterized by salinity and temperature, are also reflected in their $X \text{CO}_2$ values; the general trend of higher values with lower temperatures, as expected from increased solubility, is obvious. However, the strong minima found in $X \text{CO}_2$ are more likely resulting from biological uptake.

The data collected so far represent the molar fraction of CO_2 in moist air. Taking into account the atmospheric pressure from the DVS data file and by calculating the water vapor pressure, the fugacity of CO_2 in dry air was calculated. The data are about to be sent to the CO_2 data center in Oak Ridge, Tennessee to serve in the development of a seasonal $p\text{CO}_2$ model of the North Atlantic Ocean.

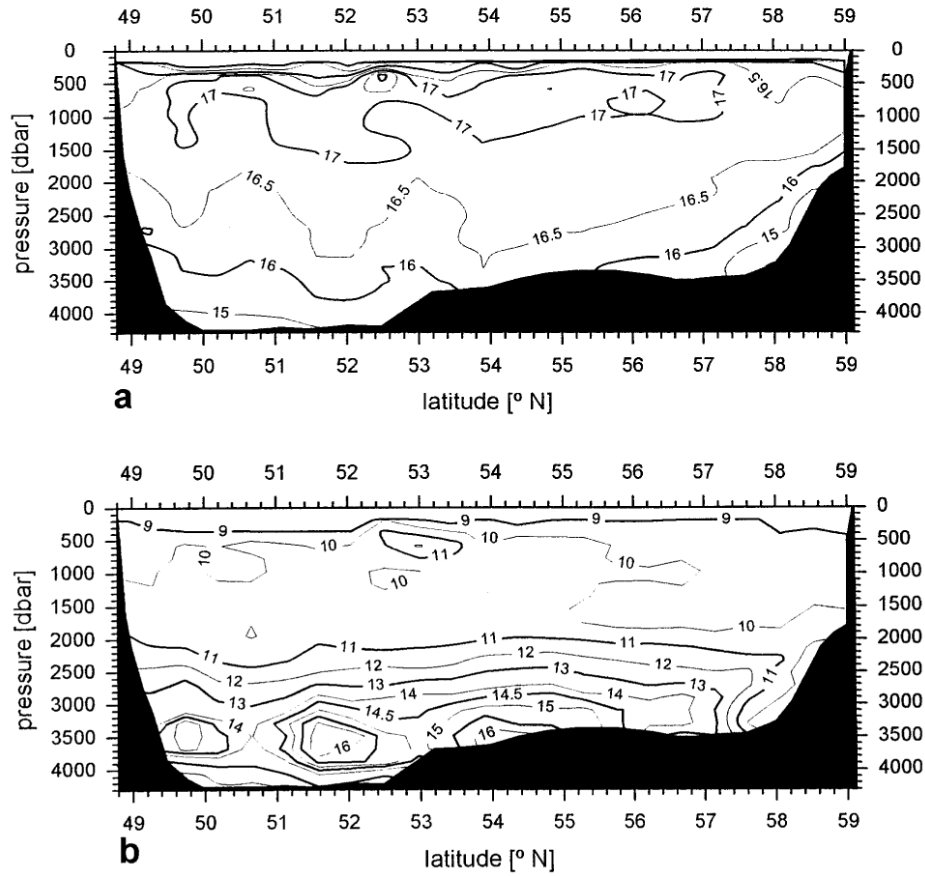
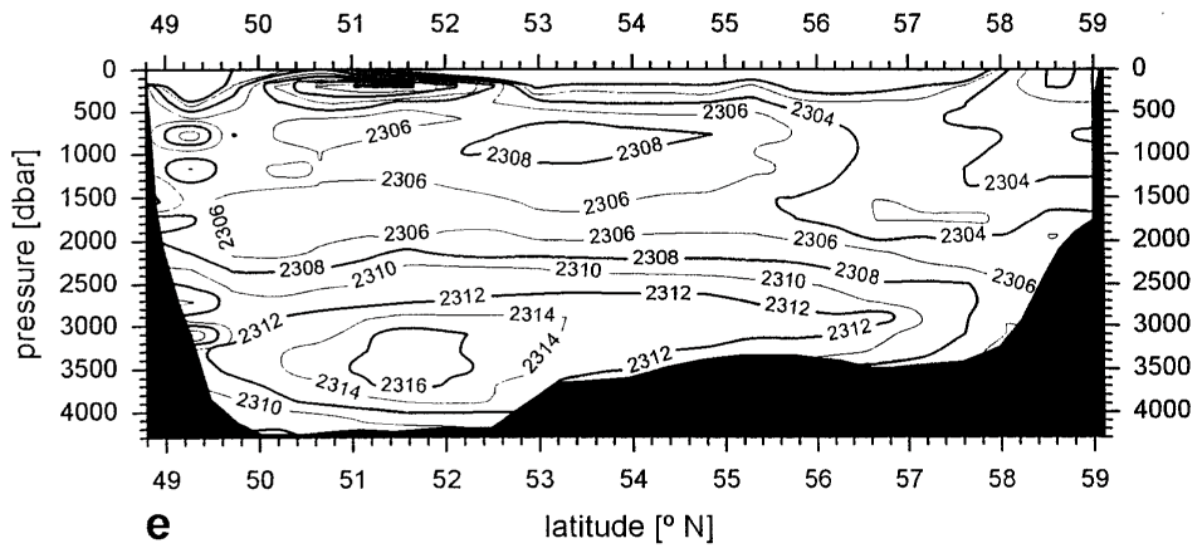
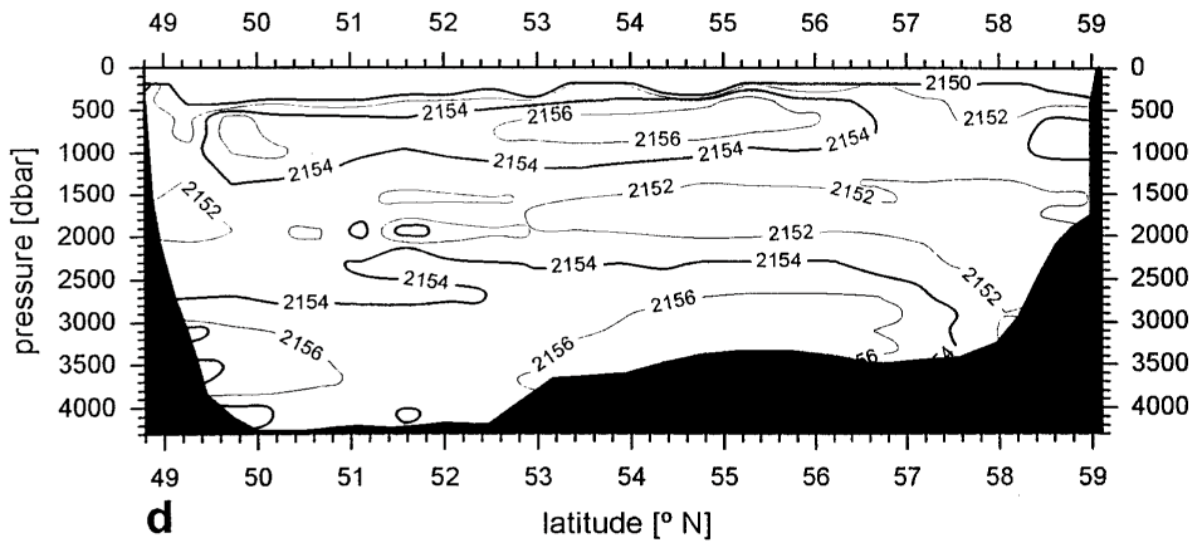
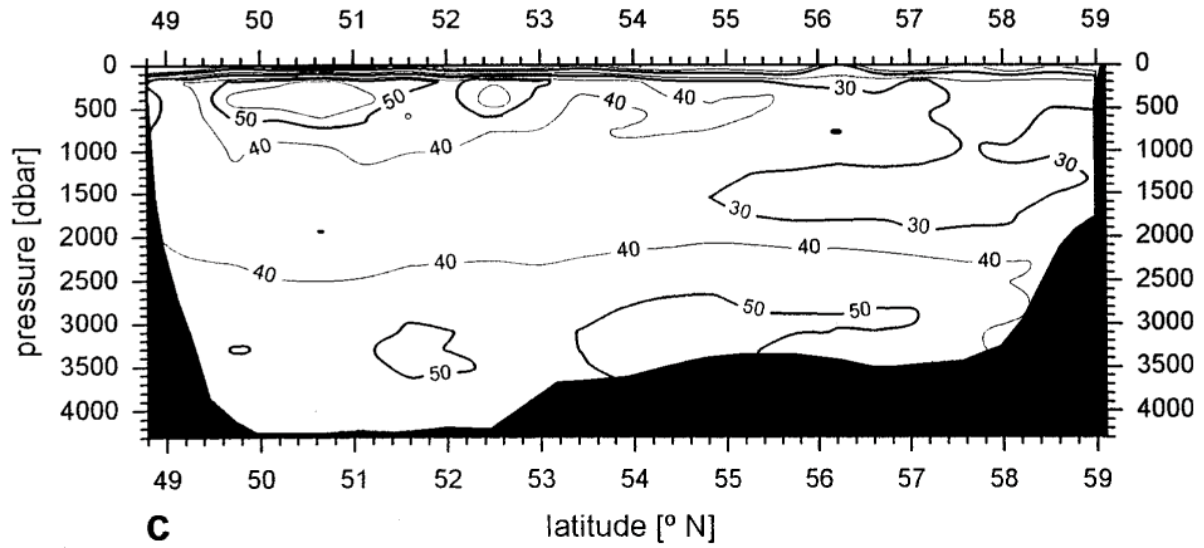


Fig. 25: isoplots of nitrate (a), silicate (b), apparent oxygen utilization (AOU, c), total dissolved inorganic carbon (C_T , d) and total alkalinity (A_T , e) between stations 381-404. Units are in $\mu\text{mol/l}$ (a-c) and $\mu\text{mol/kg}$ (d, e), respectively. (see next page)



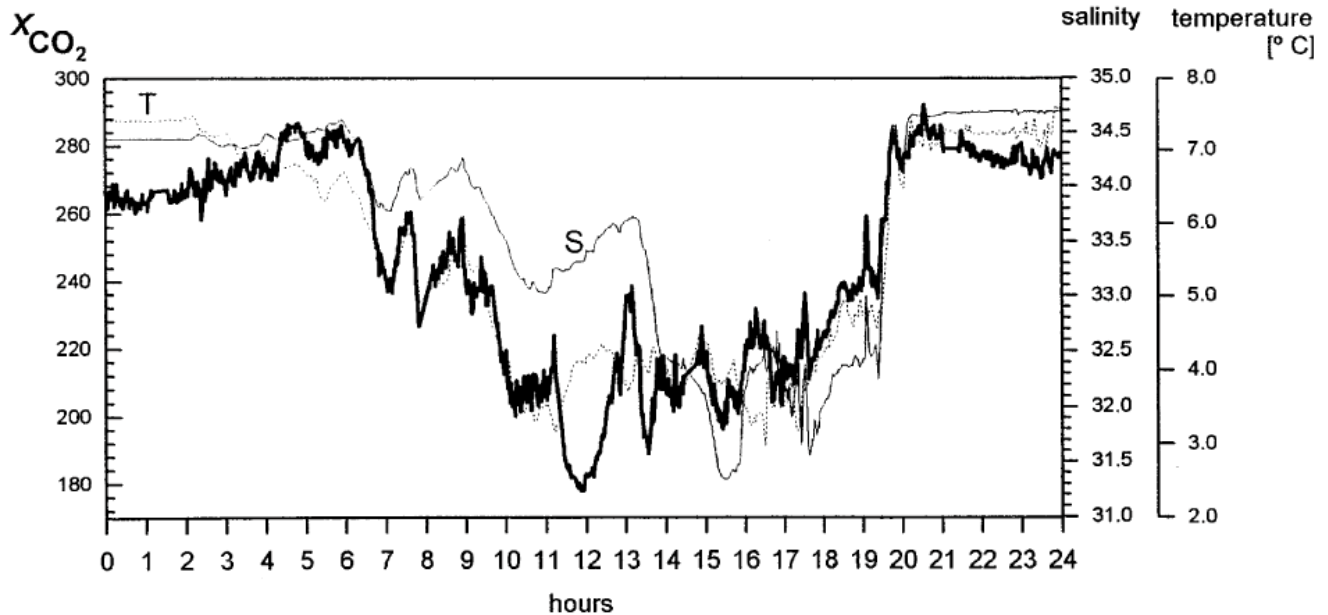


Fig. 26: Continuous registration of molar fraction of CO₂ in surface seawater on July 8, 1997 (bold line). Also included are water temperature (dotted line) and salinity (thin line). Positions at 0:00 and 24.00 hrs are ca. 53°N 51.4°W and 55.3°N 53.9°W, respectively.

5.2 WOCE and VEINS

5.2.1 Leg M39/3

5.2.1.1 Hydrographic Measurements

Hydrographic work on this cruise consisted of a routine 24 hour watch system to operate CTD/rosette casts with a L-ADCP system on station, underway, besides regular XBT drops we maintained two thermosalinograph systems TSG for T and S measurements of the surface layer, the shipboard ADCP and a rain-gauge. Routine meteorological observations were made and recorded.

Hydrographic data collection was done in a 24 hour watch system with the watch running the CTD/rosette casts on station and the underway measurements. For the CTD/rosette casts we used again the BIO label system to uniquely identify water samples and subsequent subsampling right to their analysis. For further details see M39/5.

All TSG, XBT and CTD data were transmitted to BSH in the framework of IGOSS in the relevant formats. All data will be submitted to the relevant WOCE Data Centre after final processing, quality control and annotation.

The 48°N section in the Atlantic has been sampled first during the IGY in 1957, and intensively during the 1990s. This now is the sixth survey since 1957 and the fourth during WOCE (KOLTERMANN u. LORBACHER, 1998). The hydrographic structure is dominated by the warm, salty waters from the South that cover the top 1400 m, with maximum salinities on the

European side of the section. The intermediate waters between 1400 m and 2400 m are fresh and particularly well oxygenated. Properties are set in their area of origin in the West, the subpolar gyre to the north of the section and especially in the Labrador Sea. Below 2400 m and almost down to the bottom are waters with temperatures between 2.9 °C and < 2.0 °C, with an intermediate salinity maximum in both basins at ca. 2900 m. In both basins we find remnants of Antarctic Bottom Waters AABW, best identified by the high silicate signal. The largest contribution is found in the North European Basin. On both sides of the Mid-Atlantic Ridge boundary currents are marked well in the salinity fields by distinct cores.

The largest changes below the thermocline are found in the intermediate waters dominated by the Labrador Sea Water LSW. The strong cooling and freshening observed in the 1993 survey arrived at the European continental slope in the summer of 1996; the eastward spreading has now come to a rest. The core now is detached again from the slope (fig. 27 to 29). The northward progress of the AABW observed earlier on in the 1990s has also come to rest. In the west the 1997 section shows a colder and fresher Labrador Current in the top 500 m, and at ca. 2000 m a comparably pronounced core of the Deep Western Boundary Current. Indications at present are, that the meridional overturning circulation is returning to the one-cell case last observed in the 1980s (KOLTERMANN et al., 1998a).

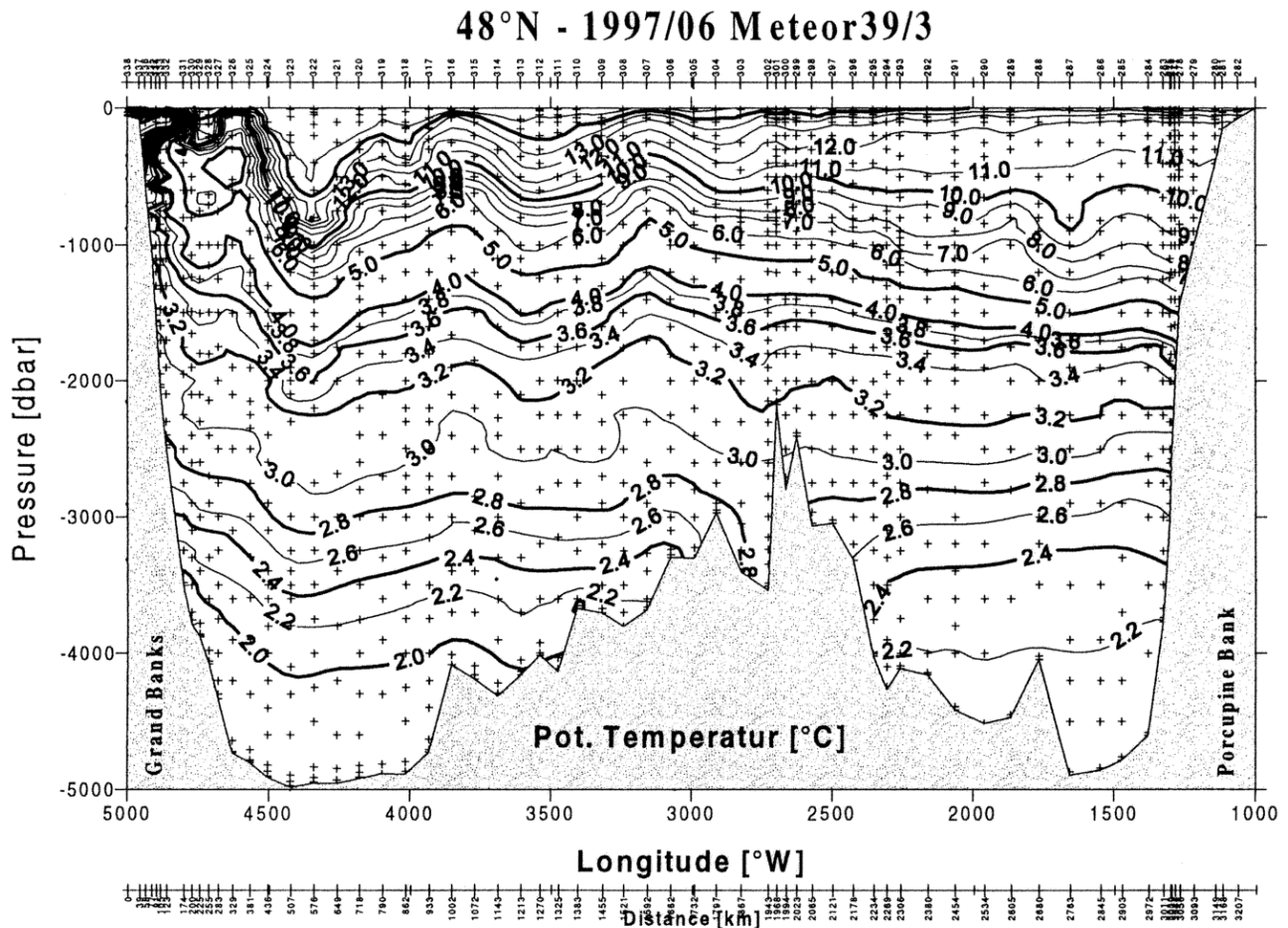


Fig. 27: Potential temperature θ along the A2 section during M39/3, June 1997.

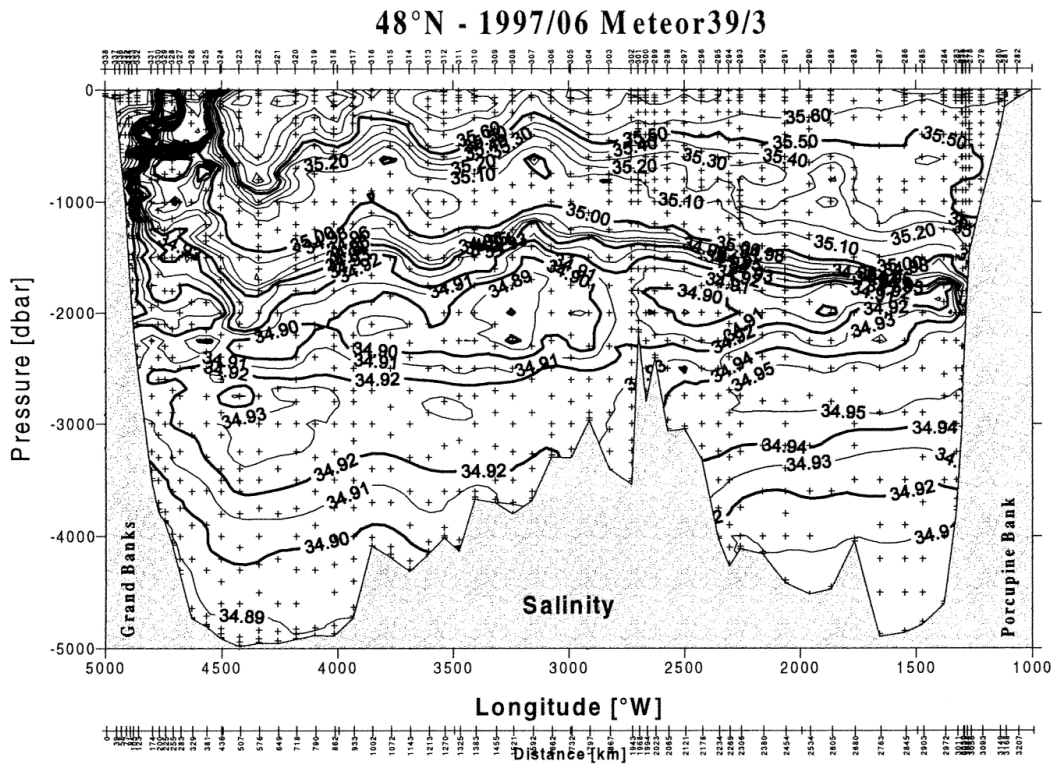


Fig. 28: Salinity S along the A4 section during M39/3, June 1997.

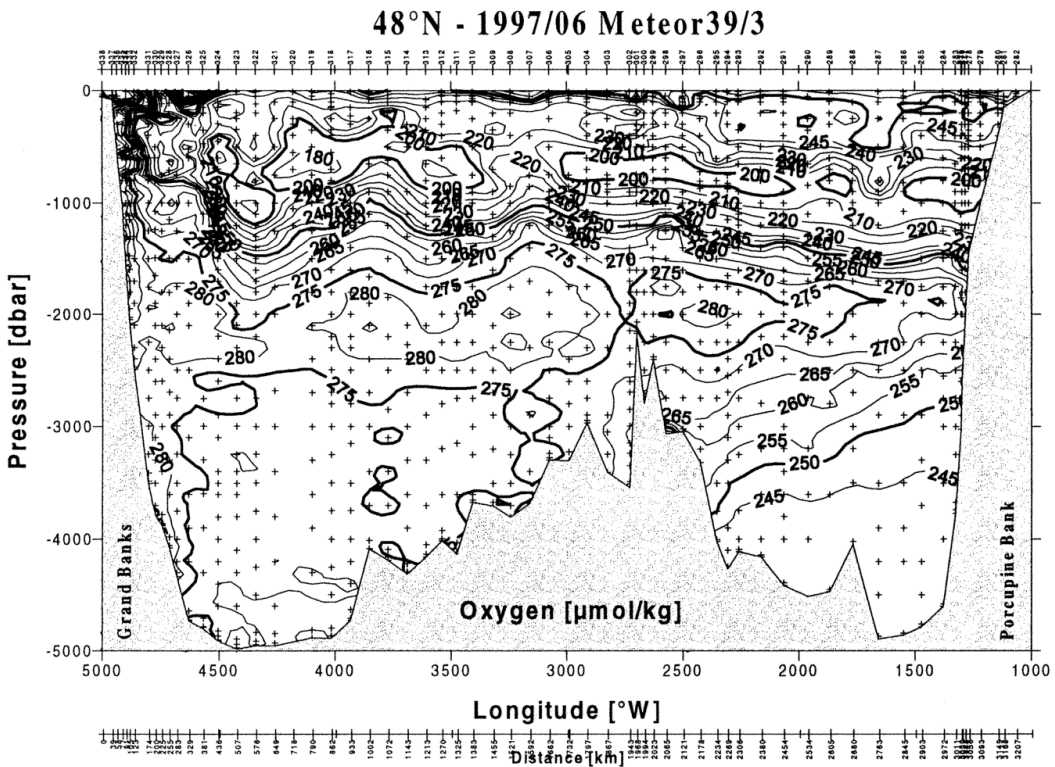


Fig. 29: Dissolved oxygen O_2 in $\mu\text{mol/kg}$ along the A2 section during M39/3, June 1997.

a) CTD Data Processing

(H.-J. Weichert)

A total of 90 CTD profiles was processed from 66 full-depth stations. Due to CTD problems at the beginning of the cruise strict control of instrument combinations and the relevant acquisition software had to be assured.

The following CTD systems were used

DHI-1	7 profiles
DHI-2	11 profiles
FSI	1 profile
BSH-2	40 profiles
NB3	31 profiles

of which for the routine operation the CTD systems NB3 from Kiel and BSH-2 were deployed for alternating shallow and deep casts.

The individual steps in processing the CTD data are documented with the following file suffices:

- *.FRM ctd_form and inserting the Header (ctd_hdinj) for conversion from raw data (counts) to physical units,
- *.ARF ctd_clean with time-lag-correction, monotonized in pressure,
- *.ARC ctd_cal with laboratory calibration polynom applied,
DHI1: pressure and temperature
DHI2: pressure
- *.FLT tsctd_filter filtered with double median and single running mean filters. This includes optional correction by hand (ctd_inter). This is the last version of processing onboard.

For processing the BSH-2 data the HDR-file had to be modified, the previous version was saved as *.HDRor. For the NB3 probe the header was introduced under DHI1 in the HDR files. This was cancelled in the final version of the data. For the oxygen channels of the NB3 further software modifications had to be made to compensate the differing sampling rates.

Despite the problems in setting up the routine CTD/rosette packages, the CTD data are of good quality. Only for three casts we needed to use manual editing programmes. One of these profiles had to be "repaired" in its bottom part. Individual comments for these three profiles are:

- #283002: distinct offset in C and T at ca. 1300 dbar, unrealistic values at the bottom. Further processing required,
- #284001: sudden offset in C only between 3000 and 3700 dbar; editing finished on board, 88
- #313001: non-linear offset in C between 1100 and 4100 dbar; to be processed again in BSH.

All data were backed-up on different media and machines. For further information see leg M39/5.

b) Bottle Data Processing

(G. Stelter)

During the cruise preliminary files *.SUM and *.SEA were produced according to the WHP Operations Manual subject to final inspection after the cruise. The *.SUM file contains all station information and is given in List 7.3.1. The *.SEA file gives all measurements available at this time from analyses of sea water samples drawn from the CTD/rosette system.

All data were merged from the onboard analysis streams into these files. They were cross-checked and inconsistencies discussed with the data originators. Corrections and comments were entered into a third, metadata, file *.DOC. For the first evaluation of the data, instrument and analysis performance from each cast profile and property/property plots were made. These were also compared to data from the previous cruises to assess the instrument performance and potentially detect changes in the ocean.

All data and the relevant information were used in a preliminary data report prepared for all participants at the end of this leg.

c) Salinity Analysis

(A. Frohse)

Salinity analysis during the cruise encountered no problems besides the usual tear and wear. The same procedure and equipment was used as described under leg M39/5. The electronic stability (SBY, zero-reading) was extremely stable (± 1 digit). Only the IAPSO batch P129 showed for two ampoules irreproducible results. We used 42 ampoules for some 100 calibration measurements, that is after ca. 40 samples. In Fig. 30 we give the mean values of the deviations of all calibration measurements from a salinity of 34.998 against station number.

For 30 samples of a sub-standard of Atlantic Water (sampled on June 1, 1997 at 52°44.97 N and 35°0.00 W from 1300 dbar depth Fig. 31 shows the deviations from the mean, 34.8973. It indicates that these deviations all lie within the 0.001 limit.

d) LADCP measurements

(F. Morsdorf, G. Stelter)

The LADCP-system (153 kHz) used on legs M39/2 and M39/5 on loan from IfMK was also used during this leg. It was attached to the rosette system. For maintenance purposes the LADCP was not used on stations 287 to 289. In total 56 profiles over the entire water depth were sampled. All profiles were analyzed on board. Navigation of the data was done using the ship's GPS-system.

e) XBT measurements

(Ch. Stransky)

For the entire length of the A2 section XBT probes were dropped after leaving the CTD station and at mid-distance points between stations. A total of 133 drops were made, resolving the

temperature field of the top 1850 m at sub-eddy scale. Probes of the T-5 type were used for most drops. Only at water depths less than 800 m Deep Blue probes were deployed. During most measurements the ship's speed was reduced to 6 kn to make maximum use of the probes maximum depth. The quality of the data is good, there were only few drops were either the probes did not work properly or other errors occurred due to bad grounding.

Data were processed on board and all profiles were submitted to BSH in near real-time.

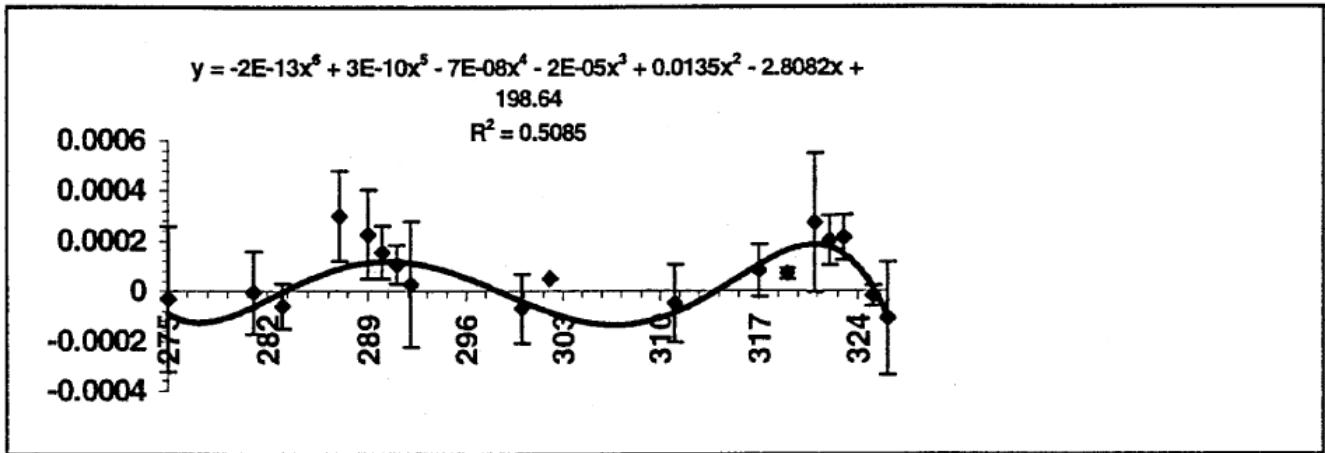


Fig. 30: Deviations of salinity measurements from the mean of all calibration measurements, IAPSO batch P129.

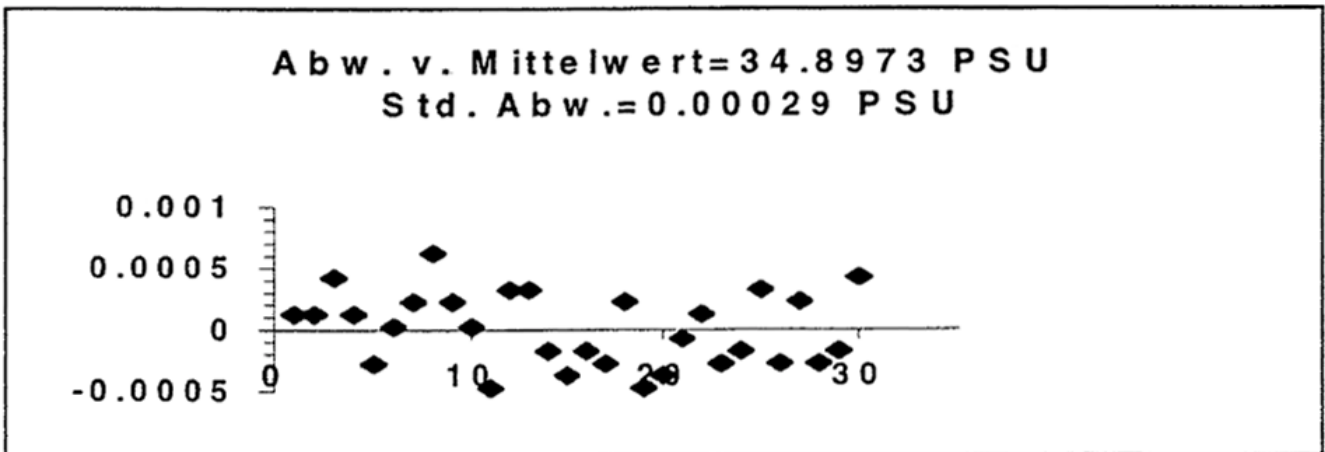


Fig. 31: Deviations of salinity measurements from the mean of 30 samples of Atlantic Water sub-standard

5.2.1.2 Nutrients and Oxygen Measurements

a) Nutrients Measurements

(R. Kramer, H. Tacke)

We have analyzed sea water samples for the nutrients ($\text{PO}_4\text{-P}$), nitrate ($\Sigma\text{nitrate}+\text{nitrite}$, $\text{NO}_3+\text{NO}_2\text{-N}$) and silicate ($\text{SiO}_4\text{-Si}$) using automatic photometric methods. For quality assurance purposes during the cruise in each analysis run we measured mixing standards 3 and 5 as a sample. In addition three calibration casts were used to estimate the overall error of these measurements. The Q-standard (sea water samples of the first rosette cast) could not be analyzed because of a failure of the air conditioning unit. All analyses were worked in continuous shifts.

Equipment

We used:

a Skalar SA 4000 Analysersystem, Matrixphotometer Typ 6250

Skalar Software 6.2

calibrated Eppendorf-, Finn- and glass pipettes for the standard solutions

calibrated flasks for the standard solutions

Methods

$\text{PO}_4\text{-P}$, measurement range: 0,01-4,0 $\mu\text{mol/l}$

According to MURPHY and RILEY (1962)

Absorption of the blue Phosphorusmolybdat complex was measured at 880 nm, proportional to the concentration. Reaction at 38°C

$\text{NO}_3+\text{NO}_2\text{-N}$, measurements range: 1,0- 30,0 $\mu\text{mol/l}$

According to BENDSCHNEIDER and ROBINSON (1952)

The colour complex was measured at 540 nm. Chemical reaction at lab temperature.

$\text{SiO}_4\text{-Si}$, range : 1,0- 50,0 $\mu\text{mol/l}$

According to KOROLEFF (1971)

The absorption of the blue Siliciummolybdat complex was measured at 810 nm, proportional to the silicate concentration. Reaction at ~30°C

Procedure:

Samples were drawn directly at the rosette bottle. PE-bottles at 250 ml were rinsed three times with the sample and filled up to the lower edge of the shoulder. The sample bottles were kept wet with the remnants of the previous sample. For the analysis samples were filled into 8 ml cups, after rinsing three times with the sample water or the standard. During the entire cruise 40 cups were in constant use and kept wet during that time.

Standards were prepared daily. For each CTD/rosette cast a linear calibration was made for all nutrient parameters.

Precision

On three stations calibration casts were added to estimate the reproducibility and overall error of measurements

Station	depth dbar	NO ₃ +NO ₂ ± std dev μmol/l	PO ₄ ± std dev μmol/l	SiO ₄ -Si ± std dev μmol/l
274/1	3500.7±0.47	21.750±0.196 0.89 %	1.432±0.034	39.298±0.23 0.60 %
320/4	3758.5±2.31	17.451±0.130 0.74 %	1.114±0.040	21.599±0.18 0.83 %
326/1	2301.3±1.41	17.429±0.102 0.59 %	1.096±0.067	14.431±0.22 1.53 %

B Oxygen Measurements

(F. Schmiel, A. Gottschalk)

Dissolved oxygen was measured by the Winkler method modified by Carpenter with a Metrohm Titroprozessor and a double platinum electrode. The dissolved oxygen content of seawater was defined as ml per liter seawater.

Precision

Multiple samples from fixed depths were taken on three calibration stations. For oxygen the overall error estimated was

Station	depth dbar	O ₂ ± std dev ml/l	percent %
274/1	3500.7 ± 0.47	6.619 ± 0.041	0.74
320/4	3758.5 ± 2.31	6.282 ± 0.012	0.19
326/1	2301.3 ± 1.41	6.326 ± 0.014	0.23

C Tracer-Oceanography (CFCs, Tritium and Helium)

(K. Bulsiewicz, U. Fleischmann, G. Fraas, R. Gleiss, V. Sommer)

The investigated tracers are carbon tetrachloride (CCl₄) and the chlorofluorocarbons (CFC) F-11, F-12, F-113 as well as tritium and the noble gases Helium and Neon. The time dependent input of the CFCs, CCl₄, tritium and helium at the ocean surface is known. The tracer concentration of the surface water is altered by mixing processes when the water descends to deeper levels of the ocean. The helium concentration is altered additionally by degassing at the sea floor and by tritium decay. Measuring the concentration of the tracers delivers information about time scales of ventilation processes of subsurface water.

The atmospheric F-11 and F-12 contents increased monotonously with different rates from the forties until the beginning of the nineties. CCl₄ increases since 1920 while F-113 started to increase 1970. CFC and CCl₄ concentrations and their ratios vary over wide ranges and are used to estimate the 'age' of water masses (i.e. time since leaving the surface). 'Younger' water is tagged with higher CFC concentrations compared with 'older' water.

Tritium and ³Helium are used to determine the 'age' by inverting the law of radioactive decay after the tritiogenic part of the ³Helium is separated from the other components. Helium can be used additionally to trace water masses with terrigenous helium as the Antarctic Bottom Water and the Mediterranean Water.

Sampling and Measurements

The CFC's F-11, F-12, F-113 and the tracer CCl₄ were measured on board on the majority of stations using a gaschromatographic system. All measurements were done according to the WHP- standards.

For Helium and tritium measurements (on shore) water samples were filled in copper tubes and glass bottles respectively on approximately every second station. A new sampling procedure for

helium was tested, for which the water is filled in flame-sealed glass ampoules. The advantage of this sampling procedure is to shorten the measuring process in the laboratory.

Altogether we occupied 53 stations and analyzed 779 water samples for CFCs. 550 samples were taken for helium and tritium. 80 water samples were taken in flame-sealed glass ampoules.

Preliminary results

The antarctic-influenced bottom water of the eastern North-Atlantic is identified in the eastern basin close to the European shelf break by the lowest CFC values (Fig. 32) deep eastern basin below 2500 meters the values are rising on isobaths from east to west. This is due to the influence of ventilated overflow water from the Norwegian Sea, which reaches the eastern basin as Iceland-Scotland-Overflow-Water and is fed into the recirculation of the Westeuropean Basin. In the depth range between 1500 and 2500 meters a maximum layer is found in both basins that is related to the Labrador Sea Water. Different cores can be seen in the CFC maximum-layer. At 30°W a core with very fresh LSW is found with extremely high CFC-values. The surface water concentrations are slightly supersaturated compared with air concentrations.

In the western basin the deepest samples of most of the station had higher CFC values than the water above. The absolute minimum was mostly reached between 300 and 1000 meters above the bottom. The elevated values at the bottom are again caused by the influence of overflow water from the Norwegian Sea, here the Denmark-Strait-Overflow-Water. Close to the North American Shelf the Deep Western Boundary Current can be identified. One core with high CFC (Fig. 33) and CCl₄ values is found in a depth of about 4000 meters and high values are found from the surface down to more than 1500 meters.

The structures described above are very similar for all tracers measured on board. There is a broad minimum in the range of the intermediate waters for CCl₄. This is caused by its instability for water above 10°C.

The preliminary results for the CFC measurements show a significant rise in tracer concentration in comparison with the data set from the WHP-A2 section 1994 (M30/2). An exception was found in the eastern basin. A LSW-core with very high concentration was found there in 1994, but not this time. In 1994 some deep stations were found in the eastern part of the North American Basin that had an obvious CFC-minimum at the bottom due to an influence of northward flowing Antarctic Bottom Water. No such stations were found this time.

The water sampling for Helium in sealed glass ampoules turned out to be quite successful [ROETHER et al. 1998]. The ampoules were safe to handle also under rough field conditions. The new method is capable of giving good data, especially for the ratios of Helium and Neon, which are the basis of our interpretation of helium data. The new sampling method has about the same blank as the copper tube sampling. But a certain air contamination still exists in the glass ampoules which shows up as an offset and a lesser reproducibility in helium concentrations compared to copper tube sampling.

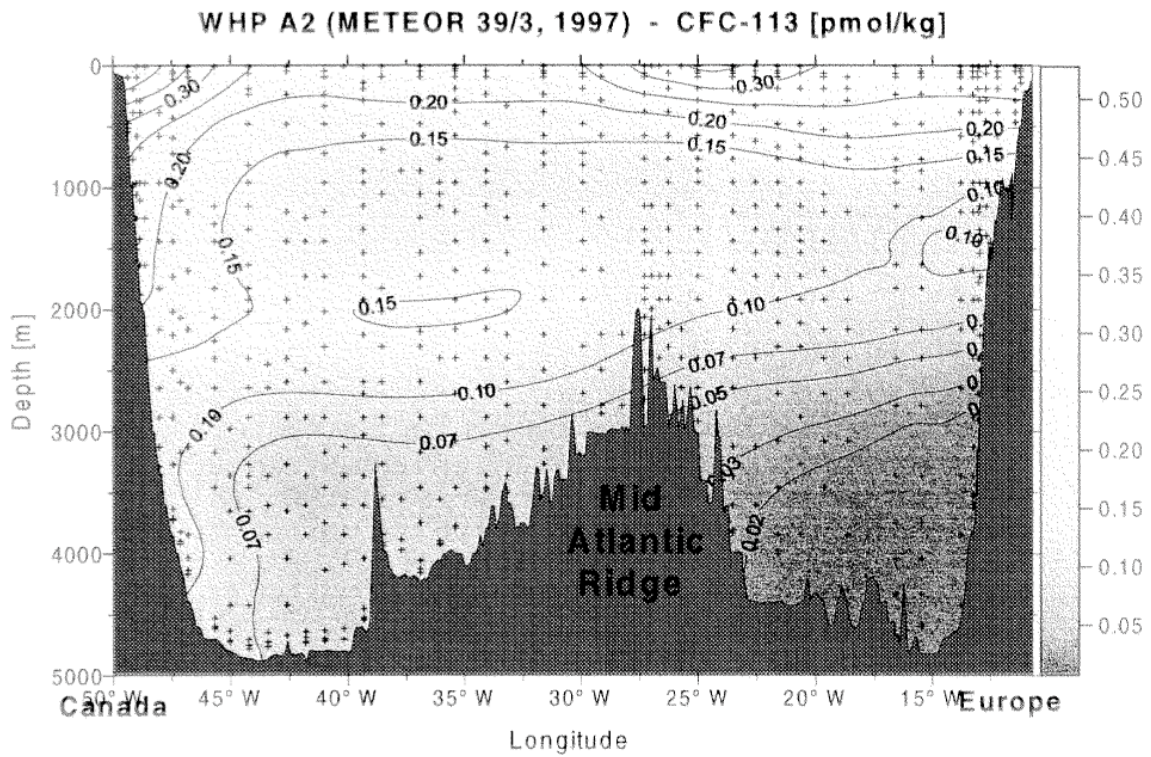


Fig. 32: CFC-113 measurements along the WHP section A2 during M39/3, June 1997.

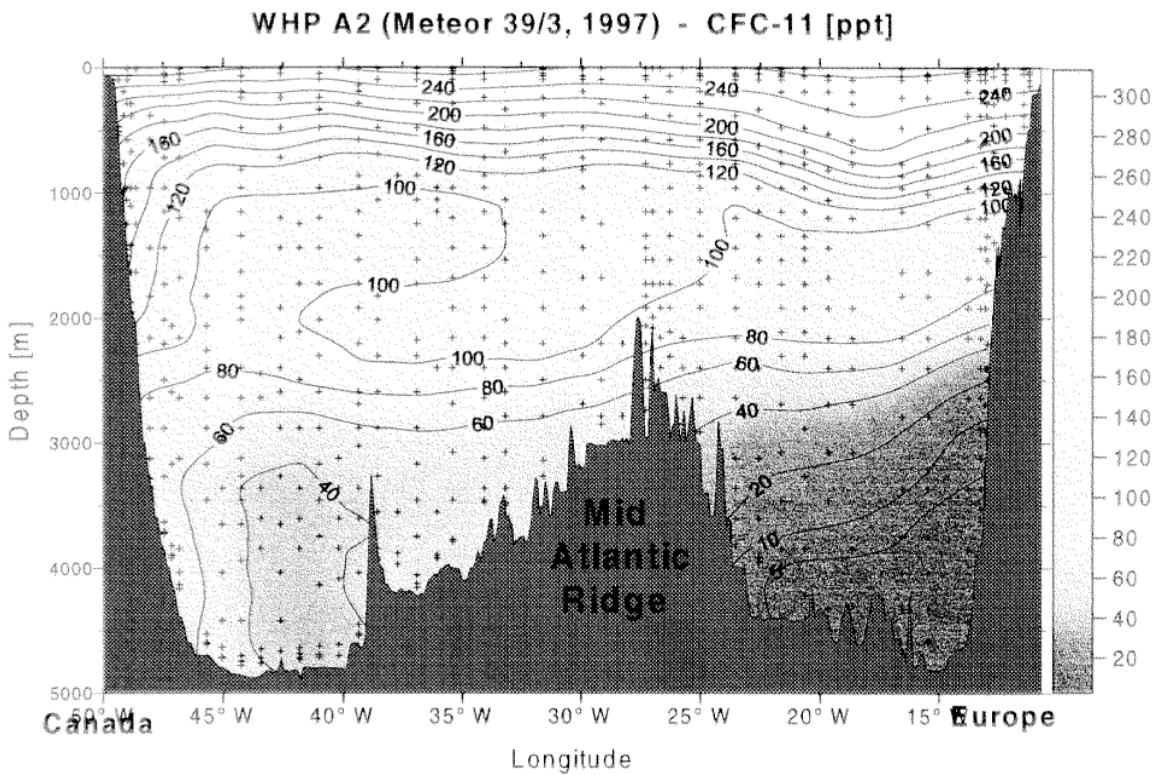


Fig. 33: CFC-11 measurements along the WHP section A2 during M39/3, June 1997.

5.2.1.4 Mooring work and float deployment
(H. Giese, K. P. Koltermann)

a) Mooring work

West of the Mid-Atlantic Ridge two moorings were recovered and re-deployed. They were set to cover over the full water-depth the eastern boundary current system which shows a complicated baroclinic structure in hydrographic surveys. Besides the question whether the core of the Labrador Sea Water LSW is arriving from the south or north a further core at ca. 2200 m with slightly higher salinities is monitored. These details are imbedded in the general circulation west of the ridge and is not clear if there is a re-circulation within the Newfoundland Basin, feeding the boundary current from the west and south or whether this re-circulation is instationary. These sites have been maintained intermittently since July 1993. Moorings deployed during the Gauss cruise G276 in May 1996 were recovered without any problems.

Each of the moorings deployed in 1996 and recovered during this cruise is made up of 5 current- meters, 3 thermistor strings and 5 SeaCats each. Further instrumentation details are given in Tab. 7.

METRANA 96		K1		46° 19,8 'N		29° 55,9 'W		23.05.1996		1230 UTC		z= 3280 m		ausge.		Gauss 276	
		Ist-						22.06.1997		700				aufge.		Meteor M39/3	
Code	STATION	tiefe	Solltiefe	bis Tiefe	Gerät	Nr	Parameter	Zusatz Nr	Temp-B	Bemerkungen							
K1/96.1	97011	449	390		RCM5	10560	VTP		25°C	2 Jahre Auslegedauer							
K1/96.2	97504	460	400		SeaCat	2056	S:T			Wassertiefe 3220 m							
K1/96.3	97603	466	410	716	IR7	1287	T1-T11	TK250:1355	low								
K1/96.4	97503	969	910		SeaCat	2055	S:T										
K1/96.5	97010	980	920		RCM5	11496	VTP										
K1/96.6	97602	1061	1000	1361	IR7	1280	T1-T11	TK300:1917	low								
K1/96.7	97502	1564	1500		SeaCat	1442	S:T										
K1/96.8	97009	1651	1590		RCM8	10587	VT										
K1/96.9	97601	1657	1600	2057	IR7	1493	T1-T11	TK400:2372	arctic								
K1/96.10	97501	2559	2500		SeaCat	2005	S:T										
K1/96.11	97008	2611	2550		RCM8	10653	VT										
K1/96.12	97500	3103	3050		SeaCat	1725	S:T										
K1/96.13	97007	3186	3100		RCM8	10586	VT										
					releaser	4751											
Bodentiefe		3280															

Tab. 7: Table of moored instrumentation recovered during M39/3.

METRANA 96		K3		45° 20,15 N		33° 13,35 W		23.05.1996		1625 UTC		z=3659		ausge.		Gauss 276	
		Ist-						23.06.1997		1600				aufge.		Meteor M39/3	
Code	STATION	tiefe	Solltiefe	bis Tiefe	Gerät	Nr	Parameter	Zusatz Nr	Temp-B	Bemerkungen							
K3/96.1	97016	400	390		RCM7	10580	VTP			2 Jahre Auslegedauer							
K3/96.2	97509	405	400		SeaCat	2075	T:S:P			Wassertiefe 3650 m							
K3/96.3	97606	412	405	462	IR7	1290	T1-T11	TK50:233	low								
K3/96.4	97015	704	700		RCM7	11995	VT										
K3/96.5	97508	765	750		SeaCat	1297	S:T										
K3/96.6	97605	807	800	1107	IR7	1279	T1-T11	TK300:1918	low								
K3/96.7	97014	1490	1480		RCM7	10582	VTP										
K3/96.8	97507	1500	1490		SeaCat	1563	S:T										
K3/96.9	97604	1507	1500	1907	IR7	1494	T1-T11	TK400:2373	arctic								
K3/96.10	97506	2008	2000		SeaCat	2003											
K3/96.11	97505	2510	2500		SeaCat	2004											
K3/96.12	97013	2553	2540		RCM8	10650	V,T										
K3/96.13	97012	3505	3500		RCM8	10585	V,T										
					releaser	1724											
Bodentiefe		3659															

Tab. 8: Table of moored instrumentation deployed during M39/3

For the deployment during this cruise the mooring instrumentation varied slightly. Mooring K1/97 was instrumented with 5 current-meters, 3 SeaCats and no thermistor strings, K3/97 was fully instrumented with 5 current-meters, 3 thermistor strings and 3 SeaCats. These moorings have been recovered without losses and problems during the Gauss cruise G316/1 in May 1998. Further instrumentation details are given in Tab. 8.

Preliminary results

At both sites the flow is largely barotropic and stationary. At the easternmost site K1 it has mainly an E-W preference, at K3 in the West is SW - NE. The main baroclinic feature is the stronger flow in the LSW layer, roughly between 1000 and 1700 m. As in previous deployments the flow is from June to December towards the East. At site K3, the western mooring, it then changes from SW to directly West, whereas at site K1 it changes direction from SW to North. The salinity and temperature data at the moorings and particularly at K1 again show the arrival and existence of the LSW in the first half of the year, roughly from December to about June/ July. In the second half temperatures and salinities increase dramatically and coincide with the increased northward component of the flow at site K1.

b) Float deployments

(K. P. Koltermann)

Three C-PALACE float were deployed during this cruise leg to add information on the larger-scale Lagrangian flow-field at 1500 m depth and monthly CTD-Profiles around the mooring sites. Sensor and mission details comply with the WOCE float programme in this region. These float with a duty cycle of 30 days therefore complement the present intense WOCE Float Programme in the Subpolar and Subtropical Gyres.

The deployment details are:

float	stat	start time	deploy. time	deploy. position
#719	302	6/20/97	6/20/97	lat: 46 54.772 N
		18:19:16	20:41:10	lon: 27 18.393 W
#720	304	6/20/97	6/21/97	lat: 46 32.419 N
		16:57:40	10:40:00	lon: 29 08.404 W
#718	307	6/22/97	6/22/97	lat: 45 49.733 N
		09:35:21	14:14:00	lon: 31 36.639 W

Note: All times are UTC.

5.2.1.5 “TCO₂ and Total Alkalinity Measurements along 48°N on the WHP section A2, 1997”

(C. Neill, E. Lewis)

Samples were collected and analyzed on ship for total alkalinity and dissolved inorganic carbon (DIC). Other samples were collected for on-shore analysis for dissolved organic carbon by Dr. Dennis Hansell of the Bermuda Biological Station for Research and for ¹³C by Dr. Arne Koertzing of the Kiel Institut of Marine Research. This report discusses the total alkalinity measurements.

Methods

General

Samples were collected and analyzed in alternating 12-hour shifts. Samples were first analyzed on the SOMMA (single operator multi-parameter metabolic analyzer) for DIC, after which they were titrated for alkalinity. DIC was analyzed first since it is affected by CO₂ exchange with the atmosphere, unlike alkalinity. Software and hardware from Kiel was used to determine the total alkalinity in units μmol/kg. All post-cruise data processing was done by Ernie Lewis.

Sample Collection and Storage

Samples were collected in 700 ml bottles with ground glass stoppers directly from the Niskin bottles, allowing for an overflow of at least one full bottle volume. They were stored in the dark at 3°C until being analyzed for DIC, then they were warmed in a water bath to 25°C before being titrated to determine total alkalinity. All samples were analyzed within 24 hours of being collected.

Instrumentation

The titrations were made using a Metrohm 665 Dosimat and a Metrohm 713 pH meter with an Orion Ross electrode and an Orion double junction reference electrode filled with 0.7 molar NaCl. The equipment is computer controlled, and other than filling and rinsing the cell, the titration and data collection is fully automatic. The cell was a plexiglass cell containing about 100 ml of sample and was thermostated to remain at 25°C. The equipment used was on loan from Dr. Ludger Mintrop of the Institut of Marine Research at Kiel. It was already on board and was used by researchers from that laboratory for the previous leg and the following leg. A glass pipette for sample delivery is an integral part of the system and was calibrated both before and after the cruise by researchers at Kiel. The volume determination performed after the cruise suffered from poor reproducibility, so the volume determined before the cruise was used: 99.014 (±.043) ml. This was used with the density of the sample (calculated from the bottle salinity and measured temperature) to determine the mass of seawater being titrated.

Titration Analysis

Samples were equilibrated at 25°C and titrated with the HCl/NaCl mixture. The EMF of the electrode pair was recorded for 20 volume additions of the acid mixture. These values were fit using Kiel's software to determine the values of alkalinity, DIC, E₀ for the electrode pair, and pK₁ for carbonic acid which result in the least square deviation from the measured values of

the EMF. The value of SSS (the rms error of the fit in units μmol) is also given. Values of DIC, E_0 , and pK_1 determined in this fashion are not reliable as they are highly correlated, but the method is very robust for determination of alkalinity. The value of SSS is sometimes an indicator of problems during a titration. Generally values $<.5$ are considered acceptable, with higher values meaning that the fit is poor, though the alkalinity value determined from that fit might still be accurate.

The strength of the acid (a mixture of HCl and NaCl) used for titration was determined by Dr. Andrew Dickson of the Scripps Institute of Oceanography to be 0.097723 mol/kg, with a density of 1.0232 kg/l at 24.13°C. Using the formula given in the DOE Handbook the density at 25°C was found to be 1.0228 kg/l, yielding a value of .099951 mol/l as the value used for the acid mixture. Since the dosimat gives the volume of the acid dispensed, this value will tell the number of equivalents (moles) of acid used to titrate the sample.

Quality Control

Replicate analyses were performed on 1 out of every 10 samples. Typically samples with Bedford ID numbers ending in 0 were sampled twice and analyzed separately as independent samples. In addition, two different batches of CRMS (Certified Reference Materials) provided by Dr. Andrew Dickson of the Scripps Institute for Oceanography and certified for alkalinity, were analyzed to check the overall accuracy as well as the precision of the analyses.

Sampling Locations

Of the more than 1500 samples which were taken on 86 casts at 66 stations, 689 samples (including 61 replicate samples) from 33 stations were analyzed for alkalinity. At least one station per day was fully analyzed, except for one day when the SOMMA was down. Samples from the following stations were analyzed for alkalinity (# of depths sampled in parentheses):

275 (19)	277 (20)	279 (13)	282 (5)	283 (22)	285 (21)
288 (19)	291 (37)	293 (31)	295 (21)	297 (21)	299 (22)
301 (22)	302 (17)	304 (21)	305 (20)	307 (20)	309 (20)
311 (10)	314 (22)	317 (23)	319 (21)	321 (18)	322 (12)
323 (32)	325 (23)	327 (22)	329 (21)	331 (6)	332 (22)
334 (13)	336 (8)	337 (4)			

Salinities Used for Calculations

Salinity is needed to convert from the volume of the pipette to the mass of seawater so the alkalinity can be expressed in $\mu\text{mol/kg}$. Errors in salinity affect alkalinity only slightly: an error of 1 in salinity will result in an error of about 1.5 $\mu\text{mol/kg}$ in alkalinity, which is less than the precision as determined by replicate analyses.

The salinity values were taken from the CTD data provided by the chief scientist. For six samples bottle salinities were not available and were estimated from CTD salinity and bottle salinities of nearby samples:

Bedford ID#	salinity
200688	35.600
200969	34.950
201238	35.843
201266	34.940
201470	36.010
201846	35.050

Sample 201468 misfired and the salinity from the SOMMA salinity cell, 36.010, was used instead of the value 30.077 given in the CTD reports.

ID values 200985-200994 and 201803-201804 were used twice. We only sampled on the second occurrence, so I deleted the first occurrence of these. All of these changes were documented in the hydrography master file.

Data

The values from the calculations are in the file M39_3AT.XLS. This file has 13 columns, one for each of the following: Bedford ID (unique for each sample), QC flag, station, cast, Niskin, salinity, pressure (dbar), alkalinity, DIC determined from the alkalinity titration, DIC determined from the SOMMA, E_0 , pK_1 , and SSS (the error of the titration fit).

QC flags were assigned to each sample as follows:

- 2 = acceptable measurement
- 3 = questionable measurement (value of SSS > .5 μmol but < 1 μmol)
- 4 = unacceptable measurement (value of SSS > 1 μmol)
- 5 = sample analysis failed (-9 entered for all values)
- 9 = sample not analyzed for alkalinity

The alkalinity analyses on the cruise were remarkably free from errors. The vast majority of the samples (666) were assigned a flag of 2. Only 17 samples were assigned a flag of 3, and 6 samples were assigned a value of 4. Two samples were assigned a flag of 5, and two samples were assigned a flag of 9.

The 6 samples which were assigned a flag of 4 all occurred during the first station (275). It is typical for electrodes to become conditioned with use and perform better than if they have been sitting unused, so the fact that all of these occurred on the first station is understandable. It is worth noting that although high values of SSS indicate that the fit is poor, it does not necessarily indicate that the alkalinity value determined from the fit is inaccurate.

The two samples with the flag 5 were those for which alkalinity titrations were started but did not finish. In one case the computer hung and the titration had to be aborted (201275); in the other the stir bar was not turned on and the titration was aborted (201178). All samples which were analyzed for DIC were also analyzed for alkalinity except for two (200602 and 200623) on the first station (274), which was used for testing purposes.

Other possible errors which may occur in alkalinity titrations include bubbles in the acid line and incomplete rinsing. In the first case, it appears that more acid was added than actually was, leading to an over- estimation of the alkalinity. In the second case, some alkalinity is titrated before any acid is added, leading to under-estimation of the alkalinity. Both of these are difficult to determine. Plots of alkalinity vs. depth show a few points which look out of profile which may be due to these reasons.

Precision and Accuracy

Precision is determined by analyzing replicate samples and by analyzing Certified Reference Materials. Accuracy is estimated from comparing values of the Certified Reference Materials with the certified values.

A total of 61 pairs of replicate samples were analyzed. The replicate sample data are summarized in file M39_3RAT.XLS. The mean difference was 2.9 $\mu\text{mol/kg}$, which is good compared to other cruises on which I have performed alkalinity measurements. Three of the replicates were between 9 and 11, which are higher than desired. This is also typical of other cruises on which I have performed alkalinity titrations.

A total of 59 analyses of Certified Reference Materials were made after they were analyzed on the SOMMA for DIC (usually three times per day). Two different batches (34 and 36) were used. Data for these are summarized in the file M39_3CAT.XLS. Results are summarized in the table below.

CRM Batch	certified alkalinity	# bottles analyzed	mean result	standard deviation
34	2284.35	44	2287.9	3.7
36	2283.83	15	2285.9	3.4

All of the 15 samples of Batch 36 which were analyzed resulted in values which were within two standard deviations of the mean. In total, 44 samples of batch 34 were analyzed. One sample was started and the cell was found to be open, thus invalidating the sample, which was not completed. One sample (bottle 217) was analyzed twice. The values obtained during the cruise ranged from 2279.2 to 2299.2. No overall drift was detected during the cruise, and the standard deviations, as well as the differences between the mean and certified values, are in line with values obtained on other cruises.

5.2.2 Leg M39/5

5.2.2.1 Hydrographic Measurements

(A. Sy, K. Bakker, R. Kramer, D. Machoczek, H. Mauritz, F. Schmiel, K. Schulze, G. Stelter, M. Stolley, N. Verch)

Operational Details

Following the WOCE Hydrographic Programme requirements, the hydrographic stations were worked in one-time survey mode. The station spacing was designed in accordance with bathymetry and varied between some 5 nautical miles (nm) and 30 nm. To increase the spatial resolution of the hydrographic sampling, temperature profiles up to 2000 m depth were also obtained by use of expendable bathythermographs (XBT).

Hydrographic casts were carried out with an NBIS MK-IIIB CTDO₂ unit, labeled "DHI-1". The underwater unit was mounted vertically inside a rosette frame with a 24-place General Oceanic pylon and 22 x 10 litre Niskin bottles uniquely marked. All bottles were equipped with stainless steel springs and grease-free O-rings to avoid contamination in CFC sampling. Also attached to the CTD/Rosette system were Benthos altimeter, SIS digital temperature meters and pressure meters (DSRT) and, instead of 2 Niskin bottles, a self contained lowered ADCP was mounted. The mean constant maximum descent rate was 1 m/s. CTDO 2 data were collected at a rate of 64 ms using a PC based data acquisition software designed by BSH. A video tape unit was operated as a backup system. Hardware and software instrumentation ran without serious problems during the whole cruise leg. The rosette system used proved to be well adapted to the CTD unit, and thus only few mistrips occurred.

The bottle sampling sequence was as follows. Oxygen samples were collected soon after the CTD system had been brought on board and after CFC and 3 He had been drawn. The sample water temperature was measured immediately after the oxygen sample had been drawn. The next samples drawn were TCO₂, ¹⁴C, ³H, nutrients (NO₂ + NO₃, SiO₃, PO₄), ¹⁸O and salinity. Salinity samples were collected as pairs of replicates to allow cross checks of ship-based and shore based salinity analysis. The rosette sampling procedure was completed by readings of electronic DSRTs for a first quick check of the scheduled bottle pressure level and for in-situ control of the CTD pressure and temperature. An overview of the bottom topography of the WOCE section and the locations of water samples is given in Fig. 34a.

47 CTDO₂/Rosette profiles at 43 stations were occupied along 5 VEINS sections and 72 CTDO₂/Rosette profiles at 69 stations during the WOCE part of the cruise (Fig. 9). 7 of the casts were used for system test purposes (cable, CTD/Rosette system performance etc.). 3 casts were used for rosette sample quality tests at stat. # 483, 501 and 534 by means of multi-trips at the same depth level. Activities, occurrences and measured parameters are summarized in the attached station listing.

To meet WOCE quality requirements, the processing and quality control of CTD and bottle data followed the published guidelines of the WOCE Operations Manual (WHPO 91-1) as far as their realisation was technically possible on this cruise. Standard CTD data processing and bottle data quality control (including salinity, oxygen and nutrient samples) were carried out on board during the cruise using BSH designed software tools. For salinity analysis of samples a standard Guildline Autosol salinometer model 8400 was used on board together with processing software

designed by SIS. Dissolved oxygen was measured by the Winkler method modified by Carpenter with a Metrohm Titroprocessor and a double platinum electrode. Nutrients were analysed with a Technicon TRAACS 800 flow autoanalyser. XBTs were dropped following the corresponding WOCE requirements (SY, 1991; HANAWA et al., 1995).

Measurements of the classical parameters were supplemented by continuous registrations of current profiles using a vessel mounted acoustic Doppler current profiler (VM-ADCP) and of sea surface temperatures and salinities using a Seabird SBE-21 thermosalinograph (TSG). CTD, TSG and XBT data were transmitted to BSH and distributed worldwide in the framework of IGOSS (Integrated Global Ocean Services System) in quasi real-time (i.e. within 30 days) as BATHY, TESAC and TRACKOB reports. All data will be submitted to the responsible WOCE Hydrographic Programme Data Assembly Centre after data processing and quality control has been finished.

Preliminary Results

A selection of property sections from bottle data and CTD data are presented in Figs. 34 and 35, which show the main water masses encountered along WHP-A1/E. Positions of XBT drops and the temperature field of the main section are shown in Figs. 36a,b.

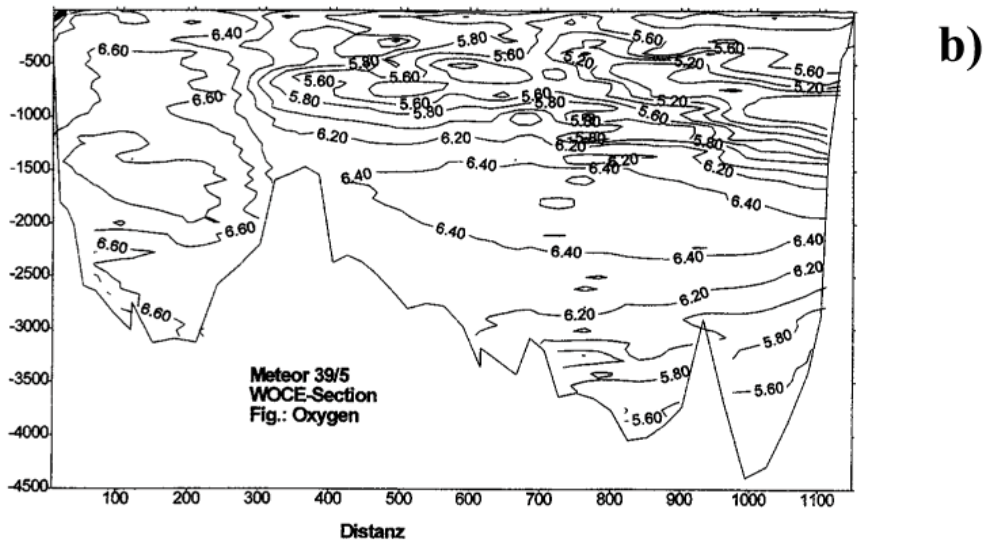
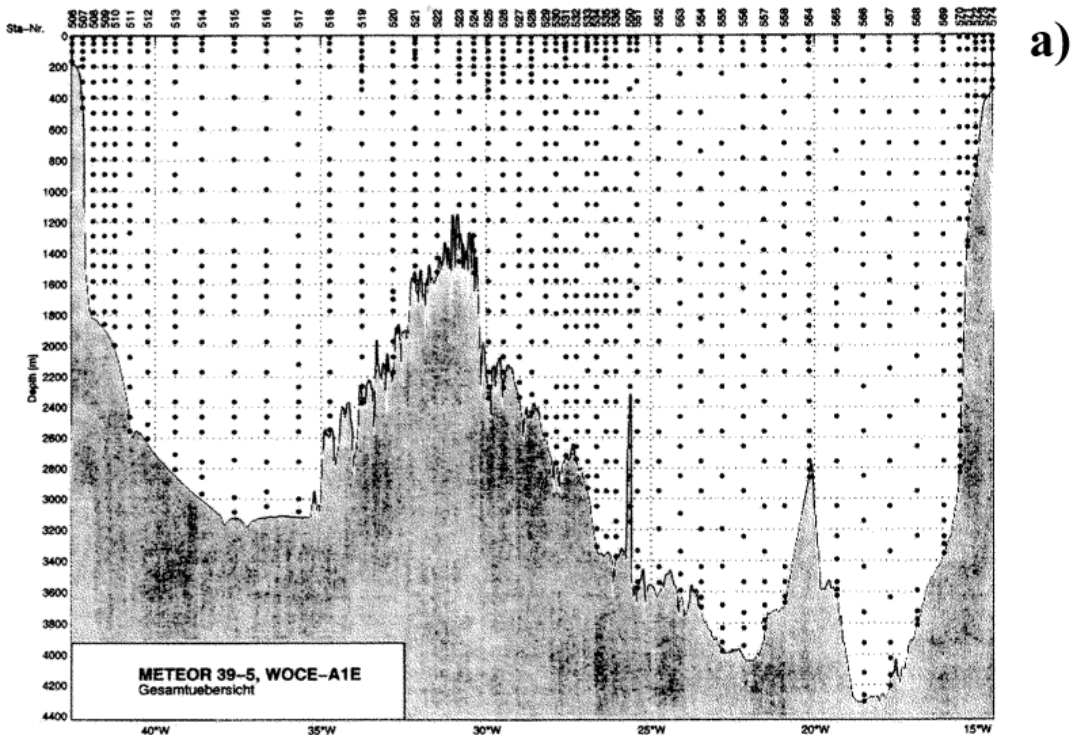
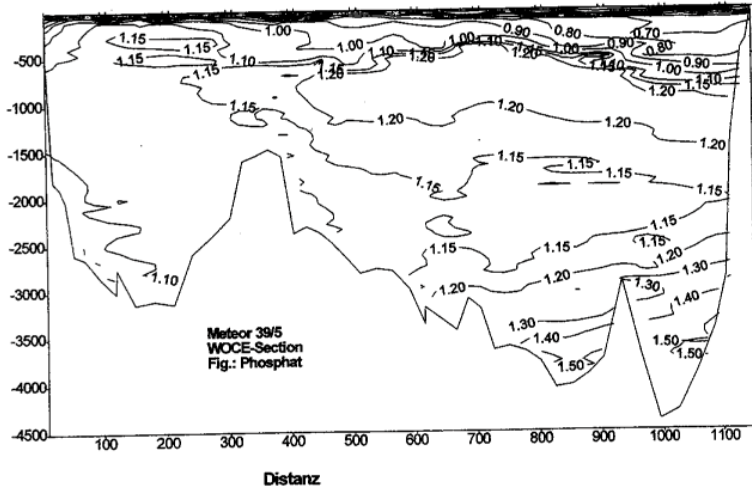
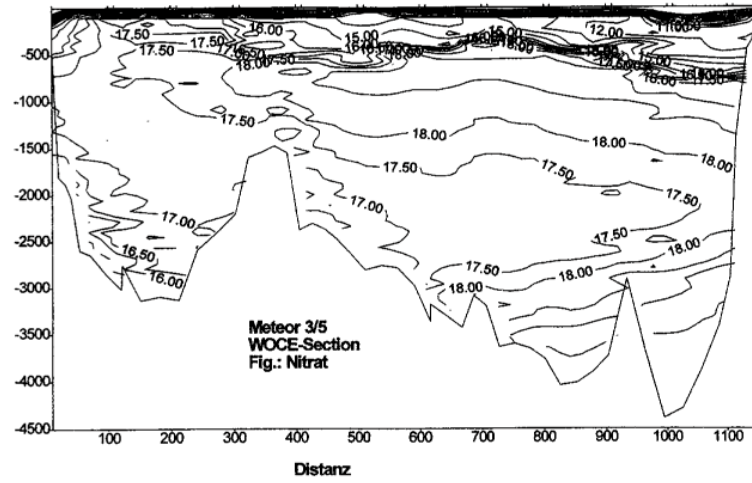


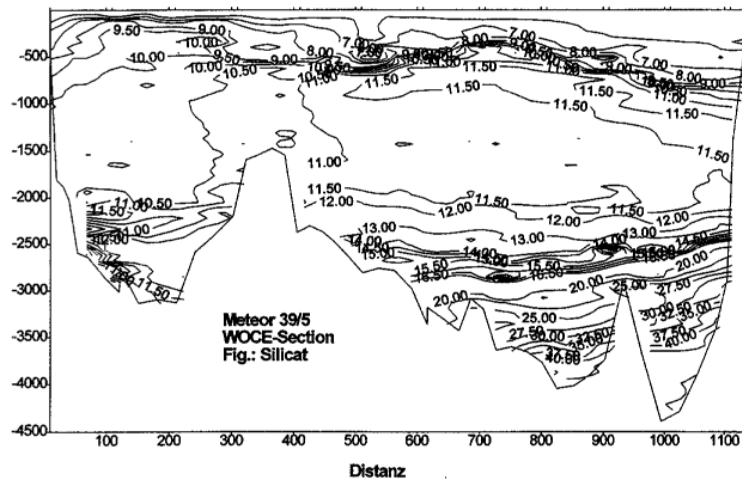
Fig. 34: a) Distribution of water samples along section WHP-A1/E, b) Sample oxygen (ml/l), c) Phosphate ($\mu\text{mol/l}$), d) Nitrate ($\mu\text{mol/l}$), e) Silicate ($\mu\text{mol/l}$). (next page)



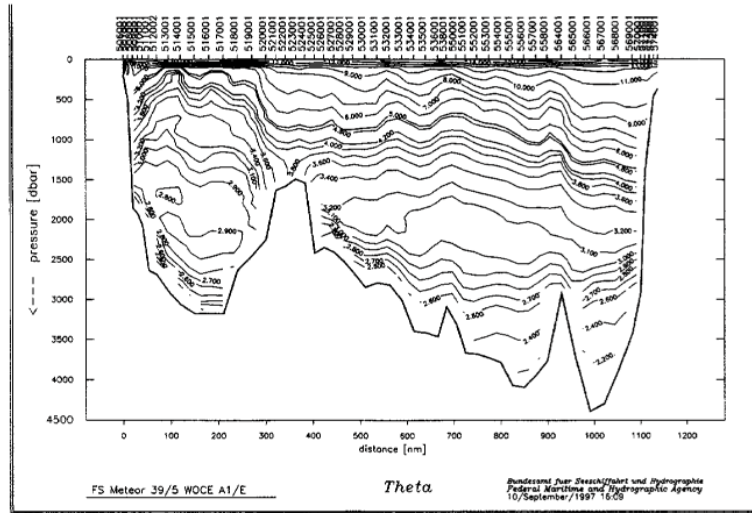
c)



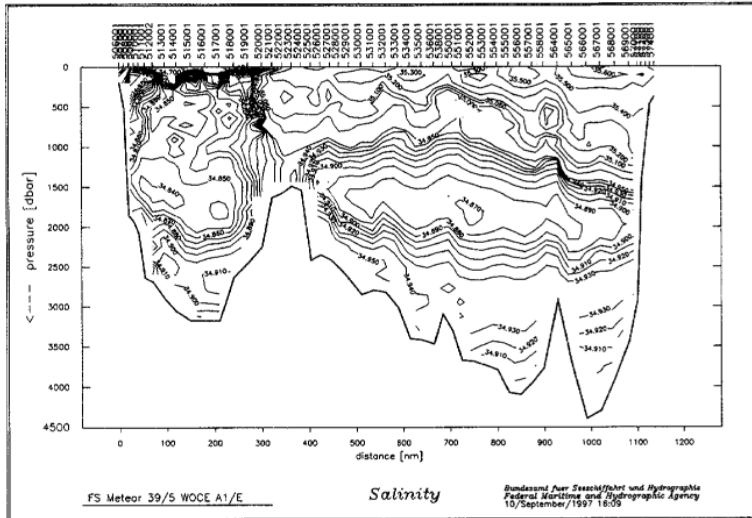
d)



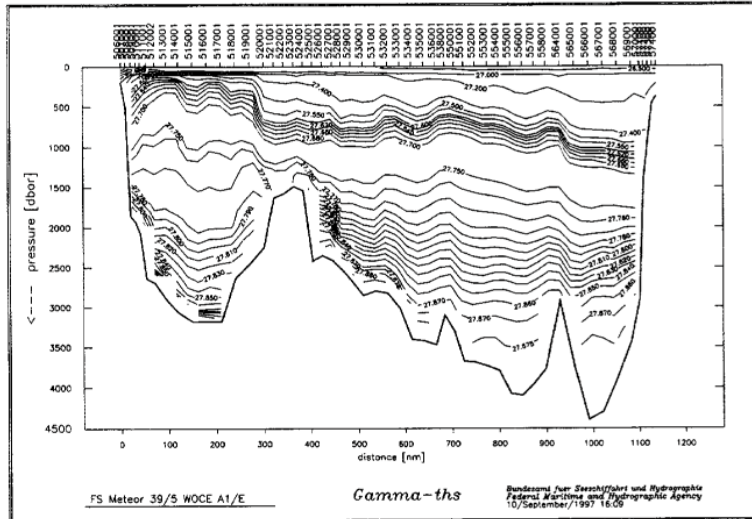
e)



a)

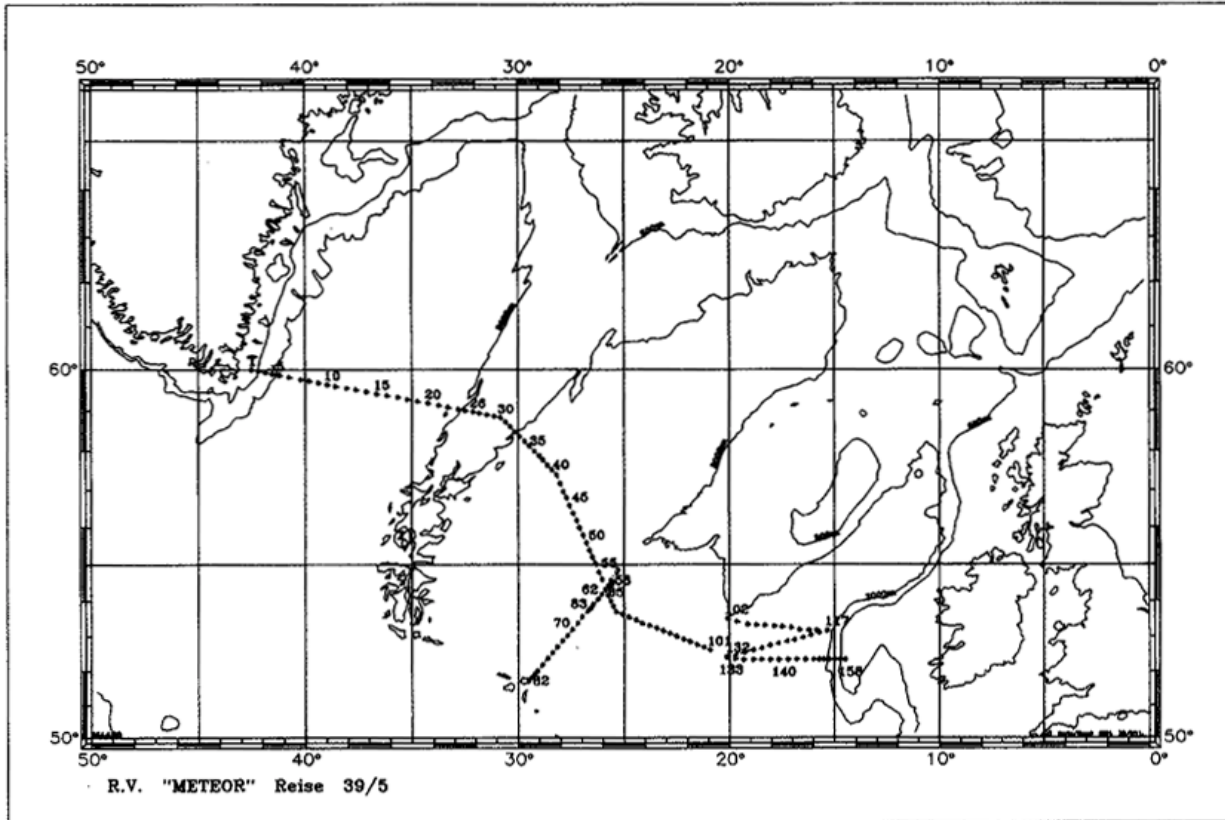


b)

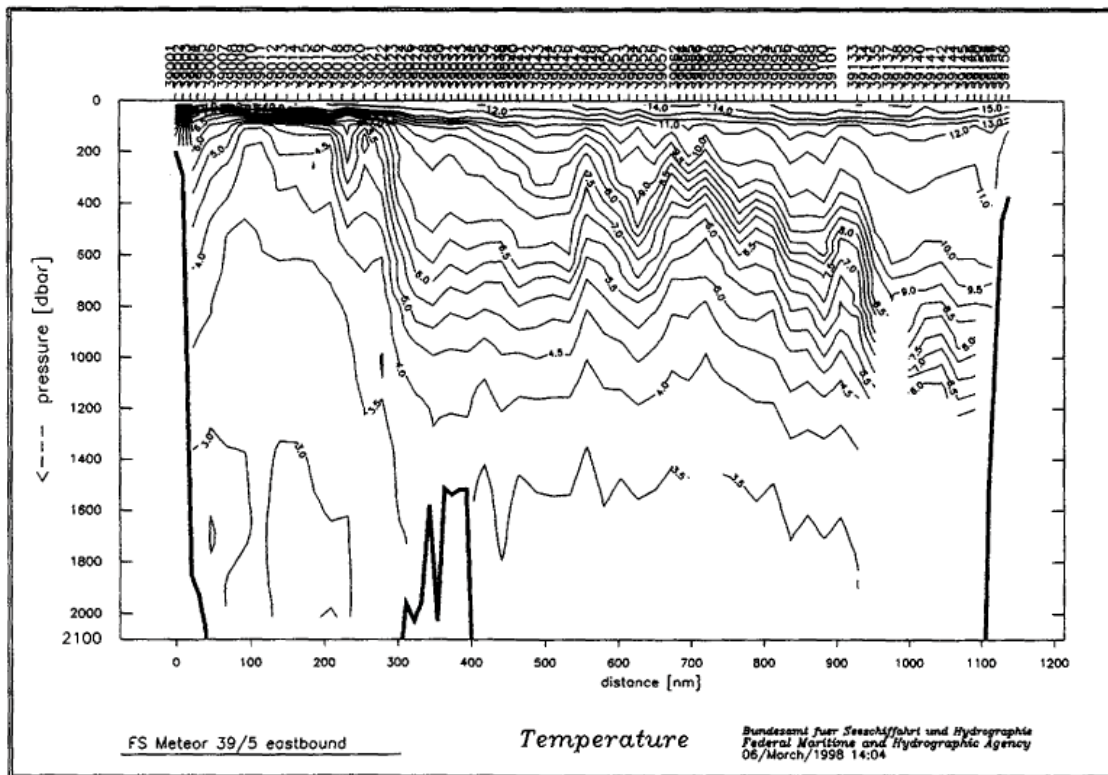


c)

Fig. 35: CTD property section WHP-A1/E, a) Temperature (°C), b) Salinity, c) Density.



a)



b)

Fig. 36: a) Positions of XBT profiles, b) XBT temperature section along WHP-A1/E.

The characteristic water mass of the upper layer is the Subpolar Mode Water (SPMW) from the North Atlantic Current which has the highest temperatures and salinities. At the continental slope off east Greenland, the influence of the East Greenland Current is visible transporting polar surface water southwards. The Intermediate Water (IW) below SPMW is characterized by an oxygen minimum (VAN AAKEN and BECKER, 1996). South of Rockall Plateau and in the same density layer as the IW the influence of Mediterranean Water is visible due to its high salinity.

The upper part of the deep layer in both basins shows the Labrador Sea Water (LSW), well marked by its low salinity and high oxygen content. In the layer below LSW we find dense overflow-type water masses with their well distinguishable cores at the East Greenland continental slope (Denmark Strait Overflow Water, DSOW) and at the eastern slope of the Reykjanes Ridge (Island Scotland Overflow Water, ISOW). Further to the east and after leaving the bottom layer in the deep basins of the Porcupine Abyssal Plain, ISOW is transformed into North East Atlantic Deep Water (NEADW) by mixing with LSW and the Lower Deep Water (LDW). LDW is marked by low salinity, low oxygen content, and a very high silicate concentration of Antarctic origin. Therefore, the name Antarctic Bottom Water (AABW) is also used instead of LDW. Here, close to the north-western terminus of the AABW tongue, we observed the core of this water mass lifting from the bottom (Fig. 37).

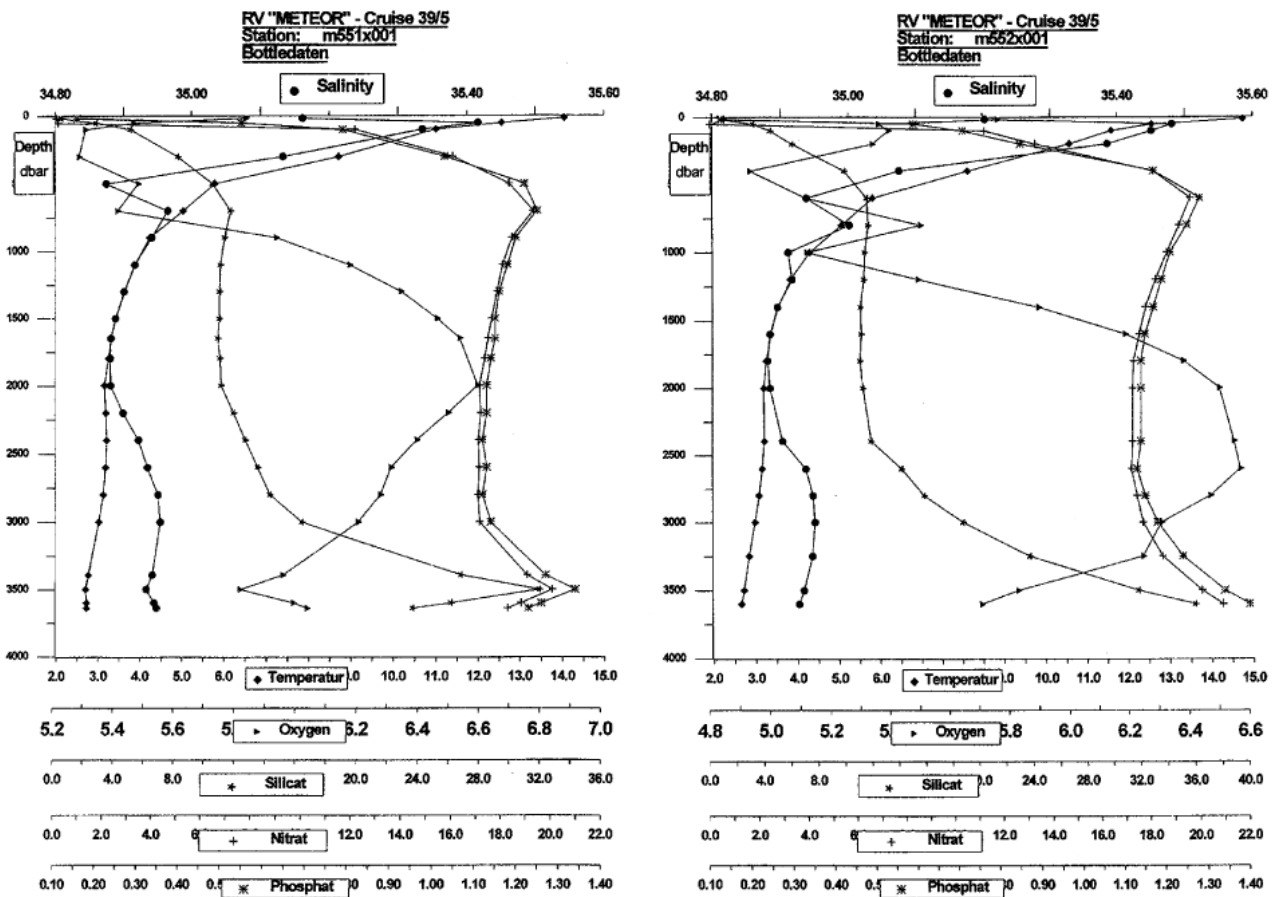


Fig. 37: Property profiles of stats. # 551 and 552.

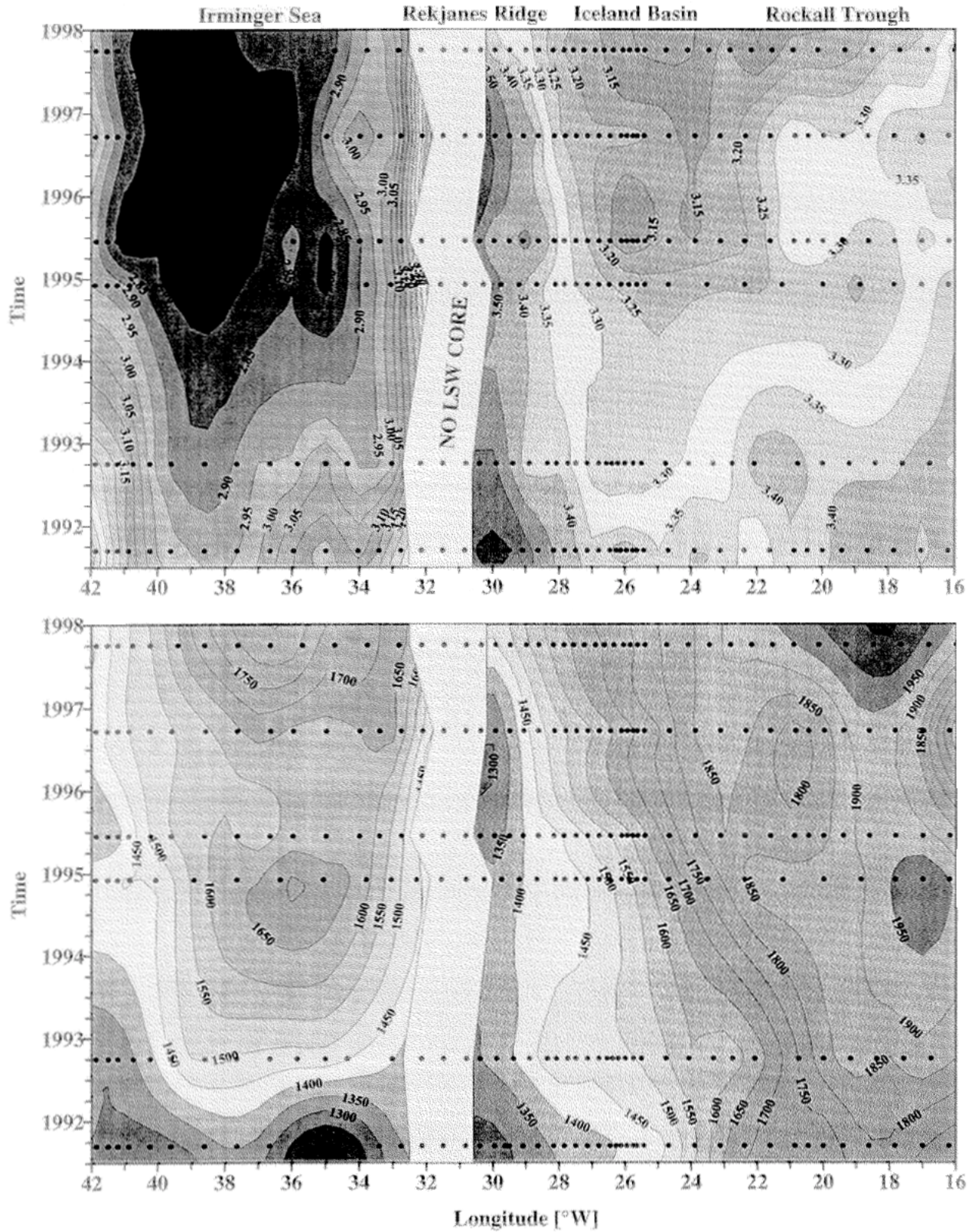


Fig. 38: Change of Labrador Sea Water core properties along WHP-A1/E from 1991 to 1998
 a) Temperature, b) Pressure.

The outstanding event in the North Atlantic of the late 80s and early 90s was the convective Labrador Sea Water formation (LAZIER, 1995) and the spreading of the new LSW vintages throughout the North Atlantic. It is believed that the LSW formation period, which reached its maximum in the winters of 1992 and 1993, is linked with the North Atlantic Oscillation (NAO) (DICKSON et al., 1996). Based on the observations along WHP sections A1 and A2, rapid changes of intermediate-depth water-mass characteristics were observed (SY et al., 1997), and we were able to trace the propagation of a series of new modes of LSW ("1988 LSW cascade") and to link these modes to the series of intensifying deep wintertime convection events after 1988 in the central Labrador Sea. The appearance of these LSW vintages is marked by substantial cooling, deepening and densification of the local LSW core. Using the T/S and CFC data independently, the trans-Atlantic travel time from the source region to the eastern boundary was estimated to be 4 - 5.5 years (SY et al., 1997). This surprisingly rapid spreading is confirmed by investigation results recently reported by CURRY et al. (1998). Observations made during cruise METEOR 39/5 reveal no appearance of newly formed LSW (i.e. of vintage 1996 or 1997) in the Irminger Sea but show clearly that the exceptional cooling of the intermediate waters is still in progress in the West European Basin (Fig. 38a). We found that the LSW core layer east of 22°W deepened by about 170 m (Fig. 38b) and that the mean temperature had decreased by -0.13°C within the last 13 months.

In the upper ocean we encountered another interesting feature. BERSCH et al. (1998) report a strong warming of the Subpolar Mode Water (SPMW) layer between June 1995 (V152) and August 1996 (V161), which they explain by the contraction of the Subpolar Gyre. The westward shift of the Subarctic Front reduces the eastward spreading of cold and less saline waters from its western part and increases the supply of warm and more saline SPMW from the North Atlantic Current. Obviously this is not a short-time event because METEOR 39/5 data show that compared to August 1996 (M39-V161) the SPMW layer remained anomalously warm also in September 1997 (Fig. 39). Preliminary estimates of the geostrophic current field reveal 3 branches of the North Atlantic Current: west of the Reykjanes Ridge between 35°W and 36°W, and south of the Rockall Plateau between 22°W and 25°W and at 19°W.

Since the early days of WOCE it has been stated that the industrial production of expendable CTDs (XCTD) had to be extended with the accuracy and precision needed for large-scale measurement of heat and salt storage of the upper ocean in the WOCE voluntary observing ship programme (WCRP, 1988). As in the past (SY, 1996) we therefore took the opportunity of this WHP cruise to test a new expendable device, designed by Tsurumi-Seiki Co. (TSK), Yokohama, against a controlled and accurate CTD reference to check the manufacturer's claimed system performance independently. The test result shows that the new XCTD system is close to provide the performance required by the oceanographic community for upper ocean thermal and salinity investigations. Details on the test procedure and results are published in SY (1998).

5.2.2.2 Tracer Measurements

a) Chlorofluorocarbon (M. Rhein, M. Reich, L. Czechel)

Technical Aspects

During leg M39/5, the Kiel CFC system worked continuously and about 1550 water samples on 99 stations have been analysed. CFC-11 analysis was successfully carried out during the cruise, the analysis of the CFC-12 peak, however, was disturbed by an unknown substance with a similar retention time as CFC-12. The unknown peak affected the precision of the CFC-12 data, but did not influence the accuracy. The blanks for CFC-11 and CFC-12 were negligible. Accuracy was checked by analysing 10 percent of the water samples twice, and was for both substances $\pm 0.5\%$. The result was confirmed by the accuracy obtained at the test stations, where several bottles were tripped at the same depths. The accuracy at these test stations was better than 0.5% for both substances. The water samples are calibrated with gas standard provided by D. Wallace, PMEL, USA and the CFC concentrations are reported on the SIO93 scale. All data were analysed on board.

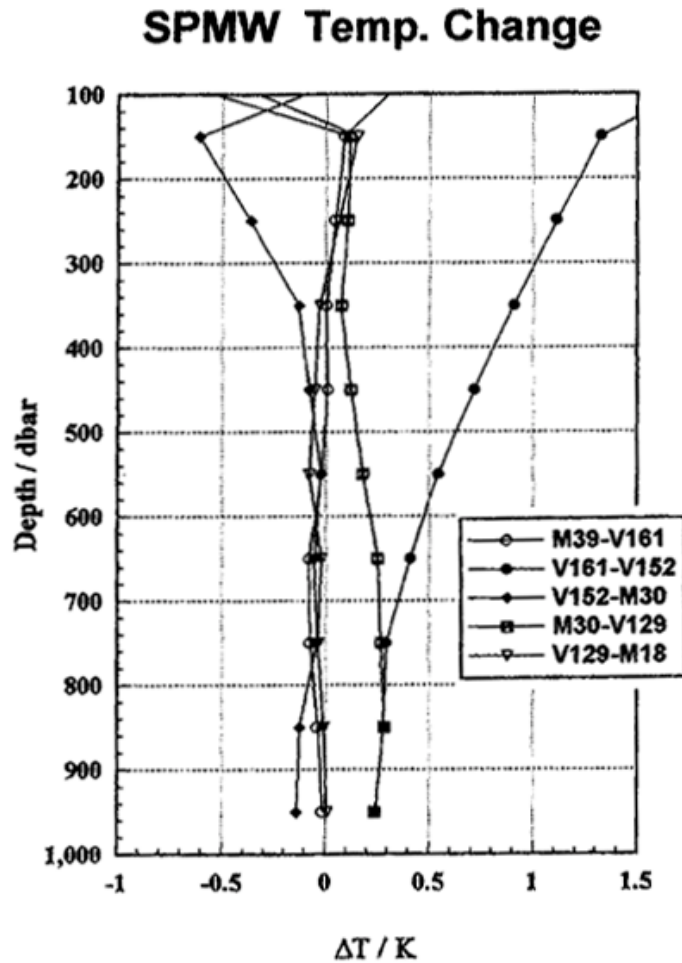
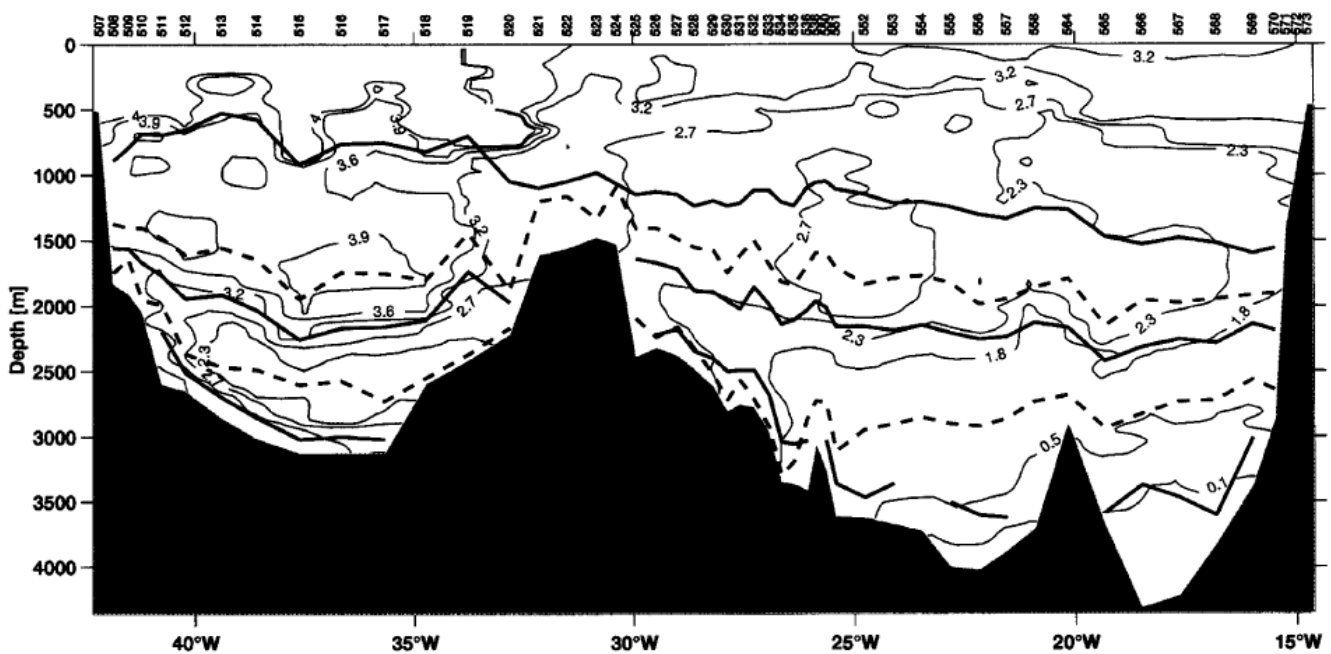


Fig. 39: Differences of horizontally averaged temperature in the SPMW layer of A1/E. Data are vertically averaged at 100 m intervals.

Leg 5 completed the Kiel CFC data set of the M39 cruise, covering the subpolar East Atlantic (M39/2) and the West Atlantic (M39/4). A first comparison of the three data sets showed that the data are internally consistent.

Preliminary Results

The aims of the CFC analysis are to study the formation and circulation of the deep water masses in the subpolar North Atlantic. At the CFC-11 section along A1/East (Fig. 40), the thick lines denote the isolines $\sigma_\theta = 27.2, 27.8, \text{ and } 27.88$, which are chosen as boundaries for the deep water components, the Labrador Sea Water (LSW) between 27.74 and 27.80 and the Iceland Scotland Overflow Water (ISOW) between 27.80 and 27.88 . In the western Atlantic one finds Denmark Strait Overflow Water (ISOW) as the densest water mass below $\sigma_\theta = 27.88$, centred on the western flank of the Irminger Sea. In the eastern Atlantic, however, this isopycnal is no longer suitable as a water mass boundary. The core of the LSW is shown with the stippled line, which denotes the salinity minimum, taken from the CTD stations. The lower stippled line represents the salinity maximum of the ISOW, which crosses into the western Atlantic through the Gibbs Fracture Zone, and thus is also called GFZW (Gibbs Fracture Zone Water).



M395, Aug – Sep 1997

11-Sep-98

bold lines: sigma 27.74, 27.8, 27.88

stippled lines: Salinity Min and Max

CFC-11

Fig. 40: CFC-11 section of WHP-A1/E.

In the western Atlantic, the CFC distributions show two intermediate maxima, which characterize in mid-depth the LSW and the DSOW, which is found near the bottom. Both water masses receive their CFC load by contact with the atmosphere in their respective formation regions. The CFC-11 minimum and the salinity maximum belong to the ISOW spilling through the GFZ. The ISOW is present in the eastern Atlantic on the flank of the Reykjanes Ridge, showing a CFC-11 maximum in the east, because the surrounding water masses are CFC poor. At the Reykjanes Ridge, the highest salinities and CFCs of the ISOW were found near the bottom. CFC poor water penetrates between the LSW and the ISOW, separating the two CFC maxima. The lowest CFC-11 concentrations were found in the LDW below 4000 m depth.

The CFC concentrations of the LSW are highest in the Irminger Sea and decrease east of the Reykjanes Ridge. Elevated CFC-11 values in the LSW east of the ridge were found near 25°W. Compared to November 1994 (METEOR cruise M30/3), the CFC-11 signal at the salinity minimum of the LSW did not change significantly in the Irminger Sea, but increase in the eastern Atlantic. The CFC-11 increase was accompanied by cooling of about 0.1°C. Both features confirm the short spreading time of LSW into the eastern Atlantic.

b) Tritium/Helium, $^{18}\text{O}/^{16}\text{O}$, SF-6 sampling
(H. Hildebrandt)

Tritium/Helium

The measuring of tracer concentrations in oceanic water samples provides important information in addition to the analysis of the classic hydrographic parameters. One particularly useful tracer is tritium (^3H) since it takes part in the hydrological cycle as $^1\text{H}^3\text{HO}$ and is therefore an almost 'ideal' tracer. Furthermore, this radioactive hydrogen isotope decays into ^3He with a mean-life of 17.93 a. Since tritium is only supplied to the oceans at the atmosphere-ocean boundary, and its input function at the surface is well known, the simultaneous measuring of the tritium and helium concentration of a water sample allows for the determination of an apparent $^3\text{H}/^3\text{He}$ age which yields important information about different water masses, such as their time of isolation from the atmosphere and the year of their formation ('vintage' age). Taking into account the information gathered from the hydrography or other transient tracers the mixing and spreading rates of these water masses can be determined as well.

For this purpose, a set of 384 tritium and helium samples was taken during M39/5, both on the VEINS and WOCE section. The main focus of the sampling was on the Labrador Sea Water and the Denmark Strait Overflow Water. The measurement of tritium concentrations and isotopic helium ratios ($^3\text{He}/^4\text{He}$) will be done after the cruise at the IUP Heidelberg using mass spectrometry techniques.

$^{18}\text{O}/^{16}\text{O}$

Due to the fractionation of the oxygen isotopes ^{18}O and ^{16}O during phase transitions of water (e.g. freezing/melting of ice) oceanic samples can have a characteristic $^{18}\text{O}/^{16}\text{O}$ ratio which allows to identify their origin and to describe the mixing rates of different water types. In particular, water containing a considerable amount of fresh water (e.g. due to ice melting or

river-runoff) shows a significantly decreased $^{18}\text{O}/^{16}\text{O}$ ratio. This ratio is usually expressed as the percent deviation from Standard Mean Ocean Water ($\delta^{18}\text{O}$).

During M39/5, a total of 120 ^{18}O samples was taken. If needed, additional measurements can be done using the water collected for tritium analysis. Most of the samples were taken in and around the East Greenland Current which is much fresher than the surrounding water due to its content of Polar Water and melted ice from the glaciers of Greenland. The analysis of the samples will again be done at the IUP Heidelberg using a mass spectrometer.

SF-6

Sulfur hexafluoride (SF₆) has recently become of interest in tracer oceanography and is already used in tracer experiments. To determine its usefulness as a transient tracer a set of 22 samples was taken during M39/5 for on-shore analysis: several surface samples, a profile in the Irminger Sea and one close to the Rockall Trough. To check the equilibration of the surface water with the atmosphere 25 air samples were taken along the WOCE A1/E section which could also yield information about spatial trends in the atmospheric concentration of SF₆.

5.2.2.3 Current Measurements

a) Vessel Mounted ADCP

(C. Mohn)

Water velocities relative to the ship were recorded continuously in the upper 600 m during the whole cruise using a ship-mounted 150 kHz ADCP. The measurements were carried out in depth intervals of 16 m within sampling intervals of 6 minutes. Data gaps occurred only at a short period of 8 hours at one day during the last week of the cruise.

The processing and a preliminary calibration of the ADCP data was performed on board using the CODAS software system developed at the University of Hawaii. The calibration of the misalignment between the transducer and the ship's axis was carried out using a short period of bottom tracking at the beginning of the cruise. The tidal correction and final calibration will be performed after the end of the cruise using a 2 day period of bottom tracking at the Celtic shelf.

During the cruise high resolution GPS position fixes from the GLONASS GPS positioning system were available, which will also be applied to the ADCP data after the cruise.

The results of the on board ADCP data processing without tidal correction are presented in Fig. 41a - c (VEINS transects) and 42a - c (WOCE transect A1E) for the three depth layers 25 - 200 m, 200 - 400 m and 400 - 600 m, respectively. The strongest currents during the VEINS transects are associated with the southwestward moving East Greenland Current with speeds up to 40 - 50 cm/s in the upper 400 m (Fig. 41a, b). Below 400 m the reduced data quality yielded a much coarser current pattern.

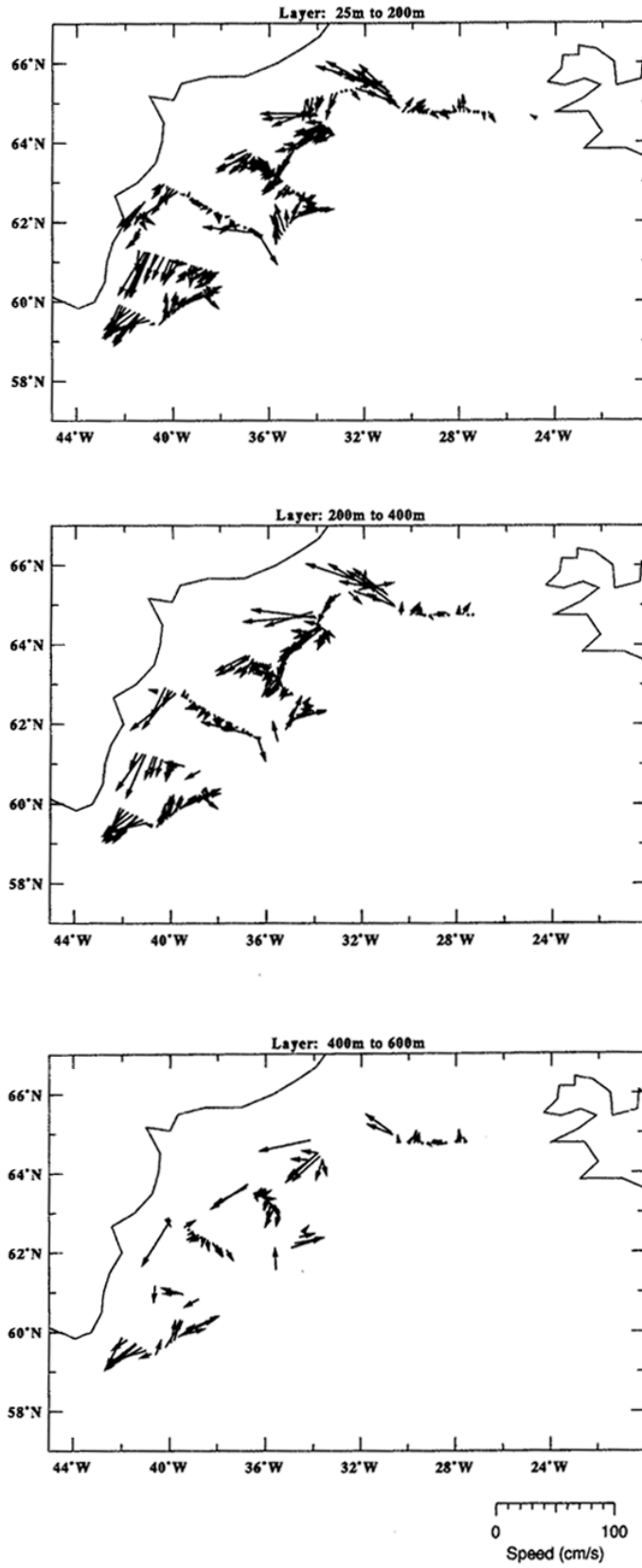


Fig. 41: VM-ADCP currents along VEINS sections

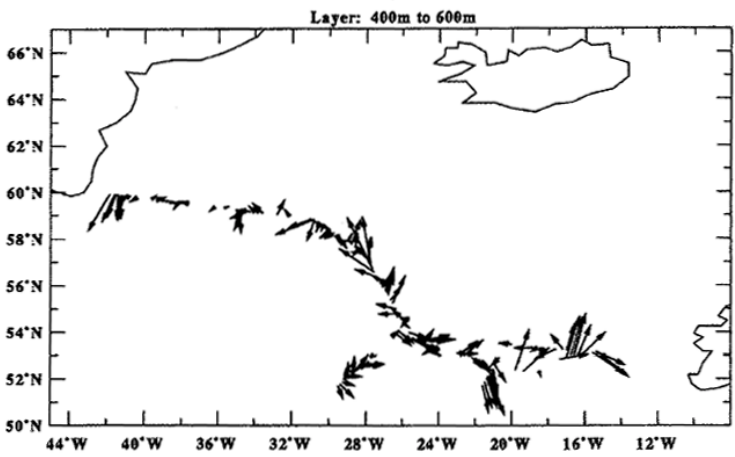
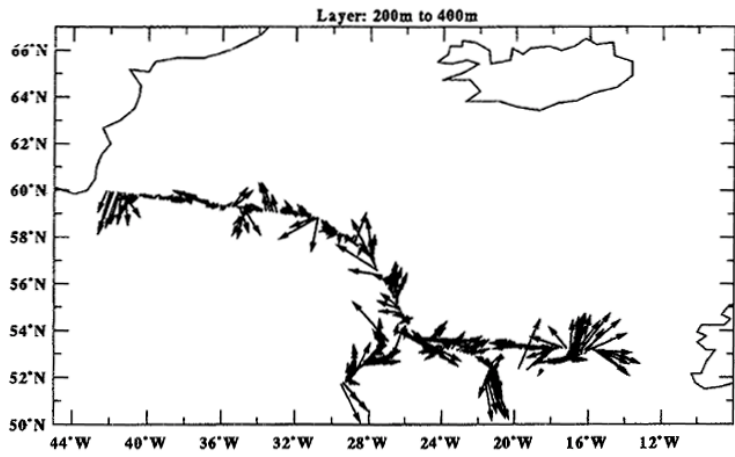
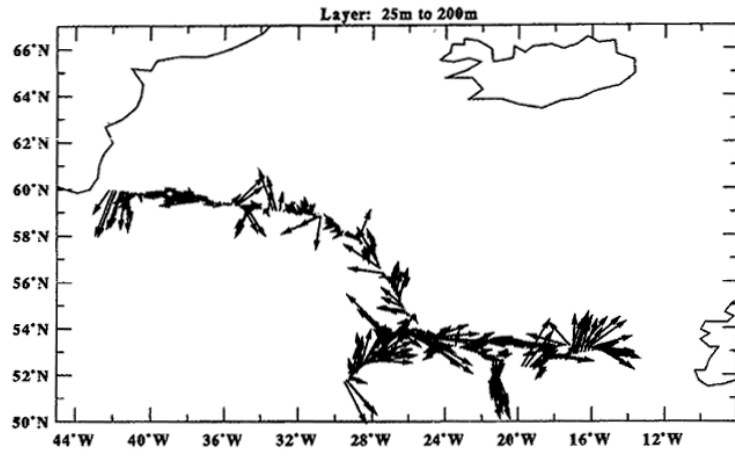


Fig. 42: VM-ADCP currents along WHP-A1/E

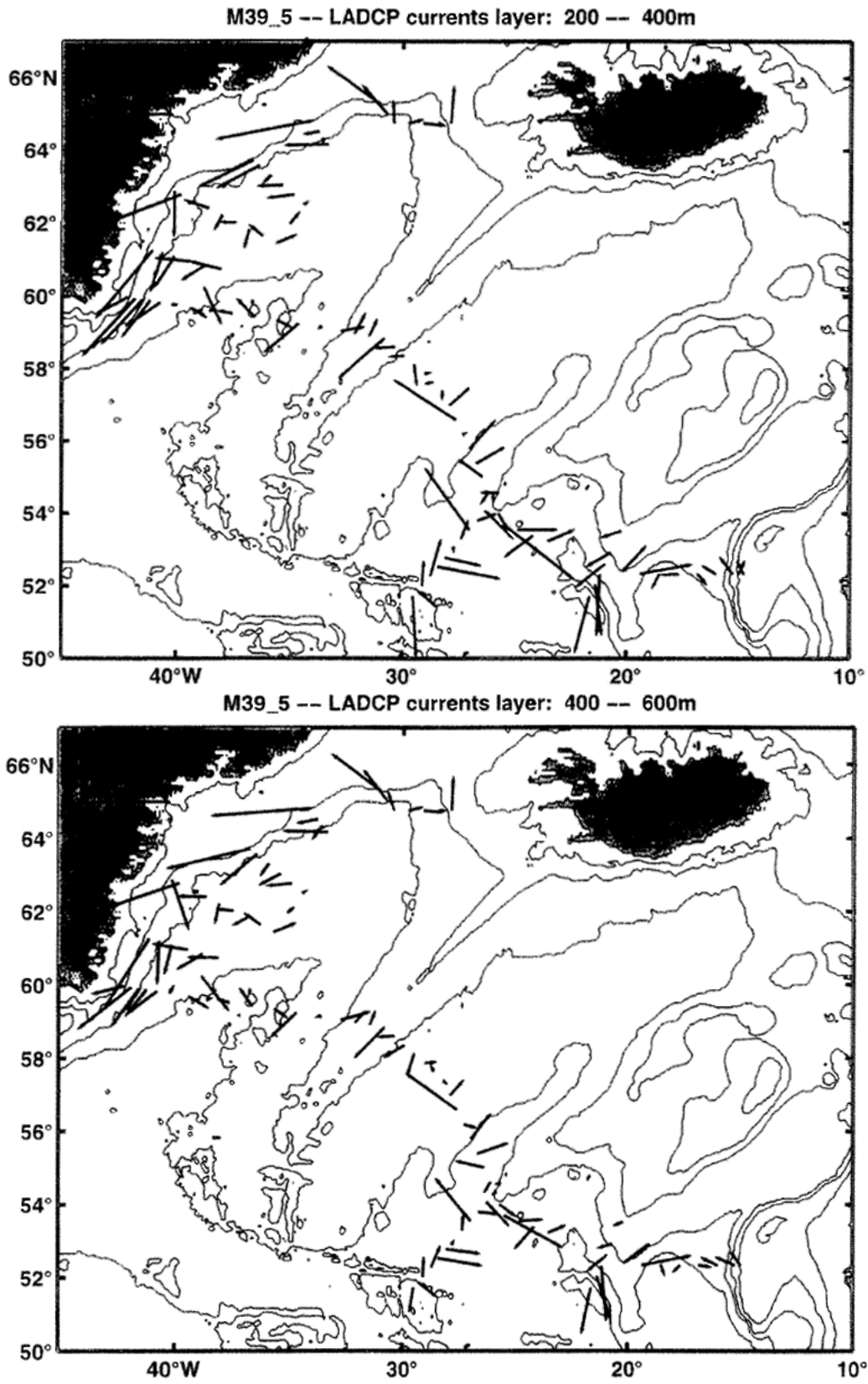


Fig. 43: LADCP currents during M39/5

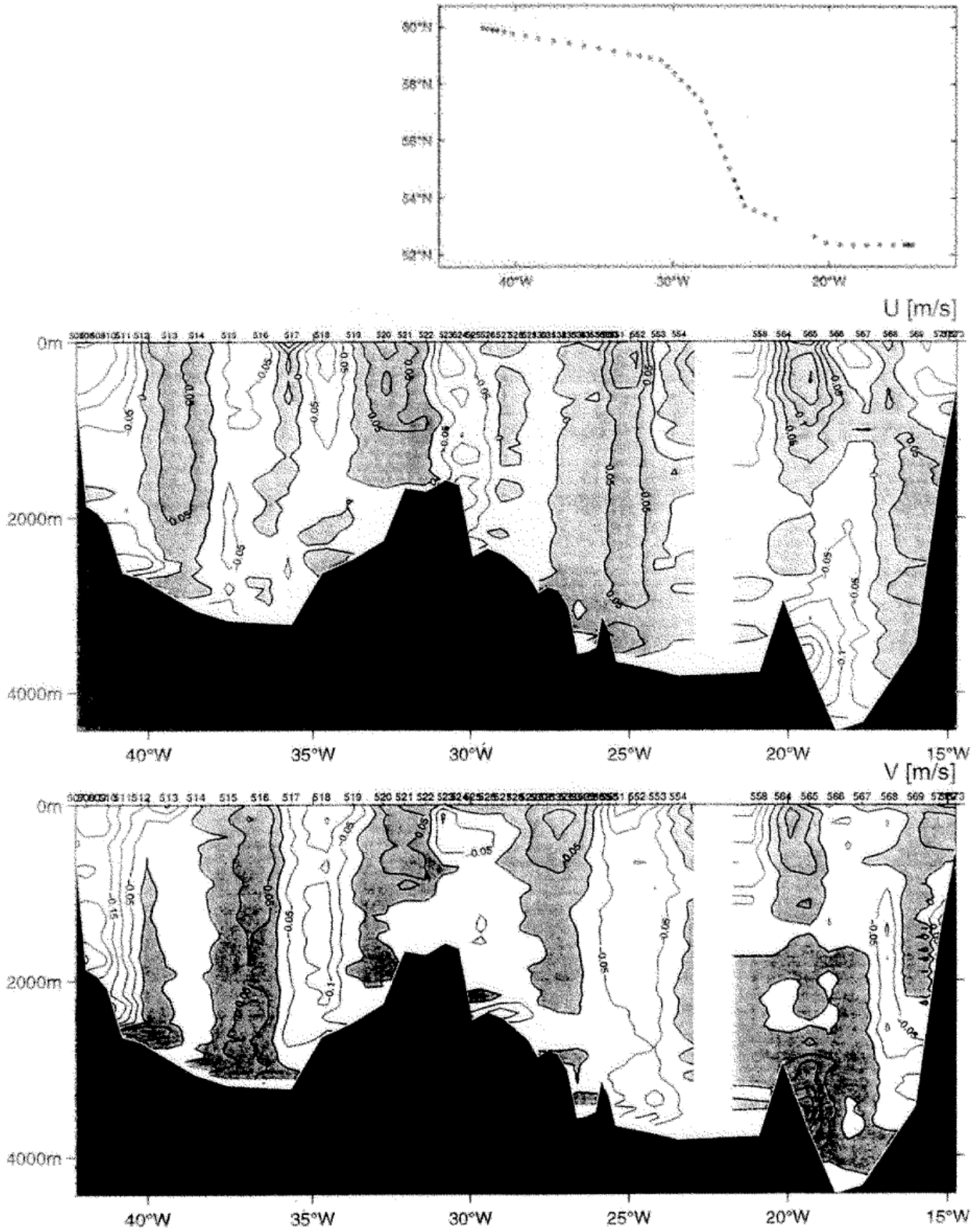


Fig. 44: LADCP section with WHP-A1/E

Along the WOCE A1E transect the East Greenland Current (40 cm/s) west of the Reykjanes Ridge is still clearly visible (Fig. 42a). A divergence of the eastward moving North Atlantic Current is visible at approximately 22°W near the Rockall Plateau. West of Porcupine Bank the northward path of the Shelf Edge Current is marked by current speeds in the order of 30-40 cm/s. A comparison between the results of the LADCP measurements and the VM-ADCP measurements at the LADCP positions at the actual state of data processing showed a satisfying agreement.

b) Lowered ADCP

(M. Rhein, M. Reich)

During leg 5, the self contained 153 kHz LADCP from IfM Kiel was used, the same system as during leg 4. The LADCP was attached to the CTD/Rosette system. On stations 555 - 557 the LADCP was removed from the rosette due to bad weather conditions. In total, 98 profiles were obtained reaching from 40 m depth about 100 m above sea floor. The longest profiles (4270 m) were sampled at stations 559 and 566, water depths = 4340 m. All profiles were analysed on board. The navigation of the LADCP was done with the GLONASS system, which worked successfully during the cruise. Comparison of the upper 600 m of the profiles with the data from the vessel mounted ADCP confirmed the good quality of the LADCP profiles (Fig. 43). The highest velocities were observed in the Irminger Sea sections off Greenland. There, the boundary current exhibits southward velocities greater than 20 cm/s throughout the water column (Fig. 44). The velocity distribution show band like structures, with high velocities reaching down to the bottom. The strongest velocity signal in the deep eastern Atlantic near 20°W at 2800 - 3900 m depth directed to the northwest (Fig. 44) are also present in the geostrophic computations.

c) Mooring Work

(J. Read, G. Hargreaves, J. Ashley)

The mooring work is summarized in the table 9 and 10.

Tab. 9: Moorings recovery programme

1. 9504 laid by Bjarni Saemundsson Nov 1995 not found by Valdivia July 1996, traced but not recovered by Bjarni Saemundsson Dec 1996 (dredge failed)
2. 9601 laid by Valdivia, July 1996 (dredge failed)
3. 9602 laid by Valdivia, July 1996 (dredge failed)
4. I.E.S laid by Poseidon August 1996 (recovered)
5. 9603 laid by Bjarni Saemundsson Dec 1996 (recovered)
6. 9604 laid by Bjarni Saemundsson Dec 1996 (recovered)
7. Veins 21 laid by Valdivia, July 1996 (recovered)
8. Veins 11 laid by Valdivia, July 1996 (dredge failed)
9. Veins 2 laid by W. Herwig 1995 not recovered by Valdivia 1996 (failed)

Tab. 10: 1997 Mooring Positions (Deployments)

MOORING	(OWNER)	LAT	LONG	DEPTH	DATE/TIME 19.08.97
FI	(FIMR)	63°38.20'N	36°47.40'W	1638 m	06:30 UTC
F2	(FIMR)	63°33.24'N	36°30.14'W	1785 m	08:12
UK1	(CEFAS)	63°28.63'N	36°17.90'W	1993 m	09:20
IES1	(POL)	63°28.73'N	36°17.87'W	1991 m	09:29
G1	(IfM-HH)	63°21.85'N	36°04.18'W	2208 m	11:31
IES20	(POL)	63°21.97'N	36°03.88'W	2209 m	11:46
UK2	(CEFAS)	63°16.65'N	35°51.47'W	2368 m	13:44
G2	(IfM-HH)	63°07.00'N	35°32.30'W	2590 m	15:15

5.2.2.4 Carbonate chemistry in the Northern Atlantic Ocean

(H. Thomas, B. Schneider, N. Gronau and E. Trost)

The investigations performed on the WOCE A1/E transect during the cruise M39/5 mainly were focussed on the air sea exchange of CO₂ and the analysis of the distribution of dissolved inorganic carbon (DIC) within the water column with respect to the biological pump. The surface distribution of the partial pressure of carbon dioxide (pCO₂) was measured continuously during the whole leg, completed by surface samples of DIC on each station. Furthermore, at each second station the depth profiles of DIC were recorded.

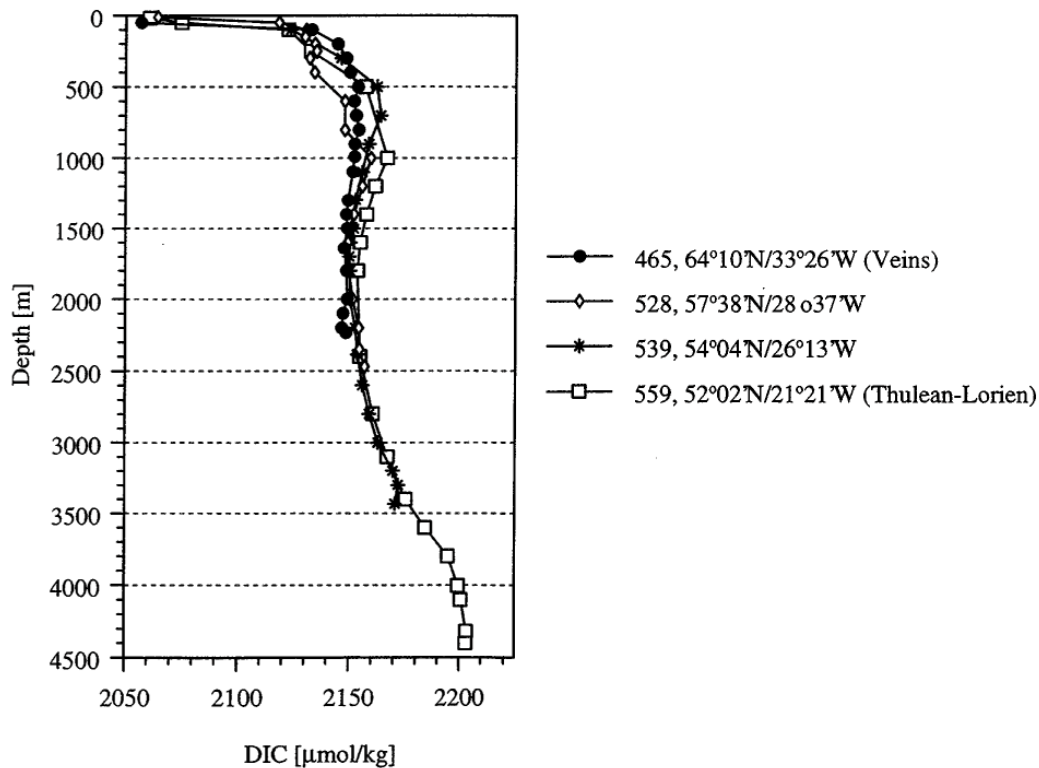


Fig. 45: 4 profiles of dissolved inorganic carbon (DIC)

Preliminary results

The common feature of the pCO₂ (raw data) is an increase from approx. 300 µatm in the northwestern part to approx. 320 µatm in the southeastern part of the investigation area. This feature corresponds to the decrease of the nutrient concentrations and oxygen saturation as well as to the increase of temperature within the surface layer showing the proceeding of the summer in the same direction. The distributions of DIC are discussed using the following 4 profiles recorded in the different regions of the cruise (Fig. 45). Along the east coast of Greenland (Veins leg) below the mixed layer an homogenous level of approx. 2150 µmol/kg DIC was found. At some stations branches of Denmark Strait Overflow Water are visible characterized by slightly lower values, because the increase of the DIC due to remineralisation of organic matter within the younger water mass is lower than within the overlying older ones. Due to the same reason along the WOCE transect the lowest values are observed within the Labrador Sea Water increasing in lower and higher depths. The highest values are found within the Antarctic Bottom Water with values of approx. 2200 µmol/kg DIC observed clearly at station 559 on the Thulean-Lorien transect.

5.3 Other programs

5.3.1 Methane

(R. Keir, G. Rehder)

Background

Methane is a trace gas in the atmosphere, and its concentration has varied over time. Proxy measurements made in ice cores indicate that over the last 200 years, the atmospheric methane has risen from about 700 to 1800 ppb volume, and, on a percentage basis, the rise has accelerated during the last decades at a rate faster than the rise of atmospheric CO₂. As with other transient tracers such as tritium and chlorofluorocarbons, the changing atmospheric concentration should result in a time dependent net input/output of methane to the ocean, the signature of which should be observable in recently formed deep waters.

In addition to the atmosphere, methane is also influenced by production and consumption within the ocean. In the upper ocean, methane appears to be generated slowly by some microbial process, judging from weak maximums that sometimes occur under the base of the mixed layer. In addition, at hydrothermal vents and cold seeps found on compressional margins, methane is released into the deep sea. Nevertheless, older deep waters generally appears to have quite low methane concentrations due to slow oxidative consumption.

Since the majority of the ocean's deep water is produced in the northern Atlantic, it is an area where the changing atmospheric exchange should influence the distribution of methane most strongly. In conjunction with the program being carried out by the SFB 460, measurements of the distribution of dissolved methane and its ¹³C/¹²C isotope ratio were carried out on M39/2. The isotope measurements should provide an indication of the extent of the methane decrease in the water column that is due to oxidation, because this process consumes the lighter isotope preferentially. On the other hand, the carbon isotope ratio of methane in the atmosphere has remained nearly constant over time, and changes in the distribution due to varying atmospheric concentration should not strongly affect the isotope ratio in the ocean.

Surface Water pCH₄

Since deep waters are formed from surface waters, one needs to observe whether the atmosphere does indeed tightly control the methane concentration in the open ocean where this formation occurs. During the entire cruise, the partial pressure of methane in the surface layer of the ocean as well as in the atmosphere was surveyed. This was accomplished by pumping from 5 meters below the surface directly to a gas equilibrator located in the wet lab. A sample of the air recirculated in the equilibrator is periodically shunted into a gas chromatograph equipped with a flame-ionization detector. Both the methane and the CO₂ partial pressure were measured, the latter by catalytic conversion to methane. These measurements were also carried out continuously on air pumped from overtop the bridge into the wet lab. The apparatus provides a semi-continuous measurement of the partial pressures in the water every twenty minutes and atmospheric measurements every 40 minutes.

The methane partial pressure in the surface water was close to that of the atmosphere over the area covered by the cruise track. During the last section as warmer waters were encountered, the methane partial pressure of the surface became slightly supersaturated, by about 5%.

The CO₂ partial pressure measurements by gas chromatography followed closely those made by the IfM group using the infrared detector. The CO₂ partial pressure was more variable than that of methane, but the surface water was always under-saturated relative to the atmosphere (see 5.1.1.3). Our measured atmospheric CO₂ concentrations agreed very well with those measured with the infrared technique, but the pCO₂ values measured in the water by gas chromatography were systematically lower than obtained from the IfM equilibrator system, by two or three percent. The reason for the discrepancy is not known, and this will be investigated subsequently ashore.

Discrete CH₄ Measurements

In order to measure the dissolved methane in discrete samples from the hydrocasts, a new procedure for separating the gas phase from the water was employed. Water from the Niskin bottles is drawn into a 200 ml glass syringe without contact to the air. The syringe is then connected to an evacuated 500 ml bottle. As the water is drawn into this bottle from the syringe, most of the dissolved gas separates from the liquid phase. Altogether, 400 ml of water from 2 syringes is added to each bottle. The gas is now led into an evacuated burette by injecting a degassed brine into the bottom of the sample through a sidearm at atmospheric pressure. At this point, 1 ml of gas is extracted and injected into a gas chromatograph equipped with a flame ionization detector. The gas remaining in the burette is collected in an evacuated vial for isotopic analysis by mass spectrometry ashore. In addition to the gas samples, on a few stations separate water samples were collected in air free bottles, and these will be returned to the shore-based laboratory for carbon isotope analysis. The dissolved gas in these samples will be stripped using helium, and the trapped methane injected directly into the mass spectrometer. These isotope measurements will be compared to those on the already separated gas samples.

Preliminary results from M39/2

The calculation of the dissolved methane concentration from the measured data involves estimation of the total volume of all dissolved gases using nitrogen solubility in seawater, which requires temperature and salinity data, and the observed dissolved oxygen measurements. Thus, the final work up of our measurements will be conducted following the cruise.

The measured methane mole fraction in the gas phase gives a qualitative indication of the dissolved concentration in the water, since the total dissolved gas volume typically varies by about $\pm 10\%$ in the northeastern Atlantic. As an example of results obtained so far, we show the vertical profiles of the methane concentration in the extracted gas at Stations 260, 262, 264 and 266 along sections F and G. Station 260 was taken directly over the rift valley of the Mid-Atlantic Ridge, just south of the Charlie Gibbs Fracture Zone. The other three stations lie progressively eastward of the ridge, reaching to the Porcupine Basin. The profiles illustrate that the vertical distribution of methane in the upper 2500 meters along this line remains relatively constant. Methane in the upper 500 to 600 m is relatively uniform at about saturation with the atmospheric partial pressure. The concentration decreases over the next 100 meters or so, and then remains fairly constant at a value somewhat less than that equivalent to the atmosphere over the 800 to 2000 m depth range.

In contrast, the deeper methane concentrations show a marked variation in their horizontal distribution. Below the rim of the rift valley, the methane concentration increases rapidly to values greater than found in the surface water. Evidently, hydrothermal venting is supplying a source to the waters within the valley, but overtop the rim, the deep circulation sweeps away the excess. Away from the ridge, in the eastern basin, the deepest waters contain quite low methane concentrations. This is apparently due to the fact that this water is relatively old, having a component of Antarctic Bottom Water that has found its way into the eastern basin through the Romanche Fracture in the Mid-Atlantic Ridge at the equator.

Preliminary results from M39/4

As for leg M39/2, the final work up of our measurements will be conducted following the cruise. However, the measured methane mole fraction in the gas phase gives a qualitative indication of the dissolved concentration in the water, since the total dissolved gas volume typically varies by about $\pm 10\%$ in the northwestern Atlantic. The vertical distribution of this property is presented along 3 sections consisting of profiles 22-33, 34-57, and 88-103. As a preliminary observation, it appears that the pattern of these distributions is quite similar to those of chlorofluorocarbon and dissolved oxygen. This clearly indicates that water mass "age" or degree of ventilation with the atmosphere has an important influence on the methane concentration in relatively recently formed waters.

In regard to methane in the upper water column, the methane partial pressure in the surface water was consistently in equilibrium with the atmosphere over the most of the area covered by the equilibrator survey. A slight over-saturation occurred during the short transit over shelf waters (200 m depth) near Greenland. A preliminary indication from the station data indicates that the upper few hundred meters of the water column generally have concentrations equivalent to the atmospheric concentration. However, a subsurface maximum was found at about 54°N on the N-S section from Cape Farvel, indicative of production in the upper water

column (Section profiles 34-57). The maximum is found at the top of the thermocline, at a depth of about 200 m.

5.3.2 Tritium/helium sampling program results from M39, legs 4 and 5 (H. Hildebrandt, M. Arnold, R. Bayer)

The preparation of the water samples obtained during M39 for analyses of the helium isotopes and the tritium content started soon after arrival of the samples at the Heidelberg laboratory. The procedure includes the quantitative extraction of helium from the water and transfer of the gases in a glass ampoule as well as storage of the degassed water for ingrowth of ^3He in a preconditioned glass bulb. The measurements are performed in a dedicated helium isotope mass spectrometer which is accessible for helium measurements of samples from M39 since January, 1998. Mass spectrometric tritium analyses may be performed after a sample storage time of typically six months and the high quality tritium data production will start in summer 1998. Nevertheless, a preview of the tritium distribution at selected positions was obtained in the meanwhile by our low-level counting facility (data precision lower than obtained from mass spectrometric measurements).

First results obtained from profiles taken along the WOCE WHP-A1/AR7 leg are shown in Figure 46 where the spatial and temporal evolution of the mean tracer content in the density range of Labrador Sea Water (LSW) is depicted. Evidently and principally according to the transient input and the radioactive decay of tritium the concentrations (upper panel of the figure) decreased since our last occupation of the leg in 1994, the same trend was observed between 1991 and 1994. The second panel attributes to the transient character and shows all the data points currently available normalized to a common date, i.e. start of 1991 (tritium concentrations are given as TU91); in this plot almost no temporal variability is visible. On the contrary the ^3He excess concentrations in LSW at least in the western part of the subpolar North Atlantic changed since 1994 (third panel, ^3He is presented in a delta notation giving the per cent deviation of the ^3He content of the samples from that of surface water in equilibrium with the atmosphere): in the Labrador Sea and in the Irminger Sea $\delta^3\text{He}$ increased from 2% to 3-4%, a feature that is probably related to the ventilation rate of LSW which, according to hydrographic observations, diminished since 1994. This is also visible from the lower panel of the figure which presents formally calculated tritium/ ^3He ages in the LSW: apparently the LSW ages obtained from the M39 cruise increased by about 3-4 years compared to the situation in 1994. Further measurements are in progress and a more detailed discussion of the tracer distribution and its variability will be performed as the data set grows.

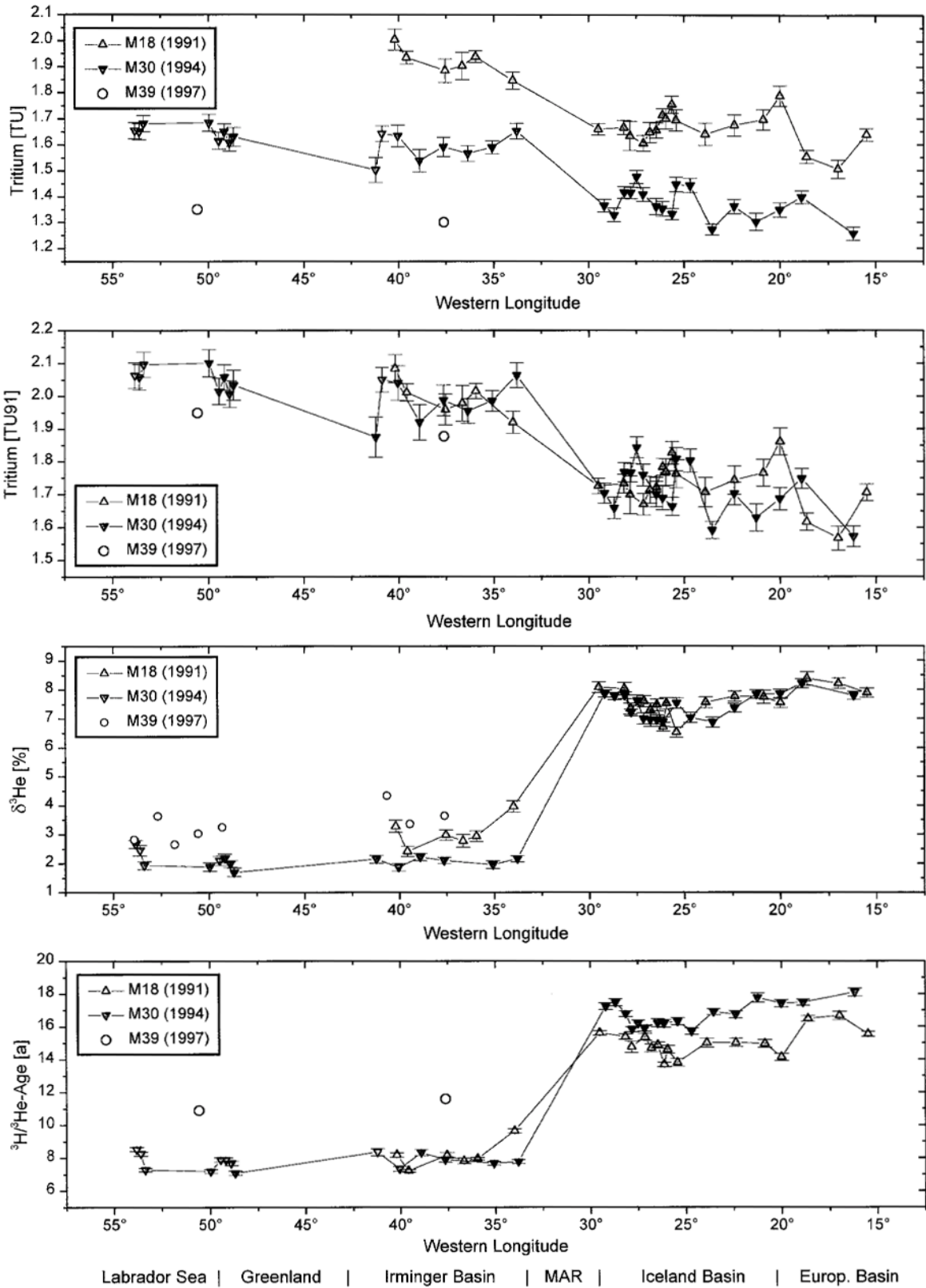


Fig. 46: Spatial and temporal evolution of tritium and delta ^3He in the density range of the Labrador Sea Water.

5.4. Paleoceanography

5.4.1 Water Column T-S Profiling

(M. Huels, S. Jung, R. Zahn)

Methods

During METEOR cruise M39/1, a CTD/Rosette water sampler was deployed at 9 stations in water depths of 500-3500 m to obtain vertical temperature and salinity profiles as well as water samples. The Seabird Electronics CTD device consisted of supplementary oxygen and transmissivity sensors, a twelve-10l-Niskin bottle rosette and a Seabird Electronics 911 Plus deck unit. The CTD/Rosette unit was coupled on-line to a PC. The raw data set will be post-processed shore-based. Firing sequences for the Niskin bottles were chosen based on the downcast T/S-profiles. Down-cast and up-cast speeds were 0.5 m/s. Close to the sea floor, down-cast speed was reduced to 0.2 m/s. In order to prevent a touchdown on the sea floor. A "pinger" echosounder was used in addition to a bottom sensor to monitor the CTD's approach to the sea-floor.

Immediately after retrieval on deck a series of water samples was siphoned off for a suite of geochemical analysis (see below). Water samples for $\delta^{18}\text{O}$ and $\delta^{13}\text{C}$ analyses were poisoned with HgCl_2 to suppress biological activity. Subsequently, these samples were closed airtight with a high-vacuum paste and taped for transport. A set of water samples was sealed airtight in glass bottles for later salinometry to check the calibration of the salinity probe. Stable isotope analysis will be performed on selected water samples post-cruise at the Leibniz Labor for Isotope Research, Kiel University.

Results

The most prominent T-S component in the hydrographic profiles is derived from warm-saline MOW that enters the Gulf of Cadiz at a depth of approximately 280 m. T-S anomalies that are associated with MOW are strongest developed in the northern Gulf of Cadiz where MOW flows along the southern Portuguese margin. Advection of MOW it has resulted in the development of the Faro Drift, a vast sediment body that consists of sediments accumulated and sorted under MOW-related current activities. Acoustic surveys of the Faro Drift show distinct subbottom reflectors that clearly document the current-induced built-up and lateral extension of the Faro Drift (see Figure 57 below) due to the advection of MOW. To trace the evolution of MOW upon its entry in the Gulf of Cadiz and further North, along the western Iberian margin, CTD stations were targeted at the flow path of MOW (Figures 47, 48).

CTD casts from stations in the Gulf of Cadiz, i.e. close to the MOW "point-source" at the Strait of Gibraltar, most distinctly display the vertical T-S-variations into the MOW. At these stations, MOW impinges on the sea floor and is recorded in elevated T-S values in the near-bottom layer (Figure 47) , it is encountered except of cast M39029. At Stations M39017 and M39021, a separation into an Upper MOW (T-S-maxima at 430 and 500 m water depth, respectively) and a Lower MOW was possible (upper boundary at 510 m and 610 m water depth, respectively; Figure 47). Along the MOW flow path, the surface of lower MOW deepens from 500-600 m water depth at Stations M39017 and -021 in the northern Gulf of Cadiz to 1000 m at Station M39029 in the outer Gulf of Cadiz. Maximum MOW temperature at Station M39029 barely reaches 10°C and remains well below MOW temperatures of >12°C at stations in the inner and northern Gulf.

Likewise, maximum salinities of some 36 at Station M39029 are distinctly lower than those recorded in the immediate MOW flow path where values exceed 36.5 (Stations M39014 and -021; Figure 47). Rapid decreases of T-S values mirror the admixture of Atlantic water masses which results in a continued decrease of the T-S anomaly as one moves out the Gulf of Cadiz and northward along the western Iberian margin (Figure 48).

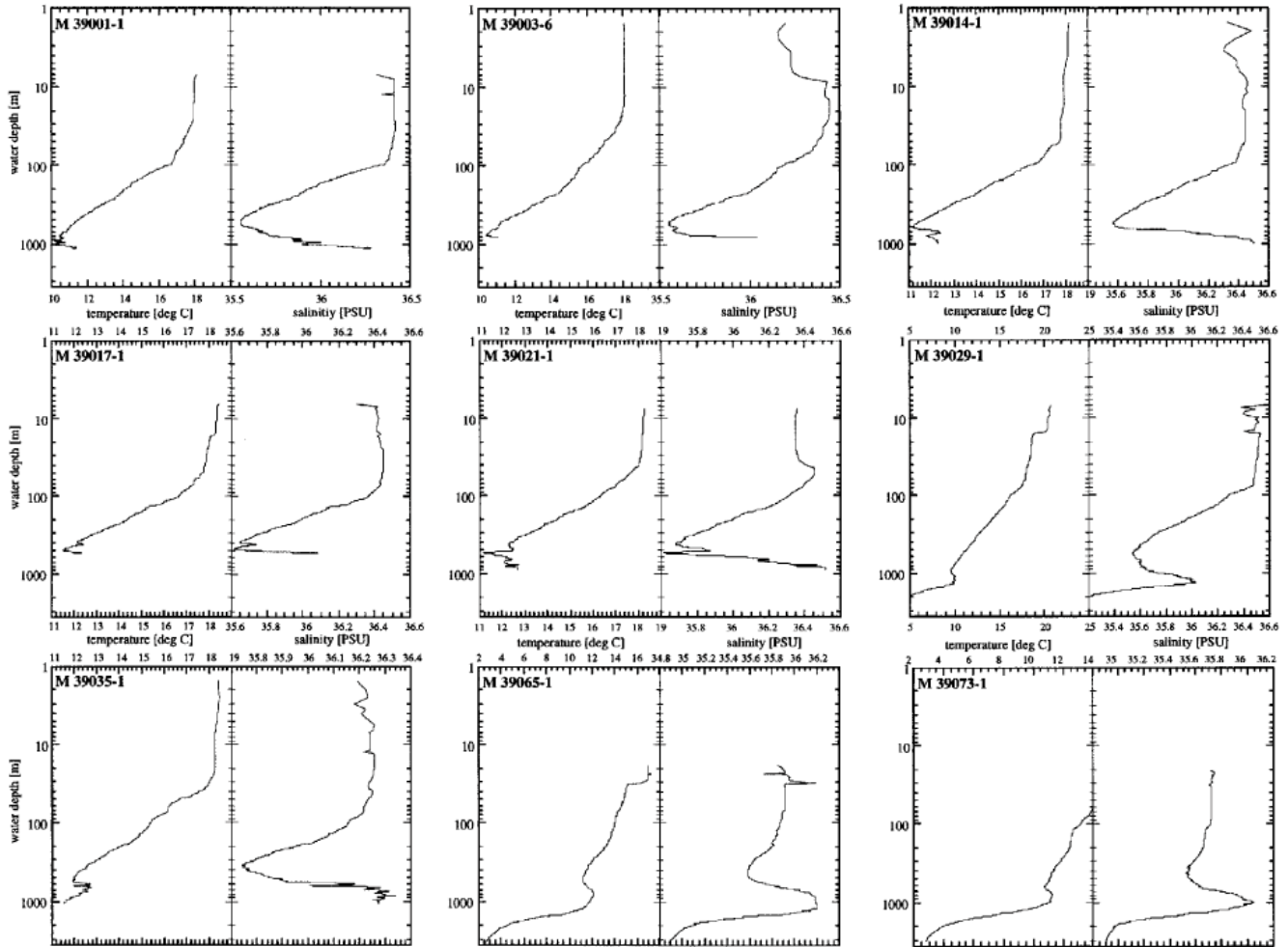


Fig. 47: Water column temperature and salinity profiles from CTD runs in the Gulf of Cadiz (M39001-029) and at the western Iberian margin (M390035-073). CTD stations were targeted at the advection path of MOW. Note logarithmic depth sale that was used to better identify T-S fine structure of the upper water column.

5.4.2 Seawater Sampling for Trace Element and Nutrient Analysis

(A. Müller, C. Willamowski)

GoFlo bottles were used to collect water samples for determination of dissolved cadmium. With a bottom weight of 40 kg, 5 to 7 bottles with volumes of 3 x 12 l and 2-4 x 2.5 l were deployed at a time. Down-cast winch speed was 0.5 m/s, up-cast speed was 0.8 m/s. Sampling depths were determined based on the CTD T-S profiles. After recovery, the GoFlo bottles were brought immediately to the laboratory to be emptied under Nitrogen atmosphere. Water samples were then filtered under clean conditions of a clean bench. 200 ml of each water sample were discarded, 1 l was filtered through a 0.45 µm membrane filter, acidified and stored at +4°C. Another liter was acidified and stored without previous filtering. Additional samples were taken for onboard phosphate analysis. Because the GoFlo bottles are not equipped with depth sensors, additional water samples were taken from the deepest bottle for salinity analysis. Comparison of the GoFlo salinity values with those from the CTD T-S profiles will serve as a control to monitor GoFlo sampling depths in addition to the wire length readings. Cd analysis will be performed post- cruise at the IfM Kiel.

Water samples for oxygen analysis (double sampling) were taken in 50 ml dark brown glass bottles from each CTD-Niskin bottle immediately after retrieval on deck. After addition of 0.5 ml of alkaline Iodide and 0.5 ml of Manganese (II) chloride, the bottles were vigorously shaken. Prior to analysis, 1 ml of sulfuric acid was carefully added and the bottles were shaken to re-dissolve precipitated hydroxides. The solution was quantitatively transferred into a beaker with distilled water. Titration was carried out immediately with 0.01 mol/l sodium thiosulphate. Shortly before disappearance of the yellow color, 1 ml of starch solution was added (solution turned blue) and titration finished as soon as the blue color disappeared.

For analysis of phosphorus concentration, 50 ml of seawater from CTD Niskin and GoFlo bottles were transferred to plastic sample containers. Subsamples of either 5 or 10 ml were taken and 0.1 (0.2) ml of two mixed reagents were added (reagent 1: 12.5 g ammonium heptamolybdate tetrahydrate $((\text{NH}_4)_6\text{Mo}_7\text{O}_{24} \cdot 4\text{H}_2\text{O})$ dissolved in 125 ml distilled water, added to 350 ml of 4.5 mol/l sulphuric acid (while well stirring) - and under mixing added 0.5 g of potassium antimonyl tartrate, $(\text{K}(\text{SbO})\text{C}_4\text{H}_4\text{O}_6)$ in 20 ml water; reagent 2: 10 g of ascorbic acid in 50 ml of 4.5 mol/l sulfuric acid and 50 ml of distilled water). Samples were transferred into a 5 ml (10 ml) cuvette and absorbency was measured at 880 nm against acidified distilled water as reference. Calibration was carried out with standard solutions of 0 to 2 µmol/l Phosphate. Water column oxygen and phosphorus profiles are shown in Figures 49 and 50. The data will be used for calibration of dissolved carbon isotope and Cd concentrations to regional nutrient inventories.

Water samples for analysis of magnesium, strontium, calcium and CO_3 - concentration were filled into 250 ml PE-bottles. Before use, all bottles were put in a 2% Mucosal-solution for at least one week after which they were rinsed three times with normal water to remove tensids and washed twice and finally filled with Milli-Q water. 1ml of concentrated hydro-chloric acid was added. The bottles were then closed and stored at room temperature for three days, subsequently turned upside-down and again kept at room temperature for three days. Then, the bottles were twice rinsed and filled with Milli-Q water, and finally 1ml of concentrated nitric

acid was added to oxidize remaining particles. The containers were then closed and remained at room temperature for three days. This step was repeated after turning the bottles upside-down. Finally, the bottles were rinsed twice with, and then filled with Milli-Q water. For conservation, 5 drops of concentrated nitric acid were added. The bottles were closed, sealed with parafilm, wrapped in foil, and stored at 4°C. The first step of the pre-sampling treatment of the duranglas bottles (250 ml/350 ml) that were used to sample for CO₃ - analysis consisted of a one day bath in 61°C hot solution of Mucosal (3%) to remove fatty compounds. Then, these bottles were rinsed once with distilled water and three times with Milli-Q water in order to remove tensids. Finally, they were dried at 62°C and wrapped in foil.

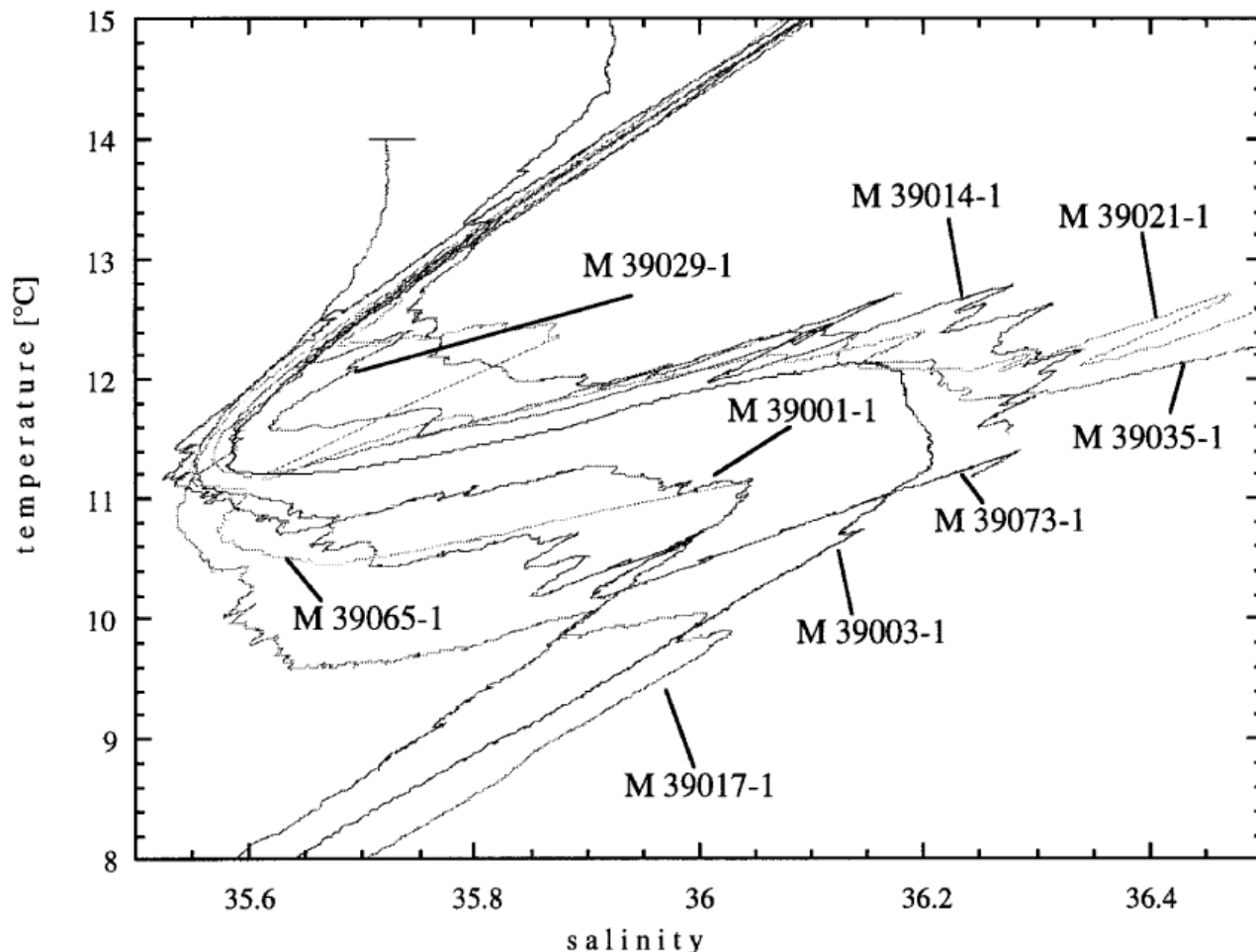


Fig. 48: T-S diagram showing the hydrographic anomaly that is associated with the advection of warm and saline MOW. Strongest T-S anomalies are recorded at stations close to the immediate flow path of MOW in the northern Gulf of Cadiz (Stations M39001, -014, -017, -021). Decreased T-S values are observed in the outer Gulf of Cadiz (M39029) and at the northern section of the western Iberian margin (M39065, -073) documenting the continued admixture of Atlantic waters.

Immediately after retrieval of the CTD/rosette water sampler (Multicorer) on deck, 250-350 ml of seawater for CO_3^- analysis were siphoned off the Niskin-bottles to prevent CO_2 -exchange with the atmosphere. The head space of the filled sample bottles was kept below 2%. All samples were poisoned with saturated mercury-II-chloride-solution (250 ml bottles with 50 μl saturated mercury-II-chloride-solution and 350 ml bottles with 75 μl saturated mercury-II-chloride-solution). The bottles were immediately closed with a Duranglas cap lubricated with Apizon-L, and subsequently sealed airtight. In a second sampling run, 250 ml of seawater (for Mg, Sr-analysis) were taken from the CTD-bottles and Multicorer tubes (the PE-bottles were emptied 1-3 h before). Prior to sampling, each bottle was washed three times with sea water. For conservation, 5 drops of hydrochloric acid were added. The bottles were then closed, sealed with parafilm, wrapped in foil, and stored at 4°C. Trace metal analysis will be performed shore-based in cooperation with the IfM Kiel.

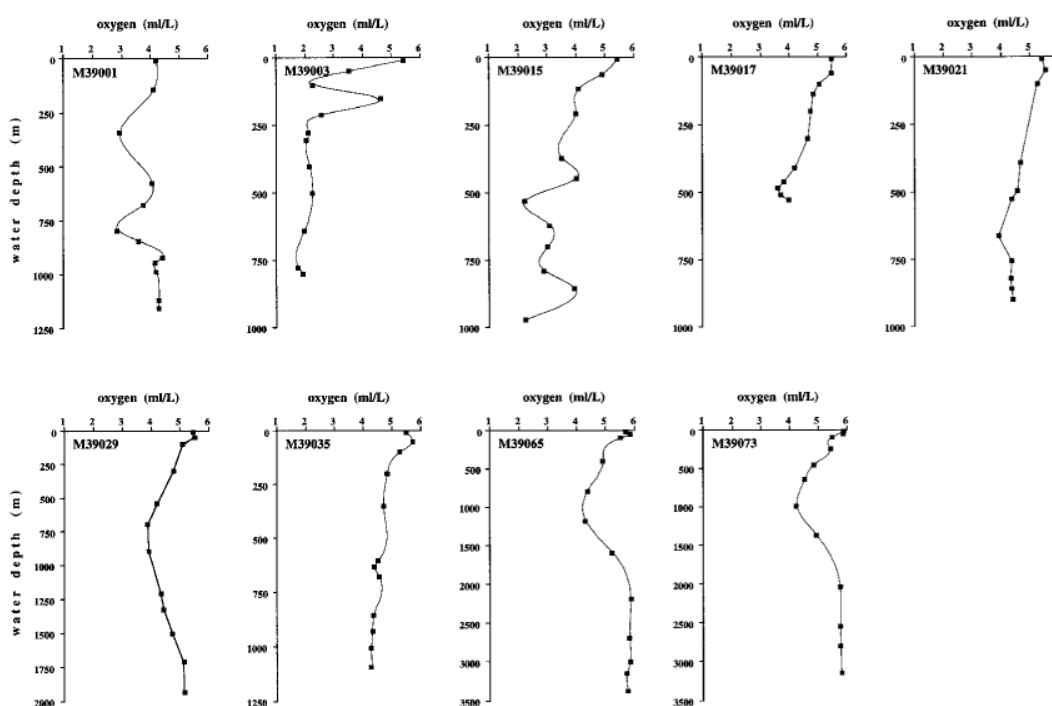


Fig. 49: Water column titration oxygen profiles from Niskin bottle water samples in the Gulf of Cadiz (M39001-029) and at the western Iberian margin (M39035-073). See Figure 2 for hydrocast positions.

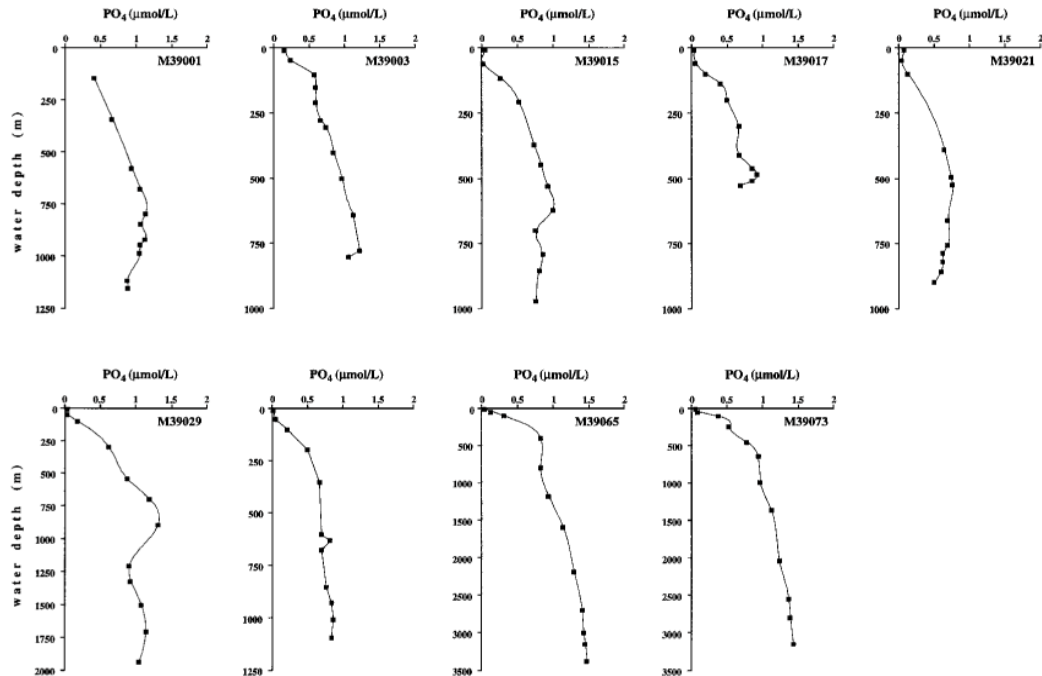


Fig. 50: Water column phosphate profiles from Niskin bottle water samples in the Gulf of Cadiz (M39001-029) and at the western Iberian margin (M39035-073). See figure 2 for hydrocast positions.

5.4.3 Shipboard Sediment Sampling and Core Flow

(G. Bozzano, C. Didie, M. Huels, S. Jung, L. Lembke, N. Loncaric, P. Schäfer, J. Schönfeld)

During M39/1 a gravity -, box-, and Multicorer as well as a grabber and a dredge were deployed for sediment sampling. Subsampling according to the detailed sampling schemes (Figures 51, 52; Table 11) was restricted to sampling of box cores, slicing of multicorer tubes, washing of grab samples and dredged material. Sampling of sediment cores was mostly postponed to a post-cruise sampling party to facilitate standard laboratory procedures and precise determination of physical properties. After retrieval of the sediment cores on deck, they were cut into 1 m sections and subsequently routinely run through the core logger. Only few sediment cores were opened for visual inspection of sediment composition and core quality. These cores were routinely cut into working and archive halves. Macroscopic core description, color scanning and core photographs were done on archive halves while sediment samples were taken from working halves.

Tab. 11: Shipboard Sample Distribution Scheme

Investigator	Device	Sample Interval	Volume
B. Bader/ P. Schäfer	GKG ¹ , BG ² , Dredge ³	surface ¹ , whole sample ^{2,3}	100 cc ¹ , macrofauna ¹
G. Bozzano	SL ^{1,2} , GKG ¹	5 cm ¹ , 1 m ²	10 cc ¹ , 4 cc ²
S. Jung/R. Zahn	GKG ¹ , SL ²	0, 2, then 5 cm ¹ , 10 cm ²	10 cc
A. Kohly/C. Didi	MUC ¹ , GKG ² ,	1 core ¹ , top of archive core ²	100 cc ²
N. Loncaric	MUC ¹ , (GKG ²), SL ³	1 core ¹ , 10 (5) cm ^{2,3}	1-3 cc and 20 cc
A. Müller	MUC ¹ , GKG ²	1 core ¹ , surface ² ,	100 cc ² ,
P. Schäfer	MUC ¹ GKG ² , SL ³	1 core ¹ , archive core ² , entire section ^{2,3} (x-ray), surface ²	x-ray slabs ^{2,3} , 100 cc ²
J. Schönfeld	MUC ¹ , GKG ² , SL ³	1 core ¹ , surface ² , 5 cm ³	3 x 88 cc ² , to be shared with Anja Müller ³
C. Willamowski	MUC	1 cm	2 cores
U. Pflaumann (onshore)	GKG	0, 2, then 5 cm	10 cc
MUC: multicorer, GKG: box corer, BG: Van Veen grab, SL: gravity corer~~			

The color scanning system consisted of a hand held Minolta photo-spectrometer and a transformer. The photo-spectrometer was coupled on-line to a Macintosh Powerbook 170, on which the ODP- software package "Spectrolog" was run for data management. During the color scanning, the sediment sections were covered by ceran wrap to prevent sediment smearing onto the measuring unit. Sediment cores were routinely scanned at 2 cm intervals.

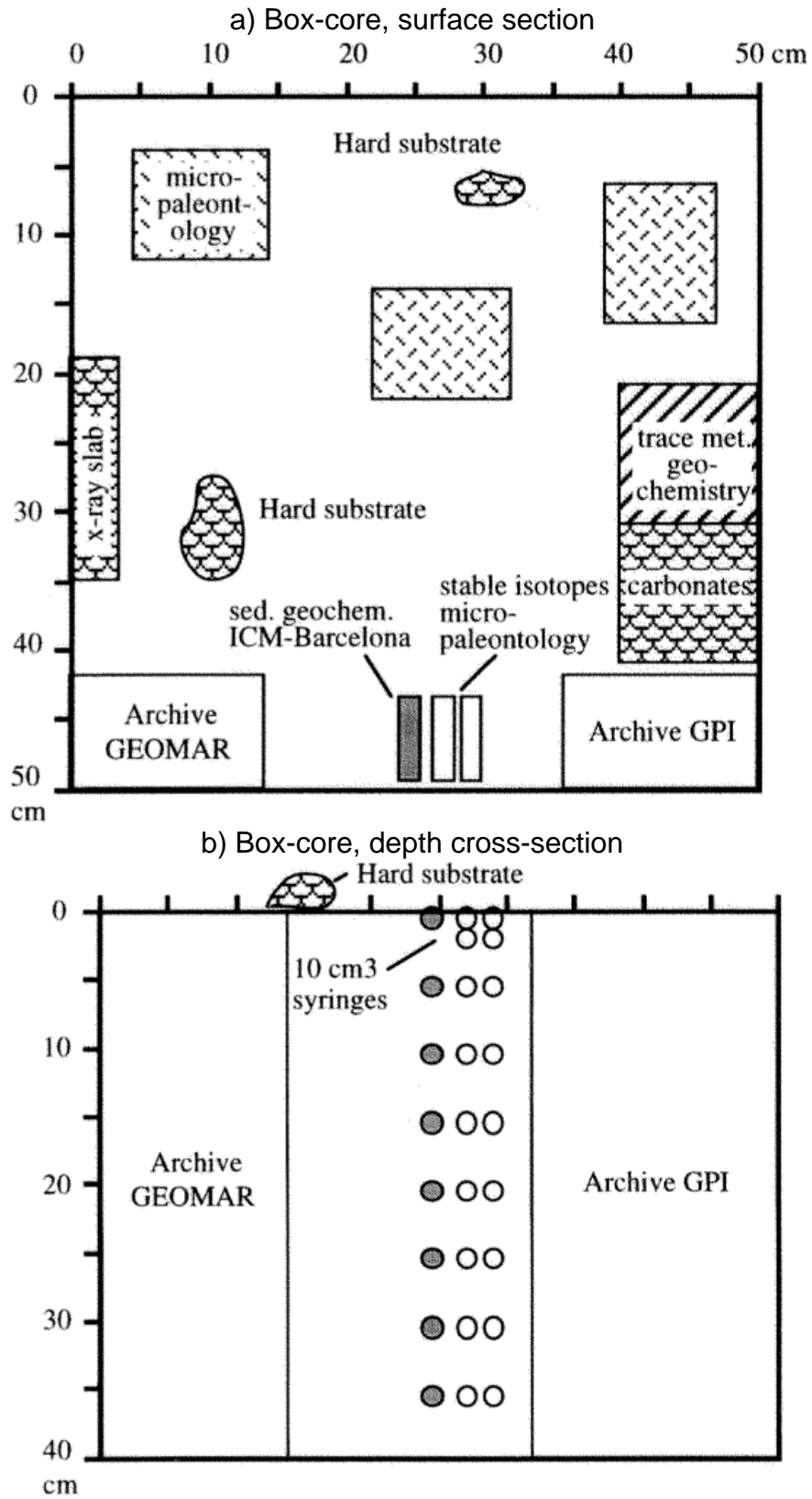


Fig. 51: M39/1 sampling scheme for Giant Box Core (GKG) sampling.

5.4.4 Plankton Hauls

(A. Kohly)

Methods

To study the transfer of living plankton assemblages (and its change) into the sediment, plankton net hauls, filtered water samples from the CTD, and sediment samples were taken. In total, 32 plankton hauls (mesh width 20 μm) from the uppermost 10-12 m were taken. All samples were treated with Formalin to stop biological activity. After settling, 3-4 drops of the concentrated plankton material were placed on a cover slip for on board microscopic analysis. The seston of mostly two liters of CTD/rosette water samples was (vacuum) pumped through a cellulose membrane filter with a pore width of 45 μm (diameter of 5 cm) (list 7.1.2). After drying, the filters were placed in plastic petri dishes, sealed in plastic bags and kept dry by using silica gel. This material will be used to investigate the vertical distribution of coccolithophors and diatoms and to compare it with the species distribution in the underlying surface sediments and sediment cores. Detailed scanning electron microscope (SEM) analyses on the plankton samples will be carried out post-cruise.

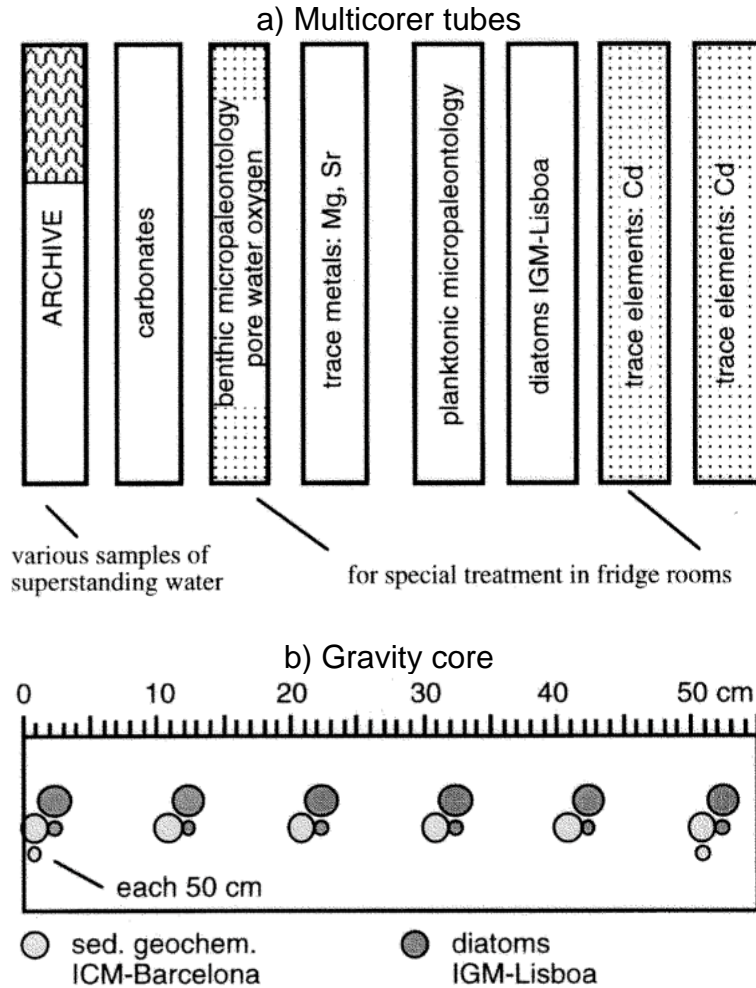


Fig. 52: M39/1 sampling schemes for (a) multicorer tubes, (b) gravity cores. Detailed sampling of gravity cores will be done post-cruise in collaboration with shore-based scientific partners.

Results: Phytoplankton and Zooplankton

Diatoms were the most abundant plankton group in most of the samples. Mainly fragile species such as *Proboscia alata*, *Bacteriastrium hyalinum*, *B. delicatulum*, *Guinardia flaccida*, *Rhizosolenia fragilissima*, *R. delicatula* and several species of the genus *Chaetoceros* were found. At one station (M39073), coincidentally a bloom of *Proboscia alata* was sampled. A list of identified phyto- and zooplankton species or groups is given in list 7.1.3. Dinoflagellates were the second most abundant plankton group; at Stations M39001, M39002, M39003, M39017, M39058 they even dominate the plankton community. Species of the genera *Ceratium*, *Dinophysis*, *Peridinium*, and *Prorocentrum* frequently occurred, whereas genera *Ceratocorys*, *Oxytoxum*, *Gonyaulax* and *Diplopeltopsis* were less abundant. Specimens of *Actiniscus pentasterias* solely occurred in samples M39006 and M39025 (list 7.1.3). Coccolithophorids were merely sampled at single stations, and never reached high concentrations. These lower than expected concentrations are probably due to the inappropriately coarse mesh width for sampling the small sized coccoliths. Furthermore, silicoflagellates (*Distephanus speculum* and/or *Dictyocha fibula*) occurred in almost 50% of the samples.

Tintinnids were the most abundant zooplankton organisms in the net hauls. Several genera were observed such as *Amphorides*, *Rhabdonella*, *Parafavella*, *Steenstrupiella*, *Dictyocystis*, *Tintinnus*, *Dadayiella* and some others with uncertain identification. Radiolarians occurred in small amounts and initial stages of their skeletons were frequent at a few stations. Both spinous and non-spinous species of planktic foraminifera were present in the net hauls.

Macro-zooplankton larvae of different organisms such as copepods and polychaets were present in most of the samples, occasionally reaching significant abundances.

In general terms, the highly diverse diatom assemblage is typical for warm water regions. The lack of spore specimen in the vegetative cells of *Chaetoceros* species indicates, that the bloom cycle had not been completed. *Chaetoceros dadayii* and *C. tetrastichon*, warm water (mediterranean type) diatoms were observed with the parasitic tintinnid (*Tintinnus inquilinus*). Areas with low diatom content (outer Gulf of Cadiz), are dominated by dinoflagellate species. This group shows a dominance of species of *Ceratium*, *Peridinium*, and *Gonyaulax*. Possibly, the diatom bloom had finished at these stations or else the surface water was too oligotrophic for high diatom abundances.

5.4.5 Porewater Oxygen Profiling: Reference for Benthic Foraminiferal Assemblage Studies

(J. Schönfeld)

Methods

The profiling instruments were mounted in a shipboard temperature-constant laboratory ("Gravimeter-Raum"). A Diamond General 768-20R needle oxygen electrode was fixed in an aluminum tube which was centered in the multicorer tube attached to the frame (Figure 53). The multicorer tube was pushed upwards with a standard laboratory lifting platform, while the electrode remained in a fixed position so that the needle was driven into the sediment. The penetration depth is displayed on a scale at the platform. The electrode current was measured with a conventional picoammperemeter. Electrode specifications and measuring procedures are described by DIAMOND GENERAL (1997).

Ambient laboratory temperature was set to the expected bottom-water temperature at least twelve hours before the measurements. The room temperature was kept constant during the measurements with variations of $\pm 0.25^{\circ}\text{C}$. The electrode was stored in deionized water during transit times and was submersed in seawater at least 4 hours before the measurements for stabilization. Calibration of the electrode was done immediately before the measurements by relating the current measurements to oxygen concentrations of two water samples which were subsequently analyzed by using a standard Winkler method (GRASHOFF, 1983). First, we determined the dissolved oxygen content of the super-standing water of the multicorer, i.e. the bottom water. A second calibration point at low oxygen values was obtained by analyzing a seawater sample through which nitrogen was bubbled for at least 30 minutes.

Immediately after retrieval of the multicorer on deck, one tube was sealed with two rubber plugs and brought to the temperature-constant laboratory. The upper lid of a second tube was

opened and the over-standing seawater was transferred into two Winkler bottles for bottom-water oxygen determination. Prior to pore water oxygen analysis with the needle probe, over-standing seawater was carefully siphoned off down to a level of 1 to 3 cm above the sediment surface. The tube was then set on the lifting platform, fixed to the frame and the tip of the electrode was moved down to a level of one millimeter above the visual upper boundary of the bottom nepheloid layer, and was fixed there. The measurement at this point was related to the oxygen concentration of the over-standing water. Oxygen readings were allowed to stabilize for 12 to 30 minutes. When the readings remained constant for more than five minutes, the data were recorded. The lifting platform was then moved upwards a few millimeters for the following measurement. The values were recorded down to either that level below the sediment surface at which the electrode current remains constant or the maximum length of the needle and holder, i.e. 80 mm.

After the measurements, the needle probe was cleaned and submerged in deionized water. The sediment was pushed out of the core tube and was cut into 5 or 10 mm thick slices which were conserved in a Rose Bengal Methanol solution.

Results: Pore water Oxygen Profiles in Selected Surface Sediment Samples

Pore-water oxygen profiles were measured at four multicorer stations, three from the Gulf of Cadiz (M39002-3, M39003-2, and M39029-6 at 1209, 800, and 1918 m water depth respectively) and one station off Cape Sines (M39035-3 at 1082 m water depth). The depth distribution of dissolved oxygen in the pore waters display a characteristic exponential mode as expected from theoretical models (BERNER, 1980; GOLOWAY and BENDER, 1982). The shape of the curves is very similar at the shallower sites whereas the deep-water site displays a much lower gradient (Figure 54). The redox boundary was recorded at depths between 3.9 and 7.1 cm below the sediment surface at the shallower sites and it was not encountered at the deep-water site from the Gulf of Cadiz indicating that oxygen consumption is low here. Relations to C_{org} contents and sedimentation rates have to be tested and will be a subject of post-cruise studies. The boundaries between low oxic, suboxic, and dysoxic pore waters are documented at different sediment depths in each core thus offering a good opportunity for a core-to-core comparison of the depth distribution of deep infaunal species as a function of oxygenation levels at different depths in the sediment.

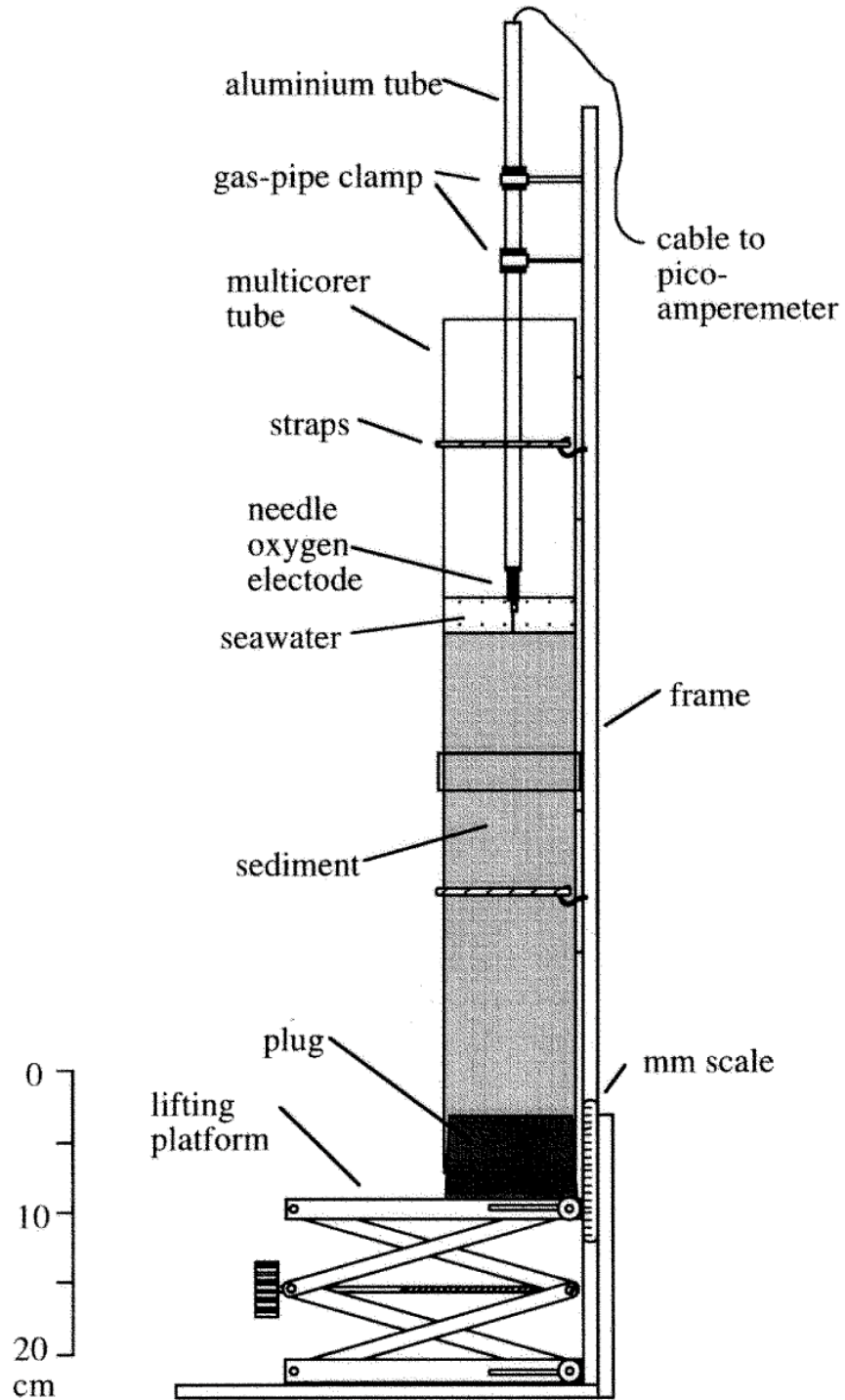


Fig. 53: Laboratory rack with oxygen needle-probe for pore water oxygen measurements. Ambient temperature in the laboratory was held constant at 8°-14°C, depending on local bottom water temperature from where the core was retrieved.

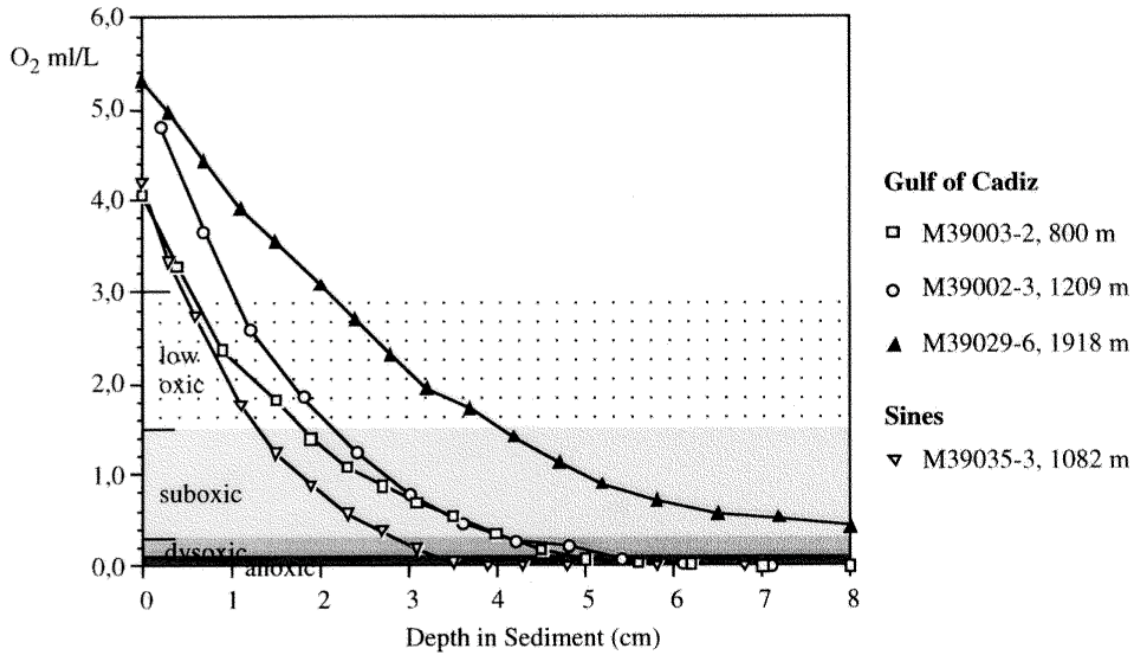


Fig. 54: Pore water oxygen profiles at four stations in the Gulf of Cadiz and off Cape Sines. Differential penetration depths of oxygen likely are a function of sedimentation rate and bottom water oxygen concentration. The data will serve as estimators for environmental control on the depth distribution of infaunal benthic foraminifera.

5.4.6 Trace Fossil Recording and Grab Sampling (P. Schäfer, B. Bader)

a) Instrumentation and Sample Conservation

Sediment samples were taken from within and outside the drift sediments in the Gulf of Cadiz as well as from three primary areas along the western Iberian continental margin at water depths of 110 to 2170 m i.e., across the MOW flow path. At least one radiograph was taken from each giant box core. Following a standard technique developed at the GPI Kiel, a thin slab was taken from each box core using a plexiglas cover of 27 to 15 cm size and 1 cm thickness, then put into plastic bags, evacuated, sealed, and stored at 4°C. Radiograph sampling of gravity cores will be done onshore.

Additional sediment samples taken with Van Veen grab and giant box core were archived in plastic bags and liners and were stored in the shipboard reefer. Surplus sediment was washed on deck through a sieve to retain the coarse fraction >1mm. This was especially important, where the carbonate content was low due to strong terrigenous input (siliciclastic sediments of the Faro drift; glauconitic quartz sand apron between 200 and 500 m water depth along the Western Iberian continental margin). Living organisms were stored in 70% alcohol or 10% formaline buffered with sea water.

b) Trace Fossil Assemblages

In general, all sediments show strong bioturbation that covers nearly the complete sediment column. *Preservation/intensity* of bioturbation, however, is poorest in the upper 5 cm of the sediment column ("Homogenous top layer" after WETZEL, 1981) and in sediments from shallow sites. A pronounced trace tiering was found in sediments from deep water sites. Both vertically and horizontally arranged feeding traces do occur. Burrows of crustaceans were observed in giant box cores as conical mounds of 5cm height; they were commonly found at shallow sites in the Gulf of Cadiz. They occur as vertical burrows with uneven burrow lining in radiographs. A preliminary description of trace fossils is given in Table 12.

At first inspection, radiographs taken from box core material revealed trace taxa of *Scolicia*, *Planolites*, *Teichichnus*, *Chondrites*, *Helminthopsis* and *Trichichnus*. On shore radiographs from gravity cores taken during METEOR cruise M39/1 (and additional material will be collected during METEOR cruise M40/1 into the Mediterranean Sea) will be studied in detail. These analysis include a visual description of bioturbation phenomena in sediment cores, the analysis of trace morphology and of trace associations from radiographs, and finally computer tomographic scans and image processing of traces in order to better illuminate their three dimensional structure. Stratigraphic and sedimentary analysis will be done post-cruise in conjunction with stable isotope analyses.

Tab. 12: Trace Fossil Occurrence in the Gulf of Cadiz and at the Western Iberian Margin Sites

Sample	water depth	Onboard sediment/trace description	
M39002-2A	-1209m	Zoophycos, Scolicia, Chondrites trace tiering	
M39002-2B	-1209m	poor trace record	trace tiering
M39003-1A	-801m	Planolites, trace tiering	
M39003-1B	-801m	Teichichnus, Planolites	Zoophycos, trace tiering
M39004-1	-966m	Chondrites, ?Helminthopsis	Zoophycos, ?Planolites
M39005-3	-118m	poor trace record	
M39006-1	-214m	crab burrows	
M39009-1	-681m	Chondrites, ? Planolites	poor trace tiering
M39010-1	-878m	Sand layer overlying silt layer	poor trace record
M39016-1	-581m	poor trace record	
M39017-5A	-533m	poor trace record	
M39017-5B	-533m	poor trace record	
M39018-1	-496m	poor trace record	
M39019-2	-730m	?Teichichnus, ?Planolites	poor trace tiering
M39020-1	-726m	trace tiering	
M39021-5	-901m	Sand layer overlying silt layer	poor trace record
M39022-1	-668m	trace tiering	
M23023-2	-730m	?Planolites, ?Trichichnus	trace tiering
M39029-3	-1917m	Zoophycos, Planolites	trace tiering
M39036-1	-1747m	Trichichnus	trace tiering
M39037-3	-2532m	?Helminthopsis	
M39058-1	-1975m	Helminthopsis, Lophoctenium	Planolites
M39059-2	-1605m	Zoophycos	

Sample	water depth	Onboard sediment/trace description	
M39061-1	-544m	poor trace record	trace tiering
M39070-1	-1220m	sand layer overlying silt layer	poor trace record
M39072-1A	-2170m	Scolicia, Zoophycos, Planolites	trace tiering
M39072-1B	-2170m	Scolicia, Zoophycos	trace tiering

c) Sediment Composition

A depth transect was sampled in the Gulf of Cadiz at water depths between 100 and 800 m along which Van Veen grab, sediment dredge, giant box corer and gravity corer were deployed. The transect was chosen so as to span the depth range of MOW and water masses immediately above and below. The Faro Drift was an important target area in the Gulf of Cadiz (Figure 2).

At the southern Portuguese margin, a depth transect from 50 to 500 m water depth was sampled with the Van Veen grab and the sediment dredge. Further samples were taken with a Van Veen grab and dredge from the isolated pinnacles of the Principes de Avis as well as from the Tejo Plateau off Cap Finisterre, grab and dredge samples were taken from 50 to 80 m water depth. Off NW Galicia, a spur of the continental shelf elevating up to 400 m water depth was sampled with a Van Veen grab. Further sediment samples were taken with a giant box corer from deeper water locations.

Sediment dredge sampling revealed pebbles and solid rock fragments, lithified coral framework and some living macroorganisms such as corals, bryozoans, and echinoids. A large amount of ship slag occurred in sediments below the major ship route in the Gulf of Cadiz and around Cabo de São Vicente. It showed intensive overgrowth by epibenthic organisms such as hydrozoans, sponges, bryozoans, serpulids, polychaetes, bivalves, and sessile foraminifers. Most of the material was dried, only few slag pieces were stored in 70% alcohol.

Van Veen grab and giant box core samples were taken along a profile in the Gulf of Cadiz between 36°03,0N/007°13,8W and 36°31,9N/006°44,0W at water depths between 110 to 850 m. Parasound profiles displayed a gentle topography and sediment accumulation is indicated by several parallel reflectors. Sediments typically consist of bioturbated silty clay to clayish silt, partly with bivalve coquinas. Surface sediments typically consist of fine- to medium grained sand with abundant biogenic fragments (echinoid spines, gastropods, bivalves, corals and bryozoans). High abundances of endobenthic species indicates a high content of fine sediment fraction (i.e. compared to the carbonaceous lag deposits in high boreal to subpolar shelf settings; SCHÄFER et al., 1996; HENRICH et al., 1997).

The deepest sampling locations (M39013-1; M39014-1,2) are characterized by a rough topography on the Parasound/Hydrosweep profiles. The sediment dredge recovered solid rocks and pebbles of red, fossiliferous sandstone colonized by a diverse epifauna (hydrozoans, bryozoans, ascidians, serpulids, actinians). Coral fragments, sea-urchins (*Cidaridiscus cidaris*) and gastropods also occurred.

Typical deep water coral reefs were not found but the considerable abundance of coral fragments in sample M39014-2 implies the nearby presence of reef-like coral structures. The

coral fragments show strong alteration (corrosion, bioerosion, epigrowth) and cementation, that either suggest a fossil age of the fragments or unusually early cementation. The lack of fine grained sediment and the abundance of sessile epibenthic suspension feeders are indicative of strong bottom currents (MOW).

The Faro drift consists of sandy, silty, and muddy contourites. The clayish silt to fine sand of the contains mainly endobenthic bivalves, associated with large solitary corals (*Flabellum* sp.) and terebratulid brachiopods. Due to increasing sediment coarseness at sites closer to the coast, the robust Van Veen grab was used at several near-shore sites. Except for a narrow erosion belt, which is indicated by slightly greater water depth and coarser sediments, clayish silt occurred up to shallowest depths of 103 m.

Sediments on the flanks of the Découvreur seamounts (M39030 to M39034) consist of silty fine to coarse sands that are enriched in pteropods, sponge spicules, and benthic and planktonic foraminifers. The tops of these seamounts are covered by blankets of coarse sand and fine gravel with high carbonate contents. This sediment includes a rich epibenthic fauna dominated by bryozoans, bivalves, and gastropods. Sediment distribution and facies types of the Découvreur seamounts correspond to that on the Principes de Avis. However, samples from the latter revealed siliceous sponges and ophiuroids.

A depth transect off Sadao (M39047 - M39054) covers the upper shelf slope between 500 and 100 m water depth and retrieved glauconitic medium to coarse sands with a high contents of small bivalves, gastropods, echinoid spines, benthic foraminifers, and skeletal debris. Sediments at depths shallower than 100 m are characterized by coarse sands with variable carbonate contents, and by well rounded pebbles 10-15 cm in diameter that were intensively encrusted by bryozoans, coralline red algae, and the foraminifer *Minicea minima*. An apron of glauconitic medium to coarse sand covering the outer shelf and uppermost slope that is found along the entire western Iberian continental margin was tracked up to the northernmost M39/1 sampling sites off Galicia.

The Tejo Plateau presumably is the most extended shelf area on the western Iberian margin where biogenic carbonate production and accumulation occurs between 50 and 200 m water depth. Coarse sand and fine gravel with a high carbonate content was found on the Tejo Plateau in water depths of 160 m. The coarse fraction >2 mm is composed of bivalves, gastropods, erect bryozoans, skeletal fragments of cirripedians (*Verruca stroemia*), and serpulids. The fraction 1- 2 mm is dominated by branchy bryozoans, bivalve debris, and benthic foraminifers. Interestingly, at Tejo Plateau the epifauna dominates the endofauna in contrast to the Gulf of Cadiz and the glauconite sand apron along the Portuguese coast. The distribution of carbonate rich sediments apparently is linked to the delivery of terrigenous material. Off Tejo Plateau, on a topographically isolated submarine mound (132 m below the sea surface) angular pebbles and solid rocks up to 50 cm in diameter were collected that were intensively overgrown by *Minicea minima*, a diverse encrusting bryozoan fauna, and serpulids.

Off Cabo Finisterre, sites between 500 and 200 m water depth revealed a glauconitic medium to coarse sand apron. Solid rocks in water depths of 50 to 70 m were colonized by large

bryozoans and corals. Solid rocks seem to be the preferred habitat for the epibenthic fauna, whereas endofaunal elements are present in glauconitic sand aprons and drift sediments.

Along the northern margin of Galicia, the shelf is bordered by a fracture zone forming a very steep topographic relief cascading into the deep Gulf of Biscaya. Glauconitic sands, poor in carbonate were found up to the northernmost position. Framed by steep walls, solid rock is exposed in 500 m water depth. Pebbles and rock boulders collected with a dredge show intensive overgrowth by sponges, bryozoans, serpulids, and benthic foraminifers. Post-cruise studies include sediment component analysis including carbonate and organic carbon contents, radiocarbon datings of carbonate skeletons, (paleo-) ecological analysis of dominant organisms, taphonomic analysis of carbonate skeletons (bioerosion, mechanical destruction, transport processes), characterization of areas of carbonate production and accumulation, and carbonate budget, terrigenous component analysis (reconstruction of sediment origin and transport patterns), and analysis of microorganisms: benthic and planktonic foraminifers, diatoms, and ostracods.

5.4.7 Geochemistry and Mineralogy

(G. Bozzano, I. Cacho)

From all opened cores samples were taken shipboard for various sedimentological and geochemical analysis. Surface samples will be used to study clay mineralogy and some cores will be selected for studying the complete mineralogical record. Additionally, three gravity cores (M39002-6, M39004-5, M39029-7) were wide spaced sampled (every 50 cm) onboard for a prospective molecular biomarker study. A total of 32 samples was collected by a 2.5 ml syringe (1 cm), stored in glass vials and immediately frozen. These samples will be processed post-cruise to determine the quality of the samples for molecular biomarker analysis. According to these results one core will be selected for a high resolution study (every 2 cm). The analysis will focus on a series of molecular biomarkers originated by marine and terrestrial organisms: C29 n- alkane, C26 n-alkan-1-ol, phytol and long chain di and tri-unsaturated alkenones (37 and 38 carbons). These compounds are present in most marine sediments and, after a lipid extraction, they can be clearly identified and quantified by gas-chromatography. Their abundance records serve as proxies either for marine paleoproductivity (Phytol and long chain alkenones) or for terrestrial input (C29 n-alkane and C26 n-alkan-1-ol). Furthermore, these compounds enable a reconstruction of the past sea surface temperature (Uk 37 unsaturation index).

5.4.8 High-Resolution Acoustic Mapping and Core Logging: Paleoceanographic Application

(K. Heilemann, F.-J. Hollender, T. Karp)

a) Instrumentation

Parasound and Hydrosweep profiling during M39/1 concentrated on sediment drifts in the northern part of the Gulf of Cadiz and were carried out as part of the STEAM MAST Project. R/V METEOR's Parasound echo-sounder applies two simultaneous primary frequencies (a fixed frequency of 18 kHz and a variable frequency of 18 to 23.5 kHz). Due to a Parametric

Effect in water, a secondary frequency is produced (2.5 to 5.5 kHz). In ocean sediments a penetration of up to 100 m can be reached. Onboard, paper plots were used for prospective studies, digital data were stored on magnetic tape for post-cruise processing. The Hydrosweep system, a multibeam echo sounder system operates at a frequency of 50 kHz. The combined use of Parasound and Hydrosweep allows a three-dimensional imaging of superficial acoustic units.

Sediment cores were logged using a GEOTEK Multi Sensor Core Logger (MSCL; P. SCHULTHEISS, GEOTEK, Surrey, UK) that provides continuous, high resolution and non-destructive measurements of physical properties that are used for stratigraphic correlation and lithologic interpretation. The MSCL used during M39/1 consisted of a p-wave logger (PWL; determination of compressional wave velocity), a gamma ray source (^{137}Cs and detector; estimation of sediment density), and a Bartington magnetic susceptibility meter. The system is fully computer-driven. Whole-round core sections were placed on a core boat and transported by a stepper motor through the tracking system for a high resolution measurement (2 cm) of physical properties. Data files are stored in ASCII format.

The p-wave-logger consists of two transducers, which send and receive a 500 kHz ultra-sound signal through the core at a rate of 1 kHz. The travel time of the signal and the diameter of the sediment core are used to calculate p-wave velocity in the sediment. The true diameter of the core liner is monitored for each measurement by an electronic caliper. A detailed discussion of MSCL application is given in SCHULTHEISS and MIENERT (1988) and SCHULTHEISS and MCPHAIL (1989).

The Gamma Ray Attenuation Porosity Evaluation (GRAPE) measurements are based on the attenuation of gamma rays in marine sediments by Compton scattering (BOYCE 1976). The attenuation of gamma rays through the core is referred to the attenuation of aluminum standards. For calibration, two pieces of a PVC liner and 20 aluminum plates (5.3 mm thick) were each placed between the source and the detector. The expected theoretical attenuation can be calculated from the density data (about 2.7 g/ccm), the thickness of the aluminum plates and the count-rate measurement of gamma rays. During the measurement, a gamma ray beam of 0.662 MeV is emitted out from a hole (6 mm) and passes through the core. The ^{137}Cs -source is shielded by a lead case. A scintillation detector (NaJ-crystal) measures the diminished radiation, which represents an indicator for wet bulk density. The physical principle of the Magnetic susceptibility meter is based on the magnetizability of atomic magnetic moments by external magnetic fields. A sensor loop with a diameter of 168 mm produces a weak, magnetic field. Interference with magnetic sediment particles induces changes of the oscillation frequency of the electric circuit. These variations are detected and transformed into the magnetic susceptibility values that are given in SI-units. A detailed description of the GEOTEK Multi Sensor Core Logger and its use in sediment logging is given by CHI (1995).

Approximately 100 m of sediment cores were logged on board during M39/1. Prior to the measurement all cores were stored horizontally for 12 hours for thermal equilibration. During the cruise (sediment) temperatures varied between 16,6 and 21,2°C. Core liners were wetted with distilled water to ensure optimum acoustic coupling between the p-wave transducers and

sediment cores. The drift of the susceptibility sensor was checked by measuring an iron ring that has a defined susceptibility signal.

Changes in acoustic and physical properties of marine sediments are closely related to the mean grain-size, bulk density, porosity, terrigenous material and percentage of sand, silt and clay. The p-wave velocity varies between 1450 m/s and 1500 m/s. In sections with a high amount of sandy components, the p-wave velocity increases up to 1600 m/s. Unrealistic high or low velocities (below 1450 or above 1600) were measured when coupling between p-wave transducer and the sediment was insufficient. In an ideal case there are no air-gaps between the liner and the sediment. But in practice the sediment does not fill the liner completely, having gaps mostly at the beginning and the end of a section. In this case the 500 kHz transducer signal is significantly weakened. Sediment gaps in the liners also distort the GRAPE measurements. For a satisfactory interpretation it would be necessary to correlate the p-wave velocity with the density data. In sections with a good correlation between compression-wave velocity and density, the physical properties can be used for interpretation of sedimentary processes. The density of marine sediments range between 1.45 and 1.9 g/ccm in the Gulf of Cadiz and at the Portuguese margin and, as expected, increases from top to bottom of these cores. Density variations on top of these general trend indicate changes of the mineralogical composition or of the water content. The magnetic susceptibility depends on the flux of terrigenous magnetic minerals. Generally susceptibility values are about 20 SI-units. In several cores prominent peaks up to 50 occur. Most magnetic susceptibility curves show a positive correlation with the curves of the p-wave-velocity and GRAPE-density.

b) PARASOUND and HYDROSWEEP Profiling in the Gulf of Cadiz

Due to good weather conditions and locally deep penetration high quality PARASOUND and HYDROSWEEP records from the Gulf of Cadiz were gained (Cadiz 4, Cadiz 5, Faro 1, Santa Maria 1, Santa Maria 2, Albufeira 1, Albufeira 2; Figure 55). Profile Cadiz 4 covers water depths from 700 m to 1100 m. Several pock marks were observed. These marks most frequently were V-shaped, either with or without levees (Figure 56). Vertically, they measure several meters, in cross sections up to one kilometer. The topography of the whole area is extremely rough. Profile Cadiz 5 covers 650 m to 1000 m water depths. The topography at the southern end of the survey box is extremely rough. This area is influenced by the tectonically active Gibraltar Fracture Zone. The other parts of the profile box has a smooth topography. The thickness of the stratified sequences in the smooth areas reaches up to 30 m and shows up to 12 reflectors. In the rough parts the penetration reaches up to 5 m, usually without subbottom reflectors.

Drift sediments in the northern Gulf of Cadiz were surveyed in three profiles. Profile Faro 1 covers the Faro Drift (Figure 57). The water depths ranges from 550 m in the North up to 800 m in the south and the profile lines were run N-S. The three-dimensional HYDROSWEEP Map shows the luv and the lee flanks of the sediment drift body. The penetration in the middle part of Faro drift body reaches up to 20 m, at the distal ends it is lower. The lines of Profile Santa Maria 1 and Santa Maria 2 were N-S oriented and show the sediment drift body east of profile Faro 1. The water depths ranged from 375 m in the north up to 950 in the south. At the northern end of the sediment drift body a channel like structure followed by a steep ascent occurred. The penetration in the middle part of the sediment drift body reaches up to 20 m, at

both ends it is about 10 m. Profile Albufeira shows the east part of the sediment drift body in the Gulf of Cadiz. The lines of Profile Albufeira have a S-N orientation. The water depth decreases from about 350 m in the North to about 1000 m in the south. The penetration in the middle part of the sediment drift body reaches up to 25 m, at the distal ends about 10 m. At the northern end of the sediment drift body the channel structure of profiles S. Maria 1-2 reappeared. The sediment thickness of the drift body increase from E to W (profile Faro 1 to profile Albufeira).

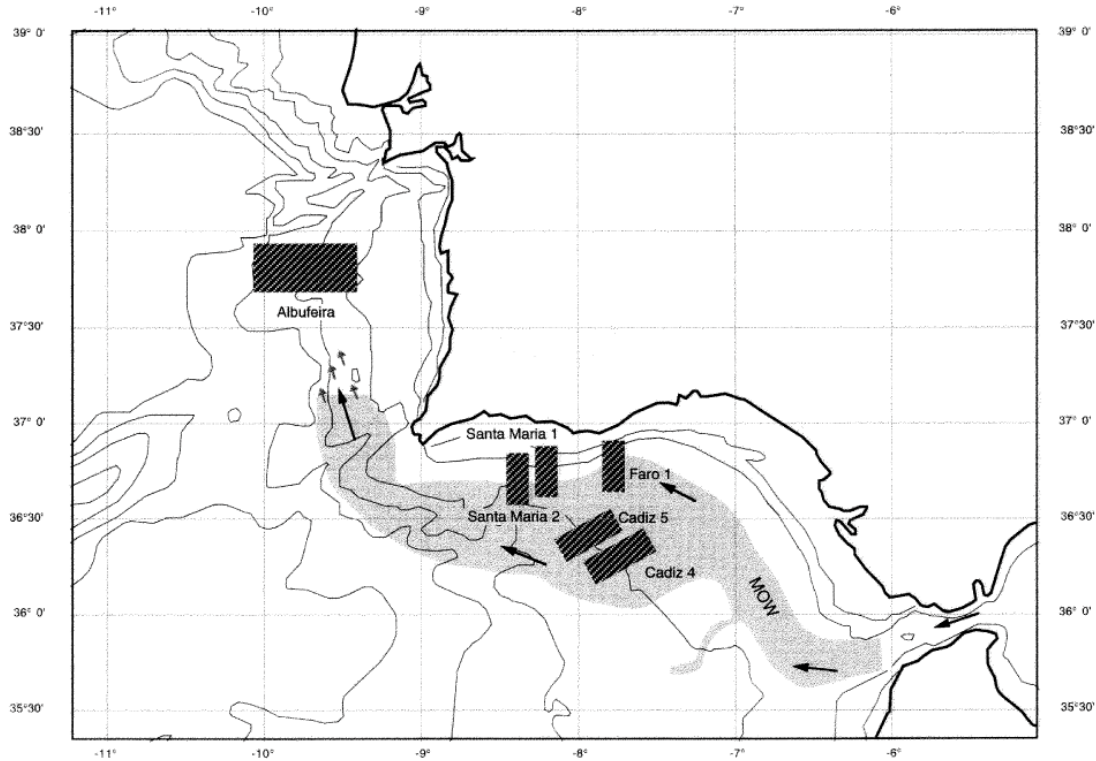


Figure 10: Location of acoustic survey boxes Cadiz 4, Cadiz 5, Faro 1, Santa Maria 1, Santa Maria 2, and Albufeira.

Fig. 55: Location of acoustic survey boxes Cadiz 4, Cadiz 5, Faro 1, Santa Maria 1, Santa Maria 2 and Albufeira.

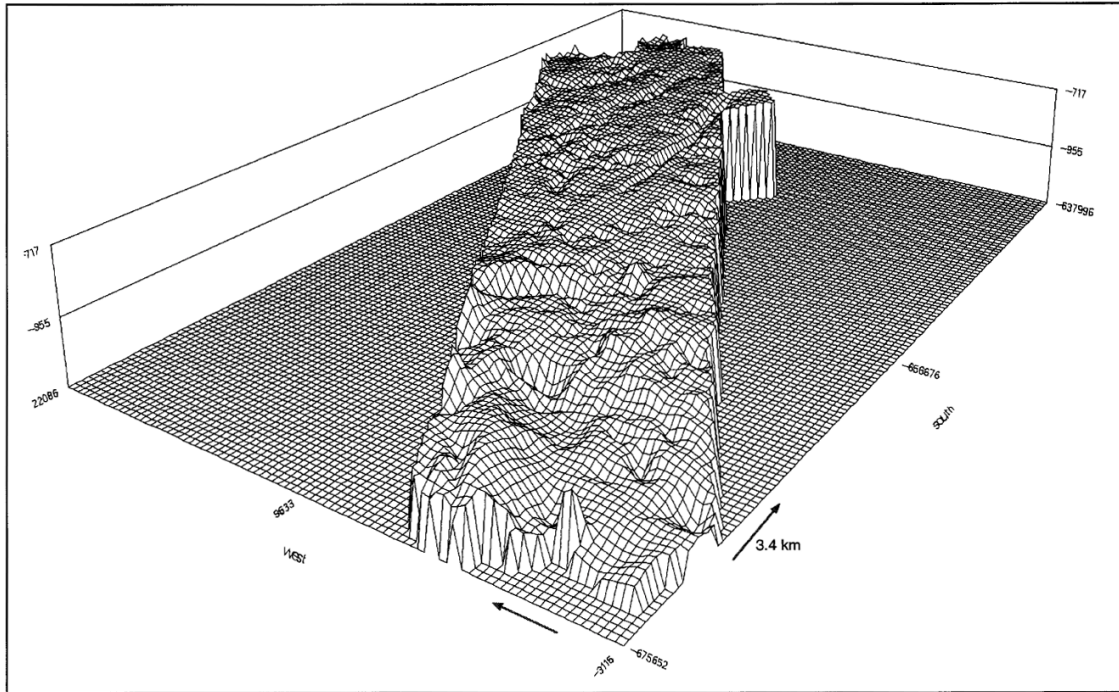


Fig. 56: Three dimensional HYDROSWEEP profile Cadiz 4. Water depths range from 760 m to 1140 m. Pock marks measure several meters in vertical direction and several hundreds of meters up to one kilometer in diameter.

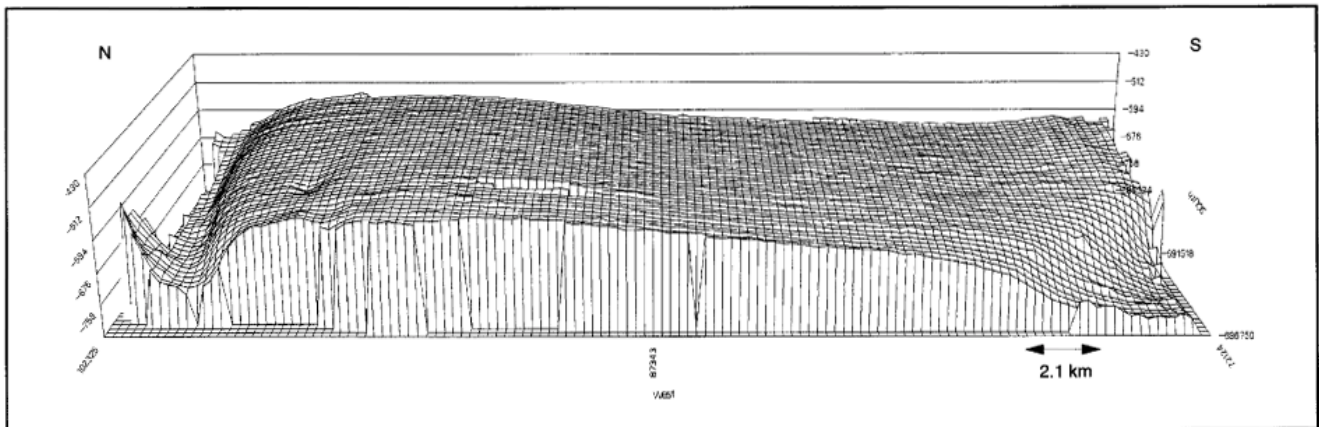


Fig. 57a: Three dimensional HYDROSWEEP profile Faro1. Shown are the luv and lee flanks of the sediment drift. Water depths range from 700 m to 1100 m.

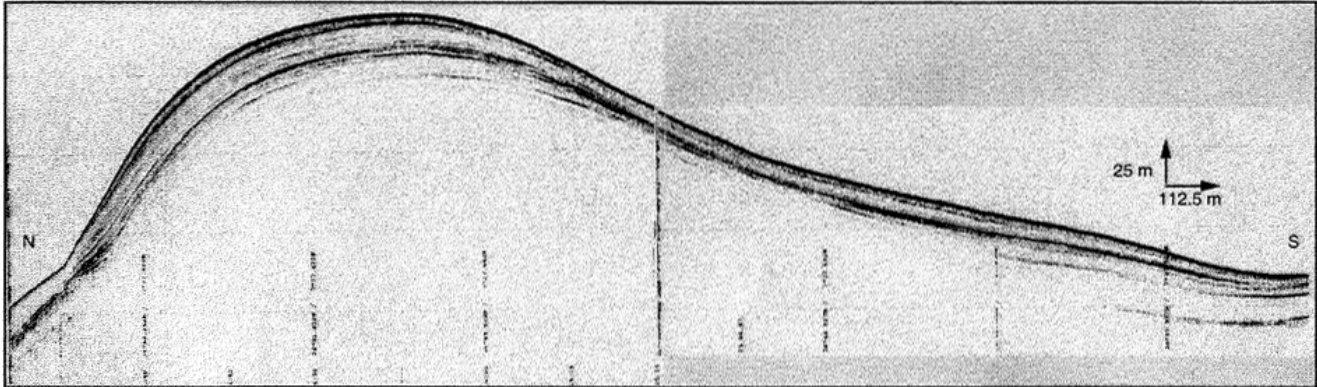


Fig. 57b: Stratified sequence of the luv and lee flank of a PARASOUND profile of the Faro Drift. Location: 36°53'N, 7°37'W/36°43'N, 7°37'W. Water depths range from 528 m in the north to 588 m in the south.

c) *Core Logs as Indicators of Climate Change*

(S. Jung, R. Zahn)

Organic and inorganic composition as well as physical properties of deep sea sediments are controlled the ocean's physical circulation and chemical cycling. Carbonate dissolution, for instance, is driven by the state of carbonate saturation of ambient water masses which, in turn, is a function of carbon input and of chemical water mass "aging". Continuous high-resolution core logging is an indispensable tool for the evaluation of sediment composition and provides valuable data of fine-scale changes of sediment parameters that are intimately tied to state of ocean circulation and, ultimately, of global climate. Magnetic susceptibility logs and color scans of M39/1 sediment cores show numerous anomalies that can be correlated e.g., with horizons of enhanced concentration of terrigenous sediment components. Such horizons have been found previously in the northern North Atlantic and at the upper Portuguese margin and have been linked to periods of enhanced iceberg melting during the last glacial period (BOND et al., 1993; LEBREIRO et al., 1996; ZAHN et al., 1997). Figure 58 gives an example of the core logs that have been obtained during M39/1. The color scans show a series of positive reflectance excursions that can be tentatively correlated to oxygen isotope anomalies in the GISP2 Greenland ice core record. The isotope anomalies signify short-lived warm (interstadial) episodes that are well known from continental European paleoclimate data bases and point to rapid climatic oscillations in the North Atlantic region (DANSGAARD et al., 1993; GROOTES et al., 1993; TAYLOR et al., 1993).

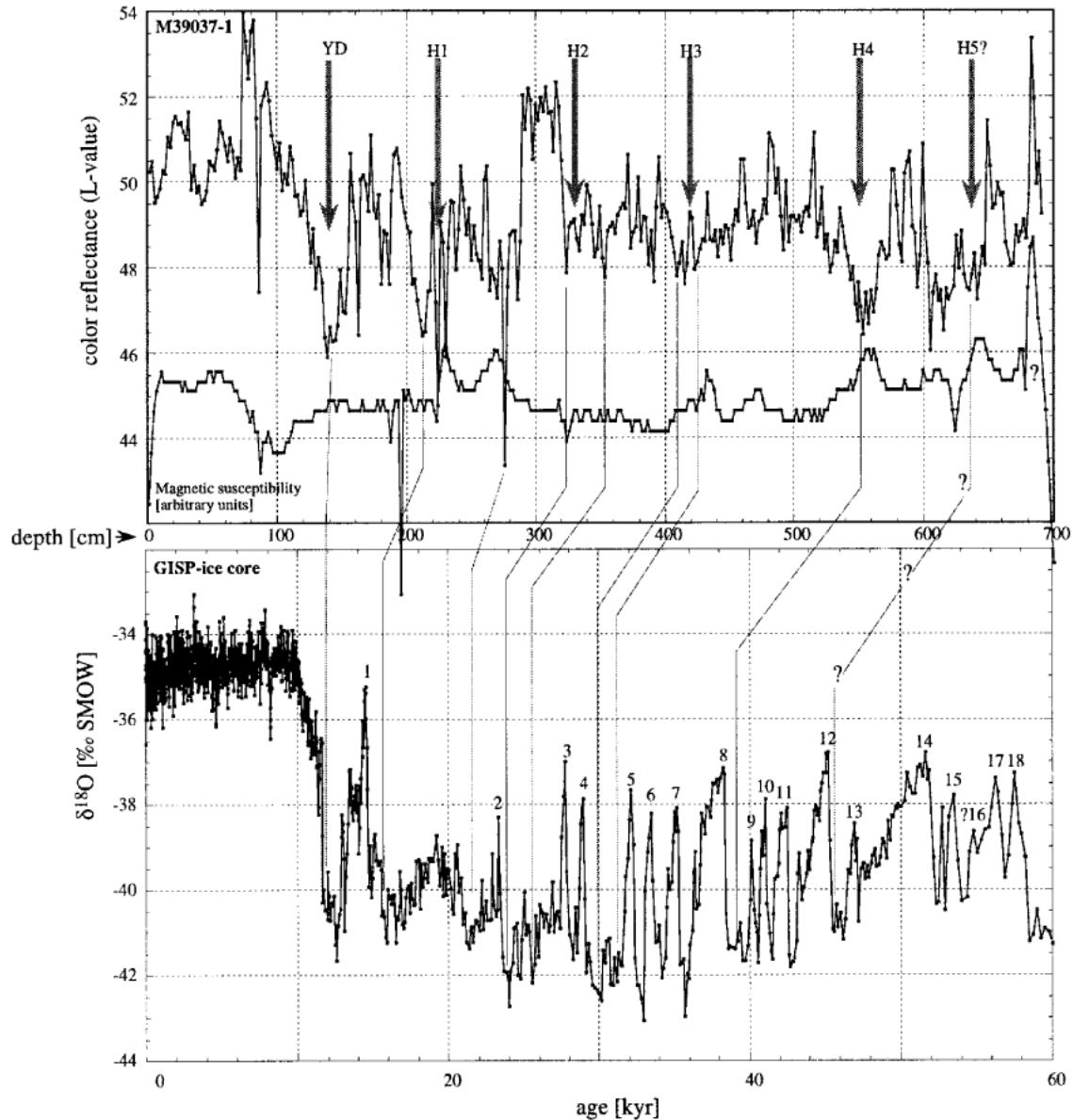


Fig. 58: Shipboard color reflectance and magnetic susceptibility logs for core M39037-1 from the western Iberian margin at 2533 m water depth (top). Arrows mark depth positions in the sediment core of 'Heinrich' meltwater events (labelled H1-H5) as predicted from reflectance minima and/or susceptibility maxima. YD=Younger Dryas cold event. The Greenland GISP2 ice core oxygen isotope record is shown for reference of northern North Atlantic climate variability (bottom). Prospective correlation between the GISP2 record and the M39037-1 color reflectance log is indicated and implies a close link between sediment property variations at the western Iberian margin and northern North Atlantic climate. Age scale along the ice core record is in 1000 years before present.

The apparent correlation between the color scan of core M39037-1 and the Greenland ice core record implies that the climate oscillations reached the western Iberian margin and conceivably affected climates of the western Mediterranean region. Planktonic isotope records that monitor surface ocean conditions will be generated for this core at the same resolution as the color scans i.e., at an average sample interval of 2 cm. This high-resolution isotope record will allow to test the predicted correlation with the ice core record as indicated in Figure 58. It will also allow to estimate the magnitude of environmental change at the western Iberian margin, far south of Greenland but reasonably close to the glacial position of the North Atlantic polar front at approximately 40°N. Statistical analysis of the planktonic foraminiferal assemblage will allow to estimate the variability of regional surface water temperature. The combined faunal and isotope data sets will help to better constrain the paleoceanographic patterns off Portugal and to determine the role of the Portugal current in transmitting northern North Atlantic climate signals as far south as Cape Blanc at 21°N off northwest Africa (WANG et al., 1995).

6 Ship's Meteorological Station

6.1 Meteorological conditions during leg M39/1 (K. Flechsenhar)

RV METEOR left Las Palmas harbor on April 18th 1997 and sailed to her first working area in the Gulf of Cadiz, where they arrived in the evening of April 20th. During this track the weather was influenced by a low centered west of Portugal, which caused northwesterly winds of 6 to 7 Bft on April 20th and 21st, and swells of about 3.5 m height. On April 22nd wind and seas decreased and from April 23rd to May 1st the scientific program was carried out under optimum conditions. On April 30th however RV METEOR for a while got into dense fog at 36.0°N8°20'W. On May 1st the ship passed Cabo de São Vicente with Westsouth-west Gale 7 to 8 Bft, and wave heights of about 3 m. This wind was primarily caused by a low approaching from the west, but its intensity was strengthened by the orographic effect of the steep cape. On May 2nd and 3rd the station works continued under fair weather off SW Portugal, but a westerly 3 m high swell caused some rolling and pitching of the ship. On May 4th, RV METEOR proceeded to the North and passed Cape Roca, height of swell now about 4 m. From May 5th on the weather was dominated by a low pressure system with center near Scotland and became rather bad. A strong southwesterly to northwesterly wind (6 to 7 Bft) made the sea very rough. During passages of cold fronts even Northwest gale 8 with gusts up to 10 occurred and the scientific was carried out under difficult conditions.

In the evening of May 7th RV METEOR passed Cape Finisterre with northwesterly winds of 5 to 6 Bft and swells of about 5 m. Until May 10th off Cape Finisterre, the Wind decreased to Bft 5, but a 5 m high swell, rolling on continuously from the North Atlantic Ocean, hampered station works. On May 10th all research operations were terminated and the ship headed towards Brest across the Bay of Biscay, wind Southwest to West 4 to 6 Bft, swell about 4 m. In the morning of May 12th RV METEOR moored in Brest.

Twice a day a weather report was compiled and published in the morning and in the evening. Additional comments were regularly given to the ship's command, the chief scientist and upon

request. The necessary data and weather maps were received from the wireless stations Bracknell and Pinneberg, as satellite pictures (satellites METEOSAT and NOAA), and by fax (forecast charts from Bracknell or Offenbach). The forecasts of weather conditions and height of sea and swell were based essentially on surface analysis charts of the North Atlantic Ocean of 00.00 and 12.00 UTC every day. Surface observations of land stations and voluntary observing merchant ships were compiled by hand and analyzed by hand.

Meteorological parameters have been measured and recorded continuously and were transferred to the ship's data collecting system. Sensors and meteorological equipment were maintained regularly, some repairs were done. Every day at 0 and 12 UTC a rawin sonde was launched with the ASAP-System, determining a vertical profile of pressure, temperature, moisture and horizontal wind up to an altitude of 20 to 25 km. The evaluated data (temps) were transmitted into the GTS of the WMO. Every hour a World Meteorological Organization (WMO) standard weather observation was practiced. 8 of them were transmitted into the WMO Global Telecommunicating System (GTS) including eye observations done by meteorological staff.

6.2 Meteorological conditions during leg M39/2 (B. Brandt)

METEOR left Brest on May 15, 1997. After intense discussion of the weather development over the next five days it was decided to go Northwest and to travel the course of METEOR cruise M39/2 in the originally intended counterclockwise direction.

The weather during the first week of the cruise was determined by high pressure over the Norwegian Sea and depressions moving from Newfoundland to the Bay of Biscay. Mostly moderate easterly winds were prevailing, bringing favourable conditions for the first cross section across the Iceland Basin to the Mid Atlantic Ridge. Only on May 20 easterly gales prevented an intended mooring which had to be postponed for one day.

On May 23 the high pressure centre began to move southward to the British Isles, and depressions now moving northwards from Newfoundland to Greenland caused prevailing winds to veer from East to South. This southerly air current was frequently accompanied by fog. On May 28 and 30 two fast moving storm depressions caused southerly gales and consequently a mooring had to be delayed until May 31 (Figure 59).

The first days of June were determined by moderate to strong northerly and later easterly winds between high pressure near Iceland and a stationary low north of the Azores. On June 5 METEOR got under the influence of a depression originating from Labrador, intensifying east of Newfoundland, and later moving east. But due to the rapid disappearance of the Icelandic anticyclone winds were only light to moderate from northeasterly directions. During the last two days of the final leg of the cruise the ship was lucky to stay near the centre of the depression with mostly moderate northeasterly winds. METEOR put in at Cork on June 8, 1997.

6.3 Meteorological conditions during leg M39/3 (B. Brandt)

After leaving Cork harbour on June 11, 1997, RV METEOR passed the rear side of a depression moving northeast across the Irish Sea with northwesterly winds up to 7 Bft. Between June 13 and 16 two weakening depressions moving from the Labrador Sea to the Bay of Biscay brought winds of 6 Bft at the most from different directions, but heavy shower activity.

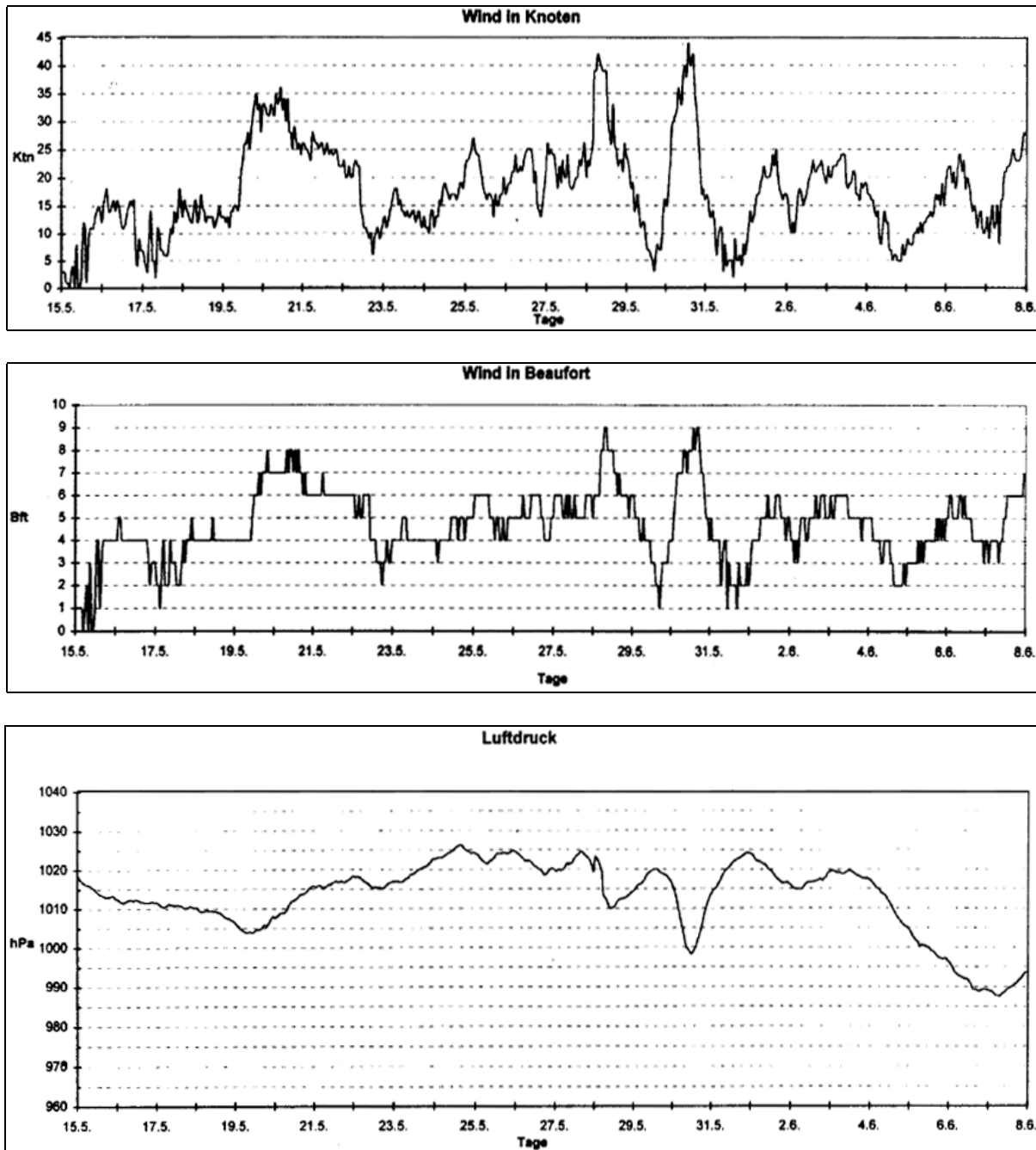


Fig. 59: Observations of wind and air pressure during Leg M39/2.

On June 17 a steady westerly air stream with sometimes high swell built up between the intensifying Azores anticyclone and a storm depression moving from Cape Farewell to the Hebrides. Westerly to northwesterly winds were mostly moderate to strong, only reaching 8 Bft on June 19. Thus conditions for the first mooring station on June 21 were rather favourable.

After passing 30° W METEOR reached the western slope of the Azores anticyclone with winds backing southwest and the air becoming warm and moist. With winds being southwesterly to southerly 6 Bft conditions were again favourable for the second mooring on June 23. On June 24 and 25 southerly winds were increasing to 7 Bft due to depressions connected with a 500mb trough stretching South from Newfoundland. Fog or drizzle was almost continuous.

With METEOR proceeding West and passing the trough line the air became clear on June 26 with light northwesterly winds increasing to 7 Bft on June 27. The final days of the cruise were determined by an almost stationary and weakening depression South of Newfoundland in the centre of which METEOR experienced light to moderate winds from variable and later north-easterly directions, accompanied by fog patches and later by widespread fog. METEOR docked in St. John's on July 2, 1997.

6.4 Meteorological conditions during leg M39/4 (G. Kahl)

When METEOR sailed from Saint John's, Nfld, on July 6, 1997, a trough trailing behind an occluded front had passed that city in the early morning hours. Moderate to strong westerly winds were blowing as the low of 1000 hPa slowly drifted southeast-wards from the Labrador coast and the ship went northward. Meanwhile, a high of 1020 hPa had formed over North Quebec, extending into the Labrador Sea by July 9, so that winds were light. However, a new low 1010 hPa had slowly formed over the New England States and moved northeast, reaching North Quebec with a central pressure of 1005 hPa on July 11. During these days the research vessel still enjoyed the presence of a wedge of high pressure 1020 hPa that extended northward from the high now 1030 hPa centered midway between Newfoundland and the Azores. The low, now of 1000 hPa moved to the south of Greenland on July 13 while moderate winds from easterly directions veering to westerlies later were experienced by METEOR returning from the vicinity of Southwestern Greenland by then. In the meantime, an area of low pressure west of Hudson Bay had elongated to the Gulf of St. Lawrence and had formed a low of 1000 hPa over the Strait of Belle Isle. Upon reaching open waters this low intensified to a complex gale 990 hPa east of Belle Isle and southeast of Cape Race. The METEOR approached her stopover destination St. Anthony from the north to northeast, thereby experiencing strong northeasterly winds but avoiding gales. During stopover time the following wedge of high pressure closed in to eliminate what little amount of clouds had been left over St. Anthony by the passage of the gale center. When METEOR put out to the Labrador Sea again another gale center had developed west of Hudson Bay and had moved to North Quebec, minimum central pressure being 990 hPa on July 17. Whereas central pressure filled somewhat, the area of strong southeasterlies extended out to the ships working area, easterly and southeasterly winds of 6 and 7 Bft being observed from July 18 to 20. Cyclonic activity on Canada's Eastern Seaboard did not cease after that date, but the ship was lucky to be in the

center of the low of 1000 hPa during July 21 to 22 when the low eventually filled and moved away northeastward. Light northwesterly winds gave way to light and variable conditions, and when METEOR visited Cape Farvel on July 25, it was calm for a few hours. The research vessel then headed south while a developing gale center made its way from the Grand Banks to the Irminger Sea, intensifying to 990 hPa while on its way. Another gale center was following closely, reaching a central pressure of under 990 hPa on July 28, too, on a position midway between Iceland and the Azores. METEOR was influenced only by moderate to strong northwesterly winds up to July 28. The gale center south of Iceland further developed into a storm center 975 hPa on July 29, the ship benefiting but shortly from the area of high pressure building to the southwest of the storm center which slowly filled thereafter. The research ship was influenced by a gale center that had developed over the region of the Great Lakes during July 26, being hardly discernible by that date but having reached a central pressure of under 990 hPa over North Quebec by July 28. The gale center then moved on to Southwestern Greenland, making its landfall with a central pressure of 980 hPa on July 30 just when METEOR visited the northern part of Flemish Cap. Southwesterly gales of 8 Bft were observed for several hours. These abated to moderate Southwesterlies when the ship headed east to reach 35 West by August 2. Another gale center 995 hPa had reached the Labrador coast and had moved quickly to southeastern Greenland, meanwhile further deepening by 5 hPa. The METEOR then headed north, Southwesterlies becoming strong almost immediately, lows crossing the North Atlantic quickly, developing into strong gale centers by the time they reached the vicinity of either Greenland or Iceland. After all, the Greenlandic Inland Ice Sheet and the East Greenland Current are a principal source of cold air masses in summer. West of Baffin Bay, a gale center 990 with a large diameter had developed. While it deepened further to 985 hPa, a secondary gale center 995 hPa developed over the northern part of Hudson Bay. This gale center, having intensified to 985 hPa, passed Hudson Strait during August 7 and moved east to southeast later to be centered west of Ireland when METEOR finished her cruise. The ship had made her way to Southeastern Greenland through strong westerlies caused by a low 1000 hPa there during August 6 and 7, then winds were light while they backed to east during the afternoon of August 8, and during the last days of her cruise the ship had to make her way to Reykjavik against strong easterlies.

6.5 Meteorological conditions during leg M39/5 (G. Kahl)

When METEOR left Reykjavik on schedule in the morning of 14.08.97, there were light southeasterly winds accompanying her out to sea. These resulted from a central low 1000 centered at 56 North 28 West. The Azores High 1027 was to be found just east of that archipelago. A secondary low 1005 which had originated somewhere along the U.S. east coast a few days earlier had made its way to the region east of Cape Race. However, winds backed to the northeast and were up to 6 Bft by 16.08. because the secondary low had become the major low of the northeastern North Atlantic by intensifying to 990 and moving up to the south coast of Iceland, the former central low now being relegated to a mere extension of the new gale center. A new low 1005 had passed Cape Race to lie northwest of the Azores, and another development was taking place over Nova Scotia.

Still another development had taken place during these few days. A low at the Labrador coast had moved up to the central part of the west Greenland coast and then it had been veering at the Polar Circle, eventually going southeast over the ice clad interior. A secondary low 1000 formed over The Irminger Sea, and this kept the METEOR from experiencing more than 5 Bft up to the 20.08. By then, the gale center south of Iceland had moved on to the Norwegian Sea and eventually to the Fram Strait, and the next low waiting in line had moved up from Newfoundland to 60 North 25 West, thereby deepening to 985.

Conditions deteriorated somewhat on 21.08. when central pressure in the gale center fell below 980 before it crossed Iceland on its way northward and began to fill. Northwesterly winds of 7 Bft were experienced for a few hours now but when the vessel approached the Greenland coast winds abated again to light northerly winds. For some time even the state of "light and variable" was reached, this being appreciated by scientific as well as ship's crew. At nightfall on 25.08. when Greenland was left behind winds were still light and visibility was of an order that is seldom observed in more southerly latitudes.

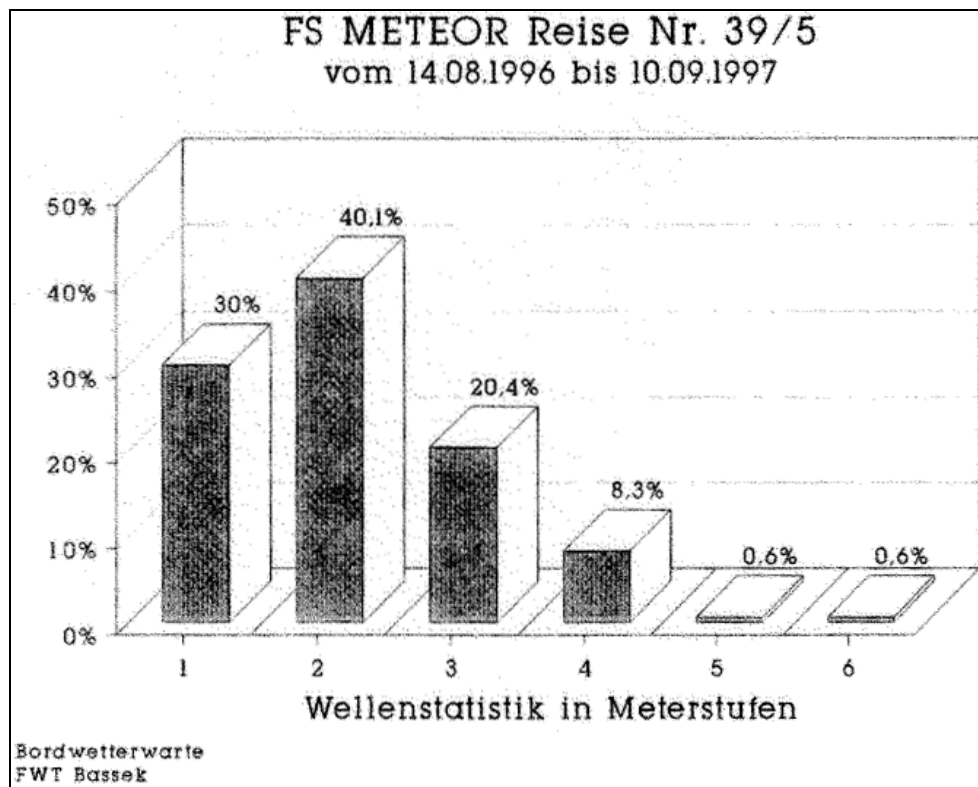
While the research vessel was on her way to the southeast, one of the lows migrating over the Atlantic at 40 to 45 North had slowed and intensified to a gale center 975 at northwestern Ireland on 27.08. This, too, moved on the Norwegian Sea and the Fram Strait so that METEOR was not bothered, the observed winds being northwesterlies about 4. During 31.08. a flat low that had moved from Labrador to our working area had seen some intensification to a central pressure of 1000 because of the cold air flowing out of the gale center passing Jan Mayen by then passed north of our position so that westerly winds of 6 Bft were observed, veering northwest and abating 4 Bft by the next day. Winds were up West 7 Bft by 03.09. to 04.09. because of a cold front originating from the last mentioned low having deepened to a gale center of 980.

On the whole, the General Circulation over the North Atlantic was weak as it should be according to the time of year, but some prominent features of the synoptic charts may be figured out:

1. Lows moving along the U.S. coast, passing the Azores and then going up to the Norwegian Sea,
2. Lows originating west of Hudson Bay, intensifying over North-Quebec to gale center strength and then moving east,
3. A few special developments like the low going up the western Greenland coast and then not continuing to Baffin Bay but choosing to go over the Inland Ice,
4. A quasi-permanent high over the region of the Great Lakes and Hudson Bay, and
5. The Azores High becoming a major feature of the synoptic Chart only during the latter part of the voyage.

Intensity of all Developments has risen during the time the voyage took. During the 03.09. the Azores High once again introduced itself to the synoptic chart at 48 North 40 West with a strength of 1025. By 07.09. this was up to 1040 at 50 North 22 West. Thereafter, it weakened but slowly and moved northeast, swinging east by 10.09. and visiting Germany one day later. The METEOR was near the core of the anticyclone, so that winds were light and variable during the last few days of probing the ocean. In other regions, however, intense gale centers reigned, the Norwegian Sea being especially hard hit by a low that became almost a storm

center 975 during 09.09., our research vessel being lucky to be left unmolested at least as far as the English Channel. Hamburg was reached by 14.09.1997. Some weather statistics of this leg are shown in Fig. 60.



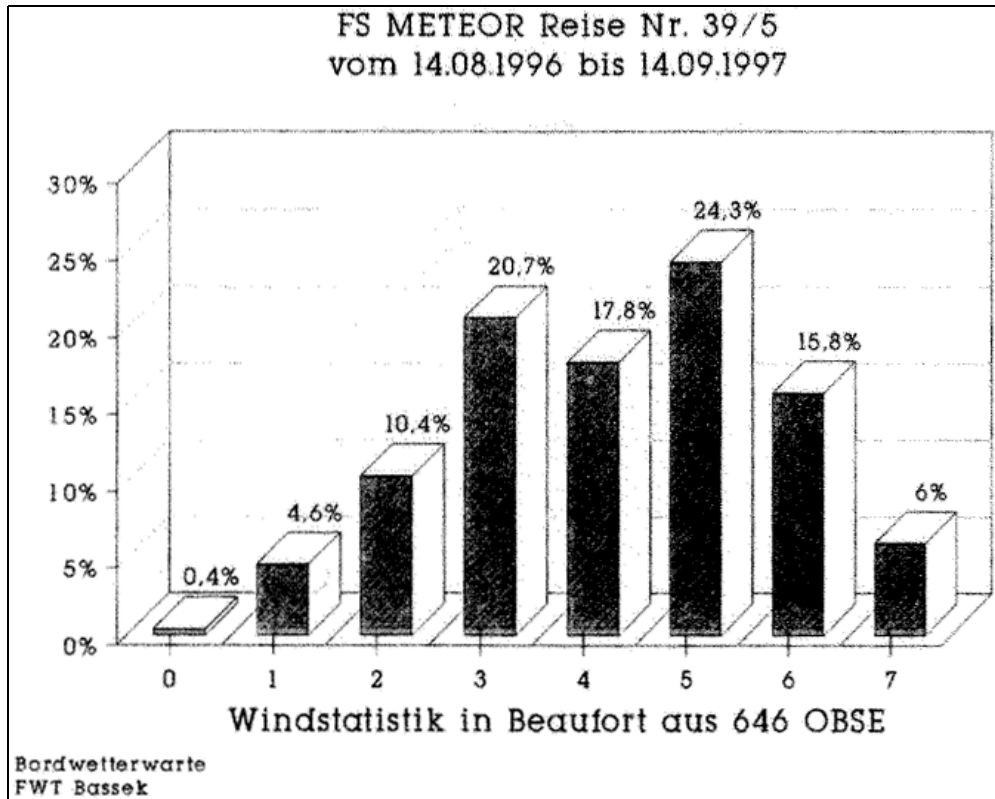


Fig. 60: Weather statistics during M39/5 for a) Wave statistics in meter steps and b) Wind statistics in Beaufort scale.

7 Lists

7.1 Leg M39/1

7.1.1 Locations for sediment and plankton/water samples

Geomar no.	Meteor no.	date	device	time (UTC)	latitude (N)	longitude (W)	water depth (m)	recovery (m)	remarks
M39001-1	121	20.04.1997	ROS/CTD	16:17	36°02.608	7°45.572	1145		Pinger at 30m,12/12 1156,1119,988,946,921,845, 797,677,576, 345,147,10
M39001-2	121	20.04.1997	GoFlo	18:53	36°02.491	7°45.606	1132		Water samples at:607,710,830,878,954,974,1022, 1052,1089, a test
M39001-3	121	20.04.1997	PN	18:30			1131		
M39001-4	121	20.04.1997	CTD	19:53	36°02.3	7°45.7	1131		CTD-Test
M39002-1	122	21.04.1997	BC	07:15	36°01.7	7°46.6	1208		Box washed out
M39002-2	122	21.04.1997	BC	08:12	36°01.7	7°46.5	1209	0.49	
M39002-3	122	21.04.1997	MUC	09:28	36°1.6	7°46.5	1205	0.38	1 tube empty
M39002-4	122	21.04.1997	PN	09:22					
M39002-5	122	21.04.1997	GC6	12:42	36°1.7	7°46.4	1205	4.7	
M39002-6	122	21.04.1997	GC12	12:05	36°1.6	7°46.4	1212	5.82	
M39002-7	122	21.04.1997	GoFlo	12:52	36°01.712	7°47.086	1214		Water samples at:231,452,500/F(S),601,774,811(S)
M39003-1	123	22.04.1997	BC	17:01	36°06.7	7°13.4	802	0.42	
M39003-2	123	22.04.1997	MUC	17:48	36°6.6	7°13.4	801	0.36-0.40	
M39003-3	123	22.04.1997	GC6	18:33	36°6.7	7°13.3	800	3.52	
M39003-4	123	22.04.1997	PN	17:15					
M39003-5	123	22.04.1997	GC12	19:26	36°6.6	7°13.3	798	0	Core bent
M39003-6	123	22.04.1997	ROS/CTD	20:41	36°6.8	7°14.1	803		Pinger at 30m,12/12 804,777,6,642,502, 401,5,303,1, 277,7,211,154,103,5,53,6,12,3
M39003-7	123	22.04.1997	GoFlo	22:26	36°6.6	7°14.0	824		Water samples at:79,181,330,429,524,664,784 (S)
M39004-1	124	23.04.1997	BC	21:01	36°14.2	7°43.9	966	0.46	
M39004-2	124	23.04.1997	MUC	21:53	36°14.2	7°43.8	968	0.40-0.44	
M39004-3	124	23.04.1997	GC6	22:49	36°14.3	7°43.8	968	5.75	
M39004-4	124	23.04.1997	GC12	23:52	36°14.2	7°43.9	968	0	Tube lost
M39004-5	124	24.04.1997	GC12	01:22	36°14.2	7°43.8	968	6.17	
M39005-1	125	24.04.1997	Grab	07:55	36°32.0	6°44.0	119	0.2-0.3	dark, olive-greyish silty finesand
M39005-2	125	24.04.1997	BC	08:33	36°32.1	6°44.1	118.3	0	not triggered
M39005-3	125	24.04.1997	BC	08:48	36°32.2	6°44.1	118	0.34	
M39006-1	126	24.04.1997	BC	09:45	36°30.7	6°46.4	214	0.34	
M39006-2	126	24.04.1997	PN	09:40					
M39007-1	127	24.04.1997	Grab	11:17	36°37.2	6°54.8	467		Finesand with abundant quartz and carbonate
M39007-2	128	24.04.1997	Grab	13:02	36°22.9	7°04.5	578		Clayish Silt with planktic Foraminifera

List of M39/1 site locations for sediment and plankton/water sampling.

Geomar no.	Meteor no.	date	device	time (UTC)	latitude (N)	longitude (W)	water depth (m)	recovery (m)	remarks
M39007-3	128	24.04.1997	GC6	13:33	36°23.0	7°04.4	579		
M39007-4	128	24.04.1997	GC8.5	14:30	36°22.8	7°04.3	577	5.77	
M39007-5	128	24.04.1997	BC	15:27	36°22.7	7°04.2	577	0.32	
M39008-5	129	24.04.1997	PN						
M39009-1	130	24.04.1997	BC	16:42	36°21.0	7°08.5	681	0.36	BC Sandstone with attached Hydrozoas, Ascidiae, Bryozoas, Porifera, Serpulidae, juvenile Pectinidae
M39010-1	130	24.04.1997	Grab	18:05	36°19.3	7°12.4	878		
M39010-2	131	24.04.1997	Grab	18:48	36°19.3	7°12.4	882		coarse sand with biogenic debris
M39011-1	132	24.04.1997	Grab	20:05	36°19.3	7°12.9	846		coarse sand w/ lithoclastic & biogenic material
M39012-1	133	24.04.1997	Grab	21:13	36°14.7	7°13.1	873		coarse sand w/ lithoclastic & biogenic material
M39013-1	134	24.04.1997	Dredge	22:28-22:59	36°19.2-36°19.2	7°12.4-7°12.7	871		boulder with sessile epifauna, seurchin
M39014-1	134	25.04.1997	Dredge	0:21-0:50	36°16.3-36°16.5	7°12.9-7°13.4	850		boulder with sessile epifauna, seurchin
M39014-2	134	25.04.1997	Dredge	1:52-2:25	36°16.2-36°16.3	7°12.8-7°13.3	847		sandstone pebbles, corals, compacted sand with biogenics
M39015-1	135	25.04.1997	ROS/CTD	05:14	36°14.240	7°43.832	970		Pinger at 30m, 12/12 373, 856, 792, 704, 622.3, 532, 448.5, 374, 203, 117, 64.3, 10.6
M39015-2	135	25.04.1997	GoFlo	07:22	36°14.2	7°43.8	967		Water samples at: 64, 374, 622, 702, 792, 856, 938(S)
M39015-3	135	25.04.1997	GC12	09:59	36°14.2	7°43.8	967	3.37	
M39016-1	136	26.04.1997	BC	14:54	36°46.7	7°42.2	581	0.33	
M39016-2	136	26.04.1997	MUC	15:37	36°46.7	7°42.1	581	0.20-0.22	4 empty liners
M39016-3	136	26.04.1997	GC6	16:08	36°46.7	7°42.2	581	2.44	
M39017-1	137	26.04.1997	ROS/CTD	20:54	36°39.0	7°24.7	527		Pinger at 30m, 12/12 529, 511, 487.5, 462, 410, 380.6, 302, 202, 138.6, 100.7, 60.6, 10.6
M39017-2	137	26.04.1997	GoFlo	22:18	36°39.0	7°24.5	533		Water samples at: 204, 304, 383, 412, 464, 490, 507
M39017-3	137	26.04.1997	GC6	23:00	36°39.0	7°24.5	533	4.1	
M39017-4	137	26.04.1997	MUC	23:42	36°38.9	7°24.6	532	0.18-0.21	5 empty liners
M39017-5	137	26.04.1997	BC	00:24	36°39.0	7°24.6	533	0.27	
M39017-6	137	26.04.1997	PN	23:32					
M39018-1	138	27.04.1997	BC	02:06	36°45.2	7°15.1	496	0.32	
M39018-2	138	27.04.1997	GC6	02:41	36°45.2	7°15.1	496	2.88	
M39019-1	139	27.04.1997	Grab	13:46	36°44.9	8°06.2	729		
M39019-2	139	27.04.1997	BC	14:22	36°44.9	8°06.1	730	0.16	
M39020-1	140	27.04.1997	BC	15:16	36°44.3	8°06.3	726	0.32	
M39020-2	140	27.04.1997	GC6	16:06-15:33-15:50	36°44.4	8°6.2	728	2	Core bent
M39020-3	140	27.04.1997	PN	15:50					

List of M39/1 site location sfor sediment and plankton/water sampling.

Geomar no.	Meteor no.	date	device	time (UTC)	latitude (N)	longitude (W)	water depth (m)	recovery (m)	remarks
M39021-1	141	28.04.1997	ROS/CTD	12:26	36°36.5	8°15.4	900		12/12 901,861,821,790,758,664,526,497,392,101,50/52,10/11
M39021-2	141	28.04.1997	GoFlo	13:44	36°36.5	8°15.3	900		Water samples at:860,875(S)
M39021-3	141	28.04.1997	Grab	14:44	36°36.5	8°15.4	903		middle sand, clay
M39021-4	141	28.04.1997	PN	14:25					
M39021-5	141	28.04.1997	BC	15:30	36°36.5	8°15.3	901	0.36	
M39022-1	142	28.04.1997	BC	17:02	36°42.7	8°15.6	668	0.36	
M39022-2	142	28.04.1997	PN	16:54					
M39022-3	142	28.04.1997	MUC	17:40	36°42.7	8°15.6	668	0.24-0.27	4 Tubes empty, not triggered
M39022-4	142	28.04.1997	GC6	18:20	36°42.7	8°15.6	668	2.66	
M39023-1	143	28.04.1997	Grab	19:41	36°44.1	8°15.3	728	full	silty middle sand, corals, brachiopods
M39023-2	143	28.04.1997	PN	19:23					
M39023-3	143	28.04.1997	BC	20:20	36°44.1	8°15.3	730	0.34	
M39024-1	144	29.04.1997	Grab	10:20	36°53.1	8°18.8	103		not closed
M39024-2	144	29.04.1997	Grab	10:31	36°52.9	8°18.8	106	full	clayish silt with endobenthic bivalves
M39024-3	144	29.04.1997	PN	10:20					
M39025-1	145	29.04.1997	Grab	11:26	36°48.2	8°18.7	272	full	clayish silt with endobenthic bivalves (Nucula)
M39025-2	145	29.04.1997	PN	11:22					
M39026-1	146	29.04.1997	Grab	12:09	36°47.7	8°19.1	308	full	clayish silt with Nucula
M39026-2	146	29.04.1997	PN						
M39027-1	147	29.04.1997	Grab	12:52	36°46.9	8°19.0	396		silty fine sand
M39027-2	147	29.04.1997	PN	12:41					
M39028-1	148	29.04.1997	Grab	13:37	36°46.2	8°18.9	545	not closed	
M39028-2	148	29.04.1997	PN	13:22					
M39028-3	148	29.04.1997	Grab	14:08	36°46.1	8°18.9	550	full	silty fine to middle sand, with Bivalves and Coralls pinger at 30m,12/12 1933,1710,1503,1326,1207,896,696,543,301,102,51,12
M39029-1	149	30.04.1997	CTD/ROS	12:53	36°2.6	8°13.8	1915		Water samples at:540,1320,1700,1890 (S)
M39029-2	149	30.04.1997	GoFlo	15:36	36°2.7	8°14.0	1914		
M39029-3	149	30.04.1997	BC	17:27	36°02.5	8°14.0	1917	0.36	
M39029-4	149	30.04.1997	GC6	18:39	36°2.5	8°14.0	1918	3.055	russian core device
M39029-5	149	30.04.1997	PN	19:00			1917		
M39029-6	149	30.04.1997	MUC	19:50	36°2.5	8°14.0	1919	0.31-0.45	
M39029-7	149	30.04.1997	GC6	21:05	36°2.5	8°13.8	1917	5.02	kiel core device
M39029-8	149	30.04.1997	GC9	22:54	36°2.5	8°13.8	1916	5.21	kiel core device
M39030-1	150	01.05.1997	Grab	09:08	37°13.5	9°12.7	159.8		carbonate fine sand to coarse sand
M39031-1	150*	01.05.1997	Grab	09:35	37°13.4	9°12.9	146.6	empty	
M39032-1	151	01.05.1997	Grab	10:08	37°12.9	9°13.5	310	not closed	
M39032-2	151	01.05.1997	Grab	10:24	37°13.0	9°13.5	193	not closed	
M39032-3	151	01.05.1997	Grab	10:43	37°12.9	9°13.5	322		silty middle to coarse sand

List of M39/1 site location sfor sediment and plankton/water sampling.

Geomar no.	Meteor no.	date	device	time (UTC)	latitude (N)	longitude (W)	water depth (m)	recovery (m)	remarks
M39033-1	152	01.05.1997	Grab	11:57	37°10.5	9°17.9	319	not closed	
M39033-2	152	01.05.1997	Grab	12:13	37°10.5	9°17.8	319	full	silty, carbonate sand
M39034-1	153	01.05.1997	Grab	12:56	37°10.9	9°17.4	197		carbonate sand
M39034-2	153	01.05.1997	Dredge	13:40	37°10.9-37°10.9	9°17.5-9°17.4	186		stones, sponge, echinodemes
M39034-3	153	01.05.1997	Drege	14:14	37°10.9	9°17.4	184		seurchins
M39035-1	154	02.05.1997	CTD/ROS	09:17	37°49.3	9°30.2	1086		pinger at 30m,12/12 1094,1005.6,928.7,856.6,679,633.3,605,354,201.6101.6,52.1,10.7
M39035-2	154	02.05.1997	GoFlo	10:52	37°49.3	9°30.2	1084		water samples at:352,601,630,675,923,1059(S)
M39035-3	154	02.05.1997	MUC	12:00	37°49.350	9°30.1	1085	0.18-0.44	
M39035-4	154	02.05.1997	PN	11:36					
M39036-1	155	02.05.1997	BC	14:07	37°48.3	9°41.0	1747	0.46	
M39036-2	155	02.05.1997	GC6	15:20	37°48.3	9°40.8	1746	5.71	
M39036-3	155	02.05.1997	PN	14:20					
M39036-4	155	02.05.1997	GC12	16:46	37°48.3	9°40.8	1745	7.17	
M39037-1	156	02.05.1997	GC12	20:18	37°48.5	9°59.77	2533	7	
M39037-2	156	02.05.1997	PN	19:51					
M39037-3	156	02.05.1997	BC	21:55	37°48.5	9°59.6	2532	0.29	
M39038-1	157	03.05.1997	Grab	03:37	37°44.7	9°28.1	508.8		silty carbonate middle to coarse sand
M39039-1	158	03.05.1997	Grab	05:16	37°44.3	9°30.8	1014	full	silty clay
M39040-1	159	03.05.1997	Grab	06:19	37°44.1	9°30.2	800		clayish silt
M39041-1	160	03.05.1997	Grab	07:18	37°43.9	9°29.6	660		silty carbonate sand
M39042-1	161	03.05.1997	Grab	08:06	37°43.7	9°29.2	568		middle sand
M39043-1	162	03.05.1997	Grab	08:54	37°43.4	9°28.5	424		mudpebbles,pebble with sessile organisms, ophiorae (Starfish)
M39043-2	162	03.05.1997	Grab	09:13	37°43.5	9°28.5	401		
M39044-1	163	03.05.1997	Grab	09:47	37°43.5	9°28.5	398		fine to middle sand with ophiorae
M39045-1	164	03.05.1997	Grab	10:33	37°43.7	9°27.6	470	not closed	
M39045-2		03.05.1997	Grab	10:54	37°43.7	9°27.6	470		
M39046-1	165	03.05.1997	Grab	11:50	37°44.1	9°26.3	740	not closed	
M39046-2	165	03.05.1997	Grab	12:25	37°44.0	9°26.3	716		
M39047-1	166	03.05.1997	Grab	14:39	37°33.8	9°11.1	451		glauconitic sand with benthic forams and bivalves
M39047-2	166	03.05.1997	PN	14:30					
M39048-1	167	03.05.1997	Grab	16:08	37°37.3	9°02.8	253		carbonate sand
M39048-2	167	03.05.1997	PN	16:03					
M39049-1	168	03.05.1997	Grab	18:48	37°42.9	8°50.5	51	not closed	
M39049-2	168	03.05.1997	PN	18:46					
M39049-3	168	03.05.1997	Grab	18:53	37°42.9	8°50.5	55	empty	

List of M39/1 site location sfor sediment and plankton/water sampling.

Geomar no.	Meteor no.	date	device	time (UTC)	latitude (N)	longitude (W)	water depth (m)	recovery (m)	remarks
M39049-4	168	03.05.1997	Grab	19:02	37°42.9	8°50.6	55		carbonate coarse sand with bivalves;pebbles with sessile epifauna
M39050-1	169	03.05.1997	Grab	19:38	37°42.1	8°52.5	93	empty	
M39050-2	169	03.05.1997	PN	19:34					
M39050-3	169	03.05.1997	Grab	19:49	37°42.1	8°52.6	93		carbonate coarse sand, pebbles with sessile epifauna
M39051-1	170	03.05.1997	Grab	20:30	37°40.7	8°55.1	127		middle sand with glauconitic
M39051-2	170	03.05.1997	PN	20:28					
M39052-1	171	03.05.1997	Grab	21:15	37°39.6	8°57.7	145.3		glauconitic middle to coarse sand
M39052-2	171	03.05.1997	PN	21:10					
M39053-1	172	03.05.1997	Grab	21:56	37°38.8	8°59.5	164		glauconitic middle to coarse sand
M39053-2	172	03.05.1997	PN	21:51					
M39054-1	173	03.05.1997	Grab	22:36	37°38.1	9°00.8	200		glauconitic middle to coarse sand
M39054-2	173	03.05.1997	PN	22:31					
M39055-1	174	04.05.1997	Grab	07:22	38°49.9	10°02.1	180		carbonate sand
M39056-1	175	04.05.1997	Grab	07:48	38°49.9	10°01.8	119		sponge
M39057-1	176	04.05.1997	Dredge	11:19	39°05.0	10°10.1	150(190)		boulders, pebbles with sessile epifauna, crinoids
M39058-1	177	04.05.1997	BC	16:50	39°02.4	10°40.8	1975	0.29	
M39058-2	177	04.05.1997	GC6	18:14	39°2.4	10°40.8	1974	3.2	
M39058-3	177	04.05.1997	PN	18:05					
M39059-1	178	04.05.1997	GC6	20:04	39°04.0	10°32.1	1605	0.95	
M39059-2	178	04.05.1997	BC	20:45	39°4.1	10°32.2	1605	0.18	
M39060-1	179	05.05.1997	BC	12:15	40°06.3	09°51.3	1166	0.3	
M39061-1	180	05.05.1997	BC	14:10	40°06.5	09°41.8	544	0.3	

7.1.2 Water sampling sites for plankton assemblage studies

Filter Nr.	Date	METEOR Station	GEOMAR Number	Latitude N	Longitude W	Water depth[m]	Water temp. [°C]	Salinity	Water filtered [l]
1	20/04/97	# 121	M39001-1	36°02,6	011°45,6	10	17.92	36.41	1
2						147	14.61	36.02	1.5
3						345	12.52	35.68	2
4						797	10.44	35.70	1.5
5						946	10.35	35.91	1.5
6						Sea floor at: 1176 m	1156	11.19	36.24
7	22/04/97	# 123	M39003-6	36°06,9	007°14,0	10	18	36.50	1.5
8						50	17	36.40	2
9						100	15.7	36.20	2
10						211	14.5	36.00	2
11						502	11.3	35.60	2
12						Sea floor at: 810 m	804	11.15	36.06
13	24/04/97	# 135	M39015-1	36°14,2	007°43,8	10	17.9	36.40	2
14						64	17.2	36.40	2
15						117	15.8	36.20	2
16						203	14.1	35.90	2
17						622	11.2	35.60	2
18						Sea floor at: 945 m	937	12.3	36.50
19	26/04/97	# 137	M39017-1	36°38,9	007°24,5	10	18.2	36.40	2
20						60	17.3	36.40	2
21						100	16.2	36.30	2
22						202	14.2	36.00	2
23						410	12.4	35.70	2
24						Sea floor at: 535 m	529	12.3	36.10
25	28/04/97	# 141	M39021-1	36°36,500	008°15,300	10	18.16	36.34	2
26						50	17.61	36.45	2
27						100	16.24	36.31	2
28						390	12.36	35.70	2
29						525	11.32	35.64	2
30						Sea floor at: 892 m	860	12.51	36.51
31	30/04/97	# 149	M39029-1	36°02,568	008°13,752	10	18.9	36.50	2
32						50	17.8	36.50	2
33						100	15.8	36.20	2
34						544	10.8	35.60	2
35						897	9.6	35.60	2
36						Sea floor at: 1950 m	1503	8	35.70

Filter Nr.	Date	METEOR Station	GEOMAR Number	Latitude N	Longitude W	Water depth[m]	Water temp. [°C]	Salinity	Water filtered [l]	
37	02/05/97	# 154	M39035-1	37°49,360	009°30,226	10	18.3	36.20	2	
38						50	16.6	36.20	2	
39						100	15.1	36.10	2	
40						354	12.6	35.70	2	
41						680	12.6	36.20	2	
42						Sea floor at: 1088 m	1005	12.6	36.30	2
43						06/05/97	# 184	M39065-1	40°34,768	010°20,962
44	50	14.57	35.91	2						
45	100	13.85	35.85	2						
46	400	11.47	35.58	2						
47	793	12.1	36.16	2						
48	Sea floor at: 3350 m	1186	11.33	36.20	2					
49	09/05/97	# 193	M39073-1	43°51,600	009°50,089					
50						50	14	35.70	1.5	
51						100	12.8	35.70	2	
52						457	11.2	35.50	2	
53						993	10.9	36.02	2	
54						Sea floor at: 3200 m	2041	3.79	34.97	2

7.1.3 Phyto- and zooplankton species found in M39/1 sampling sites

GEO MAR Number Species	M 39001	M 39002	M 39003	M 39006	M 39008	M 39017	M 39020	M 39021	M 39022	M 39023	M 39024	M 39025	M 39026	M 39027	M 39028	M 39029	M 39035	M 39037	M 39047	M 39048	M 39049	M 39050	M 39051	M 39052	M 39053	M 39054	M 39058	M 39065	M 39070	M 39073	M 39075	M 39076		
<i>Chaetoceros curvisetus</i>							x	x	x	x	x						x				x													
<i>C. tetrastichon</i> with <i>T. inquilinus</i>																												x						
<i>C. dadayii</i> with <i>T. inquilinus</i>																x		x																
<i>Chaetoceros</i> spp.				x	x	x	x	x	x	x	x	x	x	x	x	x	x	x	x	x	x	x	x	x	x	x	x	x	x	x	x	x		
<i>Rhizosolenia styliformis</i>					x		x	x			x	x	x	x	x		x			x	x	x				x	x	x	x	x				
<i>Rhizosolenia fragilissima</i>		x					x	x	x	x	x	x	x	x	x		x				x	x	x	x					x	x				
<i>Rhizosolenia indica</i>							x	x	x	x				x			x			x		x		x	x	x								
<i>Rhizosolenia stolterforthii</i>							x	x	x	x				x																				
<i>Rhizosolenia robusta</i>							x	x						x			x							x	x									
<i>Rhizosolenia hebetata</i> f. <i>semispina</i>																x	x				x	x	x	x	x	x								
<i>Proboscia alata</i>			x		x	x	x	x	x	x		x	x	x		x	x	x	x	x	x	x	x	x	x	x		x	x	x	x	x	x	
<i>Guinardia flaccida</i>								x	x	x							x			x		x		x					x				x	

Table 5, continued																																				
GEO	MAR Number	M 39001	M 39002	M 39003	M 39006	M 39008	M 39017	M 39020	M 39021	M 39022	M 39023	M 39024	M 39025	M 39026	M 39027	M 39028	M 39029	M 39035	M 39037	M 39047	M 39048	M 39049	M 39050	M 39051	M 39052	M 39053	M 39054	M 39058	M 39065	M 39070	M 39073	M 39075	M 39076			
Species																																				
<i>Bacteriastrum hyalinum</i>								X	X	X	X		X	X	X		X	X		X		X		X	X	X	X		X							
<i>Bacteriastrum delicatulum</i>																	X					X		X			X		X							
<i>Leptocyclus danicus</i>				X								X		X				X			X				X	X	X			X		X	X			
<i>Leptocyclus minimus</i>												X		X											X	X						X				
<i>Thalassiosira spp.</i>			X									X										X	X	X				X		X	X	X				
<i>Corethron hystrix</i>			X																																	
<i>Roperia tessellata</i>			X																				X													
<i>Coscinodiscus spp.</i>										X					X																			X		
<i>Odontella spp.</i>												X																					X	X		
<i>Stephanopyxis turris</i>																																		X		
<i>Ditylum brightwellii</i>																		X			X		X		X								X			
<i>Hemiaulus sinensis</i>			X	X	X	X	X	X		X			X	X			X	X	X	X	X	X	X	X	X	X	X	X	X							
<i>Skeletonema costatum</i>									X		X						X					X	X	X												
<i>Eucampia zodiacus</i>												X										X										X				
<i>Thalassionema nitzschioides</i>							X			X	X											X	X													
<i>Thalassiothrix longissima</i>											X													X						X						
<i>Gyrosigma spp.</i>											X																							X	X	
<i>Nitzschia closterium</i>																X		X					X		X		X									
<i>Nitzschia seriata group</i>			X				X	X	X	X	X		X	X			X				X	X	X	X	X	X	X	X	X		X	X	X	X		
<i>Asterionella glacialis</i>																						X														
<i>Pennales indet.</i>										X	X					X							X						X				X			
<i>Ceratium candelabrum</i>																		X												X						
<i>Ceratium cf. limulus</i>																																		X		
<i>Ceratium lineatum</i>			X	X		X	X														X			X							X	X	X			
<i>Ceratium furca</i>		X	X		X	X	X		X			X			X		X	X			X	X	X	X		X	X	X	X	X	X	X	X	X	X	
<i>Ceratium fusus</i>		X	X		X		X	X							X		X					X		X	X	X	X	X	X	X	X	X		X		
<i>Ceratium tripos</i>		X	X	X		X	X	X	X	X			X	X	X		X	X				X			X	X			X				X			
<i>Ceratium macroceros</i>		X			X		X						X				X	X			X	X	X	X	X	X	X	X	X	X	X	X	X	X		
<i>Dinophysis spp.</i>		X	X	X	X		X	X	X	X	X	X	X	X			X	X				X							X	X		X		X		
<i>Peridinium spp.</i>		X	X	X	X	X				X		X	X	X			X	X			X		X			X	X	X	X	X	X	X	X			
<i>Prorocentrum micans</i>				X			X	X	X	X		X	X									X	X		X	X										
<i>Actiniscus pentasterias</i>				X								X																								
<i>other Dinoflagellates</i>		X	X		X	X				X		X					X	X				X			X	X		X	X	X	X	X	X	X		
<i>Coccolithophores</i>		X	X	X		X	X			X			X					X				X										X	X	X	X	

Table 5, continued																																			
GEO																																			
MAR Number	M 39001	M 39002	M 39003	M 39006	M 39008	M 39017	M 39020	M 39021	M 39022	M 39023	M 39024	M 39025	M 39026	M 39027	M 39028	M 39029	M 39035	M 39037	M 39047	M 39048	M 39049	M 39050	M 39051	M 39052	M 39053	M 39054	M 39058	M 39065	M 39070	M 39073	M 39075	M 39076			
Species																																			
<i>Dictyocha fibula</i>			x	x			x			x										x									x	x					
<i>Distephanus speculum</i>						x				x							x			x	x	x	x		x						x	x	x		
<i>Tintinnus tuberculatus</i>					x					x		x	x			x	x	x	x	x				x				x							
<i>Amphorides quadrilineata</i>																														x	x			x	x
<i>Dadayiella bulbosa</i>			x		x	x						x					x		x	x	x	x	x	x	x	x	x		x						
<i>Dadayiella acutiformis</i>																						x													
<i>Dictyocysta spp.</i>																							x		x				x				x	x	
<i>Steenstrupiella steenstrupii</i>																																		x	
<i>Rhabdonella spp.</i>																			x	x	x												x	x	
<i>Parafavella sp</i>			x														x																		
<i>Xystonellopsis spp.</i>													x	x																					
<i>Epiplocyloides spp.</i>			x																																
Foraminifera, nonspinos	x				x															x	x	x													
Foraminifera, spinous	x	x			x	x	x	x	x	x							x								x	x					x	x		x	x
Larvae indet.	x	x	x	x	x	x		x	x	x	x	x				x	x	x					x		x				x	x	x	x			
Radiolarian							x									x																		x	

7.2 Leg M39/2
7.2.1 CTD Inventory

Stat	Prof	Date			Hour	Latitude	Longitude	Depth	Pmax
		YYYY	MM	DD					
199	1	1997	5	16	9.000	50.6133	-9.0631	127	104
200	2	1997	5	17	9.000	54.6656	-10.5825	342	324
201	3	1997	5	17	10.000	54.7373	-10.7316	1646	1662
201	4	1997	5	17	13.000	54.7372	-10.7184	1540	1554
202	5	1997	5	17	15.000	54.7998	-10.8638	1922	1942
203	6	1997	5	17	19.000	54.9009	-11.0960	2630	2632
204	7	1997	5	18	0.000	55.1429	-11.6393	2630	2796
205	8	1997	5	18	6.000	55.5772	-12.6013	2829	2838
206	9	1997	5	18	12.000	55.9998	-13.5626	2829	2552
207	10	1997	5	18	15.000	56.1419	-13.8858	2196	2192
208	11	1997	5	18	19.000	56.2832	-14.2142	1118	1106
209	12	1997	5	18	23.000	56.5619	-14.8277	200	174
210	13	1997	5	19	4.000	56.9964	-15.9990	1075	1056
211	14	1997	5	19	8.000	57.2823	-16.8920	1302	1276
212	15	1997	5	19	13.000	57.6181	-17.6186	1244	1228

Stat	Prof	Date			Hour	Latitude N	Longitude E	Depth m	Pmax dbar
		YYYY	MM	DD					
213	16	1997	5	19	17.000	57.9157	-18.5818	849	856
214	17	1997	5	19	22.000	58.2678	-19.5044	9999	1586
215	18	1997	5	20	4.000	58.6668	-20.6338	2909	2916
216	19	1997	5	20	11.000	59.0868	-21.8491	2408	2878
217	20	1997	5	20	17.000	59.4084	-22.8425	2516	2508
218	21	1997	5	20	22.000	59.7442	-23.8193	2636	2354
219	22	1997	5	21	4.000	60.0704	-24.7252	2287	2278
220	23	1997	5	21	13.000	60.3772	-25.6542	2287	2126
221	24	1997	5	21	16.000	60.5694	-26.2344	1927	1920
222	25	1997	5	21	20.000	60.7676	-26.8329	9999	1548
223	26	1997	5	22	0.000	60.9534	-27.3308	1364	1786
224	27	1997	5	22	3.000	61.1661	-27.9373	976	944
225	28	1997	5	22	14.000	59.6670	-29.8243	1088	1080
226	29	1997	5	22	20.000	59.2089	-28.5529	2054	2016
227	30	1997	5	23	2.000	58.7604	-27.2662	2054	2200
228	31	1997	5	23	9.000	58.2659	-26.0048	2569	2562
229	32	1997	5	23	16.000	57.7941	-24.7145	2812	2810
230	33	1997	5	23	23.000	57.3007	-23.4189	3052	3058
231	34	1997	5	24	6.000	56.8255	-22.1344	2295	2284
232	35	1997	5	24	14.000	56.2951	-20.8421	1563	1560
233	36	1997	5	25	0.000	56.0012	-23.3165	2345	2344
234	37	1997	5	25	11.000	55.6912	-25.7763	3311	3322
235	38	1997	5	25	21.000	55.4001	-27.9416	2804	2806
236	39	1997	5	26	6.000	55.1273	-30.2160	2804	2996
237	40	1997	5	26	14.000	54.9152	-31.6450	2617	2618
238	41	1997	5	26	19.000	54.7844	-32.5150	2632	2622
239	42	1997	5	27	0.000	54.6750	-33.3384	2458	2442
240	43	1997	5	27	6.000	54.5770	-34.1944	1749	1714
241	44	1997	5	27	9.000	54.5072	-34.7265	1499	1412
242	45	1997	5	27	19.000	54.2773	-32.8919	2707	2700
243	46	1997	5	28	0.000	54.3644	-33.5911	2647	2714
244	47	1997	5	28	7.000	54.0568	-32.3555	2831	2798
245	48	1997	5	28	16.000	53.5449	-31.0454	3174	3162
245	49	1997	5	28	19.000	53.5356	-31.0461	3178	3158
245	50	1997	5	28	21.000	53.5309	-31.0331	3175	3156
246	51	1997	5	29	3.000	53.2521	-30.3054	3066	3054
247	52	1997	5	29	12.000	52.9652	-29.5679	3389	3402
248	53	1997	5	29	20.000	52.4885	-28.4173	3779	3792
249	54	1997	5	31	4.000	53.8349	-31.7787	2848	2862
250	55	1997	5	31	22.000	53.2172	-35.1645	2749	2734
251	56	1997	6	1	2.000	52.8671	-34.9184	3335	3310
252	57	1997	6	1	6.000	52.7510	-35.0010	3152	3174
253	58	1997	6	1	9.000	52.6503	-34.9970	3412	3420
254	59	1997	6	1	14.000	52.3477	-35.0022	3856	3876

Stat	Prof	Date			Hour	Latitude	Longitude	Depth	Pmax
		YYYY	MM	DD		N	E	m	dbar
255	60	1997	6	1	18.000	52.0989	-35.0016	3324	3366
256	61	1997	6	2	1.000	51.3488	-34.9972	3300	3312
257	62	1997	6	2	8.000	51.4490	-33.4906	3868	3898
258	63	1997	6	2	16.000	51.6081	-32.0429	2981	3046
259	64	1997	6	3	1.000	51.7665	-30.3364	2300	2274
260	65	1997	6	3	5.000	51.7508	-30.0036	3238	3242
261	66	1997	6	3	9.000	51.8290	-29.5218	2243	2398
261	67	1997	6	3	11.000	51.8315	-29.5219	2358	2416
261	68	1997	6	3	13.000	51.8370	-29.5223	2358	2474
262	69	1997	6	3	18.000	52.0003	-28.9596	3755	3792
263	70	1997	6	4	0.000	52.3165	-28.1166	3770	3804
264	71	1997	6	4	9.000	52.9329	-26.5365	3704	3736
265	72	1997	6	4	20.000	51.7607	-24.7344	3929	3962
266	73	1997	6	5	14.000	51.0518	-20.5638	4307	4366
267	74	1997	6	5	23.000	50.7333	-18.6706	4723	4806
268	75	1997	6	5	10.000	50.4215	-16.7619	4745	4836
269	76	1997	6	5	18.000	50.5274	-15.5674	4264	4324
270	77	1997	6	6	23.000	50.6337	-14.8419	3221	3264
271	78	1997	6	7	4.000	50.7176	-14.2003	1010	1002
272	79	1997	6	7	13.000	50.9880	-12.0890	1800	1812

7.2.2 Mooring Activities

Sta. No.	Int. No.	IfM No.	Date 1997	Latitude North	Longitude West	Depth (m)	Instr. Type	Remarks incl. nominal instr. depth
<u>Current Meter Moorings</u>								
246	IM3	V388	29 May	53°14.6'N	030°16.0'W	3087	SoSo	No.23,Win.01:30Z @1407m
							ACM	No.10078@1357m
							ACM	No. 8412@2207m
							ACM	No. 9819@2507m
							ACM	No. 6159@2757m
							ACM	No. 8575@3037m
242		V386	27 May	54°17.1'N	032°57.0'W	2723	ACM	No.12051@1213m
							ACM	No. 9812@2063m
							ACM	No. 7929@2363m
							ACM	No. 7927@2673m
249		V387	31 May	53°50.2'N	031°43.6'W	2858	ACM	No.10074@1310m
							ACM	No. 9311@2258m
							ACM	No. 4570@2558m
							ACM	No. 4563@2808m

<u>Sound Source Moorings</u>								
219	IM1	V384	21 May	60°04.3'N	024°43.5'W	2281	SoSo	No. 24, Win 01:00Z @1381m
							ACM	No. 9346@1331m
							Wdog	ARGOS 2263
231	IM2	V385	24 May	56°48.7'N	022°08.0'W	2307	SoSo	No22, Win 00:30Z @1447m
								no ac. release
			(see Fig. B3)				Wdog	ARGOSS 2264
	IM3		-- see above --					

SoSo Sound source
Win window
ACM Aanderaa Current Meter
Wdog Watch Dog buoy

7.2.3 List of RAFOS Float Launches

Sta. No.	IfM No.	Date 1997	Time Z	Latitude North	Longitude West	ARGOS (DEC)	Mission (months)	Remarks
<u>RAFOS floats</u>								
203	403	17/5	22:05	54°53.9'N	011°05.8'W	12611	12	Eastern boundary Rockall Tr.
207	408	18/5	18:05	56°08.6'N	013°53.8'W	12617	18	Western boundary
215	405	20/5	07:07	58°40.4'N	020°38.4'W	12613	15	Maury Channel North
217	411	20/5	19:17	59°24.6'N	022°49.3'W	12620	24	Central Iceland Basin
220	407	21/5	14:56	60°22.8'N	025°39.4'W	12616	18	Reykjanes Ridge North
227	406	23/5	04:44	58°45.7'N	027°13.8'W	12614	15	Reykjanes Ridge South
229	404	23/5	18:32	57°47.7'N	024°42.4'W	12612	12	Central Iceland Basin
231	409	24/5	09:47	56°48.4'N	022°08.3'W	12618	21	Rockall Plateau West
234	410	25/5	13:39	55°41.5'N	025°45.8'W	12619	21	Maury Channel
245	401	29/5	00:46	53°31.9'N	031°01.6'W	4374	14	1 st float park (North)
261	402B	3/6	15:41	51°50.7'N	029°32.0'W	4375	24	2 nd float park (South)
<u>Dual Release RAFOS floats deployed by CTD probe ('Ofenrohr') (see Fig. B4)</u>								
245	412	28/5	18:07	53°32.3'N	031°02.6'W	4376	2+12	1 st float park (North)
245	413	28/5	20:38	53°31.9'N	031°02.2'W	4377	4+10	1 st float park (North)
245	414	28/5	23:14	53°32.0'N	031°01.9'W	12615	6+8	1 st float park (North)
261	415	3/6	10:28	51°50.1'N	029°31.4'W	5487	3+21	2 nd float park (South)
261	416	3/6	12:31	51°50.2'N	029°31.4'W	12610	6+18	2 nd float park (South)
261	417	3/6	14:31	51°50.3'N	029°31.6'W	12621	9+15	2 nd float park (South)

7.3 Leg M39/3
7.3.1 Station list of cruise M39/3

A2 R/V METEOR CURISE 039 leg 3 Version 1.1 February 1998; 03.03.98 Update

SHIP/CRS	WOCE	STNBR	CAST	UTC	POSITION	UNC	HT ABOVE	WIRE	MAX	NO. OF					
EXPCODE	SECT	CSTNO	TYPE	DATE	TIME	CODE	LATITUDE	LONGITUDE	NAV	DEPTH	BOTTOM	OUT	PRESS	BOTTLES	COMMENTS
06MT039/3	A2	274	01	ROS	061397	0929	BE	48 55.3 N	13 16.3 W	GPS	3719				
06MT039/3	A2	274	01	ROS	061397	1044	BO	48 55.6 N	13 16.8 W	GPS	3719	09	3731	3500	22
06MT039/3	A2	274	01	ROS	061397	1207	EN	48 55.6 N	13 17.3 W	GPS	3719				
06MT039/3	A2	275	02	ROS	061397	1416	BE	49 00.1 N	13 02.5 W	GPS	3124				
06MT039/3	A2	275	02	ROS	061397	1513	BO	49 00.2 N	13 02.5 W	GPS	3124	10	3107	3149	22
06MT039/3	A2	275	02	ROS	061397	1627	EN	49 00.3 N	13 02.5 W	GPS	3124				
06MT039/3	A2	276	01	ROS	061397	1753	BE	49 00.0 N	12 58.9 W	GPS	2570				
06MT039/3	A2	276	01	ROS	061397	1843	BO	49 00.1 N	12 58.9 W	GPS	2570	07	2565	2598	22
06MT039/3	A2	276	01	ROS	061397	1952	EN	49 00.0 N	12 59.4 W	GPS	2570				
06MT039/3	A2	277	01	ROS	061397	2149	BE	49 00.9 N	12 51.4 W	GPS	2019				
06MT039/3	A2	277	01	ROS	061397	2231	BO	49 00.9 N	12 51.6 W	GPS	2019	09	2004	2020	21
06MT039/3	A2	277	01	ROS	061397	2337	EN	49 01.1 N	12 52.2 W	GPS	2019				
06MT039/3	A2	278	01	ROS	061497	0111	BE	49 03.1 N	12 41.5 W	GPS	1509				
06MT039/3	A2	278	01	ROS	061497	0142	BO	49 03.1 N	12 41.7 W	GPS	1509	11	1489	1450	17
06MT039/3	A2	278	01	ROS	061497	0228	EN	49 03.1 N	12 41.9 W	GPS	1509				
06MT039/3	A2	279	01	ROS	061497	0436	BE	49 06.6 N	12 12.0 W	GPS	1013				
06MT039/3	A2	279	01	ROS	061497	0502	BO	49 06.6 N	12 12.1 W	GPS	1013	10	1004	0999	13
06MT039/3	A2	279	01	ROS	061497	0536	EN	49 06.7 N	12 12.5 W	GPS	1013				
06MT039/3	A2	280	01	ROS	061497	0847	BE	49 11.0 N	11 26.2 W	GPS	495				
06MT039/3	A2	280	01	ROS	061497	0900	BO	49 11.2 N	11 26.2 W	GPS	495	10	482	0469	8
06MT039/3	A2	280	01	ROS	061497	0923	EN	49 11.2 N	11 26.3 W	GPS	495				
06MT039/3	A2	281	01	ROS	061497	1036	BE	49 11.9 N	11 11.0 W	GPS	200				
06MT039/3	A2	281	01	ROS	061497	1046	BO	49 11.9 N	11 10.9 W	GPS	200	09	185	0177	5
06MT039/3	A2	281	01	ROS	061497	1104	EN	49 12.1 N	11 10.8 W	GPS	200				
06MT039/3	A2	282	01	ROS	061497	1329	BE	49 13.9 N	10 38.9 W	GPS	160				
06MT039/3	A2	282	01	ROS	061497	1338	BO	49 13.9 N	10 38.9 W	GPS	160	09	147	0150	7
06MT039/3	A2	282	01	ROS	061497	1354	EN	49 13.9 N	10 38.8 W	GPS	160				
06MT039/3	A2	283	01	ROS	061597	2315	BE	48 55.3 N	13 16.4 W	GPS	3729				
06MT039/3	A2	283	01	ROS	061697	0020	BO	48 55.5 N	13 16.2 W	GPS	3729	09	3735	3770	22
06MT039/3	A2	283	01	ROS	061697	0151	EN	48 55.9 N	13 15.9 W	GPS	3729				
06MT039/3	A2	283	02	ROS	061597	0219	BE	48 55.9 N	13 15.9 W	GPS	3723				
06MT039/3	A2	283	02	ROS	061597	0319	BO	48 55.8 N	13 15.9 W	GPS	3723	09	3564	3499	36
06MT039/3	A2	283	02	ROS	061597	0551	EN	48 55.9 N	13 15.2 W	GPS	3723				

06MT039/3	A2	284	01	ROS	061597	0734	BE	48 51.4 N	13 48.2 W	GPS	4515				
06MT039/3	A2	284	01	ROS	061597	0856	BO	48 51.5 N	13 47.9 W	GPS	4515	10	4527	4601	22
06MT039/3	A2	284	01	ROS	061597	1052	EN	48 51.8 N	13 47.7 W	GPS	4515				
06MT039/3	A2	285	01	ROS	061597	1428	BE	48 44.5 N	14 44.1 W	GPS	4717				
06MT039/3	A2	285	01	ROS	061597	1601	BO	48 44.4 N	14 44.0 W	GPS	4717	20	4730	4784	21
06MT039/3	A2	285	01	ROS	061597	1750	EN	48 44.4 N	14 43.7 W	GPS	4717				
06MT039/3	A2	286	01	ROS	061597	2059	BE	48 36.4 N	15 28.7 W	GPS	4802				
06MT039/3	A2	286	01	ROS	061597	2229	BO	48 36.4 N	15 29.1 W	GPS	4802	17	4814	4858	21
06MT039/3	A2	286	01	ROS	061597	0031	EN	48 36.8 N	15 29.6 W	GPS	4802				
06MT039/3	A2	287	01	ROS	061697	0445	BE	48 27.1 N	16 34.9 W	GPS	4818				
06MT039/3	A2	287	01	ROS	061697	0618	BO	48 27.0 N	16 34.8 W	GPS	4818		4842	4894	22
06MT039/3	A2	287	01	ROS	061697	0810	EN	48 26.8 N	16 34.9 W	GPS	4818				
06MT039/3	A2	288	01	ROS	061697	1616	BE	48 18.0 N	17 40.9 W	GPS	4016				
06MT039/3	A2	288	01	ROS	061697	1727	BO	48 18.2 N	17 41.3 W	GPS	4016		4016	4043	19
06MT039/3	A2	288	01	ROS	061697	1858	EN	48 18.3 N	17 41.7 W	GPS	4016				
06MT039/3	A2	289	02	ROS	061797	0221	BE	48 09.8 N	18 40.1 W	GPS	4395				
06MT039/3	A2	289	02	ROS	061797	0342	BO	48 09.8 N	18 40.3 W	GPS	4395		4419	4470	20
06MT039/3	A2	289	02	ROS	061797	0525	EN	48 09.8 N	18 40.6 W	GPS	4395				
06MT039/3	A2	290	01	ROS	061797	0956	BE	48 01.8 N	19 39.4 W	GPS	4471				
06MT039/3	A2	290	01	ROS	061797	1121	BO	48 01.8 N	19 36.7 W	GPS	4471	20	4476	4513	21
06MT039/3	A2	290	01	ROS	061797	1310	EN	48 01.8 N	19 40.0 W	GPS	4471				
06MT039/3	A2	291	01	ROS	061797	1837	BE	47 53.6 N	20 39.2 W	GPS	4343				
06MT039/3	A2	291	01	ROS	061797	1956	BO	47 53.6 N	20 39.7 W	GPS	4343	09	4362	4417	35
06MT039/3	A2	291	01	ROS	061797	2142	EN	47 53.2 N	20 40.0 W	GPS	4343				
06MT039/3	A2	291	02	ROS	061797	2223	BE	47 53.1 N	20 39.7 W	GPS	4333				
06MT039/3	A2	291	02	ROS	061797	2242	BO	47 53.0 N	20 39.7 W	GPS	4333	09	993	0899	12
06MT039/3	A2	291	02	ROS	061797	2312	EN	47 53.0 N	20 40.0 W	GPS	4333				
06MT039/3	A2	292	02	ROS	061897	0639	BE	47 45.9 N	21 37.8 W	GPS	4114				
06MT039/3	A2	292	02	ROS	061897	0752	BO	47 45.9 N	21 38.1 W	GPS	4114		4122	4159	22
06MT039/3	A2	292	02	ROS	061897	0924	EN	47 45.7 N	21 37.9 W	GPS	4114				
06MT039/3	A2	293	02	ROS	061897	1342	BE	47 37.6 N	22 36.0 W	GPS	4070				
06MT039/3	A2	293	02	ROS	061897	1459	BO	47 37.6 N	22 36.3 W	GPS	4070		4075	4110	22
06MT039/3	A2	293	02	ROS	061897	1638	EN	47 37.6 N	22 36.3 W	GPS	4070				
06MT039/3	A2	293	03	ROS	061897	1642	BE	47 37.4 N	22 36.3 W	GPS	4011				
06MT039/3	A2	293	03	ROS	061897	1659	BO	47 37.4 N	22 36.3 W	GPS	4011		995	0900	12
06MT039/3	A2	293	03	ROS	061897	1727	EN	47 37.2 N	22 36.4 W	GPS	4011				
06MT039/3	A2	294	02	ROS	061897	1956	BE	47 33.8 N	23 05.3 W	GPS	4224				
06MT039/3	A2	294	02	ROS	061897	2110	BO	47 33.7 N	23 05.4 W	GPS	4224		4220	4266	22
06MT039/3	A2	294	02	ROS	061897	2255	EN	47 37.6 N	23 05.5 W	GPS	4224				

06MT039/3	A2	294	03	ROS	061897	2304	BE	47 33.7 N	23 05.4 W	GPS	4234				
06MT039/3	A2	294	03	ROS	061897	2326	BO	47 33.7 N	23 05.5 W	GPS	4234	994	0874	12	
06MT039/3	A2	294	03	ROS	061897	2355	EN	47 33.6 N	23 05.5 W	GPS	4234				
06MT039/3	A2	295	01	ROS	061997	0217	BE	47 29.6 N	23 33.5 W	GPS	3988				
06MT039/3	A2	295	01	ROS	061997	0329	BO	47 29.4 N	23 33.0 W	GPS	3988	3987	4019	22	
06MT039/3	A2	295	01	ROS	061997	0508	EN	47 29.4 N	23 34.5 W	GPS	3988				
06MT039/3	A2	296	01	ROS	061997	0837	BE	47 23.0 N	24 15.9 W	GPS	3327				
06MT039/3	A2	296	01	ROS	061997	0939	BO	47 22.9 N	24 16.0 W	GPS	3327	20	3312	3320	21
06MT039/3	A2	296	01	ROS	061997	1107	EN	47 22.9 N	24 16.1 W	GPS	3327				
06MT039/3	A2	297	01	ROS	061997	1516	BE	47 16.9 N	25 00.6 W	GPS	3040				
06MT039/3	A2	297	01	ROS	061997	1613	BO	47 16.8 N	25 00.6 W	GPS	3040	3045	3046	22	
06MT039/3	A2	297	01	ROS	061997	1732	EN	47 16.1 N	25 02.1 W	GPS	3040				
06MT039/3	A2	298	01	ROS	061997	2125	BE	47 10.7 N	25 43.2 W	GPS	2977				
06MT039/3	A2	298	01	ROS	061997	2225	BO	47 10.6 N	25 43.4 W	GPS	2977	3013	2972	22	
06MT039/3	A2	298	01	ROS	061997	2345	EN	47 10.5 N	25 43.8 W	GPS	2977				
06MT039/3	A2	298	05	ROS	062097	0020	BE	47 10.5 N	25 43.6 W	GPS	3058				
06MT039/3	A2	298	05	ROS	062097	0117	BO	47 10.4 N	25 44.2 W	GPS	3058	13	3041	3066	24
06MT039/3	A2	298	05	ROS	062097	0233	EN	47 10.2 N	25 45.2 W	GPS	3058				
06MT039/3	A2	299	01	ROS	062097	0533	BE	47 06.4 N	26 17.1 W	GPS	2519				
06MT039/3	A2	299	01	ROS	062097	0621	BO	47 06.3 N	26 17.4 W	GPS	2519	2410	2404	22	
06MT039/3	A2	299	01	ROS	062097	0729	EN	47 06.2 N	26 17.9 W	GPS	2519				
06MT039/3	A2	300	01	ROS	062097	0941	BE	47 03.2 N	26 39.6 W	GPS	2802				
06MT039/3	A2	300	01	ROS	062097	1035	BO	47 03.0 N	26 39.9 W	GPS	2802	20	2782	2800	22
06MT039/3	A2	300	01	ROS	062097	1150	EN	47 02.9 N	26 40.4 W	GPS	2802				
06MT039/3	A2	301	01	ROS	062097	1329	BE	46 59.0 N	26 59.5 W	GPS	2178				
06MT039/3	A2	301	01	ROS	062097	1412	BO	46 58.9 N	26 59.6 W	GPS	2178	2162	2170	22	
06MT039/3	A2	301	01	ROS	062097	1519	EN	46 59.0 N	26 59.9 W	GPS	2178				
06MT039/3	A2	302	01	ROS	062097	1658	BE	46 54.7 N	27 18.3 W	GPS	3487				
06MT039/3	A2	302	01	ROS	062097	1801	BO	46 54.8 N	27 18.3 W	GPS	3487	3517	3541	22	
06MT039/3	A2	302	01	ROS	062097	1926	EN	46 54.7 N	27 18.3 W	GPS	3487				
06MT039/3	A2	302	02	FLT	062097	2042	EN	46 54.4 N	27 18.3 W	GPS	3487	ALACE	719	FLOAT	
06MT039/3	A2	302	02	ROS	062097	1923	BE	46 54.7 N	27 18.3 W	GPS	3501				
06MT039/3	A2	302	02	ROS	062097	1952	BO	46 54.7 N	27 18.4 W	GPS	3501	1011	0999	12	
06MT039/3	A2	302	02	ROS	062097	2023	EN	46 54.7 N	27 18.4 W	GPS	3501				
06MT039/3	A2	303	01	ROS	062197	0109	BE	46 43.5 N	28 15.9 W	GPS	3398				
06MT039/3	A2	303	01	ROS	062197	0218	BO	46 43.6 N	28 15.8 W	GPS	3398	3381	3407	22	
06MT039/3	A2	303	01	ROS	062197	0346	EN	46 43.6 N	28 15.8 W	GPS	3398				
06MT039/3	A2	304	01	ROS	062197	0812	BE	46 32.5 N	29 08.8 W	GPS	2995				
06MT039/3	A2	304	01	ROS	062197	0910	BO	46 32.6 N	29 08.7 W	GPS	2995	20	2953	2969	22

06MT039/3	A2	304	01	ROS	062197	1029	EN	46 32.4 N	29 08.5 W	GPS	2995				
06MT039/3	A2	304	02	FLT	062197	1039	EN	46 32.4 N	29 08.4 W	GPS	2995				ALACE 720 FLOAT
06MT039/3	A2	305	00	MOR	062297	1426	BE	46 19.8 N	29 55.3 W	GPS	3308				Recovery of MOORING K1/96
06MT039/3	A2	305	00	MOR	062297	2235	EN	46 21.3 N	29 55.9 W	GPS	3308				New MOORING K1/97
06MT039/3	A2	305	01	ROS	062297	2310	BE	46 19.9 N	29 55.8 W	GPS	3296				
06MT039/3	A2	305	01	ROS	062397	0011	BO	46 19.8 N	29 55.8 W	GPS	3296	19	3268	3305	21
06MT039/3	A2	305	01	ROS	062397	0128	EN	46 19.7 N	29 55.8 W	GPS	3296				
06MT039/3	A2	306	01	ROS	062297	0528	BE	46 05.0 N	30 46.4 W	GPS	3277				
06MT039/3	A2	306	01	ROS	062297	0624	BO	46 04.9 N	30 46.5 W	GPS	3277	09	3266	3300	22
06MT039/3	A2	306	01	ROS	062297	0742	EN	46 04.9 N	30 46.7 W	GPS	3277				
06MT039/3	A2	307	01	ROS	062297	1134	BE	45 50.1 N	31 36.8 W	GPS	3651				
06MT039/3	A2	307	01	ROS	062297	1245	BO	45 50.1 N	31 36.8 W	GPS	3651	19	3637	3682	22
06MT039/3	A2	307	01	ROS	062297	1410	EN	45 49.8 N	31 36.6 W	GPS	3651				
06MT039/3	A2	307	02	FLT	062297	1414	EN	45 49.5 N	31 37.7 W	GPS	3651				ALACE 718 FLOAT
06MT039/3	A2	308	01	ROS	062297	1802	BE	45 35.3 N	31 26.7 W	GPS	3772				
06MT039/3	A2	308	01	ROS	062297	1908	BO	45 35.0 N	31 26.6 W	GPS	3772	09	3782	3800	21
06MT039/3	A2	308	01	ROS	062297	2033	EN	45 34.4 N	31 26.2 W	GPS	3772				
06MT039/3	A2	309	01	ROS	062397	0015	BE	45 19.2 N	33 12.7 W	GPS	3653				
06MT039/3	A2	309	01	ROS	062397	0121	BO	45 18.9 N	33 12.2 W	GPS	3653	11	3663	3704	22
06MT039/3	A2	309	01	ROS	062397	0245	EN	45 18.7 N	33 11.9 W	GPS	3653				
06MT039/3	A2	309	02	MOR	062397	0621	BE	45 19.8 N	33 12.6 W	GPS	3653				Recovery of MOORING K3/96
06MT039/3	A2	309	02	MOR	062397	1434	EN	45 19.3 N	33 09.1 W	GPS	3567				New MOORING K3/97
06MT039/3	A2	310	01	ROS	062397	1935	BE	45 07.2 N	34 04.8 W	GPS	3619				
06MT039/3	A2	310	01	ROS	062397	2040	BO	45 07.1 N	34 04.8 W	GPS	3619	09	3625	3669	21
06MT039/3	A2	310	01	ROS	062397	2206	EN	45 07.2 N	34 04.4 W	GPS	3619				
06MT039/3	A2	311	01	ROS	062497	0153	BE	44 55.6 N	34 45.7 W	GPS	4068				
06MT039/3	A2	311	01	ROS	062497	0308	BO	44 55.4 N	34 45.4 W	GPS	4068	11	4080	4132	22
06MT039/3	A2	311	01	ROS	062497	0437	EN	44 55.2 N	34 45.3 W	GPS	4068				
06MT039/3	A2	312	01	ROS	062497	0759	BE	44 45.1 N	35 24.6 W	GPS	3953				
06MT039/3	A2	312	01	ROS	062497	0911	BO	44 45.1 N	35 24.6 W	GPS	3953	10	3965	4014	22
06MT039/3	A2	312	01	ROS	062497	1046	EN	44 44.9 N	35 24.7 W	GPS	3953				
06MT039/3	A2	313	01	ROS	062497	1403	BE	44 34.0 N	36 05.0 W	GPS	4078				
06MT039/3	A2	313	01	ROS	062497	1518	BO	44 33.7 N	36 05.2 W	GPS	4078	09	4110	4158	22
06MT039/3	A2	313	01	ROS	062497	1648	EN	44 33.6 N	36 05.1 W	GPS	4078				
06MT039/3	A2	314	01	ROS	062497	2043	BE	44 20.0 N	36 54.5 W	GPS	4233				
06MT039/3	A2	314	01	ROS	062497	2200	BO	44 19.9 N	36 54.5 W	GPS	4233	09	4255	4312	22
06MT039/3	A2	314	01	ROS	062497	2339	EN	44 19.9 N	36 54.5 W	GPS	4233				
06MT039/3	A2	315	01	ROS	062597	0337	BE	44 05.8 N	37 43.6 W	GPS	4140				
06MT039/3	A2	315	01	ROS	062597	0450	BO	44 05.6 N	37 43.6 W	GPS	4140	11	4136	4190	22

06MT039/3	A2	315	01	ROS	062597	0618	EN	44 05.3 N	37 43.7 W	GPS	4140				
06MT039/3	A2	316	01	ROS	062597	1034	BE	43 52.0 N	38 32.8 W	GPS	4044				
06MT039/3	A2	316	01	ROS	062597	1150	BO	43 51.9 N	38 32.6 W	GPS	4044	11	4048	4082	22
06MT039/3	A2	316	01	ROS	062597	1327	EN	43 51.6 N	38 32.5 W	GPS	4044				
06MT039/3	A2	316	02	ROS	062597	1342	BE	43 51.7 N	38 32.5 W	GPS	4036				
06MT039/3	A2	316	02	ROS	062597	1416	BO	43 51.6 N	38 32.4 W	GPS	4036		1991	1999	10
06MT039/3	A2	316	02	ROS	062597	1506	EN	43 51.8 N	38 32.3 W	GPS	4036				
06MT039/3	A2	317	01	ROS	062597	2001	BE	43 38.1 N	39 21.6 W	GPS	4658				
06MT039/3	A2	317	01	ROS	062597	2024	BO	43 37.9 N	39 21.3 W	GPS	4658		1188	1200	12
06MT039/3	A2	317	01	ROS	062597	2102	EN	43 37.6 N	39 20.8 W	GPS	4658				
06MT039/3	A2	317	02	ROS	062597	2106	BE	43 37.4 N	39 20.6 W	GPS	4602				
06MT039/3	A2	317	02	ROS	062597	2238	BO	43 36.2 N	39 19.8 W	GPS	4602	08	4816	4726	22
06MT039/3	A2	317	02	ROS	062697	0024	EN	43 35.0 N	39 19.6 W	GPS	4602				
06MT039/3	A2	318	01	ROS	062697	0431	BE	43 24.2 N	40 10.2 W	GPS	4780				
06MT039/3	A2	318	01	ROS	062697	0453	BO	43 24.3 N	40 10.7 W	GPS	4780	10	1188	1199	12
06MT039/3	A2	318	01	ROS	062697	0530	EN	43 24.5 N	40 10.9 W	GPS	4780				
06MT039/3	A2	318	02	ROS	062697	0536	BE	43 24.5 N	40 10.9 W	GPS	4779				
06MT039/3	A2	318	02	ROS	062697	0638	BO	43 24.7 N	40 10.5 W	GPS	4779	08	4829	4887	22
06MT039/3	A2	318	02	ROS	062697	0828	EN	43 24.7 N	40 11.9 W	GPS	4779				
06MT039/3	A2	319	01	ROS	062697	1209	BE	43 10.4 N	40 59.4 W	GPS	4798				
06MT039/3	A2	319	01	ROS	062697	1338	BO	43 10.5 N	41 00.1 W	GPS	4798	10	4832	4883	21
06MT039/3	A2	319	01	ROS	062697	1519	EN	43 10.5 N	41 00.9 W	GPS	4798				
06MT039/3	A2	320	01	ROS	062697	1839	BE	42 56.3 N	41 47.3 W	GPS	4809				
06MT039/3	A2	320	01	ROS	062697	1900	BO	42 56.0 N	41 47.6 W	GPS	4809		1194	1200	12
06MT039/3	A2	320	01	ROS	062697	1937	EN	42 55.8 N	41 48.7 W	GPS	4809				
06MT039/3	A2	320	02	ROS	062697	1943	BE	42 55.2 N	41 49.0 W	GPS	4809				
06MT039/3	A2	320	02	ROS	062697	2108	BO	42 55.2 N	41 40.0 W	GPS	4809	09	4850	4921	22
06MT039/3	A2	320	02	ROS	062697	2252	EN	42 54.3 N	41 49.9 W	GPS	4809				
06MT039/3	A2	320	04	ROS	062797	0133	BE	42 52.3 N	41 52.4 W	GPS	4880				
06MT039/3	A2	320	04	ROS	062797	0236	BO	42 51.4 N	41 53.2 W	GPS	4880		3720	3755	20
06MT039/3	A2	320	04	ROS	062797	0350	EN	42 50.7 N	41 54.1 W	GPS	4880				
06MT039/3	A2	321	01	ROS	062797	0715	BE	42 24.7 N	42 35.9 W	GPS	4837				
06MT039/3	A2	321	01	ROS	062797	0842	BO	42 41.8 N	42 36.5 W	GPS	4837	08	4903	4955	20
06MT039/3	A2	321	01	ROS	062797	1027	EN	42 41.0 N	42 37.8 W	GPS	4837				
06MT039/3	A2	322	01	ROS	062797	1345	BE	42 28.1 N	43 30.0 W	GPS	4832				
06MT039/3	A2	322	01	ROS	062797	1423	BO	42 28.4 N	43 24.4 W	GPS	4832		1395	1301	12
06MT039/3	A2	322	01	ROS	062797	1505	EN	42 28.0 N	42 24.7 W	GPS	4832				
06MT039/3	A2	322	02	ROS	062797	1523	BE	42 27.9 N	43 25.0 W	GPS	4831				
06MT039/3	A2	322	02	ROS	062797	1651	BO	42 27.3 N	43 25.6 W	GPS	4831	13	4887	4955	21

06MT039/3	A2	322	02	ROS	062797	1822	EN	42 27.9 N	43 26.7 W	GPS	4831				
06MT039/3	A2	323	01	ROS	062797	2157	BE	42 15.2 N	44 12.2 W	GPS	4865				
06MT039/3	A2	323	01	ROS	062797	2231	BO	42 15.6 N	44 12.6 W	GPS	4865		1191	1200	12
06MT039/3	A2	323	01	ROS	062797	2309	EN	42 16.0 N	44 13.3 W	GPS	4865				
06MT039/3	A2	323	02	ROS	062897	2319	BE	42 16.0 N	44 13.4 W	GPS	4863				
06MT039/3	A2	323	02	ROS	062997	0049	BO	42 16.6 N	44 14.5 W	GPS	4863	10	4915	4983	21
06MT039/3	A2	323	02	ROS	062997	0232	EN	42 17.2 N	44 15.9 W	GPS	4863				
06MT039/3	A2	324	01	ROS	062897	0636	BE	42 00.9 N	44 59.9 W	GPS	4814				
06MT039/3	A2	324	01	ROS	062897	0702	BO	42 01.6 N	45 00.9 W	GPS	4814		1228	1203	10
06MT039/3	A2	324	01	ROS	062897	0740	EN	42 20.4 N	45 01.4 W	GPS	4814				
06MT039/3	A2	324	02	ROS	062897	0755	BE	42 02.2 N	45 01.5 W	GPS	4801				
06MT039/3	A2	324	02	ROS	062897	0928	BO	42 04.4 N	45 03.2 W	GPS	4801	09	4937	4914	22
06MT039/3	A2	324	02	ROS	062897	1118	EN	42 05.8 N	45 05.1 W	GPS	4801				
06MT039/3	A2	325	01	ROS	062897	1350	BE	42 11.5 N	45 38.4 W	GPS	4720				
06MT039/3	A2	325	01	ROS	062897	1413	BO	42 12.2 N	45 38.8 W	GPS	4720		1278	1101	11
06MT039/3	A2	325	01	ROS	062897	1453	EN	42 13.1 N	45 39.3 W	GPS	4720				
06MT039/3	A2	325	02	ROS	062897	1454	BE	42 13.3 N	45 39.4 W	GPS	4714				
06MT039/3	A2	325	02	ROS	062897	1619	BO	42 14.8 N	45 40.6 W	GPS	4714	09	4835	4802	22
06MT039/3	A2	325	02	ROS	062897	1804	EN	42 17.1 N	45 40.9 W	GPS	4714				
06MT039/3	A2	326	01	ROS	062897	2045	BE	42 22.4 N	46 17.6 W	GPS	4660				
06MT039/3	A2	326	01	ROS	062897	2140	BO	42 22.3 N	46 17.5 W	GPS	4660		3029	2298	24
06MT039/3	A2	326	01	ROS	062897	2300	EN	42 22.3 N	46 17.4 W	GPS	4660				
06MT039/3	A2	326	02	ROS	062897	2333	BE	42 22.3 N	46 17.5 W	GPS	4660				
06MT039/3	A2	326	02	ROS	062997	0056	BO	42 22.4 N	46 17.7 W	GPS	4660	12	4742	4733	21
06MT039/3	A2	326	02	ROS	062997	0241	EN	42 22.5 N	46 17.4 W	GPS	4660				
06MT039/3	A2	327	01	ROS	062997	0516	BE	42 44.3 N	46 17.5 W	GPS	4660				
06MT039/3	A2	327	01	ROS	062997	0630	BO	42 22.4 N	46 17.7 W	GPS	4660	12	4298	4332	22
06MT039/3	A2	327	01	ROS	062997	0753	EN	42 22.5 N	46 17.4 W	GPS	4660				
06MT039/3	A2	328	01	ROS	062997	0940	BE	42 36.5 N	47 07.3 W	GPS	4045				
06MT039/3	A2	328	01	ROS	062997	1102	BO	42 35.6 N	47 08.1 W	GPS	4045	11	4070	4077	21
06MT039/3	A2	328	01	ROS	062997	1232	EN	42 34.6 N	47 09.0 W	GPS	4045				
06MT039/3	A2	329	01	ROS	062997	1452	BE	42 34.7 N	47 26.7 W	GPS	3825				
06MT039/3	A2	329	01	ROS	062997	1600	BO	42 44.0 N	47 27.3 W	GPS	3825	10	3846	3879	22
06MT039/3	A2	329	01	ROS	062997	1723	EN	42 43.8 N	47 27.1 W	GPS	3825				
06MT039/3	A2	330	01	ROS	062997	1934	BE	42 49.2 N	47 44.1 W	GPS	3741				
06MT039/3	A2	330	01	ROS	062997	2036	BO	42 49.4 N	47 43.9 W	GPS	3741	09	3742	3786	22
06MT039/3	A2	330	01	ROS	062997	2206	EN	42 49.8 N	47 43.8 W	GPS	3741				
06MT039/3	A2	331	01	ROS	062997	2358	BE	42 54.8 N	48 01.7 W	GPS	3486				
06MT039/3	A2	331	01	ROS	063097	0103	BO	42 55.0 N	48 01.7 W	GPS	3486	10	3465	3505	22

06MT039/3	A2	331	01	ROS	063097	0223	EN	42 55.0 N	48 01.2 W	GPS	3486				
06MT039/3	A2	332	01	ROS	063097	0506	BE	43 03.1 N	48 37.5 W	GPS	2510				
06MT039/3	A2	332	01	ROS	063097	0549	BO	43 03.0 N	48 37.6 W	GPS	2510	10	2473	2494	22
06MT039/3	A2	332	01	ROS	063097	0651	EN	43 03.1 N	48 37.6 W	GPS	2510				
06MT039/3	A2	333	01	ROS	063097	0836	BE	43 05.5 N	48 50.5 W	GPS	2072				
06MT039/3	A2	333	01	ROS	063097	0913	BO	43 05.3 N	48 50.8 W	GPS	2072	10	2043	2050	22
06MT039/3	A2	333	01	ROS	063097	1014	EN	43 04.9 N	48 51.4 W	GPS	2072				
06MT039/3	A2	334	01	ROS	063097	1206	BE	43 08.3 N	48 59.8 W	GPS	1588				
06MT039/3	A2	334	01	ROS	063097	1248	BO	43 08.4 N	48 59.7 W	GPS	1588	09	1554	1564	22
06MT039/3	A2	334	01	ROS	063097	1340	EN	43 08.4 N	48 59.4 W	GPS	1588				
06MT039/3	A2	335	01	ROS	063097	1518	BE	43 11.7 N	49 09.3 W	GPS	1049				
06MT039/3	A2	335	01	ROS	063097	1547	BO	43 11.6 N	49 09.2 W	GPS	1049	09	1022	1029	10
06MT039/3	A2	335	01	ROS	063097	1621	EN	43 11.6 N	49 09.2 W	GPS	1049				
06MT039/3	A2	336	01	ROS	063097	1803	BE	43 15.2 N	49 22.2 W	GPS	0570	05	557	560	10
06MT039/3	A2	336	01	ROS	063097	1840	EN	43 15.2 N	49 22.2 W	GPS	0570				
06MT039/3	A2	337	01	ROS	063097	1953	BE	43 20.1 N	49 34.9 W	GPS	0097				
06MT039/3	A2	337	01	ROS	063097	2000	BO	43 20.1 N	49 34.9 W	GPS	0097		77	0080	7
06MT039/3	A2	337	01	ROS	063097	2009	EN	43 20.1 N	49 34.9 W	GPS	0097				
06MT039/3	A2	338	01	ROS	063097	2223	BE	43 30.2 N	50 00.3 W	GPS	0068				
06MT039/3	A2	338	01	ROS	063097	2227	BO	43 20.2 N	50 00.3 W	GPS	0068	09	55	0057	5
06MT039/3	A2	338	01	ROS	063097	2235	EN	43 30.3 N	50 00.4 W	GPS	0068				

7.4 Leg M39/4

7.4.1 CTD-profile station list and water samples taken from the bottles

CTD-Profile	Station No.	Date	Time	Latitude	Longitude	Water Depth	Profile Depth dbar	Comment	CH ₄ -samples	He, ³ H, ¹⁸ O samples	Plankton net depth/ comment	¹⁸ O for Lamont US England GB
1	339	1997/07/07	23:03	52°57.22'N	51°21.08'W	2200	2111				200m culturing	
2	341	1997/07/08	23:03	55°19.54'N	53°53.55'W	2405	2398	K2,K6 retrieved		He(12) ³ H(12) ¹⁸ O(5)		US(4) GB(20)
3	342	1997/07/09	03:30	55°00.72'N	54°12.57'W	514	482			He(6) ³ H(6) ¹⁸ O(6)	500m conservation	US(4) GB(5)
4	343	1997/07/09	06:30	55°09.11'N	54°03.86'W	1270	1236			He(7) ³ H(7) ¹⁸ O(6)		US(5) GB(10)
	344	1997/07/09	08:35	55°15.96'N	53°57.03'W						500m conservation	

CTD-Profile	Station No.	Date	Time	Latitude	Longitude	Water Depth	Profile Depth dbar	Comment	CH ₄ -samples	He, ³ H, ¹⁸ O samples	Plankton net depth/comment	¹⁸ O for Lamont US England GB
5	346	1997/07/09	12:09	55°33.52'N	53°40.02'W	2898	2887			¹⁸ O(6)		US(4) GB(22)
6	347	1997/07/09	17:06	55°58.01'N	53°15.96'W	3230	3233			He(12) ³ H(12) ¹⁸ O(6)		US(4) GB(22)
7	348	1997/07/10	04:02	57°22.74'N	51°47.36'W	3552	3569			He(12) ³ H(12) ¹⁸ O(6)		US(4) GB(22)
8	349	1997/07/10	23:30	58°29.63'N	50°33.49'W	3552	3569	K4 retrieved		He(13) ³ H(14) ¹⁸ O(6)		US(4) GB(22)
9	350	1997/07/11	13:07	57°44.89'N	49°56.87'W	3595	3611	no LADCP		¹⁸ O(6)		
10	351	1997/07/11		57°00.03'N	49°19.05'W	3644	3651			He(12) ³ H(12) ¹⁸ O(4)		
11	352	1997/07/12	04:18	56°16.48'N	48°41.95'W	3716	3733	K3 retrieved			500m conservation	
12	353	1997/07/12	18:26	55°22.99'N	48°47.86'W	3780	3808			He(12) ³ H(12) ¹⁸ O(5)		
13	354	1997/07/13	03:00	54°32.11'N	49°06.88'W	3746	3766	no LADCP				
14	355	1997/07/13	13:43	53°41.13'N	49°26.64'W	3716	3741	K16 deployed, no LADCP		He(13) ³ H(13) ¹⁸ O(6)		US(4)
15	357	1997/07/14	01:21	53°26.08'N	50°04.04'W	3533	3565	K10 deployed, no LADCP		¹⁸ O(6)	500m conservation	US(4)
16	358	1997/07/14	06:54	53°16.06'N	50°33.11'W	3189	3192			He(12) ³ H(12) ¹⁸ O(5)		US(4)
17	359	1997/07/14	14:56	53°07.99'N	50°53.68'W	2903	2902	K9 deployed		¹⁸ O(7)		US(4)
18	361	1997/07/14	23:18	52°52.44'N	51°30.77'W	1691	1665	K7 deployed		He(9) ³ H(9) ¹⁸ O(7)	500m conservation	US(4)
19	362	1997/07/15	03:37	53°02.50'N	51°05.89'W	2601	2577			He(10) ³ H(10) ¹⁸ O(6)	500m conservation	US(4)
20	363	1997/07/15	07:56	52°58.02'N	51°18.00'W	2284	2261	K8 deployed		¹⁸ O(6)	500m culturing	US(4)
21	364	1997/07/15	17:02	52°47.93'N	51°45.05'W	550	520			He(5) ³ H(5) ¹⁸ O(6)	500m conservation	US(3)
22	366	1997/07/19	04:02	57°40.13'N	56°32.03'W	3019	3018		22		500m conservation	US(4)
23	367	1997/07/20	01:30	57°06.51'N	54°36.11'W	3260	3262	K15+K17 deployed	22		500m conservation	US(4)

CTD-Profile	Station No.	Date	Time	Latitude	Longitude	Water Depth	Profile Depth dbar	Comment	CH ₄ -samples	He, ³ H, ¹⁸ O samples	Plankton net depth/comment	¹⁸ O for Lamont US England GB
24	370	1997/07/21	12:54	55°08.92'N	54°04.21'W	1243	1234		8			
25	372	1997/07/21	23:18	55°22.02'N	53°49.10'W	2581	2558	K12 deployed	17			
26	373	1997/07/22	03:37	55°42.09'N	53°31.88'W	3020	3009		22			
27	374	1997/07/22	12:03	56°34.07'N	52°39.93'W	3509	3520	K11 deployed	21	He(12) ³ H(12)	500m conservation	GB(22)
28	375	1997/07/23	11:26	57°56.12'N	51°10.26'W	3588	3602		22	He(9) ³ H(8) SF ₆ (8)		GB(19)
29	376	1997/07/23	19:15	58°27.49'N	50°29.94'W	3552	505	K14 deployed	-		500m conservation	
30	377	1997/07/24	05:18	59°27.87'N	49°29.79'W	3413	3425		21			US(4) GB(22)
31	378	1997/07/24	10:54	59°53.97'N	49°00.02'W	3110	3113		21	He(12) ³ H(12) ¹⁸ O(4)		US(4) GB(22)
32	379	1997/07/24	16:02	60°07.77'N	48°45.76'W	2918	2917		-	He(10) ³ H(10) ¹⁸ O(4)	500m conservation	US(5) GB(17)
33	380	1997/07/24	20:56	60°18.46'N	48°34.20'W	2747	2741		21	He(10) ³ H(10) ¹⁸ O(4)	500m conservation	US(5) GB(17)
34	381	1997/07/25	20:45	59°03.07'N	43°30.05'W	1707	1692		13	He(8) ³ H(8) ¹⁸ O(3)	500m conservation	US(5)
35	382	1997/07/26	01:33	58°40.08'N	43°30.03'W	1975	1946		-	He(8) ³ H(8) ¹⁸ O(3)		US(4)
36	383	1997/07/26	05:55	58°26.27'N	43°30.31'W	2439	2425		22	He(9) ³ H(9) ¹⁸ O(4)	500m conservation	US(3)
37	384	1997/07/26	09:31	58°11.98'N	43°30.02'W	2942	2942		-			US(4)
38	385	1997/07/26	14:20	57°58.10'N	43°30.14'W	3248	3252		22	He(11) ³ H(11)	500m conservation	US(4)
39	386	1997/07/26	18:44	57°37.87'N	43°29.95'W	3417	3426		20	He(5) ³ H(5)		
40	387	1997/07/26	23:48	57°10.04'N	43°30.09'W	3449	3478		-			
41	388	1997/07/27	05:15	56°39.91'N	43°29.91'W	3502	3515		21			
42	389	1997/07/27	12:07	55°57.93'N	43°29.94'W	3348	3360		22	He(3) ³ H(3)		
43	390	1997/07/27	18:37	55°15.88'N	43°30.02'W	3329	3338		22	He(8) ³ H(8)		
44	391	1997/07/28	00:48	54°33.99'N	43°30.00'W	3410	3414		-			
45	392	1997/07/28	07:09	53°51.92'N	43°29.76'W	3625	3668		21			
46	393	1997/07/28	13:41	53°09.96'N	43°30.05'W	3661	3686		21			
47	394	1997/07/28	20:11	52°27.97'N	43°29.87'W	4190	4237		21	He(9) ³ H(9)		

CTD-Profile	Station No.	Date	Time	Latitude	Longitude	Water Depth	Profile Depth dbar	Comment	CH ₄ -samples	He, ³ H, ¹⁸ O samples	Plankton net depth/comment	¹⁸ O for Lamont US England GB
48	395	1997/07/29	01:45	51°59.84'N	43°30.00'W	4176	4218		-			
49	396	1997/07/29	07:29	51°30.07'N	43°30.02'W	4234	4289		22			
50	397	1997/07/29	14:07	50°59.92'N	43°29.98'W	4205	4259		22			
51	398	1997/07/29	22:22	50°30.03'N	43°29.99'W	4267	4305		-			
52	399	1997/07/30	05:00	49°59.99'N	43°30.00'W	4259	4310		21			US(5)
53	400	1997/07/30	10:58	49°40.04'N	43°49.97'W	4070	4111		22	He(10) ³ H(10)		US(4)
54	401	1997/07/30	16:52	49°15.65'N	44°14.86'W	3106	3113		21	He(9) ³ H(9) ¹⁸ O(5)		US(4)
55	402	1997/07/30	22:15	48°15.41'N	44°38.72'W	1573	1548		19	He(9) ³ H(7) ¹⁸ O(6)	500m conservation	US(5)
56	403	1997/07/31	02:29	49°04.30'N	44°25.89'W	2550	2538		-	He(10) ³ H(10) ¹⁸ O(4)		
57	404	1997/07/31	07:49	49°27.79'N	44°03.01'W	3845	3906		22	He(11) ³ H(11) ¹⁸ O(3)	500m conservation	
58	405	1997/07/31	18:18	50°12.05'N	41°59.78'W	4349	4412		21			
59	406	1997/08/01	02:00	50°23.97'N	40°29.68'W	4341	4407		22	He(9) ³ H(9)		
60	407	1997/08/01	10:16	50°35.97'N	39°00.12'W	4136	4192		21			
61	408	1997/08/01	18:11	50°48.01'N	37°29.86'W	4242	4308		21	He(10) ³ H(10)		
62	409	1997/08/02	02:00	50°59.94'N	35°59.91'W	4328	4380		-			
63	410	1997/08/02	08:54	51°20.11'N	34°59.97'W	3307	3316		21	He(10) ³ H(10)		
64	411	1997/08/02	13:11	51°40.12'N	35°00.04'W	3828	3859		-			
65	412	1997/08/02	17:30	51°55.02'N	34°59.94'W	3235	3223		-			
66	413	1997/08/02	20:36	52°06.11'N	34°59.92'W	3321	3343		20	He(8) ³ H(8)		
67	414	1997/08/03	00:13	52°15.17'N	34°59.88'W	3779	3849		-			
68	415	1997/08/07	03:30	52°22.62'N	35°00.02'W	3774	3744		21	He(9) ³ H(9)		
69	416	1997/08/07	07:18	52°28.03'N	34°59.88'W	2821	2774		-			
70	417	1997/08/07	09:54	52°34.04'N	35°00.22'W	2784	2752		-	He(6) ³ H(6)		
71	418	1997/08/07	12:35	52°38.54'N	35°01.18'W	3332	3369		21	He(9) ³ H(9)		
72	419	1997/08/07	19:41	53°01.99'N	35°06.84'W	3136	3270		21	He(6) ³ H(6)		
73	420	1997/08/07	23:18	53°02.05'N	35°18.94'W	2419	2421		-			
74	421	1997/08/07	01:40	53°02.06'N	35°12.35'W	3109	3108		-			
75	422	1997/08/07	05:11	52°56.67'N	34°58.45'W	3083	3110		-			
76	423	1997/08/07	08:31	52°47.56'N	34°58.11'W	3281	3214		-			
77	424	1997/08/07	11:16	52°43.11'N	34°59.61'W	3531	3537		-			
78	425	1997/08/07	14:37	52°51.97'N	34°57.45'W	3482	3510		22	He(7) ³ H(7)		

CTD-Profile	Station No.	Date	Time	Latitude	Longitude	Water Depth	Profile Depth dbar	Comment	CH ₄ -samples	He, ³ H, ¹⁸ O samples	Plankton net depth/comment	¹⁸ O for Lamont US England GB
79	426	1997/08/07	19:33	53°11.62'N	34°51.47'W	2795	2750		-			
80	427	1997/08/07	22:30	53°15.09'N	34°51.76'W	2613	2616		-	He(8) ³ H(8)		
81	428	1997/08/07	03:38	53°44.07'N	35°15.08'W	2480	2467		-	He(4) ³ H(4)		
82	429	1997/08/07	08:37	54°13.99'N	35°08.96'W	2900	2893		20	He(7) ³ H(7)		
83	430	1997/08/07	13:41	54°42.41'N	35°09.77'W	2001	1964		-			
84	431	1997/08/07	17:41	54°59.08'N	34°49.99'W	2460	2434		-			
85	432	1997/08/07	20:18	55°03.44'N	34°49.95'W	2568	2559		14	He(6) ³ H(6)		
86	433	1997/08/07	01:15	55°34.03'N	35°06.89'W	2047	2027		-			
87	434	1997/08/07	06:01	56°03.02'N	35°24.80'W	2042	2022		19			
88	435	1997/08/07	10:39	56°31.10'N	35°42.16'W	2270	2246		-			
89	436	1997/08/07	14:09	56°41.12'N	36°02.05'W	2421	2416		22			
90	437	1997/08/07	17:33	56°50.96'N	36°21.90'W	2620	2629		-			
91	438	1997/08/07	21:07	57°02.02'N	36°42.98'W	2422	2423		22			
92	439	1997/08/07	00:35	57°12.01'N	37°03.09'W	2743	2734		-			
93	440	1997/08/07	04:17	57°23.03'N	37°24.04'W	3250	3263		-			
94	441	1997/08/07	08:07	57°32.99'N	37°44.90'W	3222	3216		22			
95	442	1997/08/07	13:58	57°54.00'N	38°26.01'W	3249	3262		21	He(15) ³ H(15)		
96	443	1997/08/07	20:18	58°14.00'N	39°05.88'W	3324	3334		-			
97	444	1997/08/08	02:45	58°34.04'N	39°44.76'W	3139	3134		22			
98	445	1997/08/08	07:59	58°48.96'N	40°14.84'W	3088	3091		-			US(4) GB(20)
99	446	1997/08/08	13:22	59°01.93'N	40°39.07'W	2948	2944		21		200m culturing	US(4) GB(18)
100	447	1997/08/08	17:11	59°13.03'N	41°02.90'W	2716	2709		19			US(4) GB(20)
101	448	1997/08/08	20:45	59°23.97'N	41°26.00'W	2359	2342		6			US(4) GB(20)
102	449	1997/08/09	00:03	59°35.08'N	41°50.03'W	1942	1922		14			US(4) GB(18)
103	450	1997/08/09	02:45	59°42.47'N	42°06.94'W	1755	1730		-			GB(4)

7.5 Leg M39/5
7.5.1 Station Listing

EXPO- CODE	Section NAME	Stat No.	Cast No.	Cast Type	Date	Time UTC	Code	Position Latitude	Longitude	Code	Bottom Depth	Meter Wheel	Max. Pres.	Bottom Dist.	No. of Btles	Para meters	Comments
06MT39/5	VEINS-6	451	01	ROS/A	081497	2110	BE	64 45.0N	26 39.7W	GPS	250						
06MT39/5	VEINS-6	451	01	ROS/A	081497	2110	BO	64 45.0N	26 39.9W	GPS	250		243		10	1-8, 23	Test station
06MT39/5	VEINS-6	451	01	ROS/A	081497	2148	EN	64 45.0N	26 40.0W	GPS	250						
06MT39/5	VEINS-6	451	02	ROS/A	081497	2345	BE	64 45.0N	26 40.0W	GPS	253						
06MT39/5	VEINS-6	451	02	ROS/A	081497	2356	BO	64 45.0N	26 40.1W	GPS	250		239		10	1-8,20	
06MT39/5	VEINS-6	451	02	ROS/A	081597	0014	EN	64 45.1N	26 40.2W	GPS	250						
06MT39/5	VEINS-6	452	01	ROS/A	081597	0149	BE	64 45.1N	27 14.9W	GPS	495						
06MT39/5	VEINS-6	452	01	ROS/A	081597	0206	BO	64 45.2N	27 14.8W	GPS	494		482		8	1-8,20,23	
06MT39/5	VEINS-6	452	01	ROS/A	081597	0226	EN	64 45.2N	27 14.8W	GPS	492						
06MT39/5	VEINS-6	453	01	ROS/A	081597	0406	BE	64 45.3N	27 50.2W	GPS	902						
06MT39/5	VEINS-6	453	01	ROS/A	081597	0431	BO	64 45.4N	27 50.0W	GPS	893		902	9	11	1-8,20,23	
06MT39/5	VEINS-6	453	01	ROS/A	081597	0503	EN	64 45.5N	27 49.8W	GPS	882						
06MT39/5	VEINS-6	454	01	ROS/A	081597	0637	BE	64 45.1N	28 25.1W	GPS	1171						
06MT39/5	VEINS-6	454	01	ROS/A	081597	0703	BO	64 45.1N	28 24.9W	GPS	1168		1162	11	13	1-8,20	
06MT39/5	VEINS-6	454	01	ROS/A	081597	0740	EN	64 45.9N	28 24.9W	GPS	1164						
06MT39/5	VEINS-6	455	01	ROS/A	081597	0920	BE	64 45.2N	29 04.9W	GPS	1070						
06MT39/5	VEINS-6	455	01	ROS/A	081597	0947	BO	64 45.2N	29 04.8W	GPS	1070	1044	1058	16	13	1-8,20	
06MT39/5	VEINS-6	455	01	ROS/A	081597	1028	EN	64 45.0N	29 05.0W	GPS	1071						
06MT39/5	VEINS-6	456	01	ROS/A	081597	1209	BE	64 45.1N	29 45.1W	GPS	2139						
06MT39/5	VEINS-6	456	01	ROS/A	081597	1251	BO	64 45.2N	29 45.2W	GPS	2139		2141		22	1-10,20	
06MT39/5	VEINS-6	456	01	ROS/A	081597	1349	EN	64 45.2N	29 45.4W	GPS	2155						
06MT39/5	VEINS-6	457	01	ROS/A	081597	1533	BE	64 45.1N	30 25.2W	GPS	2236						
06MT39/5	VEINS-6	457	01	ROS/A	081597	1616	BO	64 45.2N	30 25.1W	GPS	2235		2237	12	22	1-10,20,23,26	
06MT39/5	VEINS-6	457	01	ROS/A	081597	1719	EN	64 45.4N	30 24.9W	GPS	2230						
06MT39/5	VEINS-6	458	01	ROS/A	081597	1901	BE	65 00.2N	30 42.2W	GPS	1888						
06MT39/5	VEINS-6	458	01	ROS/A	081597	1943	BO	65 00.3N	30 42.5W	GPS	1887		1887	12	22	1-10,20	
06MT39/5	VEINS-6	458	01	ROS/A	081597	2045	EN	65 00.4N	30 42.9W	GPS	1868						
06MT39/5	VEINS-6	459	01	ROS/A	081597	2257	BE	65 16.2N	31 00.0W	GPS	1192						
06MT39/5	VEINS-6	459	01	ROS/A	081597	2325	BO	65 16.2N	31 00.2W	GPS	1187		1171	20	14	1-8,20,23,26	
06MT39/5	VEINS-6	459	01	ROS/A	081697	0009	EN	65 16.5N	31 01.3W	GPS	1178						
06MT39/5	VEINS-6	460	01	ROS/A	081697	0149	BE	65 31.2N	31 15.9W	GPS	364						
06MT39/5	VEINS-6	460	01	ROS/A	081697	0202	BO	65 31.1N	31 16.0W	GPS	364		353	10	8	1-6,20	
06MT39/5	VEINS-6	460	01	ROS/A	081697	0223	EN	65 31.1N	31 16.4W	GPS	364						
06MT39/5	VEINS-5	461	01	ROS/A	081697	0937	BE	65 05.1N	34 28.0W	GPS	316						
06MT39/5	VEINS-5	461	01	ROS/A	081697	0949	BO	65 05.1N	34 28.0W	GPS	316	296	302	12	6	1-10	
06MT39/5	VEINS-5	461	01	ROS/A	081697	1007	EN	65 05.1N	34 28.1W	GPS	316						

06MT39/5 VEINS-4	475	01	MOR	081997	0906	BE	63 28.8N	36 18.0W	GPS	1993									Deployment of mooring "UK1"
06MT39/5 VEINS-4	475	01	MOR	081997	1012	EN	63 28.9N	36 18.1W	GPS										and of IES1
06MT39/5 VEINS-4	476	01	MOR	081997	1117	BE	63 22.0N	36 03.8W	GPS	1993									Deployment of mooring "G1"
06MT39/5 VEINS-4	476	01	MOR	081997	1218	EN	63 22.0N	36 03.9W	GPS										and of IES2
06MT39/5 VEINS-4	477	01	MOR	081997	1330	BE	63 16.8N	35 51.2W	GPS	2364									Deployment of mooring "UK2"
06MT39/5 VEINS-4	477	01	MOR	081997	1344	EN	63 16.6N	35 51.5W	GPS										
06MT39/5 VEINS-4	478	01	MOR	081997	1503	BE	63 07.2N	35 32.2W	GPS	2589									Deployment of mooring "G2"
06MT39/5 VEINS-4	478	01	MOR	081997	1518	EN	63 07.0N	35 32.3W	GPS										
06MT39/5 VEINS-4	479	01	ROS/A	081997	1648	BE	63 18.1N	35 57.1W	GPS	2313									
06MT39/5 VEINS-4	479	01	ROS/A	081997	1732	BO	63 17.9N	35 57.0W	GPS	2313	2317		8	22					1-10,23,26
06MT39/5 VEINS-4	479	01	ROS/A	081997	1847	EN	63 17.9N	35 57.1W	GPS	2314									
06MT39/5 VEINS-4	480	01	ROS/A	081997	2048	BE	63 02.0N	35 27.4W	GPS	2658									
06MT39/5 VEINS-4	480	01	ROS/A	081997	2138	BO	63 02.1N	35 27.4W	GPS	2656	2663	2661	14	22					1-10
06MT39/5 VEINS-4	480	01	ROS/A	081997	2257	EN	63 02.1N	35 27.3W	GPS	2654									
06MT39/5 VEINS-4	481	01	ROS/A	082097	0105	BE	62 45.9N	34 57.1W	GPS	2780									
06MT39/5 VEINS-4	481	01	ROS/A	082097	0158	BO	62 46.1N	34 57.6W	GPS	2774	2742	2781	12	21					1-10
06MT39/5 VEINS-4	481	01	ROS/A	082097	0312	EN	62 46.2N	34 57.9W	GPS										
06MT39/5 VEINS-4	482	01	ROS/A	082097	0524	BE	62 30.0N	34 27.9W	GPS	2845									
06MT39/5 VEINS-4	482	01	ROS/A	082097	0619	BO	62 30.1N	34 28.0W	GPS	2845	2815	2852	14	22					1-10,23,26
06MT39/5 VEINS-4	482	01	ROS/A	082097	0738	EN	62 30.1N	34 28.0W	GPS	2846									
06MT39/5	483	01	ROS/A	082097	1105	BE	61 58.0N	35 07.8W	GPS	2901									
06MT39/5	483	01	ROS/A	082097	1156	BO	61 58.1N	35 07.8W	GPS	2899	2848	2905	20	22					1-8,23,26 Ros. quality test #1
06MT39/5	483	01	ROS/A	082097	1306	EN	61 58.2N	35 07.8W	GPS	2898									
06MT39/5 VEINS-3	484	01	ROS/A	082097	1632	BE	61 26.1N	35 44.1W	GPS	2915									
06MT39/5 VEINS-3	484	01	ROS/A	082097	1720	BO	61 26.0N	35 43.9W	GPS	2917		2926	14	22					1-10,20
06MT39/5 VEINS-3	484	01	ROS/A	082097	1855	EN	61 26.0N	35 44.2W	GPS	2917									
06MT39/5 VEINS-3	485	01	ROS/A	082097	2120	BE	61 37.8N	36 18.2W	GPS	2804									
06MT39/5 VEINS-3	485	01	ROS/A	082097	2214	BO	61 37.9N	36 18.2W	GPS	2800	2775	2806	15	22					1-10,20
06MT39/5 VEINS-3	485	01	ROS/A	082097	2333	EN	61 38.0N	36 18.0W	GPS	2800									
06MT39/5 VEINS-3	486	01	ROS/A	082197	0201	BE	61 48.9N	36 53.0W	GPS	2685									
06MT39/5 VEINS-3	486	01	ROS/A	082197	0250	BO	61 48.9N	36 53.2W	GPS	2684	2648	2685	19	21					1-10,20
06MT39/5 VEINS-3	486	01	ROS/A	082197	0413	EN	61 49.1N	36 53.6W	GPS	2685									
06MT39/5 VEINS-3	487	01	ROS/A	082197	0640	BE	62 01.0N	37 28.3W	GPS	2563									
06MT39/5 VEINS-3	487	01	ROS/A	082197	0731	BO	62 01.0N	37 28.3W	GPS	2565	2525	2572	10	22					1-10,20,23
06MT39/5 VEINS-3	487	01	ROS/A	082197	0849	EN	62 01.0N	37 28.3W	GPS	2564									
06MT39/5 VEINS-3	488	01	ROS/A	082197	1058	BE	62 11.9N	38 03.1W	GPS	2492									
06MT39/5 VEINS-3	488	01	ROS/A	082197	1142	BO	62 12.0N	38 03.0W	GPS	2492	2470	2491	13	22					1-10,20
06MT39/5 VEINS-3	488	01	ROS/A	082197	1251	EN	62 11.9N	38 03.1W	GPS	2491									
06MT39/5 VEINS-3	489	01	ROS/A	082197	1459	BE	62 24.0N	38 38.3W	GPS	2267									
06MT39/5 VEINS-3	489	01	ROS/A	082197	1543	BO	62 24.2N	38 38.5W	GPS	2270	2201	2256	20	22					1-10,20
06MT39/5 VEINS-3	489	01	ROS/A	082197	1655	EN	62 24.3N	38 38.9W	GPS	2272									
06MT39/5 VEINS-3	490	01	ROS/A	082197	1856	BE	62 35.1N	39 13.2W	GPS	2030									
06MT39/5 VEINS-3	490	01	ROS/A	082197	1943	BO	62 35.1N	39 13.3W	GPS	2026	2004	2027	9	20					1-10,20,23,26

06MT39/5 VEINS-3	490	01	ROS/A	082197	2046	EN	62 35.2N	39 13.3W	GPS	2028									
06MT39/5 VEINS-3	491	01	ROS/A	082197	2245	BE	62 47.0N	39 49.3W	GPS	1931									
06MT39/5 VEINS-3	491	01	ROS/A	082197	2325	BO	62 46.8N	39 49.3W	GPS	1939	1963	1924	30	20	1-10,20				
06MT39/5 VEINS-3	491	01	ROS/A	082297	0026	EN	62 46.0N	39 51.2W	GPS	1939									
06MT39/5 VEINS-3	492	01	ROS/A	082297	0207	BE	62 51.8N	40 06.7W	GPS	1706									
06MT39/5 VEINS-3	492	01	ROS/A	082297	0243	BO	62 51.4N	40 07.0W	GPS	1690	1672	1694	32	18	1-8,20				
06MT39/5 VEINS-3	492	01	ROS/A	082297	0337	EN	62 51.1N	40 07.4W	GPS	1666									
06MT39/5 VEINS-3	493	01	ROS/A	082297	0514	BE	62 58.0N	40 25.0W	GPS	218									
06MT39/5 VEINS-3	493	01	ROS/A	082297	0525	BO	62 58.0N	40 25.2W	GPS	232	212	215	10	4	1-10,20				
06MT39/5 VEINS-3	493	01	ROS/A	082297	0543	EN	62 57.9N	40 25.4W	GPS	241									
06MT39/5	494	01	ROS	082297	1123	BE	62 08.6N	41 19.2W	GPS	415									
06MT39/5	494	01	ROS	082297	1135	BO	62 08.4N	41 19.1W	GPS	421		406		24	1,23	Test CTD "DHI-2"			
06MT39/5	494	01	ROS	082297	1200	EN	62 08.2N	41 19.2W	GPS	433									
06MT39/5 VEINS-2	495	01	ROS/A	082297	1817	BE	61 17.7N	41 29.5W	GPS	445									
06MT39/5 VEINS-2	495	01	ROS/A	082297	1831	BO	61 17.7N	41 29.5W	GPS	456	465	458	9	6	1-6,9,20				
06MT39/5 VEINS-2	495	01	ROS/A	082297	1852	EN	61 17.7N	41 29.5W	GPS	462									
06MT39/5 VEINS-2	496	01	ROS/A	082297	2007	BE	61 14.9N	41 05.2W	GPS	1761									
06MT39/5 VEINS-2	496	01	ROS/A	082297	2043	BO	61 14.7N	41 05.6W	GPS	1763	1726	1752	24	16	1-8,20				
06MT39/5 VEINS-2	496	01	ROS/A	082297	2133	EN	61 14.5N	41 06.2W	GPS	1760									
06MT39/5 VEINS-2	497	01	ROS/A	082397	2316	BE	61 11.1N	40 39.1W	GPS	1892									
06MT39/5 VEINS-2	497	01	ROS/A	082497	0001	BO	61 10.9N	40 39.3W	GPS	1897	1827	1878	50	20	1-10,20,23				
06MT39/5 VEINS-2	497	01	ROS/A	082497	0059	EN	61 10.5N	40 39.6W	GPS	1818									
06MT39/5 VEINS-2	498	01	ROS/A	082397	0306	BE	61 04.0N	40 07.7W	GPS	2193									
06MT39/5 VEINS-2	498	01	ROS/A	082397	0349	BO	61 03.9N	40 07.5W	GPS	2196	2160	2185	19	21	1-8,20				
06MT39/5 VEINS-2	498	01	ROS/A	082397	0501	EN	61 03.7N	40 07.8W	GPS	2197									
06MT39/5 VEINS-2	499	01	ROS/A	082397	0701	BE	60 56.9N	39 27.1W	GPS	2580									
06MT39/5 VEINS-2	499	01	ROS/A	082397	0749	BO	60 57.1N	39 27.2W	GPS	2579	2550	2583	9	20	1-10,20				
06MT39/5 VEINS-2	499	01	ROS/A	082397	0904	EN	60 57.2N	39 27.3W	GPS	2578									
06MT39/5 VEINS-2	500	01	ROS/A	082397	1110	BE	60 50.1N	38 46.9W	GPS	2816									
06MT39/5 VEINS-2	500	01	ROS/A	082397	1201	BO	60 49.9N	38 47.3W	GPS	2814	2765	2820	24	22	1-10,20,23				
06MT39/5 VEINS-2	500	01	ROS/A	082397	1315	EN	60 49.7N	38 47.0W	GPS	2813									
06MT39/5 VEINS-2	501	01	ROS	082397	1532	BE	60 44.1N	38 06.0W	GPS	2906									
06MT39/5 VEINS-2	501	01	ROS	082397	1624	BO	60 43.9N	38 06.0W	GPS	2905		2914	04	23	1-2,20	Test CTD "DHI-2"			
06MT39/5 VEINS-2	501	01	ROS	082397	1748	EN	60 43.9N	38 06.2W	GPS	2906									
06MT39/5 VEINS-2	501	03	ROS/A	082397	1858	BE	60 43.9N	38 05.8W	GPS	2906									
06MT39/5 VEINS-2	501	03	ROS/A	082397	1954	BO	60 43.9N	38 05.8W	GPS	2906	2874	2911	18	21	1-8,23	Ros. quality test #2			
06MT39/5 VEINS-2	501	03	ROS/A	082397	2102	EN	60 44.0N	38 06.3W	GPS	2907									
06MT39/5	502	01	ROS/A	082497	0023	BE	60 13.9N	38 50.0W	GPS	2877									
06MT39/5	502	01	ROS/A	082497	0116	BO	60 13.7N	38 49.6W	GPS	2879	2847	2883	18	26	1-10,20,23				
06MT39/5	502	01	ROS/A	082497	0229	EN	60 13.5N	38 49.4W	GPS	2879									
06MT39/5	503	01	MOR	082497	0911	BE	59 25.4N	40 35.7W	GPS										Rec. of mooring
06MT39/5	503	01	MOR	082497	1014	EN	59 25.5N	40 35.5W	GPS										"VEINS21"
06MT39/5	504	01	MOR	082497	1042	BE	59 23.0N	40 38.0W	GPS										Rec. of mooring "VEINS2"

06MT39/5	504	01	MOR	082497	1050	EN	59 23.0N	40 38.0W	GPS	(failed)
06MT39/5	505	01	MOR	082497	1342	BE	59 41.3N	41 26.5W	GPS	Rec. and dredging of mooring
06MT39/5	505	01	MOR	082497	2332	EN	59 41.8N	41 26.2W	GPS	“VEINS11” (failed) CTD-Tests:“DHI-1”,“DHI-2”, “NB-3”

EXPO- CODE	WOCE WHP-ID	Stat No.	Cast No.	Cast Type	Date	Time UTC	Code	Position		Code	Bottom Depth	Meter Wheel	Bottom Dist.	Max. Pres.	No. of Btles	Parameters	Comments
06Me039	A1/E	506	01	ROS/A	082597	0709	BE	59°59.8N	42°30.0W	GPS	193						
06Me039	A1/E	506	01	ROS/A	082597	0720	BO	59°59.8N	42°30.1W	GPS	193	173	10	179	4	1-6,10,20,23,26	
06Me039	A1/E	506	01	ROS/A	082597	0735	EN	59°59.8N	42°30.1W	GPS	193						
06Me039	A1/E	507	01	ROS/A	082597	0859	BE	59°58.0N	42°10.4W	GPS	497						
06Me039	A1/E	507	01	ROS/A	082597	0911	BO	59°58.9N	42°10.6W	GPS	497	480	9	478	8	1-8,10,20,23,26	
06Me039	A1/E	507	01	ROS/A	082597	0933	EN	59°58.0N	42°10.7W	GPS	497						
06Me039	A1/E	508	01	ROS/A	082597	1059	BE	59°55.9N	41°51.0W	GPS	1829						
06Me039	A1/E	508	01	ROS/A	082597	1131	BO	59°55.8N	41°51.1W	GPS	1829	1806	11	1821	20	1-10,20	
06Me039	A1/E	508	01	ROS/A	082597	1229	EN	59°55.5N	41°51.7W	GPS	1829						
06Me039	A1/E	509	01	ROS/A	082597	1406	BE	59°54.1N	41°30.7W	GPS	1902						
06Me039	A1/E	509	01	ROS/A	082597	1445	BO	59°53.9N	41°30.8W	GPS	1902	1864	22	1895	21	1-6,20,23,26	
06Me039	A1/E	509	01	ROS/A	082597	1540	EN	59°53.6N	41°31.3W	GPS	1902						
06Me039	A1/E	510	01	ROS/A	082597	1701	BE	59°52.0N	41°12.0W	GPS	2040						
06Me039	A1/E	510	01	ROS/A	082597	1741	BO	59°52.0N	41°12.0W	GPS	2040	2023	10	2038	22	1-10,23	
06Me039	A1/E	510	01	ROS/A	082597	1848	EN	59°51.9N	41°12.0W	GPS	2040						
06Me039	A1/E	511	01	ROS/A	082597	2041	BE	59°49.1N	40°45.1W	GPS	2598						
06Me039	A1/E	511	01	ROS/A	082597	2131	BO	59°49.0N	40°45.6W	GPS	2598	2576	10	2608	21	1-10,23	
06Me039	A1/E	511	01	ROS/A	082597	2246	EN	59°49.0N	40°45.9W	GPS	2598						
06Me039	A1/E	512	02	ROS/A	082697	0108	BE	59°45.9N	40°13.2W	GPS	2646						
06Me039	A1/E	512	02	ROS/A	082697	0211	BO	59°46.0N	40°12.9W	GPS	2646	2612	16	2597	22	1-8,23	
06Me039	A1/E	512	02	ROS/A	082697	0317	EN	59°45.9N	40°12.8W	GPS	2646						
06Me039	A1/E	513	01	ROS/A	082697	0546	BE	59°40.0N	39°23.8W	GPS	2854						
06Me039	A1/E	513	01	ROS/A	082697	0640	BO	59°40.9N	39°23.8W	GPS	2854	2829	9	2865	22	1-10,23,26	
06Me039	A1/E	513	01	ROS/A	082697	0806	EN	59°40.8N	39°23.7W	GPS	2854						
06Me039	A1/E	514	01	ROS/A	082697	1032	BE	59°36.0N	38°35.8W	GPS	3012						
06Me039	A1/E	514	01	ROS/A	082697	1132	BO	59°36.1N	38°35.9W	GPS	3012	3993	9	3029	22	1-10,20,23,26	
06Me039	A1/E	514	01	ROS/A	082697	1250	EN	59°35.9N	38°35.8W	GPS	3012						
06Me039	A1/E	514	02	ROS	082697	1302	BE	59°35.9N	38°35.8W	GPS	3013			3010	15	1-2	CTD “NB-3”
06Me039	A1/E	514	02	ROS	082697	1356	BO	59°35.9N	38°35.9W	GPS	3013						
06Me039	A1/E	515	01	ROS/A	082697	1817	BE	59°30.9N	37°37.1W	GPS	3126						
06Me039	A1/E	515	01	ROS/A	082697	1920	BO	59°31.0N	37°37.3W	GPS	3126	3106	11	3147	22	1-10,23,26	
06Me039	A1/E	515	01	ROS/A	082697	2043	EN	59°31.0N	37°37.4W	GPS	3126						
06Me039	A1/E	516	01	ROS/A	082697	2349	BE	59°25.0N	36°39.1W	GPS	3124						
06Me039	A1/E	516	01	ROS/A	082797	0045	BO	59°25.1N	36°39.1W	GPS	3124	3059	10	3145	22	1-8,23,26	

06Me039	A1/E	516	01	ROS/A	082797	0202	EN	59°25.1N	36°39.1W	GPS	3124					
06Me039	A1/E	517	01	ROS/A	082797	0507	BE	59°20.1N	35°40.8W	GPS	3124					
06Me039	A1/E	517	01	ROS/A	082797	0606	BO	59°20.0N	35°40.8W	GPS	3124	3102	11	3143	22	1-8,23
06Me039	A1/E	517	01	ROS/A	082797	0730	EN	59°20.0N	35°41.1W	GPS	3124					
06Me039	A1/E	518	01	ROS/A	082797	1028	BE	59°14.0N	34°44.0W	GPS	2592					
06Me039	A1/E	518	01	ROS/A	082797	1118	BO	59°13.9N	34°44.0W	GPS	2592	2568	8	2595	22	1-8,23
06Me039	A1/E	518	01	ROS/A	082797	1227	EN	59°13.7N	34°44.1W	GPS	2592					
06Me039	A1/E	519	01	ROS/A	082797	1530	BE	59°08.0N	33°45.8W	GPS	2411					
06Me039	A1/E	519	01	ROS/A	082797	1615	BO	59°07.9N	33°46.0W	GPS	2411	2399	9	2421	22	1-10,23,26
06Me039	A1/E	519	01	ROS/A	082797	1729	EN	59°08.0N	33°45.9W	GPS	2411					
06Me039	A1/E	520	01	ROS/A	082797	2031	BE	59°02.0N	32°49.2W	GPS	2209					
06Me039	A1/E	520	01	ROS/A	082797	2116	BO	59°02.0N	32°48.9W	GPS	2209	2189	11	2214	21	1-8,23
06Me039	A1/E	520	01	ROS/A	082797	2222	EN	59°02.0N	32°48.8W	GPS	2209					
06Me039	A1/E	521	01	ROS/A	082897	0037	BE	58°58.1N	32°08.9W	GPS	1609					
06Me039	A1/E	521	01	ROS/A	082897	0110	BO	58°58.1N	32°08.9W	GPS	1609	1578	22	1608	16	1-10,23,26
06Me039	A1/E	521	01	ROS/A	082897	0205	EN	58°58.0N	32°08.9W	GPS	1609					
06Me039	A1/E	522	01	ROS/A	082897	0429	BE	58°53.9N	31°29.0W	GPS	1558					
06Me039	A1/E	522	01	ROS/A	082897	0501	BO	58°54.0N	31°28.9W	GPS	1558	1536	10	1553	17	1-10,23
06Me039	A1/E	522	01	ROS/A	082897	0555	EN	58°53.9N	31°28.9W	GPS	1558					
06Me039	A1/E	523	01	ROS/A	082897	0807	BE	58°50.0N	30°50.0W	GPS	1467					
06Me039	A1/E	523	01	ROS/A	082897	0838	BO	58°49.9N	30°49.2W	GPS	1467	1457	16	1479	17	1-8,23,26
06Me039	A1/E	523	01	ROS/A	082897	0927	EN	58°49.7N	30°49.2W	GPS	1467					
06Me039	A1/E	524	01	ROS/A	082897	1132	BE	58°35.9N	30°22.1W	GPS	1513					
06Me039	A1/E	524	01	ROS/A	082897	1204	BO	58°35.9N	30°22.1W	GPS	1513	1498	18	1581	15	1-10,23
06Me039	A1/E	524	01	ROS/A	082897	1251	EN	58°36.0N	30°22.0W	GPS	1513					
06Me039	A1/E	525	01	ROS/A	082897	1503	BE	58°21.1N	29°55.9W	GPS	2384					
06Me039	A1/E	525	01	ROS/A	082897	1547	BO	58°21.0N	29°56.2W	GPS	2384	2346	27	2390	22	1-10,23,26
06Me039	A1/E	525	01	ROS/A	082897	1659	EN	58°21.2N	29°56.4W	GPS	2384					
06Me039	A1/E	526	01	ROS/A	082897	1904	BE	58°06.9N	29°29.0W	GPS	2316					
06Me039	A1/E	526	01	ROS/A	082897	1955	BO	58°06.9N	29°28.9W	GPS	2316	2215	19	2304	21	1-10,23
06Me039	A1/E	526	01	ROS/A	082897	2106	EN	58°06.9N	29°28.9W	GPS	2316					
06Me039	A1/E	527	01	ROS/A	082897	2322	BE	57°52.0N	28°59.9W	GPS	2374					
06Me039	A1/E	527	01	ROS/A	082997	0009	BO	57°52.0N	29°00.0W	GPS	2374	2354	17	2383	18	1-10,23
06Me039	A1/E	527	01	ROS/A	082997	0115	EN	57°51.9N	29°00.0W	GPS	2374					
06Me039	A1/E	528	01	ROS/A	082997	0318	BE	57°38.1N	28°37.0W	GPS	2477					
06Me039	A1/E	528	01	ROS/A	082997	0407	BO	57°38.0N	28°37.1W	GPS	2477	2461	13	2487	20	1-8,23,26
06Me039	A1/E	528	01	ROS/A	082997	0518	EN	57°37.9N	28°37.0W	GPS	2477					
06Me039	A1/E	529	01	ROS/A	082997	0719	BE	57°22.9N	28°10.9W	GPS	2615					
06Me039	A1/E	529	01	ROS/A	082997	0810	BO	57°22.9N	28°10.9W	GPS	2615	2615	14	2625	21	1-8,23
06Me039	A1/E	529	01	ROS/A	082997	0929	EN	57°22.9N	28°11.0W	GPS	2615					
06Me039	A1/E	530	01	ROS/A	082997	1205	BE	56°59.0N	27°51.9W	GPS	2801					
06Me039	A1/E	530	01	ROS/A	082997	1257	BO	56°59.0N	27°52.1W	GPS	2801	2775	17	2819	20	1-8,23
06Me039	A1/E	530	01	ROS/A	082997	1418	EN	56°59.0N	27°52.4W	GPS	2801					

06Me039	A1/E	531	01	ROS/A	082997	1658	BE	56°35.2N	27°34.4W	GPS	2758						
06Me039	A1/E	531	01	ROS/A	082997	1749	BO	56°35.3N	37°34.8W	GPS	2758	2725	19	2757	22	1-10,23,26	
06Me039	A1/E	531	01	ROS/A	082997	1905	EN	56°35.4N	37°35.3W	GPS	2758						
06Me039	A1/E	532	01	ROS/A	082997	2146	BE	56°11.0N	27°15.1W	GPS	2779						
06Me039	A1/E	532	01	ROS/A	082997	2241	BO	56°11.0N	27°15.0W	GPS	2779	2758	15	2793	22	1-8,23	
06Me039	A1/E	532	01	ROS/A	083097	0004	EN	56°11.1N	27°15.1W	GPS	2779						
06Me039	A1/E	533	01	ROS/A	083097	0249	BE	55°46.9N	26°56.9W	GPS	2966						
06Me039	A1/E	533	01	ROS/A	083097	0344	BO	55°46.9N	26°56.7W	GPS	2966	2959	13	2987	22	1-8,23,26	
06Me039	A1/E	533	01	ROS/A	083097	0504	EN	55°47.1N	26°56.6W	GPS	2966						
06Me039	A1/E	534	01	ROS/A	083097	0755	BE	55°23.0N	29°38.9W	GPS	3347						
06Me039	A1/E	534	01	ROS/A	083097	0858	BO	55°23.0N	29°38.8W	GPS	3347	3333	16	3379	22	1-8,23	Ros. quality test # 3
06Me039	A1/E	534	01	ROS/A	083097	1028	EN	55°23.0N	29°38.8W	GPS	3347						
06Me039	A1/E	534	02	ROS	083097	1203	BE	55°23.0N	26°39.0W	GPS	3340						
06Me039	A1/E	534	02	ROS	083097	1238	BO	55°23.1N	26°38.9W	GPS	3340	1760		1782	22	1-6,23	
06Me039	A1/E	534	02	ROS	083097	1322	EN	55°23.0N	26°38.9W	GPS	3340						
06Me039	A1/E	535	01	ROS/A	083097	1629	BE	55°00.2N	26°21.5W	GPS	3362						
06Me039	A1/E	535	01	ROS/A	083097	1733	BO	55°00.1N	26°21.5W	GPS	3362	3351	21		21	1-10,23,26	
06Me039	A1/E	535	01	ROS/A	083097	1904	EN	55°00.2N	26°21.4W	GPS	3362						
06Me039	A1/E	536	01	ROS/A	083097	2152	BE	54°36.1N	26°03.7W	GPS	3409						
06Me039	A1/E	536	01	ROS/A	083097	2257	BO	54°36.0N	26°03.7W	GPS	3409	3394	14	3441	22	1-8,23	
06Me039	A1/E	536	01	ROS/A	083197	0022	EN	54°35.9N	26°03.6W	GPS	3409						
06Me039		537	01	ROS/A	083197	0205	BE	54°34.0N	25°36.9W	GPS	2421						
06Me039		537	01	ROS/A	083197	0247	BO	54°33.9N	25°36.9W	GPS	2421	2388	16	2412	20	1-6,23	Eriador-Hecate
06Me039		537	01	ROS/A	083197	0358	EN	54°33.7N	25°37.3W	GPS	2421						--Section
06Me039	A1/E	538	01	ROS/A	083197	0556	BE	54°18.9N	25°51.8W	GPS	3050						
06Me039	A1/E	538	01	ROS/A	083197	0657	BO	54°18.9N	25°52.1W	GPS	3050	3065	10	3097	21	1-8,23	
06Me039	A1/E	538	01	ROS/A	083197	0820	EN	54°19.0N	25°52.2W	GPS	3050						
06Me039		539	01	ROS/A	083197	1052	BE	54°04.0N	26°13.8W	GPS	3400						
06Me039		539	01	ROS/A	083197	1155	BO	54°03.8N	26°13.7W	GPS	3400	3448	12	3431	21	1-8,23,26	
06Me039		539	01	ROS/A	083197	1318	EN	54°03.5N	26°13.5W	GPS	3400						
06Me039		540	01	ROS/A	083197	1826	BE	53°33.1N	26°56.9W	GPS	2666						
06Me039		540	01	ROS/A	083197	1919	BO	53°33.4N	26°57.2W	GPS	2666	2651	11	2681	22	1-8,23	
06Me039		540	01	ROS/A	083197	2030	EN	53°33.4N	26°57.7W	GPS	2666						
06Me039		541	01	ROS/A	090197	0136	BE	53°01.9N	27°39.8W	GPS	3632						
06Me039		541	01	ROS/A	090197	0245	BO	53°01.8N	27°39.9W	GPS	3632	3590	41	3645	21	1-8,23,26	
06Me039		541	01	ROS/A	090197	0426	EN	53°01.8N	27°39.9W	GPS	3632						
06Me039		542	01	ROS/A	090197	0836	BE	52°32.0N	28°22.7W	GPS	3683						
06Me039		542	01	ROS/A	090197	0944	BO	52°32.1N	28°22.4W	GPS	3683	3680	12	3731	22	1-10,23	
06Me039		542	01	ROS/A	090197	1120	EN	52°32.0N	28°22.3W	GPS	3683						
06Me039		543	01	ROS/A	090197	1527	BE	52°00.9N	29°05.0W	GPS	3793						
06Me039		543	01	ROS/A	090197	1636	BO	52°00.9N	29°05.0W	GPS	3793	3790	9	3846	22	1-8,23	
06Me039		543	01	ROS/A	090197	1813	EN	52°01.1N	29°05.0W	GPS	3793						
06Me039		544	01	ROS/A	090197	2053	BE	51°42.9N	29°30.2W	GPS	1839						

06Me039		544	01	ROS/A	090197	2127	BO	51°42.9N	29°30.1W	GPS	1839	1739	17	1756	17	1-6,20,23
06Me039		544	01	ROS/A	090197	2221	EN	51°42.9N	29°30.3W	GPS	1839					
06Me039		545	01	ROS/A	090297	0014	BE	51°51.9N	29°15.9W	GPS	3198					
06Me039		545	01	ROS/A	090297	0110	BO	51°52.0N	29°15.7W	GPS	3198	3170	20	3211	20	1-8,23
06Me039		545	01	ROS/A	090297	0232	EN	51°51.8N	29°15.5W	GPS	3198					
06Me039		546	01	ROS/A	090297	0544	BE	52°17.0N	28°42.0W	GPS	3121					
06Me039		546	01	ROS/A	090297	0652	BO	52°17.0N	28°42.1W	GPS	3121	3159	9	3196	21	1-8,23
06Me039		546	01	ROS/A	090297	0818	EN	52°17.1N	28°41.9W	GPS	3121					
06Me039		547	01	ROS/A	090297	1156	BE	52°46.9N	28°01.8W	GPS	3464					
06Me039		547	01	ROS/A	090297	1301	BO	52°47.0N	28°01.9W	GPS	3464	3454	18	3498	22	1-8,23
06Me039		547	01	ROS/A	090297	1427	EN	52°47.0N	28°01.8W	GPS	3464					
06Me039		548	01	ROS/A	090297	1837	BE	53°18.0N	27°19.0W	GPS	3618					
06Me039		548	01	ROS/A	090297	1947	BO	53°18.0N	27°19.1W	GPS	3618	3610	8	3664	22	1-8,23
06Me039		548	01	ROS/A	090297	2118	EN	53°18.0N	27°19.3W	GPS	3618					
06Me039		549	01	ROS/A	090397	0132	BE	53°47.9N	26°34.9W	GPS	3713					
06Me039		549	01	ROS/A	090397	0235	BO	53°47.8N	26°35.1W	GPS	3713	3709	20	3754	22	1-8,23
06Me039		549	01	ROS/A	090397	0413	EN	53°47.5N	26°35.6W	GPS	3713					
06Me039	A1/E	550	01	ROS/A	090397	0746	BE	53°59.9N	25°37.9W	GPS	3252					
06Me039	A1/E	550	01	ROS/A	090397	0848	BO	53°60.0N	25°38.0W	GPS	3252	3229	16	3274	21	1-8,23
06Me039	A1/E	550	01	ROS/A	090397	1009	EN	53°59.9N	25°37.9W	GPS	3252					
06Me039	A1/E	551	01	ROS/A	090397	1211	BE	53°41.8N	25°24.7W	GPS	3603					
06Me039	A1/E	551	01	ROS/A	090397	1318	BO	53°41.4N	25°24.4W	GPS	3603	3587	22	3638	22	1-10,23
06Me039	A1/E	551	01	ROS/A	090397	1452	EN	53°41.4N	25°24.4W	GPS	3603					
06Me039	A1/E	552	01	ROS/A	090397	1717	BE	53°33.0N	24°45.7W	GPS	3621					
06Me039	A1/E	552	01	ROS/A	090397	1825	BO	53°32.9N	24°45.7W	GPS	3621	3614	10	3663	20	1-8,23
06Me039	A1/E	552	01	ROS/A	090397	1959	EN	53°32.9N	24°45.9W	GPS	3621					
06Me039	A1/E	553	01	ROS/A	090397	2238	BE	53°22.9N	24°06.6W	GPS	3674					
06Me039	A1/E	553	01	ROS/A	090397	2347	BO	53°22.7N	24°06.9W	GPS	3674	3663	18	3712	20	1-10
06Me039	A1/E	553	01	ROS/A	090497	0118	EN	53°22.2N	24°08.4W	GPS	3674					
06Me039	A1/E	554	01	ROS/A	090497	0402	BE	53°14.0N	23°27.9W	GPS	3725					
06Me039	A1/E	554	01	ROS/A	090497	0514	BO	53°13.9N	23°28.3W	GPS	3725	3731	10	3776	22	1-8,23,26
06Me039	A1/E	554	01	ROS/A	090497	0652	EN	53°14.0N	23°28.2W	GPS	3725					
06Me039	A1/E	555	01	ROS	090497	1011	BE	53°05.0N	22°49.8W	GPS	4000					
06Me039	A1/E	555	01	ROS	090497	1127	BO	53°05.0N	22°49.9W	GPS	4000	4005	16	4064	21	1-8,23,26
06Me039	A1/E	555	01	ROS	090497	1300	EN	53°05.0N	22°49.9W	GPS	4000					
06Me039	A1/E	555	02	ROS	090497	1511	BE	53°04.8N	22°50.5W	GPS	3972					
06Me039	A1/E	555	02	ROS	090497	1615	BO	53°04.7N	22°50.3W	GPS	3972	3987	15	4047	24	1-6,SF6
06Me039	A1/E	555	02	ROS	090497	1752	EN	53°04.8N	22°50.1W	GPS	3972					
06Me039	A1/E	556	01	ROS	090497	2025	BE	52°55.0N	22°11.0W	GPS	4022					
06Me039	A1/E	556	01	ROS	090497	2140	BO	52°54.9N	22°11.3W	GPS	4022	4021	18	4080	22	1-10
06Me039	A1/E	556	01	ROS	090497	2314	EN	52°54.8N	22°11.1W	GPS	4022					
06Me039	A1/E	557	01	ROS	090597	0143	BE	52°45.9N	21°33.0W	GPS	3877					
06Me039	A1/E	557	01	ROS	090597	0300	BO	52°45.7N	21°32.9W	GPS	3877	3818	19	3931	23	1-8,23

06Me039	A1/E	557	01	ROS	090597	0431	EN	52°45.8N	21°32.8W	GPS	3877						
06Me039	A1/E	558	01	ROS/A	090597	0728	BE	52°36.8N	20°55.0W	GPS	3709						
06Me039	A1/E	558	01	ROS/A	090597	0837	BO	52°36.7N	20°55.4W	GPS	3709	3698	17	3747	22	1-8,23	
06Me039	A1/E	558	01	ROS/A	090597	1012	EN	52°36.4N	20°55.5W	GPS	3709						
06Me039		559	01	ROS/A	090597	1414	BE	52°01.9N	21°21.1W	GPS	4318						
06Me039		559	01	ROS/A	090597	1536	BO	52°01.6N	21°20.9W	GPS	4318	4333	10	4399	22	1-8,10,23	Lorien Bank -
06Me039		559	01	ROS/A	090597	1722	EN	52°01.4N	21°21.3W	GPS	4318						- E. Thulean Section
06Me039		560	01	ROS/A	090597	1923	BE	51°42.8N	21°36.1W	GPS	2712						
06Me039		560	01	ROS/A	090597	2020	BO	51°42.7N	21°36.3W	GPS	2712	2694	12	2727	21	1-6,23	
06Me039		560	01	ROS/A	090597	2145	EN	51°42.4N	21°36.6W	GPS	2712						
06Me039		561	01	ROS/A	090697	0206	BE	52°18.9N	21°08.8W	GPS	3774						
06Me039		561	01	ROS/A	090697	0314	BO	52°18.4N	21°09.0W	GPS	3774	3769	20	3801	22	1-8,23	
06Me039		561	01	ROS/A	090697	0448	EN	52°18.3N	21°09.4W	GPS	3774						
06Me039		562	01	ROS/A	090697	0850	BE	52°55.0N	20°41.0W	GPS	2901						
06Me039		562	01	ROS/A	090697	0943	BO	52°55.0N	20°41.0W	GPS	2901	2888	10	2925	22	1-8,23	
06Me039		562	01	ROS/A	090697	1100	EN	52°55.0N	20°41.0W	GPS	2901						
06Me039		563	01	ROS/A	090697	1506	BE	53°31.0N	20°13.0W	GPS	2151						
06Me039		563	01	ROS/A	090697	1544	BO	53°30.9N	20°13.2W	GPS	2151	2151	19	2171	22	1-8,23	
06Me039		563	01	ROS/A	090697	1655	EN	53°31.0N	20°13.6W	GPS	2151						
06Me039	A1/E	564	01	ROS/A	090897	0434	BE	52°24.0N	20°09.8W	GPS	2883						
06Me039	A1/E	564	01	ROS/A	090897	0528	BO	52°23.9N	20°09.9W	GPS	2883	2877	11	2916	22	1-10,20,23,26	
06Me039	A1/E	564	01	ROS/A	090897	0651	EN	52°24.0N	20°09.9W	GPS	2883						
06Me039	A1/E	565	01	ROS/A	090897	0938	BE	52°20.0N	19°19.9W	GPS	3670						
06Me039	A1/E	565	01	ROS/A	090897	1045	BO	52°20.1N	19°20.0W	GPS	3670	3666	12	3705	22	1-10,20,23,26	
06Me039	A1/E	565	01	ROS/A	090897	1206	EN	52°20.1N	19°20.1W	GPS	3670						
06Me039	A1/E	566	01	ROS/A	090897	1455	BE	52°20.0N	18°29.7W	GPS	4309						
06Me039	A1/E	566	01	ROS/A	090897	1613	BO	52°20.0N	18°29.8W	GPS	4309	4325	21	4392	21	1-10,20,23	
06Me039	A1/E	566	01	ROS/A	090897	1747	EN	52°20.1N	18°30.1W	GPS	4309						
06Me039	A1/E	567	01	ROS/A	090897	2040	BE	52°20.0N	17°40.0W	GPS	4217						
06Me039	A1/E	567	01	ROS/A	090897	2154	BO	52°20.0N	17°40.0W	GPS	4217	4231	15	4257	22	1-10,20,23,26	
06Me039	A1/E	567	01	ROS/A	090897	2326	EN	52°20.0N	17°40.0W	GPS	4217						
06Me039	A1/E	568	01	ROS/A	090997	0222	BE	52°20.0N	16°49.7W	GPS	3822						
06Me039	A1/E	568	01	ROS/A	090997	0331	BO	52°20.1N	16°49.5W	GPS	3822	3824	21	3882	22	1-10,20,23	
06Me039	A1/E	568	01	ROS/A	090997	0502	EN	52°20.2N	16°49.6W	GPS	3822						
06Me039	A1/E	569	01	ROS/A	090997	0753	BE	52°19.9N	16°00.1W	GPS	3375						
06Me039	A1/E	569	01	ROS/A	090997	0905	BO	52°20.2N	16°00.3W	GPS	3375	3382	13	3423	22	1-10,20,23,26	
06Me039	A1/E	569	01	ROS/A	090997	1025	EN	52°20.1N	16°00.6W	GPS	3375						
06Me039	A1/E	570	01	ROS/A	090997	1218	BE	52°20.0N	15°30.1W	GPS	2870						
06Me039	A1/E	570	01	ROS/A	090997	1310	BO	52°20.0N	15°30.6W	GPS	2870	2848	16	2876	22	1-6,23	
06Me039	A1/E	570	01	ROS/A	090997	1412	EN	52°20.0N	15°30.8W	GPS	2870						
06Me039	A1/E	571	01	ROS/A	090997	1527	BE	52°20.0N	15°14.8W	GPS	1394						
06Me039	A1/E	571	01	ROS/A	090997	1600	BO	52°20.1N	15°15.1W	GPS	1394		20	1388	15	1-8,10,20	
06Me039	A1/E	571	01	ROS/A	090997	1642	EN	52°20.0N	15°15.3W	GPS	1394						

06Me039	A1/E	572	01	ROS/A	090997	1754	BE	52°19.9N	14°59.8W	GPS	930					
06Me039	A1/E	572	01	ROS/A	090997	1817	BO	52°19.9N	14°59.6W	GPS	930	914	10	922	12	1-6,20
06Me039	A1/E	572	01	ROS/A	090997	1845	EN	52°20.0N	14°59.5W	GPS	930					
06Me039	A1/E	573	01	ROS/A	090997	1952	BE	52°19.9N	14°45.1W	GPS	462					
06Me039	A1/E	573	01	ROS/A	090997	2005	BO	52°20.0N	14°45.1W	GPS	462	451	13	451	8	1-8,20
06Me039	A1/E	573	01	ROS/A	090997	2024	EN	52°20.1N	14°45.1W	GPS	462					
06Me039	A1/E	574	01	ROS/A	090997	2141	BE	52°20.0N	14°30.0W	GPS	370					
06Me039	A1/E	574	01	ROS/A	090997	2152	BO	52°20.0N	14°29.9W	GPS	370	360	11	360	6	1-6,20
06Me039	A1/E	574	01	ROS/A	090997	2207	EN	52°20.0N	14°29.9W	GPS	370					

8 Concluding remarks and acknowledgements

The 39th voyage of RV METEOR served a multi-disciplinary group of projects in the North Atlantic Ocean. All groups and institution involved helped to support the coordination work. Special thanks is expressed to Deutsche Forschungsgemeinschaft (DFG) for making available the ship time and funding for cruise M39. Projects of the Sonderforschungsbereich 460 were also founded by the DFG.

The principle investigators further acknowledge financial support received from the German Ministry of Education and Research (BMBF) through various grants under the German WOCE programs for preparation and evaluation of the research carried out on cruise M39.

It is our particular pleasure to thank captains and crew of all cruise legs for the flexible friendly and very helpful attitude during deployments of the complex moored arrays and the various kinds of shipboard measurement programs.

9 CHLOROFLUOROCARBON REPORTS

9.1 WOCE LINE A02_06MT39_2

1997.MAY.15 - 1997.JUN.6

CFC PIs: Monika Rhein and Olaf Plähn

Institut für Meereskunde, 24105 Kiel, Germany
now at: Institut. für Ostseeforschung, 18119 Rostock, Germany
email: monika.rhein@io-warnemuende.de,
oplaehn@ifm.uni-kiel.de

CFC-Lab: Martina Elbrächter and Kristin Bahrenfuss
Institut für Meereskunde, 24105 Kiel, Germany
email: melbraechter@ifm.uni-kiel.de

Region: subpolar East Atlantic, 51°N - 62°N, 38°W - 12°W

Sample collection and technique

The water samples were drawn from pre-cleaned 10 L Niskin bottles with gas tight 100 mL glass syringes (Becton and Dickinson). CFCs were measured on board with a GC-ECD (Electron Capture Detector) technique first described by Bullister and Weiss [1988]. About 15-25 mL were transferred to a purge and trap unit. The CFCs were separated on a packed stainless steel column filled with Porasil C and detected with an ECD. The carrier gas is ECD pure Nitrogen, which was additionally cleaned by molsieves (13X mesh 80/100).

All 'O' rings and valves as well as the nylon stopcocks (of the syringes) were removed and washed in isopropanol and baked in a vacuum oven for 24 hours prior the cruise. The Niskin bottles were cleaned with isopropanol. The rubber bands on all bottles were replaced by stainless steel springs. The personnel for all water sampling and handling procedures at the bottles wore one-way gloves to protect the valves from grease.

A standard gas (ALM 0383034, 120.5 ppt CFC-12, 266.4 ppt CFC-11, kindly provided by D. Wallace, IfM Kiel) was used to convert the ECD signal in concentrations. The CFC concentrations are reported in pmol kg⁻¹ on the S1093 scale (R. Weiss, SIO).

Performance

During leg M39/2, the Kiel CFC system worked continuously and about 1200 water samples on 66 stations had been analyzed. The survey was dedicated to the circulation of the deep water masses. During periods of dense station spacing, sampling was focused on the water column below 800 m depth.

Accuracy was checked by analyzing about 350 water samples twice. It was found to be 0.7%, for CFC-11 and 0.8% for CFC-12 (Figure 1). The system blanks for CFC11 and CFC-12 were negligible. The blanks were determined by degassing CFC free water, produced by purging ECD clean Nitrogen permanently through 5 L seawater. The blanks were lower than $0.004 \text{ pmol kg}^{-1}$ for both components. As no CFC poor water is available in the subpolar North Atlantic, the Niskin bottle blanks could not be checked directly. We could only estimate an upper bound of the blank by the measurements in the deep Rockall Trough, where CFC-poor water is found. On our cruises in the Northern Indian Ocean and the Tropical Atlantic, where CFC free deep water is available, the blanks of the pre-cleaned bottles were lower than $0.003 \text{ pmol kg}^{-1}$ for both components (CFC-12 and CFC-11).

The temporal evolution of the ECD efficiency is shown in Figure 2. The efficiency for the CFC-12 component was very stable. The efficiency of CFC-11 was more variable, especially between profile 50-60 (stations 245-255). Major changes occurred, when the drying agent (magnesiumperchlorate) in the purge and trap unit was exchanged or the molsieves had to be baked and therefore exchanged. To correct the temporal drift, a calibration curve with 4-6 different standard gas volumes was carried out before and after each station, the change between these curves is thought to occur linear with time.

CFC concentrations are calculated by using the two neighbored calibration points, assuming that the calibration curve is linear between these points.

At first we used sample volumes, precalibrated by the company (Machery and Nagel, Germany) for the analysis of standard gas. It turned out that these volumes could be off by more than 5%, affecting the precision of the measured oceanic CFC concentrations by the same amount. Therefore, in 1998, the volumes for the gas standard measurements (nominal 2 mL and 5 mL) were calibrated against two 'master' volumes by D. Wallace's group (IfM Kiel), who had done this task also for the CO₂ community. CFC measurements of the air inside the vessel and especially in the lab were carried out frequently in order to check for contamination. In general, the CFC concentrations in both places were only a few percent higher than in clean air. Clean air measurements were carried out occasionally by sampling air from the ship's compass bridge or forecastle.

Problems

At some stations, the CFC-12 peak was disturbed by a high N₂O level of the samples.

Comments

Leg 2 is the first part of the Kiel CFC data set of the Meteor 39 cruise. Along the first section (Ireland-Reykjanes-Ridge) the lowest CFC concentrations - less than

1 pmol kg⁻¹ for CFC-11 were measured at the bottom of the Rockall Trough (Figure 3). Along the eastern flank of the Reykjanes-Ridge, TSOW spreads southward, with a mean CFC-11 signal of 2.5 pmol kg⁻¹ at 60°N. Along its pathway the concentration decreases, and perpendicular to the flow direction, the concentration gradient increase. In the flow through the Charly- Gibbs- Fracture Zone (CGFZ), the CFC-11 concentration was 2.3 pmol kg⁻¹ in the core of the TSOW, at the northern edge of the fracture zone. The largest CFC signal of the LSW was measured southwest of the CGFZ with concentrations of more than 3.2 pmol kg⁻¹. Spreading eastwards this strong signal decreases steadily [Sy et al., 1997]. In the density range between 27.75 and 27.78, the average CFC-11 concentration was less than 2 pmol kg⁻¹ in the Rockall Trough and about 2.7 pmol kg⁻¹ in the Iceland Basin. Along the 51°N-section the LSW signal was observed east of 15°W, marked by oxygen and CFC-11 maxima. The mean CFC ratio within a depth-range of 500-2500 m is about 2.1 (Figure 4), which is similar to the observation during the other cruises in this region. The accuracy of the ratio is less than 0.1 if the CFC-11 concentration is larger than 0.15 pmol kg⁻¹. The scatter increase considerably when the CFC concentrations become smaller.

The surface saturation of CFC-11 relative to the atmospheric value of 266 pptV varied between 93-107% (Figure 5). The supersaturations in the eastern part of the 51°N-section are presumably caused by recent mixing of cold water from the north with warmer water from the south, while the air sea gas exchange had not enough time to equilibrate with the atmosphere. Similar high saturations were found off Newfoundland, where the cold Labrador Current meets the warmer North Atlantic Current [Körtzinger et al., 1999].

- Note, that this is not a WOCE cruise, and the data are not in the WOCE format!
- The data are only for personal use.
- If you want, them for other purposes, you need the consent of Monika Rhein.

References

- Bullister J. L. and R. F. Weiss (1988). Determination Of CCl₃F and CCl₂F₂ in Seawater and Air. *Deep-Sea Res.*, 35, p. 839-853.
- Körtzinger, A., M. Rhein, and L. Mintrop (1999). Anthropogenic CO₂ and CFCs in the North Atlantic Ocean - A comparison of Man-made Tracer. *Geophys. Res. Lett.*, 26, p. 2065-2068.
- Sy, A., M. Rhein,, J.R.N. Lazier, K.P. Koltermann., J. Meincke, A. Putzka, and M. Bersch (1997). Surprisingly Rapid Cooling of Newly Formed Intermediate Waters Across the North Atlantic Ocean. *Nature*, 386, p. 675-679.

Appendix

the station file 'meteor392.sum' includes:

1. station number
2. year
3. month
4. day
5. hour: minutes in decimal system
6. latitude: minutes in decimals
7. longitude: minutes in decimals
8. water depth (m)
9. depth of CTD profile (m)

the bottle file 'meteor392.sea' includes:

1. station number
2. bottle number
3. depth (dbar)
4. in-situ temperature (IC)
5. salinity (psu)
6. CFC-12 (pmol kg⁻¹)
7. CFC-11 (pmol kg⁻¹)
8. WOCE quality flag for CFC-12 and CFC-11

Technical information

Gas chromatograph	Shimadzu GC 14
GC column	stainless steel, packed with Porasil C
Cooling trap	with Porapak T and Porasil C
Trap temperatures	-30°C, 100°C
Column temperature	70°C, isothermal
ECD temperature	300°C
Electron Capture Detector	Shimadzu
Software for chromatogram analysis	Shimadzu CLASS LC 10 (1.63)
Standard gas	ALM 0383034, D. Wallace, PMEL
Precision	CFC-11: 3%, CFC-12: 3%
Accuracy	CFC-11: 0.7%, CFC-12: 0.8%
Blanks	negligible

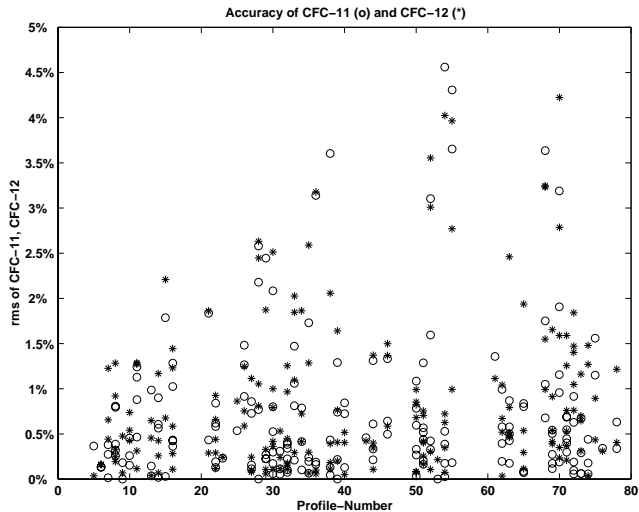


Figure 1: Accuracy (%) of the CFC-12 and CFC-11 replicate samples against profile number.

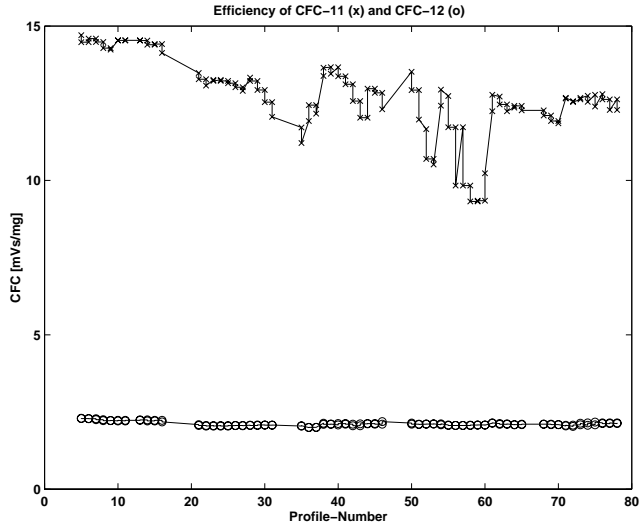


Figure 2: *Temporal evolution of the efficiency of the ECD (mVs/mg standard) for the 5 mL sample volume.*

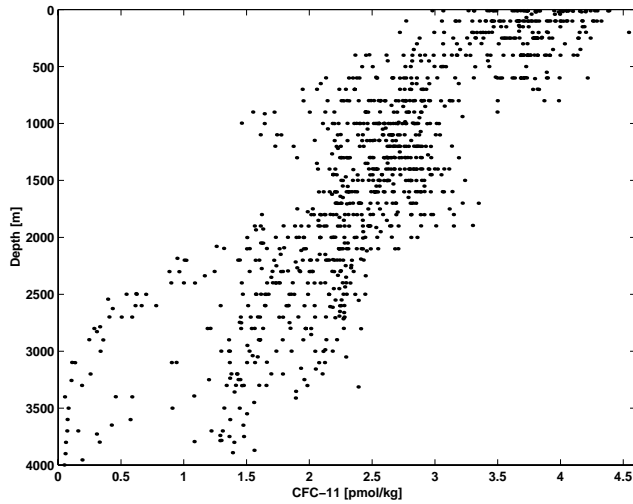


Figure 3: *Cruise Meteor 39/2, all CFC-11 data [pmol kg^{-1}] versus depth.*

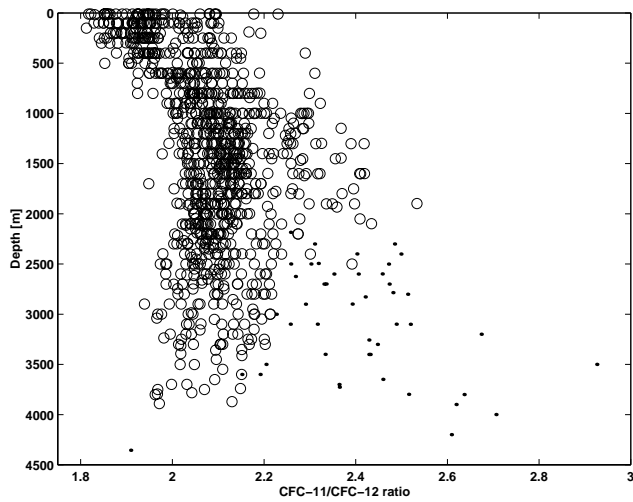


Figure 4: *All CFC-11/CFC-12 ratios measured during Meteor 39/2; CFC-11 concentrations larger than 1 pmol kg^{-1} are marked by circles.*

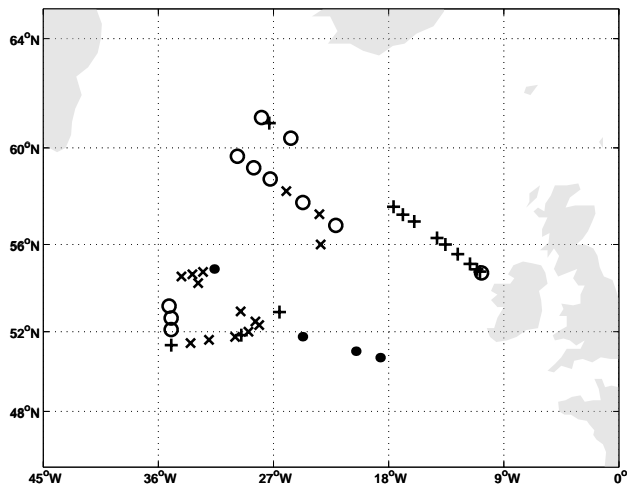


Figure 5: *CFC-11 surface saturation relative to the concentration in the atmosphere (266 pptV), plus: <95%, circle: 95-100%, cross: 100-105%, dot: >105%.*

9.2 WOCE LINE A02_06MT39_3
1997.JUN.11 - 1997.JUL.03

The data reported here were acquired by Prof. Dr. Roether

Institut für Umweltphysik, University Bremen
Tracer Ozeanographie
P.O. Box 330 440
28334 Bremen
phone: +421 218 3511
email: wroether@physik.uni-bremen.de

For questions about the data please contact Uli Fleischmann

Institut für Umweltphysik, University Bremen
Tracer Ozeanographie
P.O. Box 330 440
28334 Bremen
phone: +421 218 4317
email: ufleisch@physik.uni-bremen.de

Region: 48°N on the WHP section A2; 42°N - 49°N, 10°W - 50°W

CHLOROFLUOROCARBONS

CFC11, CFC12, CFC113 and CCL4 have been measured on the cruise. A capillary column (DBVRX, ID 0.45mm) was used. A Bremer standard was used that has been calibrated against the SIO93 scale using standard gas from Ray Weiss. CFC measurements have been assigned individual errors. The overall performance is described below:

The CCl₄ concentrations had to be corrected. CCl₄ concentrations have been raised by 3% to account for insufficient extraction from the water sample.

The ratios of CFC-11/CFC-12 and CFC-113/CFC-12 are rising rapidly and consistently on all stations in the deep eastern basin with very low CFCs (283-295), partially even above the highest values that ever existed. The profiles of individual tracers look quite reasonable. CFC-11 and CFC-113 have been flagged questionable (3) wherever this occurred.

Flags have generally been assigned by looking at individual profiles together with neighbouring profiles. Obvious deviations that did not correspond to any hydrographic property change have been flagged out.

Flags for the CFCs

	2	3	4	6	9
	good	quest	bad	rep	not
F-11	712	37	13	7	781
F-12	734	17	10	8	781
F-113	715	33	14	7	781
CCl ₄	740	7	14	8	781

Reproducibility:

F-11:	0.8 %
F-12:	1.0 %
F-113:	4.0 %
CCl ₄ :	1.6 %

Precision:

F11:	0.002 pmol/kg or a relative error of 0.5% (whichever is greater)
F12:	0.001 pmol/kg or a relative error of 0.4% (whichever is greater)
F-113:	0.001 pmol/kg or a relative error of 3.3% (whichever is greater)
CCl ₄ :	0.005 pmol/kg or a relative error of 0.7% (whichever is greater)

Mean water blank, detection limit:

F-11:	0.12 fmol/kg ± 0.56
F-12:	0.01 fmol/kg ± 0.23
F-113:	2.04 fmol/kg ± 1.96
CCl ₄ :	0.11 fmol/kg ± 0.37

For F-11 a waterblank of 4 fmol/kg has been subtracted. This accounts for possible bottle/system contaminations eventually causing the high CFC-11/CFC-12 ratios wherever the CFCs are very low. But the ratios stayed too high even though (see above).

Air measurements:

Theoretical values for 1997 (northern hemisphere) (SIO-1993 Scale):

F-11	F-12	F-113	CCl ₄
263.8	537.5	83.2	99.5

Individual air measurements performed during the cruise (SIO 93 scale):

Sta	F12	F11	F113	CCl ₄	qual
pptv	pptv	pptv	pptv		
289	535.2	262.2	84.36	100.8	6666
299	537.9	264.94	84.29	100.1	6666
309	537.1	263.3	84.05	100.0	6666
310	536.6	264.5	83.00	100.9	6666
318	536.3	266.7	84.65	101.0	6666
329	531.9	264.5	82.93	99.54	6666
uncertainties of the air measurements					
	0.3 %	0.5 %	0.9 %	2.1 %	

Helium and tritium measurements during this cruise have been measured by the Institut für Umweltphysik Bremen as well and will be reported later.

9.3 WOCE LINES AR05, AR07W_06MT39_4
1997.JUL..07 - 1997.AUG.07

CFC PIs: Monika Rhein and Olaf Plähn

Institut für Meereskunde, 24105 Kiel, Germany
now at:

Institut für Ostseeforschung, 18119 Rostock, Germany
email: monika.rhein@io-warnemuende.de
oplaehn@ifm.uni-kiel.de

CFC-Lab: Martina Elbrächter and Kristin Bahrenfuss
Institut für Meereskunde, 24105 Kiel, Germany
email: melbraechter@ifm.uni-kiel.de

Region: North Atlantic, Labrador Sea 48 N _ 61 N, 58 W _ 35 W

SAMPLE COLLECTION AND TECHNIQUE

All samples were collected from 10 L Niskin bottles. The bottles had been cleaned prior to the cruise using isopropanol. All 'O' rings, valves, and taps were removed, washed in isopropanol and baked in a vacuum oven for 24 hours. The rubber bands on all bottles were replaced by stainless steel springs. The personnel for all water sampling and handling procedures at the bottles wore one-way gloves to protect the valves from grease.

About 100 mL of water were taken from the water bottles with gastight glass syringes (Becton and Dickinson). Then 15-25 mL of the samples were transferred to a purge and trap unit and analyzed on board following the procedures described in Bullister and Weiss [1988]. The CFCs were separated on a packed stainless steel column filled with Porasil C and detected with an Electron Capture Detector (ECD). The carrier gas was ECD pure Nitrogen, which was additionally cleaned by molsieves (13X mesh 80/100). A standard gas -- kindly provided by D. Wallace, IfM Kiel (ALM 0383034) -- was used to convert the ECD signal in concentrations. The CFC concentrations are reported in pmol kg⁻¹ on the SIO93 scale (R. Weiss, SIO).

PERFORMANCE

During the cruise M39/4 the Kiel CFC system worked continuously. Both CFC components CFC-11 and CFC-12 had been sampled on 97 CTD stations and 1850 water samples had been analyzed. The survey was dedicated to the circulation of the deep water masses. During periods of dense station spacing, sampling was focused on the water column below 800 m depth.

Accuracy was checked by analyzing 213 water samples twice, and the mean rms was 0.7% for CFC-11 and 1.2% for CFC-12. The latter varied owing to the intensity of the unknown peak affecting the integration of the CFC-12 peak (Figure 1). The rms of CFC-11 and CFC-12 at the station 366-367 (profiles 22-23) were higher than average, caused by frequent malfunctions of the caliper used to determine the volume of the water sample. After replacement, the accuracy was back to normal. The system blanks for CFC-11 and CFC-12 were negligible. The blanks were determined by degassing

CFC free water, produced by purging ECD clean Nitrogen permanently through 5 L seawater. The blanks were lower than $0.005 \text{ pmol kg}^{-1}$ for both, CFC-11 and CFC-12.

The Niskin bottle blanks on this cruise could not be determined directly, as CFC-free deep water is not present in the western subpolar North Atlantic. We assume that the bottle blanks are similar to the other cruises. Measurements in the deep Rockall Trough (on leg 5), where CFC-poor water was found, showed that the bottle blanks were lower than $0.01 \text{ pmol kg}^{-1}$. On our cruises in the Northern Indian Ocean and the Tropical Atlantic, where CFC free deep water is available, the blanks of the pre-cleaned bottles were lower than $0.003 \text{ pmol kg}^{-1}$ for both components.

The temporal evolution of the ECD efficiency is shown in Figure 2. During the cruise the efficiency decreased about 20%. Major changes occurred, when the drying agent (magnesiumperchlorate) in the purge and trap unit or the molsieves for purifying the carrier gas were exchanged.

To correct the temporal drift, a calibration curve with 4-6 different standard gas volumes was carried out before and after each station. The change between these curves is thought to occur linear with time. As a typical example, the two calibration curves for station 366 are presented in Figure 3. CFC concentrations were calculated by using the two neighboured calibration points, assuming that the calibration curve is linear between these points.

At first we used sample volumes, precalibrated by the company (Machery and Nagel, Germany) for the analysis of standard gas. It turned out that these volumes could be off by more than 5%, affecting the precision of the measured oceanic CFC concentrations by the same amount. Therefore, in 1998, the volumes for the gas standard measurements (nominal 2 mL and 5 mL) were calibrated against two 'master' volumes by D. Wallace's group (IfM Kiel), who had done this task also for the CO₂ community. CFC measurements of the air inside the vessel and especially in the lab were carried out frequently in order to check for contamination. In general, the CFC concentrations in both places were only a few percent higher than in clean air. Clean air measurements were carried out occasionally by sampling air from the ship's compass bridge or forecastle.

PROBLEMS

CFC-11 analysis was successfully carried out during the cruise, the analysis of the CFC-12 concentrations, however, was partly impeded by an unknown substance with a similar retention time as CFC-12. In the data-file, the CFC-12 component got the quality flag '3'.

COMMENTS

Leg 4 is part of the 1997 Kiel CFC data set including the M39 legs 2 and 5 in the subpolar North Atlantic. During the cruise the WHP section AR7 was repeated. The surface saturation of CFC-11 relative to the atmospheric values of 226 ppt varied from 105-117% in the Labrador Sea to 98-105% east of 45 °W [Körtzinger et al., 1999]. The high supersaturations off the shelf in the Labrador Sea (Fig. 4) are presumably caused by recent mixing of cold and CFC rich water with warmer water from the south, while the air sea gas exchange had not enough time to equilibrate with the atmosphere.

In Figure 5 all CFC-11 concentrations measured during the cruise Meteor 39/4 are shown. In the whole water column the concentrations span a large range. For example, the CFC-11 concentrations

in the Labrador Sea Water (LSW) varied along the AR7- section between 4.0 - 4.6 pmol kg⁻¹. South of the Gibbs Fracture Zone the values in this water mass did not exceed 3.5 pmol kg⁻¹.

- Note, that this is not a WOCE cruise, and the data are not in the WOCE format!
- The data are only for personal use. If you want them for other purposes, you need the consent of Monika Rhein.

REFERENCES

- Bullister, J.L. and R.F. Weiss (1988). Determination of CCl₃F and CCl₂F₂ in seawater and air. *Deep-Sea Res.*, 35, p. 839-853.
- Körtzinger, A., M. Rhein, and L. Mintrop (1999). Anthropogenic CO₂ and CFCs in the North Atlantic Ocean -- A comparison of man-made tracer. *Geophys. Res. Lett.*, 26, p. 2065 - 2068.

APPENDIX

the station file 'meteor394.sum' includes:

- 1 station number
- 2 year
- 3 month
- 4 day
- 5 hour: minutes in decimal system
- 6 latitude: minutes in decimals
- 7 longitude: minutes in decimals
- 8 water depth (m)
- 9 depth of CTD profile (m)

the bottle file 'meteor394.sea' includes:

- 1 station number
- 2 bottle number
- 3 depth (dbar)
- 4 in-situ temperature (°C)
- 5 salinity (psu)
- 6 CFC-12 (pmol kg⁻¹)
- 7 CFC-11 (pmol kg⁻¹)
- 8 WOCE quality flag for CFC-12 and CFC-11

TECHNICAL INFORMATION

Gas chromatograph	Shimadzu GC 14
GC column	stainless steel packed with Porasil C
Cooling trap	with Porapak T and Porasil C
Trap temperatures	-30°C, 100°C
Column temperature	70°C, isothermal
ECD temperature	300°C
Electron capture detector	Shimadzu
Software for chromatogram analysis	Shimadzu CLASS LC 10 (1.63)
Standard gas	ALM 0383034, D. Wallace, PMEL
Precision	CFC-11: 3%, CFC-12: 10%
Accuracy	CFC-11: 0.7%, CFC-12: 1.2%
Blanks	negligible

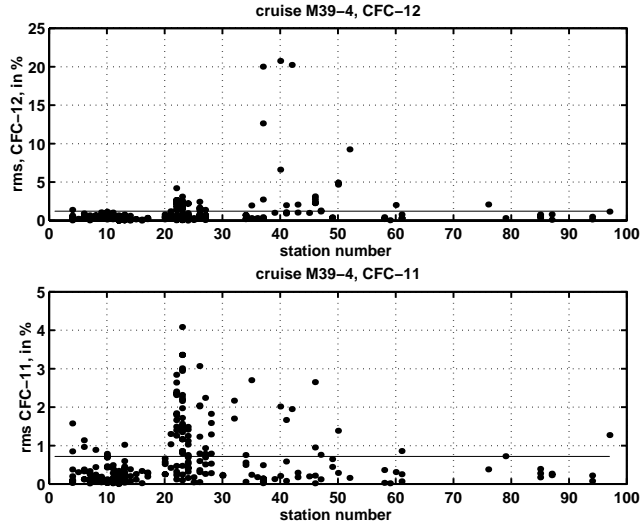


Figure 1: Accuracy (%) of the CFC-12 (a) and CFC-11 (b) replicate samples against station number. The line represents the mean accuracy of the CFC-12 and CFC-11 samples, respectively. Note the different scales for (a) and (b).

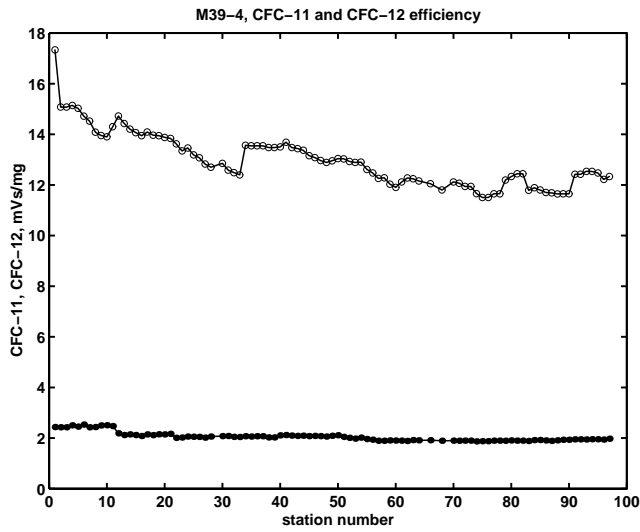


Figure 2: Temporal evolution of the efficiency of the ECD (mVs/mg standard) for the 5 mL sample volume.

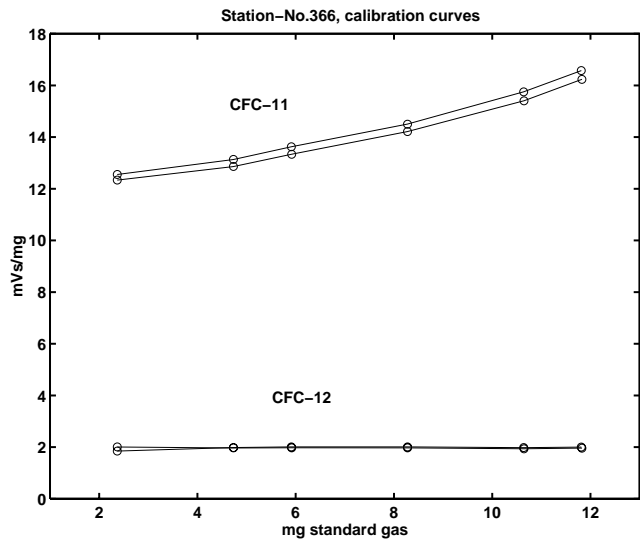


Figure 3: An example of the calibration curve for CFC-12 and CFC-11 before and after the CFC measurements of station 366.

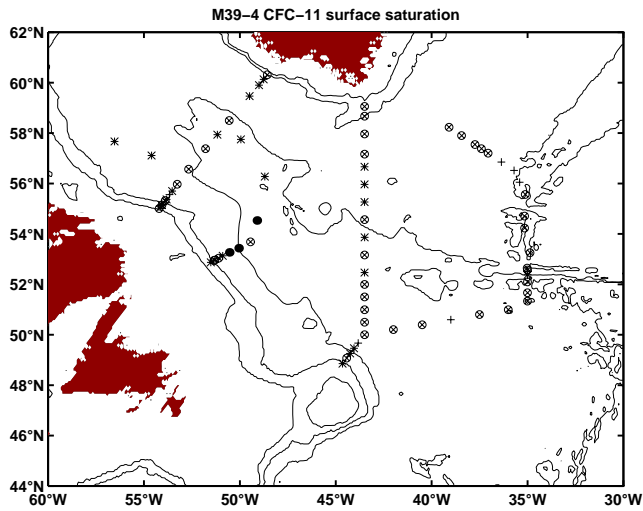


Figure 4: *M39/4*, CFC-11 surface saturation relative to 266 ppt CFC-11, black dot: 110-117%, star: 110-105%, circle with cross: 105-100%, and cross: 100-98%.

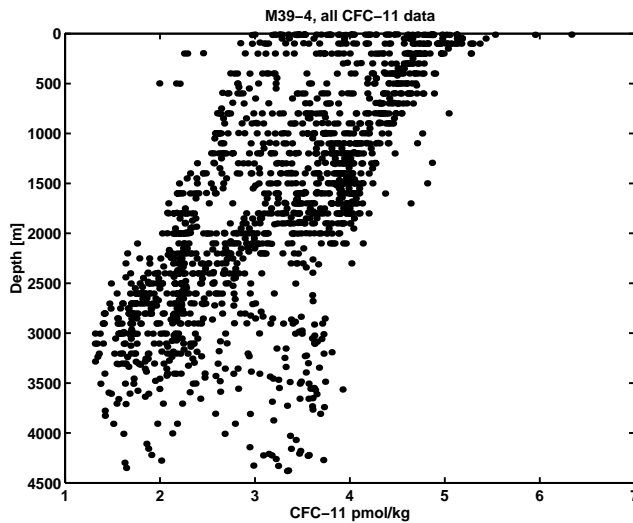


Figure 5: *Cruise M39/4*, all CFC-11 data [pmol kg^{-1}] versus depth.

9.4 WOCE LINES AR07E, AR25_06MT39_5
1997.AUG.14 - 1997.SEP.14

CFC Pls: Monika Rhein

Institut für Meereskunde, 24105 Kiel, Germany

now at:

Institut für Ostseeforschung, 18119 Rostock, Germany

email: monika.rhein@io-warnemuende.de

oplaehn@ifm.uni-kiel.de

CFC-Lab: Martina Elbrächter and Kristin Bahrenfuss

Institut für Meereskunde, 24105 Kiel, Germany

email: melbraechter@ifm.uni-kiel.de

Region: Subpolar North Atlantic

Sample collection and technique

The water samples were drawn from precleaned 10 L Niskin bottles with gas tight 100 mL glass syringes (Becton and Dickinson). CFCs were measured on board with a GC-ECD (Electron Capture Detector) technique first described by Bullister and Weiss [1988]. About 15-25 mL were transferred to a purge and trap unit. The CFCs were separated on a packed stainless steel column filled with Porasil C and detected with an ECD. The carrier gas is ECD pure Nitrogen, which was additionally cleaned by molsieves (13X mesh 80/100). All 'O' rings and valves as well as the nylon stopcocks (of the syringes) were removed and washed in isopropanol and baked in a vacuum oven for 24 hours prior the cruise. The Niskin bottles were cleaned with Isopropanol. The rubber bands on all bottles were replaced by stainless steel springs. The personnel for all water sampling and handling procedures at the bottles wore one-way gloves to protect the valves from grease.

A standard gas (ALM 0383034, 120.5 ppt CFC-12, 266.4 ppt CFC-11 kindly provided by D. Wallace, IfM Kiel) was used to convert the ECD signal in concentrations. The CFC concentrations are reported in pmol kg^{-1} on the SIO93 scale (R. Weiss, SIO).

Performance

During leg Meteor 39/5, the Kiel CFC system worked continuously and about 1550 water samples on 99 stations had been analysed. The survey was dedicated to the circulation of the deep water masses. During periods of dense station spacing, sampling was focused on the water column below 800 m depth.

Accuracy was checked by analysing about 10% of the water samples twice. The result was confirmed by the accuracy obtained at the test stations, where several bottles were dripped at the same depths. The accuracy at these test stations was better than 0.5% for both substances (Figure 1). The system blanks for CFC-11 and CFC-12 were negligible. The blanks were determined by degassing CFC free water, produced by

purging ECD clean Nitrogen permanently through 5 L seawater. The blanks were lower than $0.005 \text{ pmol kg}^{-1}$ for both components.

The Niskin bottle blanks on this cruise could not be determined directly, as CFC-free deep water is not present in the subpolar North Atlantic. We could only estimate an upper bound of the blank by the measurements in the deep Rockall Trough, where CFC-poor water is found. CFC-11 concentrations in the deep water were similar to the values found at the R/V Meteor cruise 30/3, November 1994 (Figure 2). Owing to these measurements the bottle blanks are lower than $0.01 \text{ pmol kg}^{-1}$. On our cruises in the Northern Indian Ocean and the Tropical Atlantic, where CFC free deep water is available, the blanks of the precleaned bottles were lower than $0.003 \text{ pmol kg}^{-1}$ for both components (CFC-12 and CFC-11).

The temporal evolution of the ECD efficiency is shown in Figure 3. During the cruise the efficiency decreased about 25%. Major changes occurred, when the drying agent (magnesium perchlorate) in the purge and trap unit was exchanged. To correct the temporal drift of the ECD, a calibration curve with 4-6 different standard gas volumes was carried out before and after each station. The change between these curves is thought to occur linear with time. As a typical example, the two calibration curves for station 512 are presented in Figure 4. CFC concentrations are calculated by using the two neighbored calibration points, assuming that the calibration curve is linear between these points.

At first we used sample volumes, precalibrated by the company (Machery and Nagel, Germany) for the analysis of standard gas. It turned out that these volumes could be off by more than 5%, affecting the precision of the measured oceanic CFC concentrations by the same amount. Therefore, in 1998, the volumes for the gas standard measurements (nominal 2 mL and 5 mL) were calibrated against two 'master' volumes by D. Wallace's group (IfM Kiel), who had done this task also for the CO₂ community. CFC measurements of the air inside the vessel and especially in the lab were carried out frequently in order to check for contamination. In general, the CFC concentrations in both places were only a few percent higher than in clean air. Clean air measurements were carried out occasionally by sampling air from the ship's compass bridge or forecastle.

Problems

CFC-11 analysis was successfully carried out during the cruise. The analysis of the CFC-12 peak, however was disturbed by an unknown substance with a similar retention time as CFC-12. The unknown peak affected the precision of the CFC-12 data, but did not influence the mean accuracy very much (Figure 1).

During the analysis of the stations 470-483, the efficiency declined rapidly (Fig. 3). The CFC-11 measurements during this time had been flagged with '3'.

Comments

Leg 5 completed the Kiel CFC data set of the Meteor 39 cruise, covering the subpolar East Atlantic (leg 2) and the West Atlantic (leg 4). The second part of the cruise was again a repeat of the WHP section A1E/AR7E.

The surface saturation of CFC-11 relative to the atmospheric value of 266 pptV varied from 104-107% in the northern Irminger Sea to 98-101% in the eastern Atlantic (Figure 5). The supersaturations west of Iceland and off the shelf in the northern Irminger Sea are presumably caused by recent mixing of cold and CFC rich water from the East Greenland Current with warmer water from the south, while the air sea gas exchange had not enough time to equilibrate with the atmosphere. Similar high saturations were found off Newfoundland, where the cold Labrador Current meets the warmer North Atlantic Current [Körtzinger et al., 1999].

In Figure 6 all CFC-11 data measured during the cruise are shown. In general, the concentrations decrease eastward, as the values are higher in the Irminger Sea than east of the Reykjanes Ridge [Sy et al., 1997]. The high concentrations below 2500 m depth characterized the CFC-rich Denmark Strait Overflow Water (DSOW), which can be found at Greenland slope. Compared to the data collected during the cruise Meteor 30/3 in November 1994 [Sy et al., 1997], the CFC-11 signal of the Labrador Sea Water (LSW) did not change significantly in the Irminger Sea, but increased in the eastern Atlantic.

References

- Bullister, J.L. and R.F. Weiss (1988). Determination of CCl₃F and CCl₂F₂ in Seawater and Air. *Deep-Sea Res.*, 35, p. 839-853.
- Körtzinger, A., M. Rhein, and L. Mintrop (1999). Anthropogenic CO₂ and CFCs in the North Atlantic Ocean - A comparison of Man-made Tracer. *Geophys. Res. Lett.*, 26, p. 2065-2068.
- Sy, A., M. Rhein, J.R.N. Lazier, K.P. Koltermann, J. Meincke, A. Putzka, and M. Bersch (1997). Surprisingly Rapid Cooling of Newly Formed Intermediate Waters Across the North Atlantic Ocean. *Nature*, 386, p. 675-679.

Appendix

the station file 'meteor395.sum'

includes:

1. 1 station number
2. 2 year
3. 3 month
4. 4 day
5. 5 hour: minutes in decimal system
6. 6 latitude: minutes in decimals
7. 7 longitude: minutes in decimals
8. 8 water depth (m)
9. 9 depth of CTD profile (m)

the bottle file 'meteor395.sea'

includes:

1. 1 station number
2. 2 bottle number
3. 3 depth (dbar)
4. 4 in-situ temperature (°C)
5. 5 salinity (psu)
6. 6 CFC-12 (pmol kg⁻¹)
7. 7 CFC-11 (pmol kg⁻¹)
8. 8 WOCE quality flag for CFC-12 and CFC-11

Technical information

Gas chromatograph	Shimadzu GC 14
GC column	stainless steel, packed with Porasil C
Cooling trap	with Porapak T and Porasil C
Trap temperatures	-30°C, 100°C
Electron capture detector	Shimadzu
Column temperature	70°C, isothermal
ECD temperature	300°C
Software for chromatogram analysis	Shimadzu CLASS LC 10 (1.63)
Standard gas	ALM 0383034, D. Wallace, IfM Kiel
Precision	CFC-11: 3%, CFC-12: 10%
Accuracy	CFC-11: 0.5% , CFC-12: 1.5%
Blanks	negligible

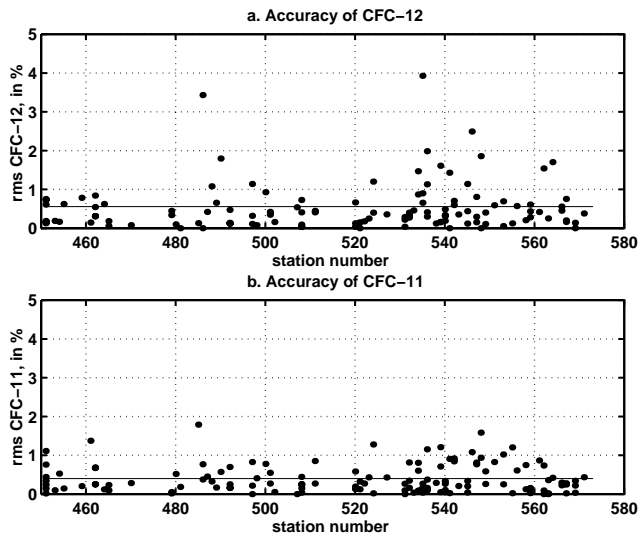
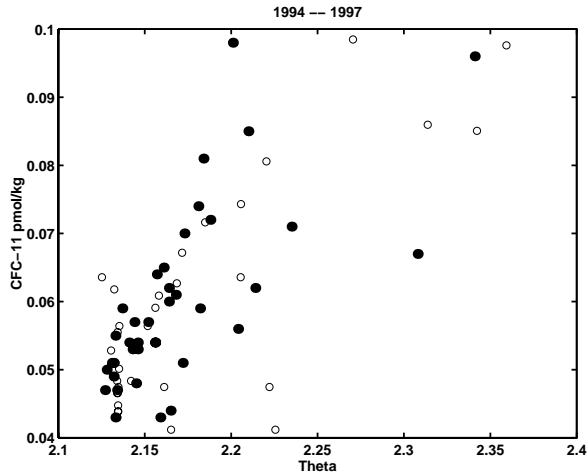


Figure 1: Accuracy (%) of the CFC-12 (a) and CFC-11 (b) replicate samples against station number. The lines represent the mean accuracy of the CFC-12 and CFC-11 samples, respectively. In (a), 9 replicates with an accuracy >5% are omitted.



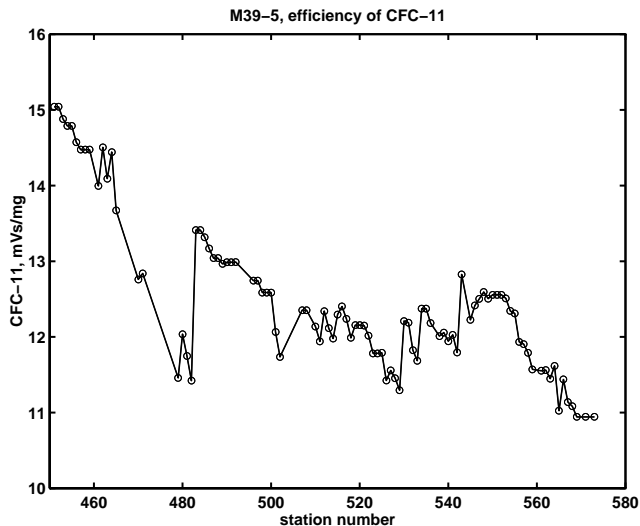


Figure 3: Temporal evolution of the efficiency of the ECD (mVs/mg standard) for the 5 mL sample volume versus station number.

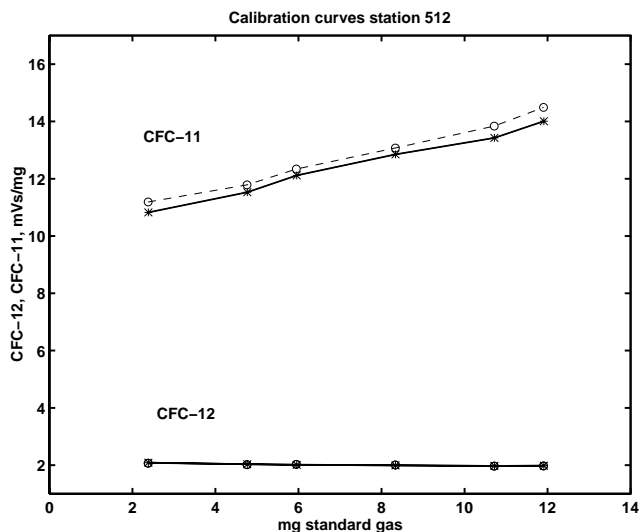


Figure 4: Calibration curve for CFC-12 and CFC-11 before (- -) and after (-) the CFC measurements of station 512.

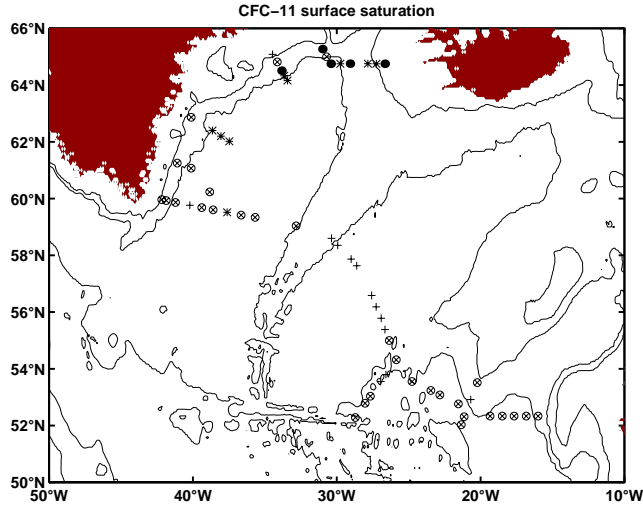


Figure 5: *CFC-11 surface saturation relative to the concentration in the atmosphere (266 pptV), black dot: 105-107%, star: 105-103%, circle with cross: 103-100%, and cross: 100-98%.*

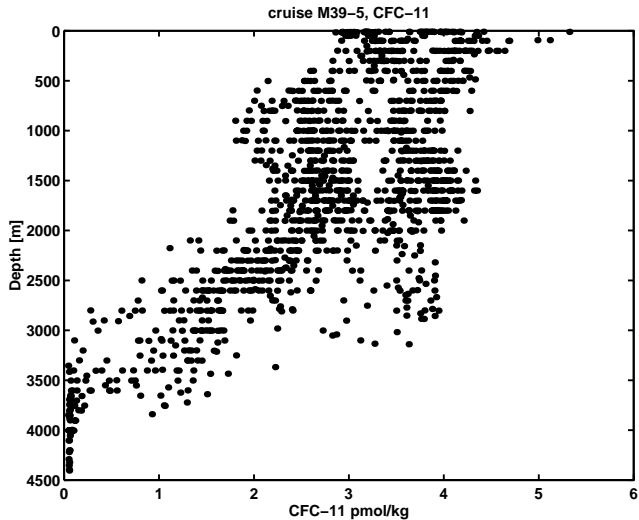


Figure 6: *Cruise Meteor 39/5, all CFC-11 data [pmol kg⁻¹] versus depth.*

10 References

- ALTENBACH, A., M. SARNTHEIN and G. WEFER (1989): Productivity record in benthic foraminifera.- In W. H. Berger and V. S. Smetacek (Ed.): *Productivity of the Ocean, Present and Past*-John Wiley, New York, 255-269.
- ALVE, E. (1995): Benthic foraminiferal distribution and recolonization of formerly anoxic environments in Drammensfjord, southern Norway. *Mar. Micropaleontol.*, **25**, 169-186.
- AMBAR, I., M. R. HOWE and M. I. ABDULLAH (1976): A physical and chemical description of the Mediterranean Outflow in the Gulf of Cadiz-*Deutsche Hydrographische Zeitschrift*, **29** (2), 58-68.
- AUFFRET G.A., PASTOURET, L., CHAMLEY, H., and LANOIX, F. (1974): Influence of the prevailing current regime on sedimentation in the Alboran Sea. *Deep Sea Res.*, Vol. **21**, 839-849.
- BAAS, J.H., SCHÖNFELD, J. and ZAHN, R., manuscript. Mid-depth oxygen drawdown during Heinrich Events: evidence from benthic foraminiferal community structure, trace fossil tiering, und benthic $d^{13}C$ at the Portuguese Margin. Submitted to *Marine Geology*.
- BARAZA, J. and ERCILLA, G. (1996): Gas-charged sediments and large pockmark-like features on the Gulf of Cadiz slope (SW Spain). *Marine and Petroleum geology*, Vol.13, No **2**, 253-261.
- BERNAT, M., CHURCH, T., and ALLEGRE, C.J. (1972): Barium and strontium concentrations in Pacific and Mediterranean sea water profiles by direct isotope dilution mass spectrometry. *Earth Planet. Sci. Letters*, **16**, 75-80.
- BERNER, R.A. (1980): *Early diagenesis. A theoretical approach.* 241 pp., Princeton University Press; Princeton.
- BERNSTEIN, R.E., BYRNE, R.H., BETZER, P.R., and GRECO, A.M. (1991): Morphologies and transformations of celestite in seawater: The role of acantharians in strontium and barium geochemistry. *Geochim. Cosmochim. Acta*, **56**, 3273-3279.
- BERSCH, M., J. MEINCKE and A. SY (1998): Interannual thermohaline changes at the eastern margin of the North Atlantic subpolar gyre 1991-1996. *Deep-Sea Res.* (in press).
- BOND, G., HEINRICH, H., BROECKER, W., LABEYRIE, L., MCMANUS, J., ANDREWS, J., HUON, S., JANTSCHIK, R., CLASEN, S., SIMET, C: TEDESCO, K., KLAS, M., BONANI, G., and IVY, S. (1992): Evidence for massive discharges of icebergs into the North Atlantic ocean during the last glacial period. *Nature*, **360**, 245-249.
- BOND, G., BROECKER, W., JOHNSON, S., MCMANUS, J., LABEYRIE, L., JOUZEL, J., and BONANI, G. (1993): Correlations between climatic records from North Atlantic sediments and Greenland ice. *Nature*, **365**, 143-147.
- BOYCE, R.E. (1976): Definitions and laboratory techniques of compressional sound velocity parameters and wet-water content, wet-bulk density, and porosity parameters by gravimetric and gamma ray attenuation techniques. In Schlanger, S., O., Jackson, E. D. et al. (eds.), *Init.Rep. DSDP*, **33**, 931-958.
- BOYLE, E.A. and L. D. KEIGWIN (1987): North Atlantic thermohaline circulation during the last 20,000 years: Link to high latitude surface temperature- *Nature*, **330**, 35-40.
- BOYLE, E.A. (1988): Cadmium: chemical tracer of deepwater paleoceanography, *Paleoceanography*, **4**, 471-489.

- BOYLE, E.A. (1994): A comparison of carbon isotopes and cadmium in the modern and glacial maximum ocean: can we account for the discrepancies?, in R. Zahn, T.F. Pedersen, M. Kaminski and L. Labeyrie (eds.), *Carbon Cycling in the Glacial Ocean: Constraints on the Ocean's Role in Global Change*, NATO ASI Series I, Vol. **17**, 167-194.
- BOZZANO, G. (1996): La sedimentazione e la mineralogia dei depositi del Mare di Alboran: significato paleoceanografico e paleoclimatico. Graduation thesis. University of Genoa. 140pp.
- BRASS, G.W. and TUREKIAN, K.K. (1974): Strontium distribution in Geosecs oceanic profiles. *Earth Planet. Sci. Letters*, **23**, 141-148.
- BROECKER, W.S. and E. MAIER-REIMER (1992): The influence of air and sea exchange on the carbon isotope distribution in the sea, *Global Biogeochem. Cyc.*, **6**, 315-320.
- BROECKER, W.S. and PENG, T.-H. (1982): *Tracers in the sea*. Eldigio Press, New York.
- BROWN, S.J. (1996): Controls on the trace metal chemistry of foraminiferal calcite and aragonite. Ph.D. thesis, Univ. of Cambridge, 231 pp., October 1996.
- CHI, J. (1995): Multi-Sensor-Kern-Logging-Methoden zur Bestimmung von physikalischen Sedimenteigenschaften. Berichte aus dem Sonderforschungsbereich 313, Univ. Kiel, **58**, 125 p.
- CORLISS, B.H., D.G. MARTINSON and T. KELTER (1986): Late Quaternary deep-ocean circulation-*Geological Society of America Bulletin*, **97**, 1106-1121.
- CULBERSON, D.H. (1991): Dissolved Oxygen. In: WHP Operations and Methods, WHP Office Report, WHPO **91-1**, 15 pp.
- CURRY, R., M.S. MCCARTNEY and T. JOYCE (1998): Oceanic transport of subpolar climate signals to mid-depth subtropical waters. *Nature*, **391**, 575-577.
- DANSGAARD, W., J.J. JOHNSON, B.H. CLAUSEN, D. DAHL-JENSEN, N.S. GUNDESTRUP, C.U. HAMMER, C.S. HVIDBERG, J.P. STEFFENSON, A.E. SVEINBJÖRNDOTTIR, J. JOUZEL, and G. BOND (1993): Evidence for general instability of past climate from a 250-kyr ice-core record, *Nature*, **364**, 218-220.
- DIAMOND GENERAL (1997): Instructions for use 768-20R needle oxygen electrode with internal reference. 6 pp., Diamond General Development Corp.; Ann Arbor.
- DICKSON, R.R., J. LAZIER, J. MEINCKE, P. RHINES and J. SWIFT (1996): Long-term coordinate changes in the convective activity of the North Atlantic. *Prog. Oceanogr.*, **38**, 241-295.
- DOE (1994): Handbook of methods for the analysis of various parameters of the carbon dioxide system in sea water; version 2, Dickson, A.G. and Goyet, C (eds.) ORNL/CDIAC-74.
- DÖSCHER, R., C.W. BÖNING and P. HERRMANN (1994): Response of Circulation and Heat Transport in the North Atlantic to Changes in Thermohaline Forcing in Northern Latitudes: A Model Study. *J. Phys. Oceanogr.*, **24**(11), 2306-2319.
- DUPLESSY, J.-C., N. J. SHACKLETON, R. G. FAIRBANKS, L. D. LABEYRIE, D. OPPO, and N. KALLEL (1988): Deepwater source variations during the last climatic cycle and their impact on the global deepwater circulation, *Paleoceanography*, **3**, 317-341.
- DWYER, G.S., CRONIN, TH.M., BAKER, P.A., RAYMO, M.E., BUZAS, J.S., and CORREGE, TH. (1995): North Atlantic deepwater temperature changes during late Pliocene and late Quaternary climatic cycles. *Science* **270**, 1347-1351.
- FREW, R.D. and K.A. HUNTER (1992): Influence of Southern Ocean waters on the cadmium-phosphate properties of the global ocean, *Nature*, **360**, 144-146.
- FREW, R.D. (1995): Antarctic bottom water formation and the global cadmium to phosphorus relationship, *Geophys. Res. Lett.*, **22**, 2349-2352.

- GOLOWAY, F. and BENDER, M. (1982): Diagenetic models of interstitial nitrate profiles in deep sea suboxic sediments. *Limnol. Oceanogr.*, **27**, 624-638.
- GRASHOFF, K. (1983): Determination of oxygen. In: Grashoff, K. (Hrsg), *Methods of seawater analysis*, 2nd ed., 61-72, Verlag Chemie; Weinheim.
- GRASSHOFF, K., M. EHRHARDT and K. KREMLING (eds.): (1983): *Methods of Seawater Analysis*; 2nd edition, Verlag Chemie, Weinheim.
- GROOTES, P.M., M. STUIVER, J.W.C. WHITE, S. JOHNSEN, and J. JOUZEL (1993): Comparison of oxygen isotope records from the GISP2 and GRIP Greenland ice cores, *Nature*, **366**, 552-554.
- GROUSSET, F.E., JORON, J.L., BISCAYE, P.E., LATOUCHE, C., TREUIL, M., MAILLET, N., FAUGERPS, J.C., and GONTHIER, E. (1988): Mediterranean Outflow through the Strait of Gibraltar since 18,000 years B.P.: mineralogical and geochemical arguments. *Geo-Marine Letters*, Vol. **8**, 25-34.
- HANAWA, K., P. RUAL, R. BAILEY, A. SY and M. SZABADOS (1995): A new depth-time equation for Sippican or TSK T-7, T-6 and T-4 expendable bathythermographs (XBT). *Deep-Sea Res.*, **42**, 1423-1451.
- HASTINGS, D., RUSSELL, A., and EMERSON, S. (1996): Foraminiferal Mg as a paleotemperature-proxy in the equatorial Atlantic and Caribbean surface oceans. AGU Fall Meeting, San Francisco, Abstract.
- HARMAN, R.A. (1964): Distribution of foraminifera in the Santa Barbara Basin, California. *Micropaleontology*, **10**, 81-96.
- HARVEY, J.G. and A. THEODOROU (1986): The circulation of Norwegian Sea overflow water in the eastern North Atlantic-*Oceanologica Acta*, **9**, 393-402.
- HENRICH, R., FREIWALD, A., BICKERT, T., SCHAEFER, P. (1997): Evolution of an Arctic open-shelf carbonate platform, Spitsbergen Bank (Barents Sea). - In: N.P. James and J.A.B. Clarke (eds.), *Cool-Water Carbonates*, SEPM Special Publication, **56**, 163-181.
- HERMELIN, J.O.R. (1992): Variations in the benthic foraminiferal fauna of the Arabian S: a response to changes in upwelling intensity? In: Summerhayes, C.P., Prell, W.J. and Emeis, K.C.(Editors). *Upwelling systems: Evolution since the Miocene*. *Geol. Soc Spec. Publ.*, **64**, 151-166.
- HOWE, M. R. (1982): The Mediterranean Water outflow in the Gulf of Cadiz-*Oceanogr. Mar. Biol. Ann. Rev.*, **20**, 37-64. IOC (1993): *Manual of quality control procedures for validation of oceanographic data*. UNESCO, *Manual and Guides* **26**, 436 pp.
- JOHNSON, K.M., K.D. WILLS, D.B. BUTLER, W.K. JOHNSON and C.S. WONG (1993): Coulometric total carbon dioxide analysis for marine studies: maximizing the performance of an automated gas extraction system and coulometric detector. *Mar. Chem.*, **44**, 167- 187.
- JUNG, S. J. A. (1996): Wassermassenaustausch zwischen dem NE-Atlantik und dem Europäischen Nordmeer während der letzten 300 000/80 000 Jahre im Abbild stabiler O- und C-Isotope.- Sonderforschungsbereich 313 "Veränderungen der Umwelt: Der nördliche Nordatlantik", Report No. 61.
- KAIHO, K. (1994): Benthic foraminiferal dissolved-oxygen index and dissolved oxygen levels in the modern ocean. *Geology*, **22**, 719-722.
- KIRKWOOD, D. S. and A. R. FOLKARD (1986): Results of the ICES salinity sample-bottle intercomparison. *ICES C.M.*, 16 pp.

- KOLTERMANN, K.P., A. SOKOV, V.TERECHECHENKOV, S. DOBROLIUBOV, K. LORBACHER and A. SY (1998a): Decadal Changes in the Thermohaline Circulation of the North Atlantic. *Deep-Sea Res.* (under review).
- KOLTERMANN, K.P. and K. LORBACHER (1998b): The changes in the Hydrography of the North Atlantic along 48°N during WOCE. (subm. *J. Geophys. Res.*).
- KÖRTZINGER, A., H. THOMAS, B. SCHNEIDER, N. GRONAU, L. MINTROP and J.C. DUINKER (1996): At-sea intercomparison of two newly designed underway $p\text{CO}_2$ systems - Encouraging results. *Mar. Chem.*, **52**, 133-145.
- KÖRTZINGER, A., MINTROP, L., and DUINKER, J.C., 1998. On the penetration of anthropogenic CO_2 in the North Atlantic Ocean.. *J. Geophys. Res.*, 103: 18681-18689
- KOUTSOUKOS, E.A.M., LEARY, P.N. and HART, M.B. (1990): Latest Cenomanian-earliest Turonian low-oxygen tolerant benthonic foraminifera: a case study from the Sergipe basin (N.E. Brazil) and the western Anglo-Paris basin (southern England). *Palaeogeogr., Palaeoclimatol., Palaeoecol.*, **77**, 145-177.
- KRAUSS, W. (1986): The North Atlantic Current. *Journ. Geophys. Res.*, **91**, 5061-5074.
- LAZIER, J. (1995): The salinity decrease in the Labrador Sea over the past thirty years. In: *Climate on decade-to-century time scales*, p. 295-305. National Academy of Sciences Press. Washington, D.C. (1995).
- LEBREIRO, S.M., J.C. MORENO, I.N. MCCAVE and P.P.E. WEAVER (1996): Evidence for 'Heinrich' layers off Portugal (Torre Seamount: 39°N, 12°W), *Mar. Geol.*, **131**, 47-56.
- LOUBERE, P. (1994): Quantitative estimation of surface ocean productivity and bottom water oxygen concentration using benthic foraminifera. *Paleoceanography*, **9**, 723-737.
- LUTZE, G.F. and COULBOURN, W.T. (1984): Recent benthic Foraminifera from the continental margin of northwest Africa: community structures and distribution. *Mar. Micropaleontol.*, **8**, 361-401.
- LYNCH-STIEGLITZ, J., A. VAN GEEN, and R.G. FAIRBANKS (1996): Interocean exchange of glacial North Atlantic Intermediate Water: evidence from subantarctic Cd/Ca and carbon isotope measurements, *Paleoceanography*, **11**, 191-201.
- MASLIN, M.A., SHACKLETON, N.J., and PFLAUMANN, U. (1995): Surface water temperature, salinity and density changes in the Northeast Atlantic during the last 45.000 years: Heinrich events, deep water formation and climatic rebounds. *Paleoceanography*, **10**, 527-544.
- MCCARTNEY, M. S., (1992): Re-circulating components to the deep boundary current of the northern North Atlantic-*Progress in Oceanography*, **29**, 283-383.
- MCCORKLE, D.C., MARTIN, P.A., LEA, D. W. and KLINKHAMMER, G.P. (1995): Evidence of a dissolution effect on benthic foraminiferal shell chemistry: ^{13}C , Cd/Ca, Ba/Ca and Sr/Ca results from the Ontong Java Plateau. *Paleoceanography*, **10**, 699-714.
- MILLERO, F. J., ZHANG, J.-Z., LEE, K., and CAMPBELL, D. M., 1993. Titration alkalinity of seawater. *Mar. Chem.*, **44**, 153-165.
- MINTROP, L., The VINDTA manual, Version 2.0 (June 1996), *unpubl.*
- MULLINEAUX, L.E. and LOHMANN, G.P. (1981): Late Quaternary stagnations and recirculation of the eastern Mediterranean: changes in the deep water recorded by fossil benthic foraminifera. *J. Foram. Res.*, **11**, 20-37.
- MURPHY, J. and J.P. RILEY (1962): A modified single solution method for the determination of phosphate in natural waters, *Anal. Chim. Acta*, **27**, 31-36.

- NELSON, C.H., BARAZA, J. and MALDONADO, A. (1993): Mediterranean undercurrent sandy contourites, Gulf of Cadiz, Spain. *Sedimentary Geology*, Vol. **82**, 103-131.
- NÜRNBERG, D. (1995): Magnesium in tests of *Neogloboquadrina pachyderma* sinistral from high northern and southern latitudes. *J. Foram. Res.* **25** (4), 350-368.
- NÜRNBERG, D., BIJMA, J., and HEMLEBEN, C. (1996a): Assessing the reliability of magnesium in foraminiferal calcite as a proxy for water mass temperatures. *Geochimica et Cosmochimica Acta*, **60** (5), 803-814.
- NÜRNBERG, D., BIJMA, J., and HEMLEBEN, C. (1996b): Erratum to "Assessing the reliability of magnesium in foraminiferal calcite as a proxy for water mass temperatures." *Geochimica et Cosmochimica Acta* **60** (13), 2483-2484.
- OPPO, D. W. and S. J. LEHMAN (1993): Mid-depth circulation of the subpolar North Atlantic during the last glacial maximum-*Science*, **259**, 1148-1152.
- PALANQUES, A., DIAZ, J.I., and FARRAN, M. (1995): Contamination of heavy metals in the suspended and surface sediment of the Gulf of Cadiz (Spain): the role of sources, currents, pathways and sinks. *Oceanologica Acta*, Vol. **18**, 469-477.
- REIMERS, C.E., JAHNKE, R.A. and MCCORCLE, D.C. (1992): Carbon fluxes and burial rates over the continental slope and rise off central California with implications for the global carbon cycle. *Global Biogeochem. Cycles*, **6**, 199-224.
- ROETHER, W., A. PUTZKA, K. BULSIEWICZ, G. FRAAS, O. KLATT, W. PLEP, C. RUETH and B. SCHLENKER; (1998): Advances in Tracer Measurements; International WOCE Newsletter; No. **30**.
- SARNTHEIN, M., K. WINN, S. JUNG, J.-C. DUPLESSY, L. LABEYRIE, H. ERLLENKEUSER, and G. GANSSEN (1994): Changes in east Atlantic deepwater circulation over the last 30,000 years: eight time slice reconstructions, *Paleoceanography*, **9**, 209-267.
- SAUNDERS, P.M. (1994): The flux of overflow water through the Charlie-Gibbs Fracture Zone. *J. Geophys. Res.*, **99** (C6), 12,343-12,355.
- SCHÄFER, P., HENRICH, R., ZANKL, H., BADER, B. (1996): Carbonate production and depositional patterns of BRYOMOL-carbonates on deep shelf banks in mid and high Northern Latitudes. - *Göttinger Arb. Geol. Palaeont.*, **Sb 2**, 101-110.
- SCHMITZ JR., W. J. J. and M. S. MCCARTNEY (1993): On the North Atlantic Circulation-*Reviews of Geophysics*, **31** (1), 29-49.
- SCHÖNFELD, J. (1997): The impact of the Mediterranean Outflow Water (MOW) on Benthic foraminiferal assemblages and surface sediments at the southern Portuguese continental margin. *Mar. Micropaleontol.*, **29**, 211-236.
- SCHULTHEISS, P.J. and MCPHAIL, S.D. (1989): An automated P-wave logger for recording fine scale compressional wave velocity structure in sediments. In Rudiman, W., Sarnthein, M. et al. (eds.) *Proc. ODP Sci. Res.*, **108**, 407-413.
- SCHULTHEISS, P.J., MIENERT, J. and Shipboard Scientific Party (1988): Whole-core p-wave velocity and gamma ray attenuation logs from Leg 108 (Sites 657 through 668). In Rudiman, W. Sarnthein, M. et al. (eds.) *Proc. ODP Init. Rep. (Pt.A)* **108**, 1015-1046.
- SY, A. (1985): An alternative editing technique for oceanographic data. *Deep-Sea Res.*, **32**, 1591-1599.
- SY, A. (1991): XBT measurements. In: WHP Operations and Methods, WHP Office Report WHPO **91-1**, 19 pp.

- SY, A. (1996): Summary of field tests of improved XCTD/MK-12 system. Intern. WOCE Newsletter, No. **22**, 11-13. SY, A. and H.-H. HINRICHSEN (1986): The influence of long-term storage on the salinity of bottled seawater samples. Dt. Hydr. Z., **39**, 35-40.
- SY, A. (1998): At-sea test of a new XCTD system. Intern. WOCE Newsletter, **31**, 45-47.
- SY, A., M. RHEIN, J. LAZIER, K.P. KOLTERMANN, J. MEINCKE, A. PUTZKA and M. BERSCH (1997): Surprisingly rapid spreading of newly formed intermediate waters across the North Atlantic Ocean. *Nature*, **386**, 675-679.
- SY, A., K.P. KOLTERMANN and U. PAUL (1997b): Observing opposing temperature changes in the upper and intermediate layers of the North Atlantic Ocean. Intern. WOCE Newsl., **26**, 30-33.
- TALLEY, L.D. and M.S. MCCARTNEY (1982): Distribution and circulation of Labrador Sea Water, *J. Phys. Oceanogr.*, **12**, 1189-1205.
- TAYLOR, K.C., C.U. HAMMER, R.B. ALLEY, H.B. CLAUSEN, D. DAHL-JENSEN, A.J. GOW, N.S. GUNDESTRUP, J. KIPFSTUHL, J.C. MOORE and E.D. WADDINGTON (1993): Electrical conductivity measurements from GISP 2 and GRIP Greenland ice cores- *Nature*, **366**, 549-552.
- TAYLOR, K.C., G.W. LAMOREY, G.A. DOYLE, R.B. ALLEY, P.M. GROOTES, P.A. MAYEWSKI, J.W.C. WHITE, and L.K. BARLOW (1993): The 'flickering switch' of late Pleistocene climate change, *Nature*, **361**, 432-436.
- UNESCO (1988): The acquisition, calibration, and analysis of CTD data. Unesco technical papers in marine science, **54**, 92 pp.
- VAN AKEN, H.M. and C.J. DE BOER (1995): On the synoptic hydrography of intermediate and deep water masses in the Iceland Basin. *Deep-Sea Res.*, **42**, 165-189.
- VAN AAKEN, H.M. and G. BECKER (1996): Hydrography and through-flow in the north eastern North Atlantic Ocean: the NANSEN project. *Prog. Oceanogr.*, **38**, p. 297 - 346.
- VAN GEEN, A., ADKIND, J.F., BOYLE, E.A., NELSON, C.H., and PALANQUES, A. (1997): A 120 yr record of widespread contamination from mining of the Iberian pyrite belt. *Geology*, Vol. **25**, No. 4, 291-294.
- VEUM, T., E. JANSEN, M. ARNOLD, I. BEYER and J.-C. DUPLESSY (1992): Water mass exchange between the North Atlantic and the Norwegian Sea during the past 28,000 years-*Nature*, **356**, 783-785.
- WANG L., SARNTHEIN, M., DUPLESSY, J.-C., ERLLENKEUSER, H., JUNG, S., and PFLAUMANN, U. (1995): Paleo sea surface salinities in the low-latitude Atlantic: the $\delta^{18}\text{O}$ record of *Globigerinoides ruber* (white), *Paleoceanography*, **10**, 749-761.
- WCRP (1988): World Ocean Circulation Experiment Implementation Plan. WMO/TD No. **242** and **243**. WOCE International Planning Office, Wormley, England.
- WETZEL, A. (1981): Ökologische und stratigraphische Bedeutung biogener Gefüge in quartären Sedimenten am NW-afrikanischen Kontinentalrand.-METEOR Forsch.-Ergebnisse, Reihe C, **34**, 1-47.
- WHP (1994): WOCE operations manual. Vol. 3, Section 3.1, Part 3.1.3. WHP Office Report WHPO **91-1**, Woods Hole, USA.
- ZAHN, R. (1997): North Atlantic thermohaline circulation during the last glacial period: evidence for coupling between melt water events and convective instability, *GEOMAR Rept.*, **63**, 133 p.

- ZAHN, R., SARNTHEIN, M., and ERLLENKEUSER, H. (1987): Benthic isotope evidence for changes of the Mediterranean outflow during the late Quaternary. *Paleoceanography*, **2**, 543-559.
- ZAHN, R. and R. KEIR (1994): Tracer-nutrient correlations in the upper ocean: observational and box model constraints on the use of benthic foraminiferal $\delta^{13}\text{C}$ and Cd/Ca as paleo-proxies for the intermediate-depth ocean, in R. Zahn, T.F. Pedersen, M. Kaminski and L. Labeyrie (eds.), *Carbon Cycling in the Glacial Ocean: Constraints on the Ocean's Role in Global Change*, NATO ASI Series I, Vol. **17**, 195-221.
- ZAHN, R., J. SCHÖNFELD, H.-R. KUDRASS, M.-H. PARK, H. ERLLENKEUSER, and P. GROOTES (1997): Thermohaline instability in the North Atlantic during melt water events: stable isotope and ice-rafted detritus records from Core SO75-26KL, Portuguese Margin, *Paleoceanography*, **12**, 696-710.
- ZENK, W. (1975): On the origin of the intermediate double-maxima in T/S profiles from the North Atlantic. *"METEOR" Forsch.-Ergebn.*, **A(16)**, 35-43.
- ZENK, W. and L. ARMI (1990): The complex spreading pattern of Mediterranean Water off the Portuguese continental slope, *Deep-Sea Res.*, **37**, 1805-1823.